Antigen Perception in T Cells

Matthew J Wither

A dissertation

submitted in partial fulfillment of the

requirements for the degree of

Doctor of Philosophy

University of Washington

2023

Reading Committee:

Dr. Hao Yuan Kueh, Chair

Dr. Jesse Zalatan

Dr. Herbert Sauro

Program Authorized to Offer Degree:

Bioengineering

University of Washington

Abstract

Antigen Perception in T Cells

Matthew J Wither

Chair of the Supervisory Committee:

Dr. Hao Yuan Kueh

Department of Bioengineering

The immune system's threat detection hinges on T cells' ability to perceive differences in the quality and quantity of peptide-major histocompatibility complex (pMHC) antigens. Our T cells are tolerant to the vast majority of antigens they sense, as these pMHCs are derived from our own endogenous proteome and represent "self". In the case of a viral infection, virus-derived pMHC antigens are perceived by T cells as a threat and elicit an effector response to clear the infection. This fundamental perception of "self" vs "foreign" is based on antigen quality. Self pMHCs have a relatively low affinity for the T cell antigen receptor (TCR), while foreign pMHCs have relatively high TCR binding affinities. The current paradigm states that this affinity discrimination is enabled by a signaling network downstream of the TCR that performs kinetic proofreading during antigen sensing, whereby only long-lasting TCR binding events resulting from interactions with high

affinity foreign pMHCs pass a series of proofreading reactions and further propagate the signal. However, numerous *in vitro* and *in vivo* studies have shown that T cells do not respond uniformly to variations in the quality and quantity of foreign antigens, but rather tailor their response to each unique threat. This suggests an unresolved signal transmission mechanism within the TCR signaling network that regulates T cell responses in a tunable, and not simply all-or-none fashion.

The Erk and NFAT signaling pathways connect TCR engagement to gene regulation, and thus their combined signaling dynamics may transmit information about pMHC inputs. We formed this hypothesis from two main bodies of evidence. First, signaling pathway dynamics, including dynamics of the Erk pathway, are known to transmit extracellular signal information in many other contexts to enable input-specific cellular responses. Second, NFAT and the Erk-activated transcription factor AP-1 work cooperatively to regulate gene expression in activated T cells, and disruption of their cooperativity leads to distinct phenotypes. Therefore, it is plausible that signaling activity of these two pathways, in combination, over the course of initial activation can tune gene expression in T cells to generate antigen-specific responses.

To test this idea, we developed a dual reporter mouse strain and a quantitative imaging assay that together enable simultaneous monitoring of Erk and NFAT dynamics in live T cells over day-long timescales as they respond to varying pMHC inputs. We found that both pathways initially activate uniformly across various pMHC inputs but diverge over longer (9+ hrs) timescales, enabling independent encoding of pMHC affinity and dose. Next, we combined signaling perturbations and variable pMHC stimulation with RNA sequencing and mathematical modeling to uncover multiple temporal and combinatorial mechanisms for decoding these late signaling dynamics to generate

pMHC-specific transcriptional responses. Our results underscore the importance of long timescale signaling dynamics in T cell antigen perception and establish a framework for understanding T cell responses under diverse contexts. Our findings, while only scratching the surface of the complexity and sophistication of T cell signaling and transcriptional regulation, point to a strategy for improving T cell-based therapies by engineering precise temporal control over signaling inputs.

TABLE OF CONTENTS

LIST OF FIGURES

ACKNOWLEDGEMENTS

I offer my sincerest gratitude and appreciation to my advisor, Dr. Hao Yuan Kueh. I had the privilege of joining his lab when it was first started at UW, and I remember doing my first experiments having to fish supplies out of boxes. I didn't think much of it at back then, but looking back now makes me appreciate the journey we've been on. You gave me creative freedom, and helped me to learn from my mistakes and to be patient. These qualities not only help me in science but in all aspects of life, and for that I thank you, Kueh.

I thank my supervisory committee, Dr. Jesse Zalatan and Dr. Herbert Sauro, for your guidance throughout my graduate work. You have helped me become a better thinker and scientist.

I thank all my fellow lab members, past and present for their support and friendship over our years together. I cherish all of our joint successes and failures, and am proud of how much we've grown.

I thank my family and closest friends for providing unconditional love and support during this challenging adventure. Without you I would have never even made it to the starting line.

Most importantly, I thank my wife, Brittany for joining me on life's adventure midway through my Ph.D. You are an exceptional person and being with you made the final few years of this work so much better. I am crazy excited for what comes next for our family.

Sections 1.2 and 1.4, Chapter 2, Chapter 3, Section 4.1, and Appendices A-C were part of a manuscript submitted for publication in *Proceedings of the National Academy of Sciences* at the time of writing:

Wither, M.J., White, W.L., Pendyala, S., Leanza, P.J., Fowler, D., Kueh, H.Y. **Antigen Perception in T cells by Long-Term Erk and NFAT Signaling Dynamics**. 2023

Chapter 1. Introduction

1.1 Signal Encoding in Biological Systems

To maintain homeostasis, all cells must alter their physiological state in response to changing environments. At the tissue level, this includes anything from a change in available glucose, amino acids, or oxygen, to the presence of inflammation, tissue damage, or a pathogen. To respond to these changes, cells transmit information about their environment, contained in the identity and quantity of extracellular signals (i.e. ligands), through biochemical signaling pathways to downstream effectors that execute a response. In a typical case, a signal, such as an inflammatory cytokine, binds a ligand-specific receptor on the cell surface which activates one or more signal transduction pathway(s) to transmit the information to the nucleus. There, transcription factors and other gene regulatory components induce a change in cell state through changes in gene expression. Signal transduction pathways (herein referred to simply as signaling pathways) are responsible for encoding and transmitting ligand information from the cell surface to the nucleus where the encoded information can then decoded at the level of gene transcription and translation[1].

This encoding process is complicated by a limitation in the number of signaling components available to encode and transmit information, as well as having to operate in noisy environments. All cell types, from lymphocytes to cardiomyocytes to hepatocytes transmit signal information

through a common set of signaling pathways that display cell to cell variability in component concentrations and background activity. To overcome this, cells often encode the identity and quantity of signals through complex signaling behaviors, such as in oscillatory or transient activation of downstream kinases and transcription factors (TFs) (**Fig. 1.1 – Dynamic encoding**). By utilizing distinct dynamic responses for different signals, cells are able to rely on a limited set of shared signaling components to transmit information and generate signal-specific responses [1–5]. The earliest reports of dynamic encoding involved the Erk/MAPK pathway [6,7] and has since become apparent in a wide range of signaling pathways and cell types including Erk/MAPKs [8–13], BMP signaling [14], Notch [15], NF-kB [16–22], IFN signaling [23,24], NFAT [25], and p53 [26–28] in mammalian cells, and Crz1 [29] and Msn2 [30] in yeast. This range of contexts points to dynamic encoding as being a general phenomenon in biological systems.

Furthermore, many surface receptors, including the T cell antigen receptor activate multiple signaling pathways in parallel [31–33]. Multiple pathway activities can then result in regulation of target genes in a combinatorial fashion, such as in the cooperativity or antagonism of two or more transcription factors at promotor or enhancer elements of gene loci [34–37]. This suggests that not only can ligand information be encoded in dynamic responses of signaling pathways, but it can be encoded jointly within the dynamics of two or more pathways (**Fig. 1.1 – Combinatorial encoding**). Indeed, combinatorial encoding has been observed in several contexts [38]. For instance, many immune receptors activate the NF-kB and MAPK pathways simultaneously to encode distinct signals [39] and it has been shown that macrophages encode quantitative differences in Toll-like receptor signals [40], as well as distinct bacterial threats [41] through differential combinatorial activities of NF-kB and MAPK. Additionally, various growth factors activate multiple signaling

pathways including Erk and Akt, and the combinatorial activities of these two kinases have been shown to encode growth factor identity in mammary epithelial cells by differentially regulating the transcription factor FOXO3 [42]. Both dynamic and combinatorial encoding serve to increase specificity [4,39] and signal-to-noise ratio [5] of the response and enable accurate information transmission through noisy intra- and extracellular environments. Evidence of signal encoding through dynamic and combinatorial signaling responses continues to emerge in a growing number of cell types and contexts, but understanding its role across more biological contexts has been limited by the need for advanced microscopy setups and signaling reporters that are not readily implemented in primary cells.

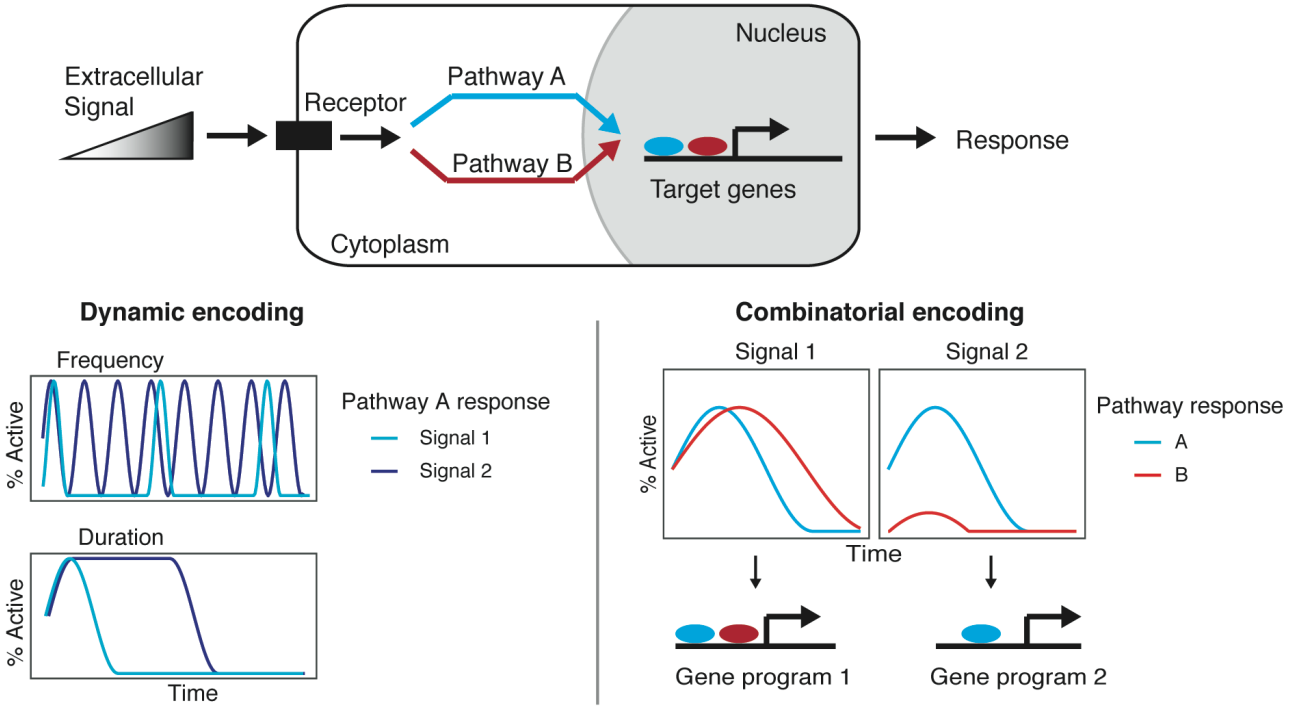

Figure 1.1 Dynamic and Combinatorial Signal Encoding.

Various extracellular signals (ligands) are present at a range of concentrations that may change over time. A ligand binds to its ligand-specific receptor and activates downstream signaling pathway(s). Signaling pathway activity is then translated into changes in gene expression which results in cellular responses. **Dynamic encoding** by a signaling pathway involves transmitting extracellular signal information through its dynamic (temporal) activity, such as in the frequency or duration of the pathway's activity. **Combinatorial encoding** involves transmitting extracellular signal information through the joint dynamics of multiple signaling pathways. Information encoded within signaling pathways can be decoded by regulatory elements (i.e. TF binding sites) that produce different transcriptional outputs from different combinatorial signaling inputs.

1.2 Decoding Signaling Dynamics

Ligand information transmitted from the cell surface to the nucleus must be accurately decoded to elicit changes in gene expression that give rise to ligand-specific responses. For example, macrophages, innate immune cells that coordinate with other immune cells to defend against pathogens, respond differently to inflammatory (i.e. TNF) versus pathogen derived (i.e. lipopolysaccharide) signals, and do so by first encoding the signal information through differential NF-kB dynamics [16,21]. Without decoding mechanisms in place to translate this information into distinct gene expression profiles, macrophages would lose the ability to elicit stimulus-specific responses. Decoding mechanisms generally rely on some form of transcriptional control, such as accessibility of the gene locus to transcriptional regulators and the presence of *cis*-regulatory elements controlling transcriptional output, or post-transcriptional control, such as mRNA stability. Importantly, as ligand information is encoded through dynamic signaling responses, the decoding mechanisms must be able to interpret temporal information.

Elucidating the precise mechanisms used to decode the dynamic response of a signaling pathway is rather difficult as quantitative measurements of signaling activity must be coupled to gene expression or protein abundance in single cells [4,16,43]. Mathematical modeling, however, provides a practical approach to identifying putative decoding mechanisms but is limited to identifying mechanisms that are sufficient to explain experimental observations, and not necessarily those that can reliably predict transcriptional responses. One of the best studied decoding mechanisms involves the Erk signaling pathway. As mentioned above, Erk signaling in various cell types can encode signal information through its dynamic response [12]. How are these different dynamics decoded to generate distinct phenotypes? A set of "Immediate-early genes (IEGs)," including the

prototypic member and transcription factor c-Fos [44], are expressed immediately upon activation of Erk, however, undergo rapid degradation. Only with sustained Erk activity will c-Fos become phosphorylated by active Erk and stabilized in the nucleus to mediate gene transcription [10]. This regulation between Erk and c-Fos represents a coherent feed-forward circuit[45] that enables decoding of the input signal duration. Further, another set of genes induced by Erk signaling, "immediate-late genes," are also transcribed upon Erk activation, but have long mRNA half-lives and serve to translate the duration of Erk signaling into response amplitude as opposed to the short half-lives of IEGs that control response duration [46]. Here, post-transcriptional regulatory mechanisms, specifically mRNA and protein stability, enable decoding of dynamic Erk signaling. Similarly, mRNA stability also plays a role in decoding pulsatile activity of the tumor-suppressor p53 in response to different stress signals [47].

Another well-studied system of dynamic encoding, the NF-kB pathway, relies too on mRNA stability for decoding, but in combination with other transcriptional mechanisms [18]. In fibroblasts, stimulus-specificity is achieved additionally by decoding the duration of NF-kB activity through a chromatin remodeling step, in which LPS-specific gene loci are contained in an inactive chromatin state prior to stimulation. Sustained NF-kB activity opens these chromatin regions to activate gene transcription, a process that occurs slowly in order to be selective towards long duration signaling. This chromatin-mediated regulatory mechanism controls cell fate decisions in other contexts where cell state, and even lineage commitment is regulated through slow chromatin opening steps [48–52], and represents a robust strategy for temporal signal decoding.

Lastly, *cis*-regulatory elements that control transcription at an individual gene locus are known to contain binding sites for varying TFs [53,54]. Distinct TF binding sites, or combinations of binding sites can decode signaling pathway activity through Boolean logic of temporal TF activity (**Fig. 1.1 – Combinatorial encoding**) [35,37], which is known to play a role in the activation of many T cell response genes [55,56]. A prototypic example of AND logic in the control of gene expression occurs at the *Il2* promoter. Binding sites for the NFAT and AP-1 TFs require combined signaling inputs from both components to drive expression [57]. As Il-2 plays a fundamental role in T cell responses, the signaling inputs required to induce Il-2 expression have been manipulated in engineered T cells to improve tumor clearance in mouse models [58], and indicates that engineering the signaling decoding mechanisms of functionally relevant genes is a viable strategy for developing cell-based therapeutics.

1.3 Antigen Sensing in T Lymphocytes

The immune system can mount tailored responses to different pathogenic threats while sparing healthy cells and tissues in the body. This remarkable selectivity stems from T cells' ability to obtain information about the challenge from peptide antigens presented on major histocompatibility complex ligands (pMHCs) [59–61]. pMHCs that bind the T cell receptor (TCR) with high affinity derive exclusively from foreign sources, due to the sharp affinity threshold for negative selection in the thymus [62,63]. On the other hand, pMHCs with lower TCR binding affinity can derive either from foreign sources or self. The dose of pMHCs presented to the T cell yields complementary information about the perceived threat: high doses of pMHCs can convey pathogen virulence or infection severity, or simply reflect high abundance of self-antigen.

Despite the importance of antigen sensing in immunity, how T cells perceive and integrate information about pMHC affinity and dose to generate tailored functional responses remains incompletely understood. Early studies suggested that T cells respond to high affinity pMHCs while ignoring high doses of low affinity pMHCs [64–70]. This selectivity was proposed to result from kinetic proofreading in the TCR signaling pathway [66,71–79], which enables selective responses to pMHCs with long binding lifetimes. However, while there is compelling evidence for kinetic proofreading [80,81], T cells do not ignore low-affinity pMHC ligands [82–84]. More recent studies indicate that T cells enact a common gene activation program amid different pMHC affinities, albeit with varying kinetics [85,86]. pMHC differences can tune these gene programs [85], thereby modulating downstream differentiation outcomes [87–90]. with their dose and affinity exerting distinct regulatory effects [91–93]. These findings suggest that the TCR signaling network can sense pMHC affinity and dose to translate this information into distinct functional outcomes.

As the Erk and NFAT signaling pathways are primary links between TCR engagement and the regulation of gene transcription (**Fig. 1.2**) [31], they are well-positioned to convey pMHC information in the cell. Upon pMHC engagement, the TCR activates a series of intracellular signaling molecules, culminating in the activation of both the Erk and NFAT pathways. Both signaling pathways activate within minutes upon antigen encounter, and over these short timescales, they appear to do so in an all-or-one, "digital" manner, with activated cells showing similar signaling levels regardless of pMHC affinity or dose [66,94–98]. However, T cells can be exposed to pMHCs for up to 24 hrs after initial encounter *in vivo* [99,100] through stable contacts with dendritic cells in lymph nodes. Over these longer timescales, it is unclear whether NFAT and Erk signaling remains uniform to varying pMHC inputs, or whether they may show variable responses to different pMHC inputs only upon prolonged exposure. Indeed, longer timescale dynamics of

signaling pathways (~hrs) is important for input encoding in other systems [8,16,21,28]. However, their roles in T cell antigen perception remain unclear, as all measurements of TCR signaling in T cells, to our knowledge, have been performed over short timescales (<3 hrs).

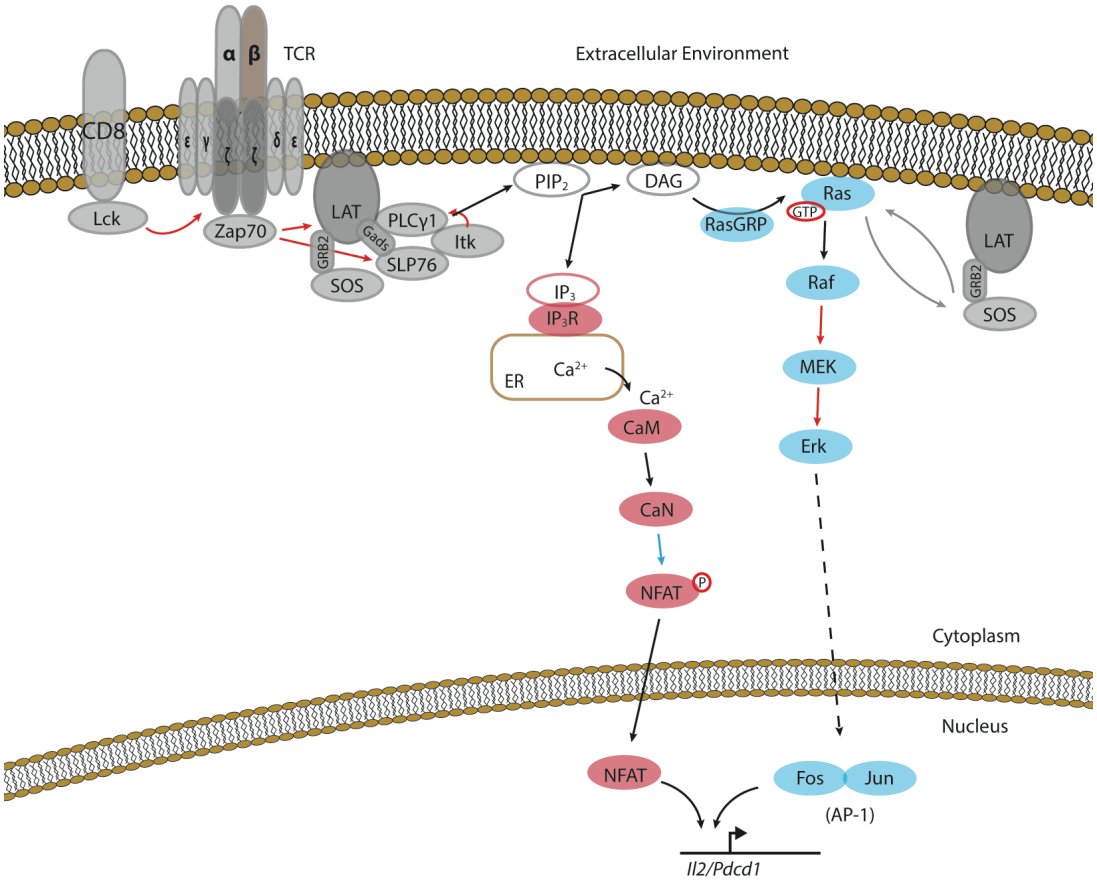

Figure 1.2 T Cell Receptor Signaling Network.

Ligation of a pMHC antigen with the alpha and beta chains of the T-cell receptor (TCR) and the CD8 co-receptor triggers a series of proximal signaling events localized at the plasma membrane. Lck phosphorylates the immunoreceptor tyrosine-based activation motifs (ITAMs) of the CD3 zeta chains, which is then able to recruit ZAP-70. ZAP-70 activates the adaptor proteins LAT and SLP76, which recruit Itk, PLCγ1, Gads, GRB2, and SOS. Itk activates PLCγ1, which generates the 2nd messengers DAG and IP_3 from PIP_2 [31,101]. IP_3 binds its receptor on the ER (IP_3R) to release intracellular Ca^{2+} stores. Increased cytosolic Ca^{2+} activates calmodulin (CaM), which activates calcineurin (CaN), which de-phosphorylates NFAT and enables its translocation into the nucleus. DAG recruits RasGRP to the membrane, which activates Ras through the exchange of GDP for GTP. Active RasGTP allosterically enhances SOS activity, which further activates Ras [102]. Ras activates Raf (MAPKKK), which activates MEK (MAPKK), which activates Erk (MAPK). Activated Erk phosphorylates numerous targets, including Fos. In the nucleus, Fos dimerizes with Jun to form the Activator protein 1 (AP-1) transcription factor. NFAT and AP-1 regulate transcription of numerous T cell activation genes, prominently though cooperative binding at regulatory elements of many gene loci (i.e. *Il2, Pdcd1*). Red lines indicate phosphorylation, blue lines represent de-phosphorylation.

Signaling through the NFAT and Erk pathways leads to nuclear accumulation and activation of the NFAT transcription factor (TF) and AP-1 family transcription factors (TFs) respectively [31,34,101]. As these TFs can show different modes of cooperation by which they regulate their target genes, they could enable cells to translate pMHC-specific Erk and NFAT signaling activities to distinct transcriptional responses. NFAT and AP-1 can bind to composite DNA binding sites for both TFs in a cooperative manner [37,103], a mode of action that underlies regulation of many T cell activation and effector genes (*Irf4, Il2ra* [104]). Disruption of NFAT:AP-1 impairs T cell effector responses and results in an inability to clear chronic infections and tumors [55,105]. At the same time, NFAT can work independently from AP-1, a mode of regulation associated with exhaustion- or anergy- associated genes (e.g. *Pdcd1*) [37,55,56,106–108]. These different *cis*-regulatory mechanisms may allow T cells to generate distinct genomic programs to different pMHC inputs.

1.4 Dissertation Specific Aims

The goal of my research presented here was to identify a mechanism by which T cells perceive differences in pMHC affinity and dose in order to generate pMHC-specific responses. This long-standing question has remained poorly understood despite decades of investigation into T cell receptor signaling and gene regulation in T cells. We used an approach that leveraged modern sequencing technologies, along with our own newly developed live-imaging assay to investigate antigen (pMHC) perception in T cells via the TCR signaling network, specifically Erk and NFAT, based on principles of combinatorial and dynamic encoding. Our approach consisted of the following aims:

Aim 1: Quantify Erk and NFAT signaling dynamics in live T cells responding to variable pMHC inputs.

To investigate the role for Erk and NFAT signaling dynamics in translating information about pMHC input affinity and dose into distinct downstream gene regulatory responses, we sought to measure their dynamics in living T cells over daylong timescales, over which T cells contact antigen-presenting cells, and over which the gene regulatory responses unfold [99]. To do so, we first developed a dual-pathway fluorescent reporter mouse strain that concurrently monitors Erk and NFAT signaling activity in the same cell. We then utilized an *in vitro* imaging assay to quantify the first 30 hrs of Erk and NFAT signaling dynamics in $CD8^+$ T cells responding to precise alterations in pMHC affinity and dose. Our results reveal, for the first time, pMHC-dependent long-term Erk and NFAT response dynamics in single $CD8^+$ T cells.

Aim 2: Identify gene regulatory mechanisms that decode Erk and NFAT signaling activity.

We hypothesized that differential Erk and NFAT signaling dynamics could be decoded by gene regulatory mechanisms to produce distinct transcriptional responses. We therefore used RNA sequencing to correlate specific affinity- and dose-dependent gene programs with pMHC-specific long-term Erk and NFAT signaling dynamics. Through clustering and regression analyses and mathematical modeling, we proposed a model whereby diverse pMHC-dependent gene expression and functional programs are enabled, in part, by the dynamic regulation of Erk and NFAT signaling.

1.5 REFERENCES

1. Behar, M. & Hoffmann, A. Understanding the temporal codes of intra-cellular signals. *Curr. Opin. Genet. Dev.* **20**, 684–693 (2010).
2. Li, P. & Elowitz, M. B. Communication codes in developmental signaling pathways. *Development* **146**, dev170977 (2019).
3. Makadia, H. K., Schwaber, J. S. & Vadigepalli, R. Intracellular Information Processing through Encoding and Decoding of Dynamic Signaling Features. *PLOS Comput. Biol.* **11**, e1004563 (2015).
4. Purvis, J. E. & Lahav, G. Encoding and Decoding Cellular Information through Signaling Dynamics. *Cell* **152**, 945–956 (2013).
5. Selimkhanov, J. *et al.* Accurate information transmission through dynamic biochemical signaling networks. *Science* **346**, 1370–1373 (2014).
6. Marshall, C. J. Signaling: Transient versus Sustained Extracellular Signal-Regulated Kinase Activation. 7 (1995).
7. Traverse, S., Gomez, N., Paterson, H., Marshall, C. & Cohen, P. Sustained activation of the mitogen-activated protein (MAP) kinase cascade may be required for differentiation of PC12 cells. Comparison of the effects of nerve growth factor and epidermal growth factor. *Biochem. J.* **288**, 351–355 (1992).
8. Albeck, J. G., Mills, G. B. & Brugge, J. S. Frequency-Modulated Pulses of ERK Activity Transmit Quantitative Proliferation Signals. *Mol. Cell* **49**, 249–261 (2013).
9. Johnson, H. E. & Toettcher, J. E. Signaling Dynamics Control Cell Fate in the Early Drosophila Embryo. *Dev. Cell* **48**, 361-370.e3 (2019).

10. Murphy, L. O., Smith, S., Chen, R.-H., Fingar, D. C. & Blenis, J. Molecular interpretation of ERK signal duration by immediate early gene products. *Nat. Cell Biol.* **4**, 556–564 (2002).
11. Regot, S., Hughey, J. J., Bajar, B. T., Carrasco, S. & Covert, M. W. High-sensitivity measurements of multiple kinase activities in live single cells. *Cell* **157**, 1724–1734 (2014).
12. Wilson, M. Z., Ravindran, P. T., Lim, W. A. & Toettcher, J. E. Tracing Information Flow from Erk to Target Gene Induction Reveals Mechanisms of Dynamic and Combinatorial Control. *Mol. Cell* **67**, 757-769.e5 (2017).
13. Aoki, K. *et al.* Stochastic ERK Activation Induced by Noise and Cell-to-Cell Propagation Regulates Cell Density-Dependent Proliferation. *Mol. Cell* **52**, 529–540 (2013).
14. Antebi, Y. E. *et al.* Combinatorial Signal Perception in the BMP Pathway. *Cell* **170**, 1184-1196.e24 (2017).
15. Nandagopal, N. *et al.* Dynamic Ligand Discrimination in the Notch Signaling Pathway. *Cell* **172**, 869-880.e19 (2018).
16. Lane, K. *et al.* Measuring Signaling and RNA-Seq in the Same Cell Links Gene Expression to Dynamic Patterns of NF-κB Activation. *Cell Syst.* **4**, 458-469.e5 (2017).
17. Nelson, D. E. *et al.* Oscillations in NF- B Signaling Control the Dynamics of Gene Expression. *Science* **306**, 704–708 (2004).
18. Sen, S., Cheng, Z., Sheu, K. M., Chen, Y. H. & Hoffmann, A. Gene Regulatory Strategies that Decode the Duration of NFκB Dynamics Contribute to LPS- versus TNF-Specific Gene Expression. *Cell Syst.* S240547121930465X (2020) doi:10.1016/j.cels.2019.12.004.
19. Tay, S. *et al.* Single-cell NF-B dynamics reveal digital activation and analogue information processing. *Nature* **466**, 267–271 (2010).

20. Werner, S. L., Barken, D. & Hoffmann, A. Stimulus Specificity of Gene Expression Programs Determined by Temporal Control of IKK Activity. *Science* **309**, 1857–1861 (2005).
21. Adelaja, A. *et al.* Six distinct NFκB signaling codons convey discrete information to distinguish stimuli and enable appropriate macrophage responses. *Immunity* **54**, 916-930.e7 (2021).
22. Cheng, Q. J. *et al.* NF-κB dynamics determine the stimulus specificity of epigenomic reprogramming in macrophages. *Science* **372**, 1349–1353 (2021).
23. Jetka, T., Nienałtowski, K., Filippi, S., Stumpf, M. P. H. & Komorowski, M. An information-theoretic framework for deciphering pleiotropic and noisy biochemical signaling. *Nat. Commun.* **9**, 4591 (2018).
24. Olagnier, D. & Hiscott, J. Type I and type III interferon-induced immune response: It's a matter of kinetics and magnitude. *Hepatology* **59**, 1225–1228 (2014).
25. Yissachar, N. *et al.* Dynamic Response Diversity of NFAT Isoforms in Individual Living Cells. *Mol. Cell* **49**, 322–330 (2013).
26. Batchelor, E., Loewer, A., Mock, C. & Lahav, G. Stimulus-dependent dynamics of p53 in single cells. *Mol. Syst. Biol.* **7**, 488 (2011).
27. Lahav, G. *et al.* Dynamics of the p53-Mdm2 feedback loop in individual cells. *Nat. Genet.* **36**, 147–150 (2004).
28. Purvis, J. E. *et al.* p53 Dynamics Control Cell Fate. *Science* **336**, 1440–1444 (2012).
29. Cai, L., Dalal, C. K. & Elowitz, M. B. Frequency-modulated nuclear localization bursts coordinate gene regulation. *Nature* **455**, 485–490 (2008).

30. Hao, N. & O'Shea, E. K. Signal-dependent dynamics of transcription factor translocation controls gene expression. *Nat. Struct. Mol. Biol.* **19**, 31–39 (2012).
31. Brownlie, R. J. & Zamoyska, R. T cell receptor signalling networks: branched, diversified and bounded. *Nat. Rev. Immunol.* **13**, 257–269 (2013).
32. D'Arcangelo, G. & Halegoua, S. A branched signaling pathway for nerve growth factor is revealed by Src-, Ras-, and Raf-mediated gene inductions. *Mol. Cell. Biol.* **13**, 3146–3155 (1993).
33. Jo, E.-K., Yang, C.-S., Choi, C. H. & Harding, C. V. Intracellular signalling cascades regulating innate immune responses to Mycobacteria: branching out from Toll-like receptors. *Cell. Microbiol.* **9**, 1087–1098 (2007).
34. Brignall, R. *et al.* Integration of Kinase and Calcium Signaling at the Level of Chromatin Underlies Inducible Gene Activation in T Cells. *J. Immunol.* ji1602033 (2017) doi:10.4049/jimmunol.1602033.
35. Cheng, C. S. *et al.* Iterative Modeling Reveals Evidence of Sequential Transcriptional Control Mechanisms. *Cell Syst.* **4**, 330-343.e5 (2017).
36. Lin, Y., Sohn, C. H., Dalal, C. K., Cai, L. & Elowitz, M. B. Combinatorial gene regulation by modulation of relative pulse timing. *Nature* **527**, 54–58 (2015).
37. Macián, F., López-Rodríguez, C. & Rao, A. Partners in transcription: NFAT and AP-1. *Oncogene* **20**, 2476–2489 (2001).
38. Luecke, S., Sheu, K. M. & Hoffmann, A. Stimulus-specific responses in innate immunity: Multilayered regulatory circuits. *Immunity* **54**, 1915–1932 (2021).
39. Hoffmann, A. Immune Response Signaling: Combinatorial and Dynamic Control. *Trends Immunol.* **37**, 570–572 (2016).

40. Gottschalk, R. A. *et al.* Distinct NF-κB and MAPK Activation Thresholds Uncouple Steady-State Microbe Sensing from Anti-pathogen Inflammatory Responses. *Cell Syst.* **2**, 378–390 (2016).
41. Lane, K., Andres-Terre, M., Kudo, T., Monack, D. M. & Covert, M. W. Escalating Threat Levels of Bacterial Infection Can Be Discriminated by Distinct MAPK and NF-κB Signaling Dynamics in Single Host Cells. *Cell Syst.* **8**, 183-196.e4 (2019).
42. Sampattavanich, S. *et al.* Encoding Growth Factor Identity in the Temporal Dynamics of FOXO3 under the Combinatorial Control of ERK and AKT Kinases. *Cell Syst.* **6**, 664-678.e9 (2018).
43. Jeknić, S., Kudo, T. & Covert, M. W. Techniques for Studying Decoding of Single Cell Dynamics. *Front. Immunol.* **10**, 755 (2019).
44. Monje, P., Hernández-Losa, J., Lyons, R. J., Castellone, M. D. & Gutkind, J. S. Regulation of the Transcriptional Activity of c-Fos by ERK: A NOVEL ROLE FOR THE PROLYL ISOMERASE PIN1*. *J. Biol. Chem.* **280**, 35081–35084 (2005).
45. Gerardin, J., Reddy, N. R. & Lim, W. A. The Design Principles of Biochemical Timers: Circuits that Discriminate between Transient and Sustained Stimulation. *Cell Syst.* **9**, 297-308.e2 (2019).
46. Uhlitz, F. *et al.* An immediate–late gene expression module decodes ERK signal duration. *Mol. Syst. Biol.* **13**, 928 (2017).
47. Hafner, A. *et al.* p53 pulses lead to distinct patterns of gene expression albeit similar DNA-binding dynamics. *Nat. Struct. Mol. Biol.* **24**, 840–847 (2017).
48. Ng, K. K. *et al.* A stochastic epigenetic switch controls the dynamics of T-cell lineage commitment. *eLife* **7**, e37851 (2018).

49. Pease, N. A. *et al.* Tunable, division-independent control of gene activation timing by a polycomb switch. *Cell Rep.* **34**, 108888 (2021).
50. Abadie, K., Pease, N. A., Wither, M. J. & Kueh, H. Y. Order by chance: origins and benefits of stochasticity in immune cell fate control. *Curr. Opin. Syst. Biol.* **18**, 95–103 (2019).
51. Li, P. & Leonard, W. J. Chromatin Accessibility and Interactions in the Transcriptional Regulation of T Cells. *Front. Immunol.* **9**, (2018).
52. Berry, S., Dean, C. & Howard, M. Slow Chromatin Dynamics Allow Polycomb Target Genes to Filter Fluctuations in Transcription Factor Activity. *Cell Syst.* **4**, 445-457.e8 (2017).
53. Kel, O. V., Romaschenko, A. G., Kel, A. E., Wingender, E. & Kolchanov, N. A. A compilation of composite regulatory elements affecting gene transcription in vertebrates. *Nucleic Acids Res.* **23**, 4097–4103 (1995).
54. Kel, A. *et al.* Composite Module Analyst: a fitness-based tool for identification of transcription factor binding site combinations. *Bioinformatics* **22**, 1190–1197 (2006).
55. Martinez, G. J. *et al.* The Transcription Factor NFAT Promotes Exhaustion of Activated CD8 + T Cells. *Immunity* **42**, 265–278 (2015).
56. Macián, F., García-Rodríguez, C. & Rao, A. Gene expression elicited by NFAT in the presence or absence of cooperative recruitment of Fos and Jun. *EMBO J.* **19**, 4783–4795 (2000).
57. Jain, J. *et al.* The T-cell transcription factor NFATp is a substrate for calcineurin and interacts with Fos and Jun. *Nature* **365**, 352–355 (1993).
58. Allen, G. M. *et al.* Synthetic cytokine circuits that drive T cells into immune-excluded tumors. *Science* **378**, eaba1624 (2022).

59. Corse, E., Gottschalk, R. A. & Allison, J. P. Strength of TCR-Peptide/MHC Interactions and In Vivo T Cell Responses. *J. Immunol.* **186**, 5039–5045 (2011).

60. Zikherman, J. & Au-Yeung, B. The role of T cell receptor signaling thresholds in guiding T cell fate decisions. *Curr. Opin. Immunol.* **33**, 43–48 (2015).

61. Richard, A. C., Frazer, G. L., Ma, C. Y. & Griffiths, G. M. Staggered starts in the race to T cell activation. *Trends Immunol.* **42**, 994–1008 (2021).

62. Daniels, M. A. *et al.* Thymic selection threshold defined by compartmentalization of Ras/MAPK signalling. *Nature* **444**, 724–729 (2006).

63. Gascoigne, N. R. J., Zal, T. & Alam, S. M. T-cell receptor binding kinetics in T-cell development and activation. *Expert Rev. Mol. Med.* **3**, 1–17 (2001).

64. Alam, S. M. *et al. T-cell-receptor affinity and thymocyte positive selection*. vol. 381 (1996).

65. Alam, S. M. *et al.* Qualitative and Quantitative Differences in T Cell Receptor Binding of Agonist and Antagonist Ligands. *Immunity* **10**, 227–237 (1999).

66. Altan-Bonnet, G. & Germain, R. N. Modeling T Cell Antigen Discrimination Based on Feedback Control of Digital ERK Responses. *PLoS Biol.* **3**, e356 (2005).

67. Hogquist, K. A., Jameson, S. C. & Bevan, M. J. Strong agonist ligands for the T cell receptor do not mediate positive selection of functional CD8+ T cells. *Immunity* **3**, 79–86 (1995).

68. Kersh, G. J. & Allen, P. M. Structural basis for T cell recognition of altered peptide ligands: a single T cell receptor can productively recognize a large continuum of related ligands. *J. Exp. Med.* **184**, 1259–1268 (1996).

69. Kersh, G. J., Kersh, E. N., Fremont, D. H. & Allen, P. M. High- and Low-Potency Ligands with Similar Affinities for the TCR: The Importance of Kinetics in TCR Signaling. *Immunity* **9**, 817–826 (1998).

70. Lyons, D. S. *et al.* A TCR Binds to Antagonist Ligands with Lower Affinities and Faster Dissociation Rates Than to Agonists. *Immunity* **5**, 53–61 (1996).

71. McKeithan, T. W. Kinetic proofreading in T-cell receptor signal transduction. *Proc. Natl. Acad. Sci.* **92**, 5042–5046 (1995).

72. Ganti, R. S. *et al.* How the T cell signaling network processes information to discriminate between self and agonist ligands. *Proc. Natl. Acad. Sci.* **117**, 26020–26030 (2020).

73. Wu, P. *et al.* Mechano-regulation of Peptide-MHC Class I Conformations Determines TCR Antigen Recognition. *Mol. Cell* **73**, 1015-1027.e7 (2019).

74. Dushek, O. & van der Merwe, P. A. An induced rebinding model of antigen discrimination. *Trends Immunol.* **35**, 153–8 (2014).

75. Chakraborty, A. K. & Weiss, A. Insights into the initiation of TCR signaling. *Nat. Immunol.* **15**, 798–807 (2014).

76. François, P., Voisinne, G., Siggia, E. D., Altan-Bonnet, G. & Vergassola, M. Phenotypic model for early T-cell activation displaying sensitivity, specificity, and antagonism. *Proc. Natl. Acad. Sci. U. S. A.* **110**, E888-97 (2013).

77. Liu, B., Chen, W., Evavold, B. D. & Zhu, C. Accumulation of Dynamic Catch Bonds between TCR and Agonist Peptide-MHC Triggers T Cell Signaling. *Cell* **157**, 357–368 (2014).

78. Fernandes, R. A. *et al.* A cell topography-based mechanism for ligand discrimination by the T cell receptor. *Proc. Natl. Acad. Sci.* **116**, 14002–14010 (2019).

79. Hong, J. *et al.* A TCR mechanotransduction signaling loop induces negative selection in the thymus. *Nat. Immunol.* **19**, 1379–1390 (2018).

80. Tischer, D. K. & Weiner, O. D. Light-based tuning of ligand half-life supports kinetic proofreading model of T cell signaling. *eLife* **8**, e42498.

81. Yousefi, O. S. *et al.* Optogenetic control shows that kinetic proofreading regulates the activity of the T cell receptor. *eLife* **8**, e42475 (2019).

82. Achar, S. R. *et al.* Universal antigen encoding of T cell activation from high-dimensional cytokine dynamics. *Science* **376**, 880–884 (2022).

83. Yin, Y., Li, Y. & Mariuzza, R. A. Structural basis for self-recognition by autoimmune T-cell receptors. *Immunol. Rev.* **250**, 32–48 (2012).

84. Bridgeman, J. S., Sewell, A. K., Miles, J. J., Price, D. A. & Cole, D. K. Structural and biophysical determinants of αβ T-cell antigen recognition. *Immunology* **135**, 9–18 (2012).

85. Richard, A. C. *et al.* T cell cytolytic capacity is independent of initial stimulation strength. *Nat. Immunol.* **19**, 849–858 (2018).

86. Ma, C. Y., Marioni, J. C., Griffiths, G. M. & Richard, A. C. Stimulation strength controls the rate of initiation but not the molecular organisation of TCR-induced signalling. *eLife* **9**, e53948 (2020).

87. Conley, J. M., Gallagher, M. P., Rao, A. & Berg, L. J. Activation of the Tec Kinase ITK Controls Graded IRF4 Expression in Response to Variations in TCR Signal Strength. *J. Immunol.* **205**, 335–345 (2020).

88. Allison, K. A. *et al.* Affinity and dose of TCR engagement yield proportional enhancer and gene activity in CD4+ T cells. *eLife* **5**, e10134 (2016).

89. Fiege, J. K. *et al.* The Impact of TCR Signal Strength on Resident Memory T Cell Formation during Influenza Virus Infection. *J. Immunol.* **203**, 936–945 (2019).

90. Solouki, S. *et al.* TCR Signal Strength and Antigen Affinity Regulate CD8 $^{+}$ Memory T Cells. *J. Immunol.* **205**, 1217–1227 (2020).

91. Keck, S. *et al.* Antigen affinity and antigen dose exert distinct influences on CD4 T-cell differentiation. *Proc. Natl. Acad. Sci.* **111**, 14852–14857 (2014).

92. Gottschalk, R. A. *et al.* Distinct influences of peptide-MHC quality and quantity on in vivo T-cell responses. *Proc. Natl. Acad. Sci.* **109**, 881–886 (2012).

93. Gottschalk, R. A., Corse, E. & Allison, J. P. TCR ligand density and affinity determine peripheral induction of Foxp3 in vivo. *J. Exp. Med.* **207**, 1701–1711 (2010).

94. Gallagher, M. P., Conley, J. M. & Berg, L. J. Peptide Antigen Concentration Modulates Digital NFAT1 Activation in Primary Mouse Naive CD8+ T Cells as Measured by Flow Cytometry of Isolated Cell Nuclei. *ImmunoHorizons* **2**, 208–215 (2018).

95. Das, J. *et al.* Digital Signaling and Hysteresis Characterize Ras Activation in Lymphoid Cells. *Cell* **136**, 337–351 (2009).

96. Gallagher, M. P. *et al.* Hierarchy of signaling thresholds downstream of the T cell receptor and the Tec kinase ITK. *Proc. Natl. Acad. Sci.* **118**, e2025825118 (2021).

97. Lin, J. J. Y. *et al.* Mapping the stochastic sequence of individual ligand-receptor binding events to cellular activation: T cells act on the rare events. *Sci. Signal.* **12**, eaat8715 (2019).

98. Podtschaske, M. *et al.* Digital NFATc2 Activation per Cell Transforms Graded T Cell Receptor Activation into an All-or-None IL-2 Expression. *PLOS ONE* **2**, e935 (2007).

99. Beuneu, H. *et al.* Visualizing the Functional Diversification of CD8+ T Cell Responses in Lymph Nodes. *Immunity* **33**, 412–423 (2010).

100. Celli, S., Garcia, Z. & Bousso, P. CD4 T cells integrate signals delivered during successive DC encounters in vivo. *J. Exp. Med.* **202**, 1271–1278 (2005).

101. Smith-Garvin, J. E., Koretzky, G. A. & Jordan, M. S. T Cell Activation. *Annu. Rev. Immunol.* **27**, 591–619 (2009).

102. Roose, J. P., Mollenauer, M., Ho, M., Kurosaki, T. & Weiss, A. Unusual Interplay of Two Types of Ras Activators, RasGRP and SOS, Establishes Sensitive and Robust Ras Activation in Lymphocytes. *Mol. Cell. Biol.* **27**, 2732–2745 (2007).

103. Chen, L., Glover, J. N., Hogan, P. G., Rao, A. & Harrison, S. C. Structure of the DNA-binding domains from NFAT, Fos and Jun bound specifically to DNA. *Nature* **392**, 42–48 (1998).

104. Schuh, K. *et al.* The Interleukin 2 Receptor ␣ Chain/CD25 Promoter Is a Target for Nuclear Factor of Activated T Cells. 5.

105. Mognol, G. P. *et al.* Exhaustion-associated regulatory regions in CD8 \textlesssup\textgreater+\textless/sup\textgreater tumor-infiltrating T cells. *Proc. Natl. Acad. Sci.* **114**, E2776–E2785 (2017).

106. Vaeth, M. & Feske, S. NFAT control of immune function: New Frontiers for an Abiding Trooper. Preprint at https://doi.org/10.12688/f1000research.13426.1 (2018).

107. Pereira, R. M., Hogan, P. G., Rao, A. & Martinez, G. J. Transcriptional and epigenetic regulation of T cell hyporesponsiveness. *J. Leukoc. Biol.* **102**, 601–615 (2017).

108. Macián, F. *et al.* Transcriptional Mechanisms Underlying Lymphocyte Tolerance. *Cell* **109**, 719–731 (2002).

Chapter 2. Encoding pMHC Information by Long-term Erk and NFAT Signaling.

2.1 Development of Dual Pathway Reporter Mouse Strain

To address the question of how T cells encode antigen information, we sought to quantify the dynamic responses of the Erk and NFAT signaling pathways downstream of the TCR. To do this, we developed a reporter system to concurrently measure the activities of both pathways in live $CD8^+$ T cells. This system consists of (1) The N-terminal regulatory domain of mouse NFATc2 (residues 1-399) fused to mRuby3 [1,2]; (2) An Erk kinase-translocation reporter (Erk-KTR) [3] fused to BFP; and (3) Histone 2B (H2B) fused to iRFP for nuclear segmentation (**Fig. 2.1A**). We generated a "dual-pathway reporter" (DPR) mouse strain with this reporter cassette inserted into the Rosa26 locus downstream of a loxP-flanked STOP codon (*Rosa26*$^{LSL\text{-}DPR}$). *Rosa26*$^{LSL\text{-}DPR/LSL\text{-}DPR}$ mice were crossed to the P14 transgenic TCR strain to enable stimulation with altered peptide ligands for the cognate $gp_{33\text{-}41}$ peptide from LCMV complexed to H-2Db MHC-1 [4]. DPR^+/P14 mice were then crossed to a Cre-ERT2 strain and treated with tamoxifen for reporter induction (**Fig. 2.1B**).

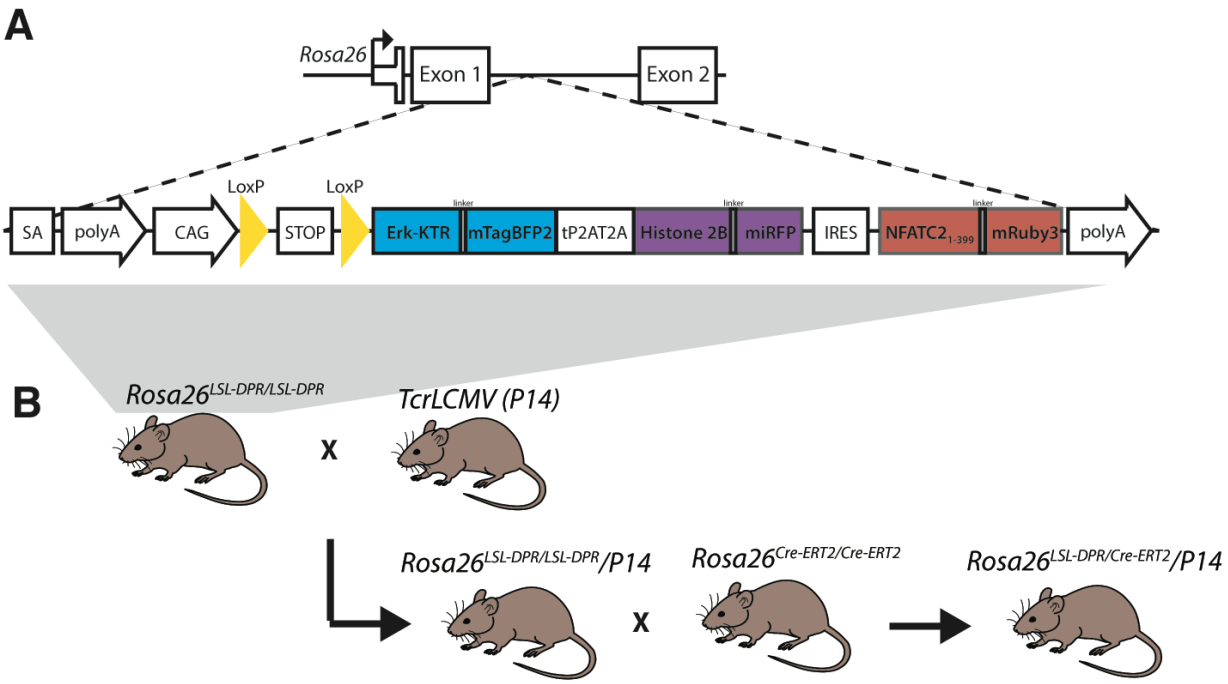

Figure 2.1 Dual-Pathway Reporter Mouse Strain.

(**A**) Schematic of the reporter transgene insertion into the mouse Rosa26 locus. Homologous recombination was done by Biocytogen Corp. using their CRISPR-based EGE^{TM} method.
(**B**) Breeding strategy used to generate all mice for this study.

2.2 Quantification of Erk and NFAT Activity in Stimulated T Cells

To measure Erk and NFAT dynamics in DPR^{+}/P14 (reporter) CD8^{+} T cells responding to pMHCs of different doses and affinities, we developed a quantitative imaging assay where T cells are cultured on purified, surface-immobilized pMHCs [5–7] to ensure they experience uniform, defined inputs and then imaged at regular intervals with time-lapse microscopy (**Fig. 2.2A**). To test whether T cells activate in this reductionist system, we isolated reporter T cells, stimulated them with a high affinity $gp_{33\text{-}41}$ pMHC variant (M9C, K_D = 2.3 μM) [8], and imaged them at four minute intervals for one hour. We then quantified each pathway's activity as the ratio of reporter signal in the active compartment to total signal (**Fig. 2.2B**). Upon cell contact with the M9C pMHC-coated surface both Erk and NFAT reporters activated within minutes (**Fig. 2.2C**), consistent with the rapid activation of these pathways upon TCR engagement [9,10], and remained active for the duration of the observation. Activation was abolished by MEK (Trametinib; MEKi) and Calcineurin (Cyclosporin A; CsA) inhibitor treatment to block activation of Erk and NFAT, respectively (**Fig. 2.2B – "MEKi + CsA"**), providing a baseline for reporter inactivity.

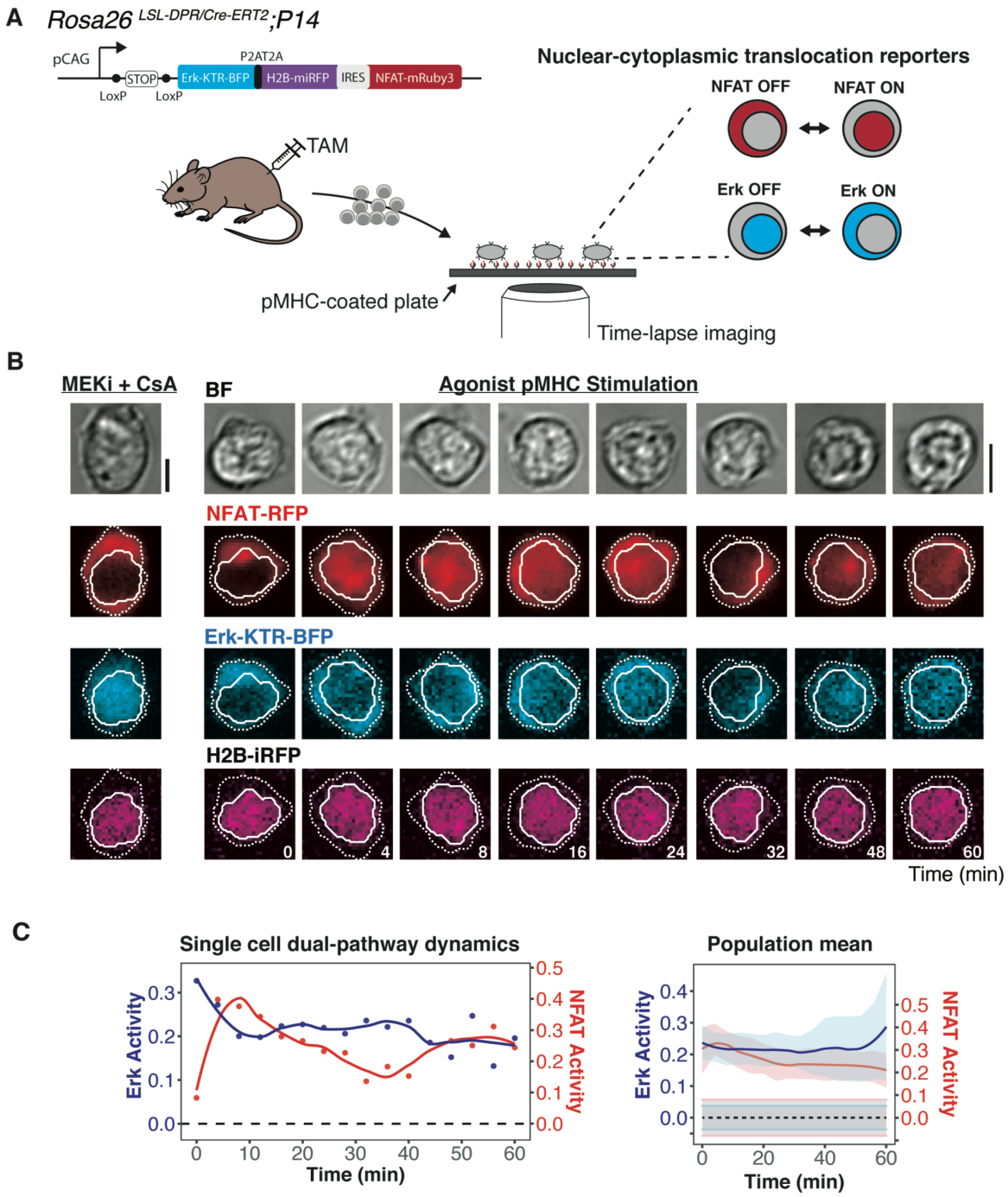

Figure 2.2 Live Imaging Platform to Measure Long-term Erk and NFAT Responses in Live CD8 T cells.

(A) Fluorescent translocation reporters for Erk and NFAT signaling pathways were inserted into the *Rosa26* locus to generate our dual-pathway reporter (DPR) mouse strain. Following

tamoxifen injection into DPR mice bred to Cre-ERT2 and P14 TCR mice, $CD8^+$ T cells are isolated and stimulated with plate-bound pMHC antigens specific for the P14 TCR. Time-lapse imaging followed by automated cell segmentation and tracking enables quantification of Erk and NFAT dynamic responses in live single cells. The NFAT reporter translocates from the cytoplasm to the nucleus when active (mirroring endogenous NFAT1). Erk-KTR translocates from the nucleus to cytoplasm when active [3].
(B) Representative cell images of reporter T cells responding to a saturating dose of agonist pMHC, compared to a negative control cell treated with inhibitors of NFAT (Cyclosporin A, CsA) and Erk (Trametinib, MEKi). An H2B-iRFP fusion protein is co-expressed with the translocation reporters to enable nuclear segmentation and tracking. Nuclear and cytoplasmic segmentation masks are shown in solid and dashed lines, respectively. Scale bars = 5 um.
(C) Quantification of Erk and NFAT activity for the cell shown in (B). Population mean +/- SD from 107 stimulated cells is shown on the right. Pathway activities are baseline subtracted using the mean pathway activities from negative control cells and shown as dashed lines with SD in gray shading.

2.3 pMHC-Dependent Erk and NFAT Signaling Dynamics

Both Erk and NFAT pathways activate in a digital, all-or-none manner within the first hour of exposure to varying pMHC inputs [9,11–13]. However, T cells can form stable contacts with dendritic cells for up to 24 hrs after initial contact [14,15], and may respond divergently to differing pMHC affinity and dose only over these longer timescales. To test this hypothesis, we utilized our dual reporter system to continuously monitor Erk and NFAT signaling activity in T cells over 30 hrs of stimulation with five pMHC conditions that vary in affinity or dose (**Fig. 2.3A**). We selected pMHC conditions based on a titration of the high affinity pMHC agonist, gp33-M9C, and the lower affinity partial agonist, gp33-L6F (K_D = 19 uM) [8] and the resulting expression of the T cell activation marker CD69 [16] (**Fig. 2.3B and Fig. 2.5B-C**). To assess T cells' ability to sense pMHC affinity, we chose saturating doses of each pMHC (2 and 20 pmol M9C vs. 20 and 80 pmol L6F), which yield equivalent CD69 activation potencies [16]. To assess T cells' ability to sense pMHC dose, we chose a dose of M9C (0.2 pmol) just below that needed for half-maximal CD69 activation. We then isolated reporter $CD8^+$ T cells, stimulated them with each of these five pMHC conditions, and acquired images at 1 hr. intervals for 30 hours (**Appendix A**). We quantified the average Erk and NFAT activities in single cells from time lapse movies (**Fig. 2.3C**) and extracted Erk and NFAT activity traces for ~1,500 cells over the first 15 hrs (**Fig. 2.3D**).

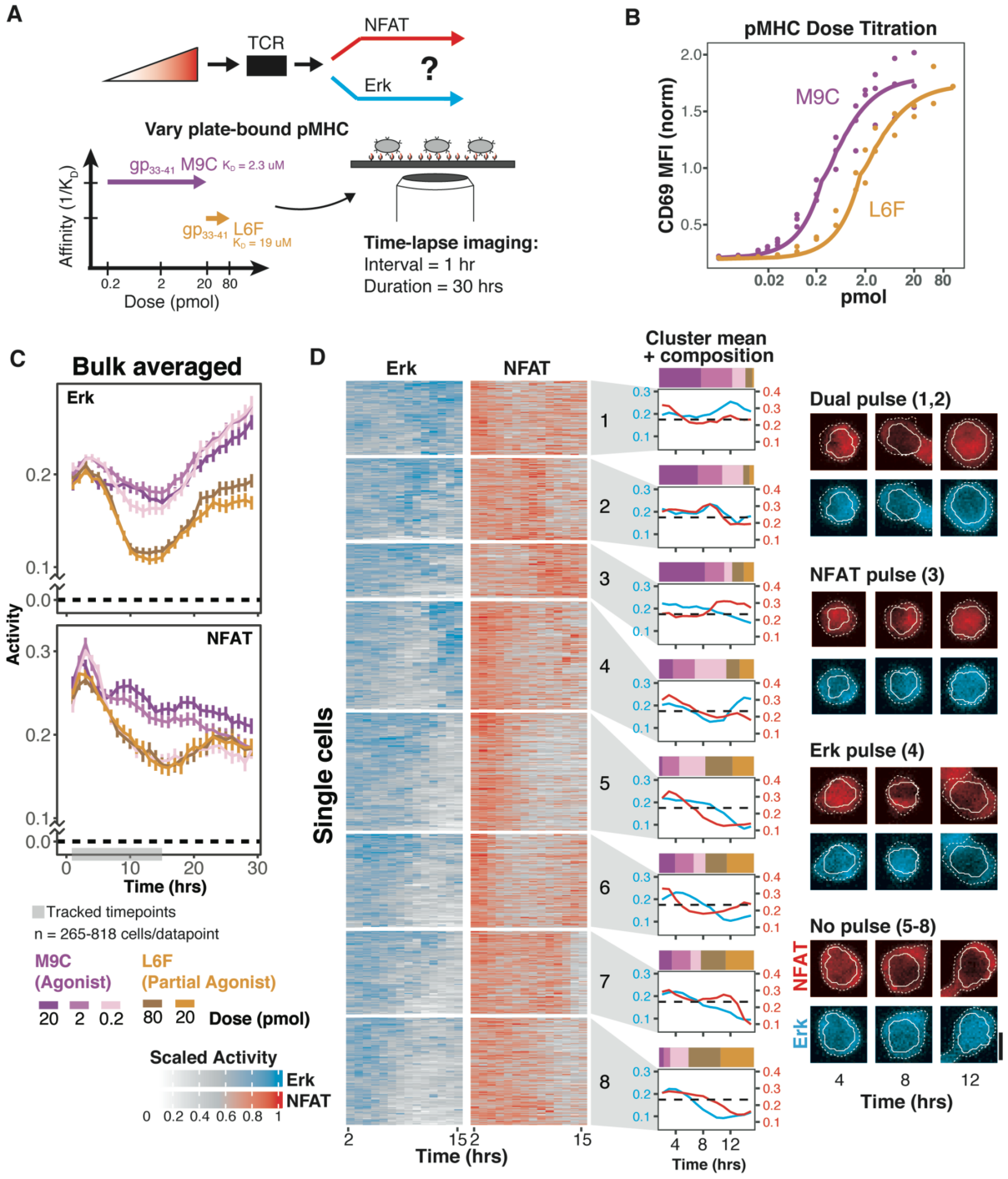
A
TCR
NFAT
Erk
?
Vary plate-bound pMHC
gp33-41 M9C KD = 2.3 uM
gp33-41 L6F KD = 19 uM
Affinity (1/KD)
0.2 2 20 80
Dose (pmol)
Time-lapse imaging:
Interval = 1 hr
Duration = 30 hrs
B
pMHC Dose Titration
CD69 MFI (norm)
M9C
L6F
0.02 0.2 2.0 20 80
pmol
C
Bulk averaged
Erk
NFAT
Activity
Time (hrs)
Tracked timepoints
n = 265-818 cells/datapoint
M9C (Agonist)
L6F (Partial Agonist)
20 2 0.2 80 20 Dose (pmol)
Scaled Activity
Erk
NFAT
0 0.2 0.4 0.6 0.8 1
D
Erk
NFAT
Cluster mean + composition
Single cells
Time (hrs)
Dual pulse (1,2)
NFAT pulse (3)
Erk pulse (4)
No pulse (5-8)
NFAT
Erk
4 8 12
Time (hrs)

Figure 2.3 Erk and NFAT Signaling Varies with pMHC Affinity and Dose over Long Timescales.

(A) The T cell receptor can bind many different pMHC ligands with varying affinities and at varying doses. To test if Erk and NFAT signaling depends on pMHC affinity and dose, we stimulated reporter T cells with various doses of two altered peptide ligands (APLs) that bind the P14 TCR with ~8 fold difference in binding affinity and measured Erk and NFAT activities in single cells over 30 hrs of stimulation.
(**B**) P14 Jurkat T cell dose-response curve based on CD69 upregulation 4 hrs after stimulation with each of the two APLs. Y-axis is MFI normalized to the EC_{50} for each peptide.
(C) Mean +/- 99% confidence intervals for Erk and NFAT activity over the first 30 hrs of stimulation with each of the five pMHC conditions from ~180k cell images from two independent replicates with 265-818 cells (~600 on average) per data point.
(D) A balanced distribution of 1,100 single cell activity traces (220 cells per condition) from the data in (C) were clustered on their scaled dual-pathway signaling activities from 2-15 hrs using a global alignment kernel-based time series clustering method [17]. The mean unscaled response, and the proportion of cells from each pMHC condition for each cluster is shown to the right of the heatmap, with dashed lines indicating the mean Erk and NFAT level across all cells in the analysis. On the far right are representative cell images for four broad types of combinatorial Erk and NFAT responses classified from the eight clusters indicated in parentheses. Nuclear and cytoplasmic segmentations are shown in solid and dashed lines, respectively. Scale bar = 5 um.

Upon stimulation by different pMHC inputs, both pathways activated, as expected, and reached similar maximal levels of activity within the first hour after pMHC encounter (**Fig. 2.3C and Fig. 2.4A**). Notably, lowering pMHC dose by a hundred-fold did not reduce maximal Erk and NFAT activity levels but reduced the rate of digital NFAT activation (**Fig 2.4B**), consistent with prior studies showing that TCR signal strength modulates the speed at which T cells acquire a common activation program [9,18,19]. However, after several hours of continued stimulation, divergent signaling dynamics emerged in a pMHC-dependent manner (**Fig. 2.3C-D**). Mean Erk activity dropped after 8-20 hrs of stimulation with L6F, but remained high for M9C at both high and low doses. In contrast, mean NFAT activity dropped rapidly for all doses of L6F, as well as for low dose of M9C, but remained persistently higher with higher doses of M9C. These signaling differences were not due to differences in pMHC stability, as both L6F and M9C were found to show negligible reduction in activity over these timescales when plate-immobilized (**Fig. 2.5A**). Furthermore, similar pMHC-dependent differences were also observed in non-reporter T cells immunostained for endogenous ppErk or nuclear-localized NFAT1, indicating that our reporter system faithfully captures pMHC-dependent Erk/NFAT signaling states in T cells (**Fig. 2.5D-E**). Thus, different pMHC inputs elicit distinct long-term Erk and NFAT signaling dynamics following uniform initial activation.

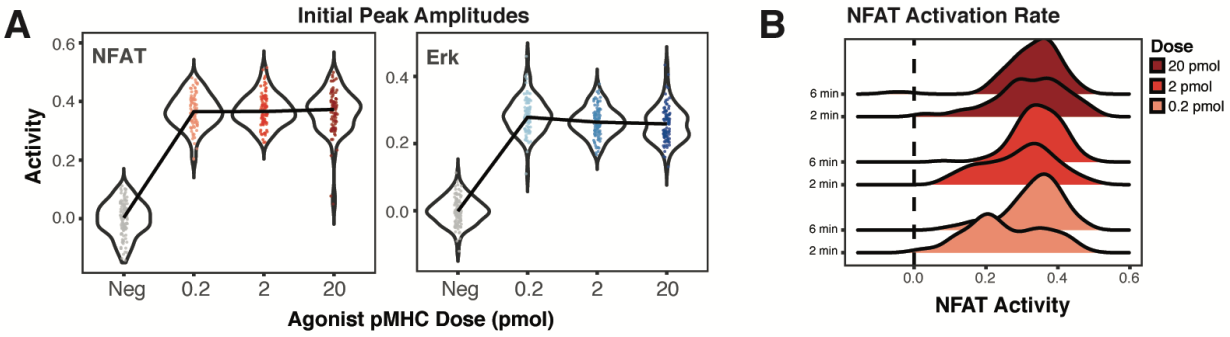

Figure 2.4 Digital Activation of Erk and NFAT in T cells.

(A) Reporter T cells stimulated with a 100-fold dose range of agonist pMHC (M9C) show invariant initial peak amplitudes for both Erk and NFAT signaling responses, as determined by the maximum activity in the first 12 minutes (4 frames) of stimulation.
(B) Distribution of NFAT activities between the first (~2 min) and second (~6 min) frames are shown for the three doses indicated. The fraction of cells that activate NFAT within 2 minutes of TCR stimulation is graded and increases with increased pMHC dose. By 6 minutes, all doses produce similar NFAT activation.

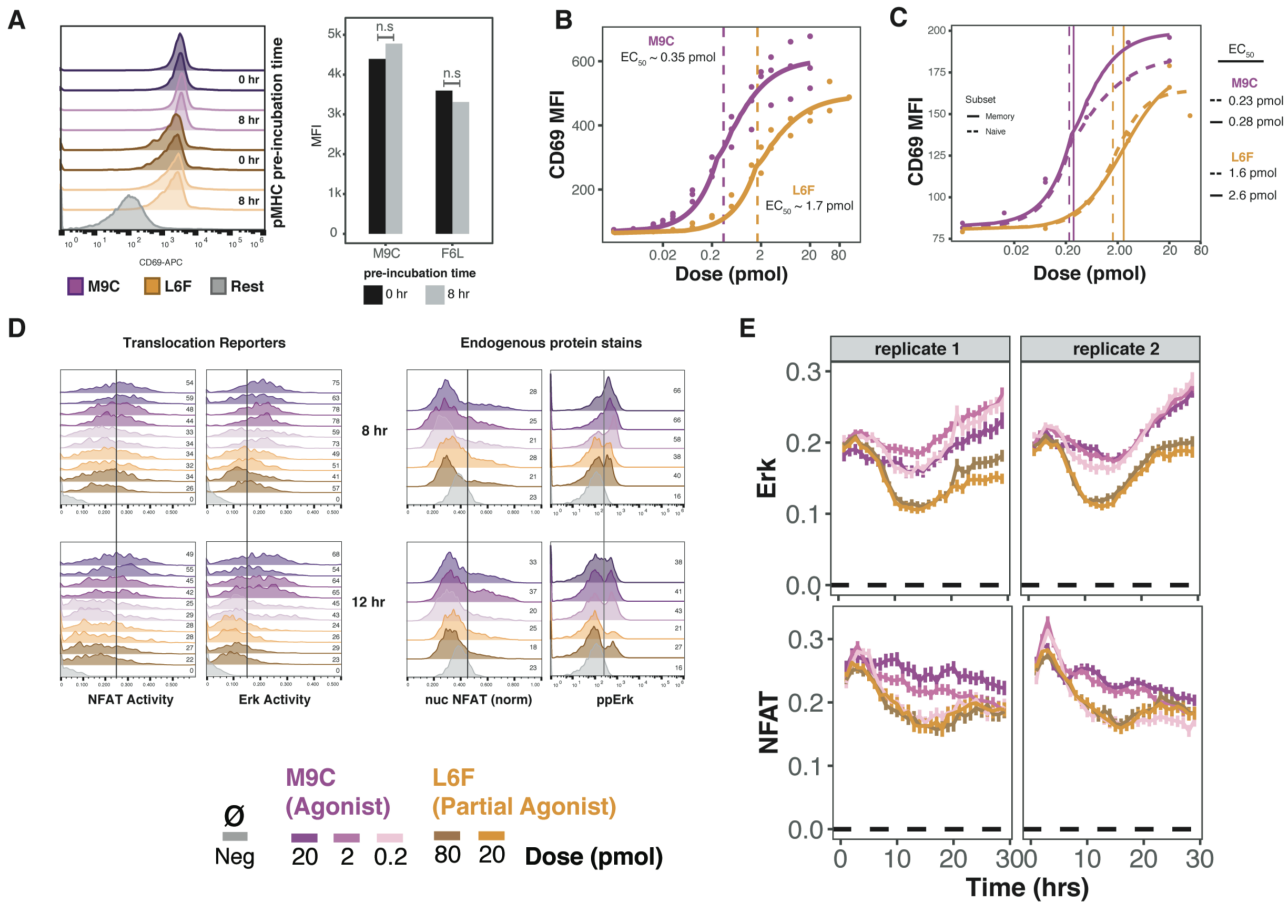

Figure 2.5 Validation of Erk and NFAT Signaling Assay.

(A) Both altered peptide ligands (M9C and F6L) used in this study remain active (i.e properly folded) for at least 8 hrs at 37°C. T cells were assayed for CD69 expression 4 hrs after stimulation on pMHC-coated plates that were pre-incubated with 20 pmol of each APL for 8 hrs at 37°C, or coated immediately prior to cell seeding. No difference in CD69 MFI was observed between pre-incubation times for each APL, as determined by t-test.
(B) Raw CD69 MFI dose-response curves for P14 Jurkat T cells for both pMHC ligands used. EC_{50}s are indicated in dashed lines. Flow analysis is done after 4 hrs of stimulation.
(C) CD69 dose-response curves, as in B, for naive ($CD62L^+/CD44^-$) and memory ($CD62L^+/CD44^+$) murine P14 $CD8^+$ T cells. EC_{50}s are indicated in dashed and solid vertical lines.
(D) Comparison of Erk and NFAT activity measurements between live translocation reporters and endogenous NFAT1 and ppErk staining. For endogenous protein staining, T cells were stimulated identically to cells stimulated for live imaging and fixed, permeabilized, and stained for NFAT1 or ppErk at 8 and 12 hrs post stimulation. Non-stimulated cells were used as a negative control for endogenous protein staining. Nuclear NFAT1 was measured with fluorescent microscopy and normalized to total NFAT1 fluorescence. ppErk intensity was

measured with flow cytometry. Vertical lines are shown for reference, with the fraction of cells to the right of the line indicated.
(E) Our live-cell imaging and automated image analysis pipeline is robust and reproducible based on results from two independent experiments performed several weeks apart with separate litters of mice. Plots show mean +/- 99% CI Erk and NFAT activity over 30 hrs of stimulation from ~90k total cells per experiment stimulated with five different pMHC conditions (same as in Fig 2.3C).

2.4 pMHC Affinity and Dose Encoding

We next determined the dynamic features of Erk and NFAT signaling in single cells that encode information about pMHC affinity and dose. To identify relevant features, we performed hierarchical clustering on the pMHC-dependent signaling responses of 1,100 single cells from the 5 different pMHC conditions. We identified eight cell clusters that showed similar Erk and NFAT activation initially after pMHC encounter, but differed in their distinct long-term signaling dynamics (**Fig. 2.3D**). While some cell clusters showed a monotonic decay in the activity of both pathways (clusters 5-8), others showed a second pulse of activity from either NFAT (cluster 3), Erk (cluster 4) or from both pathways (clusters 1-2). Different clusters were enriched for cells stimulated with different pMHC inputs, suggesting a role for these pulsed dynamics in encoding pMHC affinity and dose information. To further explore this possibility, we quantified the incidence and dynamic features of Erk and NFAT pulsing in single cells and analyzed how the dynamics vary across different pMHC conditions (**Fig. 2.6A-E**).

From this analysis, we found that high doses of M9C elicited a second Erk and NFAT pulse with high probability, whereas equivalently high doses of L6F elicited substantially lower probabilities of generating second Erk and NFAT pulses (**Fig. 2.6B**). Strikingly, lowering the dose of M9C had a distinct effect from using the lower-affinity L6F at an equivalent dose, selectively reducing the second NFAT pulse probability while maintaining high Erk pulse probabilities. We also observed pMHC-dependent effects on pulse dynamics, such that even when L6F stimulation elicited second pulses, they had reduced amplitude and earlier onset compared to those elicited with M9C (**Fig. 2.6B-C**). We observed the same trends when using early and late integrated activities as an alternate measure of the pulsatile activity (**Fig. 2.6E**). Taken together, these results indicate that

Erk and NFAT pulse features encode pMHC inputs, with Erk pulsing encoding information about antigen affinity and NFAT pulsing encoding information about antigen dose.

To quantify the extent to which late NFAT and Erk pulsing dynamics enables discrimination between different pMHC inputs, we trained a random forest classification model to distinguish between three different pMHC dose and affinity regimes using quantified pulse dynamics ("pulse features") (**Fig. 2.6F-G**). As a comparison, we also trained this model to use either the full time series for both pathways, or their early or late integrated activities. We found that the model trained on the full time series responses can discriminate between the three pMHC regimes with reasonable precision (~75%). While early integrated activity provided little discriminatory power (~33% precision), as expected (**Fig. 2.6G**), long-term pulsing dynamics (~55% precision) and integrated activity (~60% precision) also enabled discrimination of the three input regimes. Additionally, discriminating pMHC affinity was diminished when information contained within the Erk response was removed from the model, while discriminating pMHC dose was diminished when information contained within the NFAT response was removed (**Fig. 2.7**), thereby suggesting the independent encoding of pMHC dose and affinity though NFAT and Erk signaling, respectively.

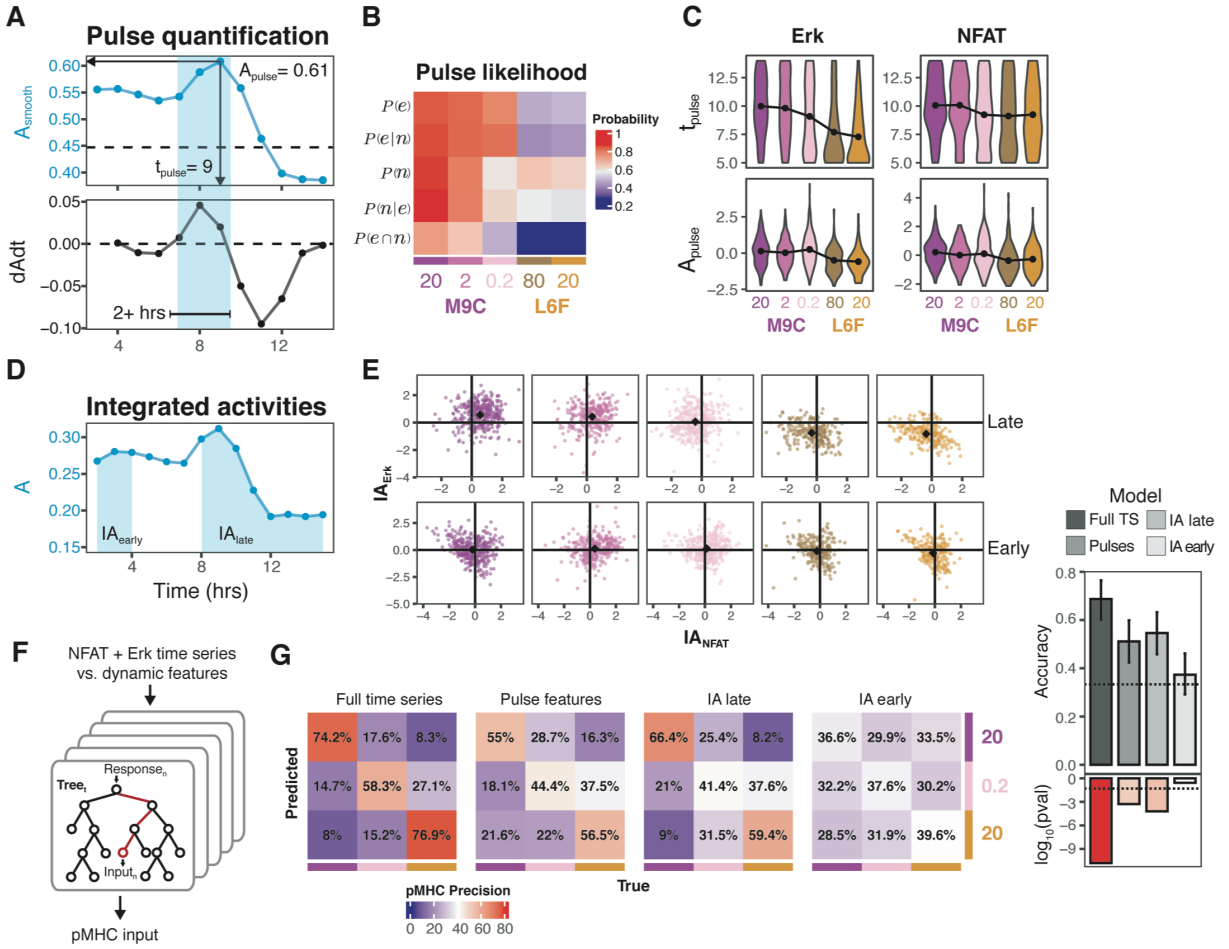

Figure 2.6 T cells Independently Encode pMHC Affinity and Dose Information through Late Erk and NFAT Pulsatile Dynamics.

(A) Quantification of pulsatile dynamics from single cell traces.
(B) Probabilities of NFAT and/or Erk pulses occurring for each pMHC condition.
(C) Distributions of pulse time and scaled amplitude by pMHC condition, gated on cells with a pulse for the respective pathway. Black connected dots represent distribution means.
(D) Quantification of early and late integrated activities from single cells.
(E) 2D scatter plots of scaled early and late integrated activities for Erk and NFAT in each cell, separated by pMHC condition with colors matching those in (C). Black diamond is the mean for each condition. n = 1,510 total cells.
(F) A random forest machine learning classification model was used to make predictions on the input pMHC condition given a dual-pathway signaling response in single cells. Four different random forest models were trained with different signaling predictors including: Full time series, pulse features (t_{pulse} + A_{pulse}), IA_{late}, and IA_{early} for both pathways.

(G) Random forest model precision in predicting the input pMHC affinity and dose regime (high dose, high affinity; low dose, high affinity; high dose, low affinity) for each of the four sets of signaling predictors. Accuracy of each model is quantified on the right with the $\log_{10}$(p-values) beneath (dashed line is p-value = 0.05), testing if the model accuracy is greater than that by random chance (Accuracy = 0.33). Error bars represent 95% confidence intervals obtained from an exact binomial test.

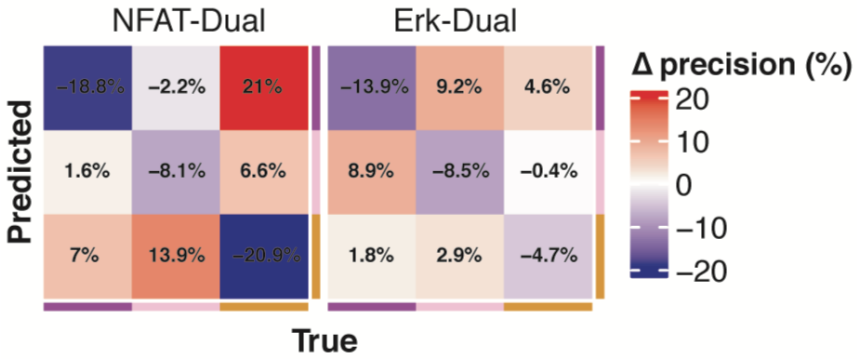

Figure 2.7 Joint Encoding of pMHC Affinity and Dose through Combined Erk and NFAT Dynamics.

Precision matrices resulting from the "Full time series"-trained random forest classification model being subtracted from those of models trained on either the NFAT or Erk time series responses. The resulting "Δ precision" matrices indicate the effect of removing information from the Erk ("NFAT-Dual") or NFAT ("Erk-Dual") pathways.

2.5 METHODS

Mice

The dual-pathway reporter mouse strain (*Rosa26*$^{DPR/DPR}$) was generated on a B6 background by Biocytogen Corp. using their EGE™ (CRISPR/Cas9) method. A *Rosa26* targeting vector [20] was generated to contain a tri-cistronic reporter cassette encoding Erk-KTR [3] fused to mTagBFP2, Histone 2B fused to iRFP, and residues 1-399 of mouse NFATc2 fused to mRuby3 [1]. *Rosa26*$^{DPR/DPR}$ mice were crossed to LCMV-specific transgenic TCR (P14) mice [21] (Jackson Labs, Strain # 004694) and bred to homozygosity. These mice were then crossed to Cre-ERT2 mice (Jackson Labs, Strain # 008463), generating *Rosa26*$^{DPR/Cre\text{-}ERT2}$*/TcrLCMV* offspring. 8 week old male and female *Rosa26*$^{DPR/Cre\text{-}ERT2}$*/TcrLCMV* mice were injected with four doses of tamoxifen over four consecutive days [22]. Briefly, tamoxifen (ApexBio Cat. no. B5965) was prepared at 30 mg/ml in corn oil (Spectrum Chemical Cat. no CO136) and filtered through a 0.2 um filter. The solution was warmed to 37^{0}C and 100 ul was administered via intraperitoneal injection for each dose. Induced male and female mice were used for imaging experiments 4-12 weeks after tamoxifen induction. 8-16 week old *Rosa26*$^{DPR/DPR}$*/TcrLCMV* male and female mice were used for all non-imaging experiments (**Fig 2.1**). All mice were used in accordance with Institutional Animal Care and Use Committee guidelines for the University of Washington.

Cell lines

A monoclonal P14 CD8$^+$ Jurkat T cell line was generated by transducing *Tcrb*-KO Jurkat T cells (a gift from Phil Greenberg) with lentiviruses containing the P14 TCRα and TCRβ chains, and mouse CD8α and CD8β1 chains. Individual CD3$^+$/CD8a$^+$ cells were sorted on an BD Aria III into a 96-well plate.

pMHC-coated plate*s*

The day prior to T cell stimulation, glass-bottom (MatTek Cat. no. PBK96G-1.5-5-F) or tissue-culture 96-well plates were prepared as previously described [5] with minor modifications. Plates were coated with 2 ug Retronectin (TaKaRa Cat. no. T110A), 1 ug anti-mouse CD11a (LFA1), and 2 ug NeutrAvidin (Thermo Fisher Scientific, Cat # 31000) in 100 ul PBS per well and incubated overnight at 4°C. The next day, the plates were washed 3x with 100 ul PBS and blocked with 100 ul 1% BSA in PBS for 1 hr at 37°C. The BSA solution was then aspirated and 100 ul of pMHC in PBS was added and incubated for 90 minutes at 4°C. Two altered peptide ligands specific for the P14 TCR; biotinylated monomeric H-2D^b MHC loaded with either gp33-M9C (KAVYNFATM) or gp33-L6F (KAVYNLATC) [8], were provided by the NIH tetramer facility and serially diluted in cold PBS. The molar quantities of pMHC indicated in the text and figures corresponds to the total amount of pMHC incubated in each well in 100 ul PBS (100 ul of 10 ug/ml pMHC solution ~ 20 pmol pMHC). Following incubation with pMHC, the wells were washed 2x with 100 ul PBS prior to cell seeding. For the pMHC pre-incubation assay (**Fig. 2.5A**), plates were prepared as indicated above, but either seeded with cells immediately after coating, or incubated with 100 ul media at 37°C for 8 hrs prior to cell seeding.

T cell stimulation

Mice were euthanized with CO_2, and their spleens removed. Single cell suspensions were made by homogenizing the spleen between frosted cover slips into FACS buffer (1X HBSS, 0.5% BSA). RBCs were lysed and CD8$^+$ T cells were isolated using the Miltenyi CD8$^+$ negative selection kit (Miltenyi Biotec, Cat # 130-104-075). For live-imaging experiments, enriched CD8$^+$ T cells were flow sorted for cells expressing the fluorescent reporters using a BD Aria III. For

RNA-sequencing and flow cytometry experiments, enriched $CD8^+$ T cells from Cre-ERT2 negative mice were used. For dose-response titration experiments, P14 $CD8^+$ Jurkat cells were cultured in RPMI 1640 with L-Gln, 10% heat-inactivated FBS, 100 U/ml pen/strep, 10 mM HEPES, 1 mM NaPyruvate, 50 uM BME. For dose-response titration experiments using primary cells, enriched $CD8^+$ T cells were sorted for naive ($CD62L^+/CD44^-$) and memory ($CD62L^+/CD44^+$) cells. Primary $CD8^+$ T cells were cultured in AIM-V media (Thermo Fisher Scientific, Cat # 12055091) supplemented with 50 uM BME. To culture rested cells for scRNA-seq and flow cytometry experiments, this media was supplemented with 10% heat-inactivated FBS, 5 ng/ml hIL-7 (Peprotech Cat # 200-07), and 50 ng/ml mIL-15 (Peprotech Cat # 210-15). All cells were cultured at 37°C with 5% CO_2. 25k (live-cell imaging), 75k (bulk RNA-seq), 100k (scRNA-seq), or 80k (flow cytometry) T cells were seeded into each well of a 96-well pMHC-coated plate in 200 ul media and centrifuged at 80g for 2 min to settle the cells to the plate surface.

Live-cell imaging

Time lapse images were acquired using a 63X (0.75 NA) glycerol objective on a Leica DMi8 inverted fluorescence microscope equipped with hardware autofocus and an incubation chamber maintaining a 37°C, 5% CO2 environment. Images were taken with a Photometrics Prime 95B camera. Automated acquisition software (MetaMorph, Molecular Devices) was used to acquire differential interference contrast (DIC) images every 20 min and fluorescence images every 60 min for 30 hr acquisitions. Fluorescence images were acquired in three channels: BFP (405 Ex; 440/40 Em), RFP (561 Excitation; 600/50 Em), and near-IR (640 Ex, 700/75 Em) using an LED illuminator (SpectraX, Lumencor). For 1 hr acquisitions, all channels were acquired at four

minute intervals, and cells were seeded immediately after the start of the acquisition and allowed to fall into the field of view during the image acquisition to capture the time of pMHC contact (+/- 4 minutes). For 30 hr acquisitions, cells were spun onto the plate surface, as indicated above, and the first image was taken after 1 hr of incubation.

Image processing

Image pre-processing, cell segmentation, and tracking was performed with a custom pipeline developed in MATLAB (Mathworks) as described previously [23,24] (**Fig. 2.8A**), modified to enable nuclear and cytoplasmic segmentations. Nuclear masks are generated by segmenting H2B-iRFP images. Cytoplasmic masks are generated by first creating a weighted average image of all three fluorescent images (BFP + RFP + iRFP), segmenting the resulting image to yield a total cell mask, then subtracting the nuclear mask. Cells are then linked from frame to frame to generate single-cell traces of signaling activity, which are then manually validated for inclusion in downstream analyses. To quantify localization of reporters in each compartment, we calculate the median nuclear fluorescence and the 0.75 quantile of cytoplasmic fluorescence, since we observed uneven distribution of fluorescence in the cytoplasm. With these quantities, we determined pathway activities as follows:

$$Erk\ Activity\ =\ BFP_{cyt}/(BFP_{cyt} + BFP_{nuc})$$

$$NFAT\ Activity\ =\ RFP_{nuc}/(RFP_{cyt} + RFP_{nuc})$$

We quantified two additional metrics for downstream quality control: (1) the fraction of H2B-iRFP signal in the nucleus, and (2) the fraction of the total mask area where the nuclear mask (M_{nuc}) does not overlap the cytoplasmic mask (M_{cyt}):

$$Nuclear\ H2B\ =\ iRFP_{nuc}/(iRFP_{cyt} + iRFP_{nuc})$$

$$non\ overlapping\ \ nuclear\ area\ =\ Area(M_{nuc} - M_{cyt})/Area(M_{nuc} \cup M_{cyt})$$

These two metrics allow for automated exclusion of out of focus cells, dead cells, and clumped cells that would produce inaccurate pathway activity measurements (**Fig. 2.8B**).

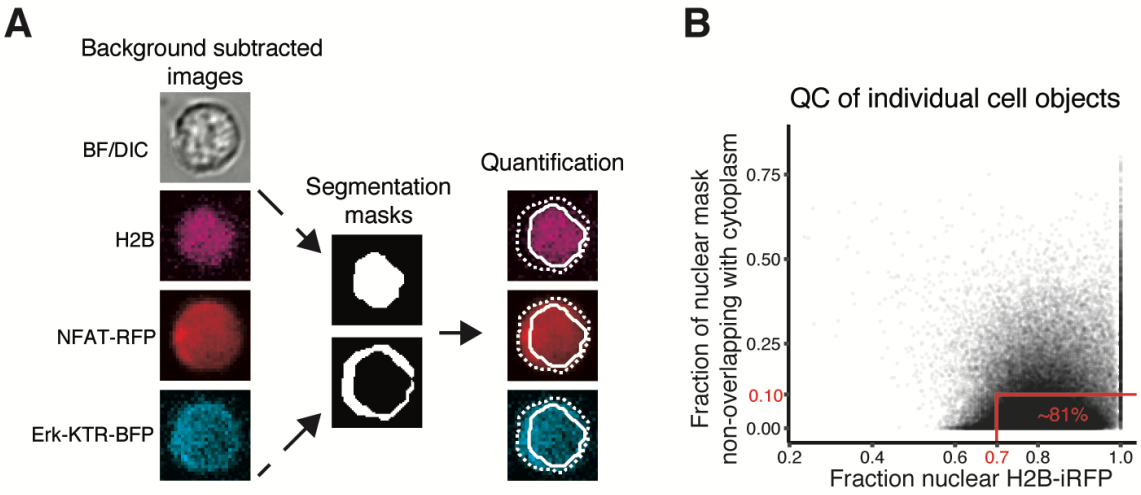

Figure 2.8 Image Processing and Quality Control Workflow.

(A) Image processing and quantification workflow done in MATLAB.
(**B**) Quality control filtering of cell objects was done in R. ~ 90k individual cell images pass QC per experiment, indicated by the red boundary gate.

For NFAT1 staining analysis, images were processed as above, but with nuclear masks generated from segmented DRAQ5 images, and total cell masks generated by dilating the nuclear mask. NFAT1 fluorescence was integrated within the nuclear and total cell masks and nuclear NFAT1 was reported as the integrated nuclear signal normalized to total signal.

Computational analysis of Erk and NFAT signaling

Quality control

Following image processing, quantified cell objects were exported from MATLAB and imported into R for analysis. Individual cell objects were first filtered based on their fraction of nuclear H2B-iRFP signal (> 0.7 for inclusion) and the fraction of their nuclear mask non-overlapping with the cytoplasmic mask (< 0.1 for inclusion) (**Fig. 2.8B**). For each of two independent live-imaging experiments, ~90k individual cell objects passed QC and proceeded to further quality control for single cell time traces. We limited our single cell time traces to 16 hrs because tracking single cells for longer than 16 hrs proved too difficult for a robust and reliable analysis. For inclusion in downstream analysis, single cell traces needed to have at least 10 measured time points. The traces that passed were then smoothed and had missing data points interpolated with local regression. Lastly, cell traces were trimmed down to 2-15 hrs due to a high prevalence of missing leading and trailing time points which cannot be interpolated, and only those cells with no missing values after this stage were included in the single cell signaling analyses. A total of 1,510 single cell traces from one experimental replicate for five pMHC conditions were used.

Single cell dual-pathway clustering

For single cell dual-pathway clustering, a balanced distribution of single cell traces from each condition was generated by downsampling the traces for each condition to match that of the lowest condition, yielding 220 single cells per condition for each of the five pMHC conditions. To perform multivariate clustering using dual-pathway responses, each pathway's activities were scaled from zero to one before clustering. The 1,100 bivariate 14-dimensional vectors (14 timepoints for each pathway) were clustered with the *dtwclust* package (v 5.5.11) [25] in R using the global alignment kernel distance [17], which allows for calculating distances between multivariate single cell responses. Parameters used with the *tsclust* function were: k = 8, type = "partitional", distance = "gak". The use of 8 partitions was empirically determined.

Quantification of dynamic features

Occurrence of a second signaling pulse was determined using two measures: (1) a 3 hr sliding window of time-integrated areas to further smooth the single cell activity traces (A_{smooth}), and (2) the derivative of the smoothed trace (dAdt). Based on these two traces for each single cell response, a pulse was detected in each pathway if there were at least 2 consecutive hours with dAdt > 0 and $A_{smooth} > (0.95 \times \bar{A}_{smooth})$. $\bar{A}_{smooth}$ was calculated as the mean smoothed activity for each pathway from all analyzed cells. If a pulse was detected, the time of pulse (t_{pulse}) was defined as the latest positive dAdt within the pulse window, and the pulse amplitude (A_{pulse}) was defined as the smoothed activity value at t_{pulse},and then scaled (z-score). To simplify the analysis, and due the rare occurrence of a third pulse within this timescale, only the earliest pulse per pathway per cell was used in our analyses. Early and late integrated activities for each pathway were calculated using the activity traces prior to the additional smoothing used for pulse

detection, and computed using the 2-4 hr and 8-15 hr activities, respectively. Integrated activities were scaled (z-score).

Machine learning classification models

We first created 25 data "folds" for cross-validation using the *createMultiFolds* function from the *caret* package (v 6.0-93) in R. For each of 5, 5-fold splits, single cell traces were divided into 5 partitions while preserving the frequency of cell traces from each pMHC condition. 1 of the 5 partitions was then held out from that fold, and used for model validation. The remaining 4 partitions were used for model training. In this process, 25 independent training and validation datasets were generated such that each and every single cell trace was used to train 20 models, and held out and used for validation for the other 5 models. With these 25 data folds, we performed a nested cross-validation training and validation workflow [26] whereby for each fold, a random forest classification model with 500 decision trees was trained and subsequently validated on the hold out partition using the *randomForest* package (v 4.7-1.1) in R. Here, each hold out partition was downsampled to create a balanced distribution of single cell traces from each pMHC condition for model validation. In this workflow, 25 independent models were trained and validated to yield 25 sets of pMHC input predictions based on various Erk and NFAT signaling predictors noted in the main text. A confusion matrix was generated from each model's predictions, and the resulting matrices averaged to yield a final precision matrix. Overall accuracy was extracted from each model and averaged to yield the reported model accuracies. Model accuracy p-values were generated by the *confusionMatrix* function in the *caret* package.

2.6 REFERENCES

1. Lodygin, D. *et al.* A combination of fluorescent NFAT and H2B sensors uncovers dynamics of T cell activation in real time during CNS autoimmunity. *Nat. Med.* **19**, 784–790 (2013).
2. Marangoni, F. *et al.* The Transcription Factor NFAT Exhibits Signal Memory during Serial T Cell Interactions with Antigen-Presenting Cells. *Immunity* **38**, 237–249 (2013).
3. Regot, S., Hughey, J. J., Bajar, B. T., Carrasco, S. & Covert, M. W. High-sensitivity measurements of multiple kinase activities in live single cells. *Cell* **157**, 1724–1734 (2014).
4. Pircher, H. *et al.* Molecular analysis of the antigen receptor of virus-specific cytotoxic T cells and identification of a new V alpha family. *Eur. J. Immunol.* **17**, 1843–1846 (1987).
5. Lever, M. *et al.* Architecture of a minimal signaling pathway explains the T-cell response to a 1 million-fold variation in antigen affinity and dose. *Proc. Natl. Acad. Sci.* **113**, E6630–E6638 (2016).
6. Abu-Shah, E. *et al.* Human CD8 $^{+}$ T Cells Exhibit a Shared Antigen Threshold for Different Effector Responses. *J. Immunol.* **205**, 1503–1512 (2020).
7. Trendel, N. *et al.* Perfect adaptation of CD8+ T cell responses to constant antigen input over a wide range of affinities is overcome by costimulation. *Sci. Signal.* **14**, (2021).
8. Boulter, J. M. *et al.* Potent T cell agonism mediated by a very rapid TCR/pMHC interaction. *Eur. J. Immunol.* **37**, 798–806 (2007).
9. Gallagher, M. P. *et al.* Hierarchy of signaling thresholds downstream of the T cell receptor and the Tec kinase ITK. *Proc. Natl. Acad. Sci.* **118**, e2025825118 (2021).
10. Lin, J. J. Y. *et al.* Mapping the stochastic sequence of individual ligand-receptor binding events to cellular activation: T cells act on the rare events. *Sci. Signal.* **12**, eaat8715 (2019).

11. Altan-Bonnet, G. & Germain, R. N. Modeling T Cell Antigen Discrimination Based on Feedback Control of Digital ERK Responses. *PLoS Biol.* **3**, e356 (2005).
12. Das, J. *et al.* Digital Signaling and Hysteresis Characterize Ras Activation in Lymphoid Cells. *Cell* **136**, 337–351 (2009).
13. Podtschaske, M. *et al.* Digital NFATc2 Activation per Cell Transforms Graded T Cell Receptor Activation into an All-or-None IL-2 Expression. *PLOS ONE* **2**, e935 (2007).
14. Beuneu, H. *et al.* Visualizing the Functional Diversification of CD8+ T Cell Responses in Lymph Nodes. *Immunity* **33**, 412–423 (2010).
15. Celli, S., Garcia, Z. & Bousso, P. CD4 T cells integrate signals delivered during successive DC encounters in vivo. *J. Exp. Med.* **202**, 1271–1278 (2005).
16. Daniels, M. A. *et al.* Thymic selection threshold defined by compartmentalization of Ras/MAPK signalling. *Nature* **444**, 724–729 (2006).
17. Cuturi, M. Fast global alignment kernels. in *Proceedings of the 28th International Conference on International Conference on Machine Learning* 929–936 (Omnipress, 2011).
18. Richard, A. C. *et al.* T cell cytolytic capacity is independent of initial stimulation strength. *Nat. Immunol.* **19**, 849–858 (2018).
19. Gallagher, M. P., Conley, J. M. & Berg, L. J. Peptide Antigen Concentration Modulates Digital NFAT1 Activation in Primary Mouse Naive CD8+ T Cells as Measured by Flow Cytometry of Isolated Cell Nuclei. *ImmunoHorizons* **2**, 208–215 (2018).
20. Srinivas, S. *et al.* Cre reporter strains produced by targeted insertion of EYFP and ECFP into the ROSA26 locus. *BMC Dev. Biol.* **1**, 4 (2001).
21. Pircher, H. *et al.* T cell tolerance to Mlsa encoded antigens in T cell receptor V beta 8.1 chain transgenic mice. *EMBO J.* **8**, 719–727 (1989).

22. Donocoff, R. S., Teteloshvili, N., Chung, H., Shoulson, R. & Creusot, R. J. Optimization of tamoxifen-induced Cre activity and its effect on immune cell populations. *Sci. Rep.* **10**, 15244 (2020).
23. Ng, K. K. *et al.* A stochastic epigenetic switch controls the dynamics of T-cell lineage commitment. *eLife* **7**, e37851 (2018).
24. Kueh, H. Y. *et al.* Asynchronous combinatorial action of four regulatory factors activates Bcl11b for T cell commitment. *Nat. Immunol.* **17**, 956–965 (2016).
25. Sardá-Espinosa, A. Time-Series Clustering in R Using the dtwclust Package. *R J.* **11**, 22 (2019).
26. Vabalas, A., Gowen, E., Poliakoff, E. & Casson, A. J. Machine learning algorithm validation with a limited sample size. *PLOS ONE* **14**, e0224365 (2019).

Chapter 3. Decoding Erk and NFAT Dynamics at the Level of Gene Regulation

3.1 Classifying Diverse Modes of Erk and NFAT Decoding

Genes downstream of TCR signaling integrate AP-1 and NFAT inputs in distinct ways. Therefore, tuning the activation of each TF through the differential long-term Erk and NFAT dynamics we discovered could plausibly lead to distinct gene expression programs. To explore this possibility, we used RNA-sequencing to identify gene programs that depend on Erk and NFAT signaling at long timescales. We subjected $CD8^+$ T cells to strong stimulation (2 pmol M9C) to elicit maximal signaling, then treated cells with either MEKi and/or CsA after 9 hrs (**Fig. 3.1A**), when signaling activities diverge for different pMHC inputs (**Fig. 2.3**). Live imaging confirmed that the inhibitors indeed reduced signaling of their target pathways as expected (**Fig. 3.1B**). Cells were then subjected to bulk RNA sequencing after 30 hrs of stimulation and analyzed for differential gene expression to identify targets of late Erk and/or NFAT signaling. This analysis identified 1,089 differentially expressed genes (DEGs) regulated by Erk and/or NFAT signaling, with substantial overlap between their target genes (**Fig. 3.2**), consistent with the cooperativity of NFAT and AP-1 in regulating target gene expression. We classified each gene as being strongly (s) or weakly (w) regulated based on their magnitude of expression fold change upon signaling inhibition (**Fig. 3.1C**).

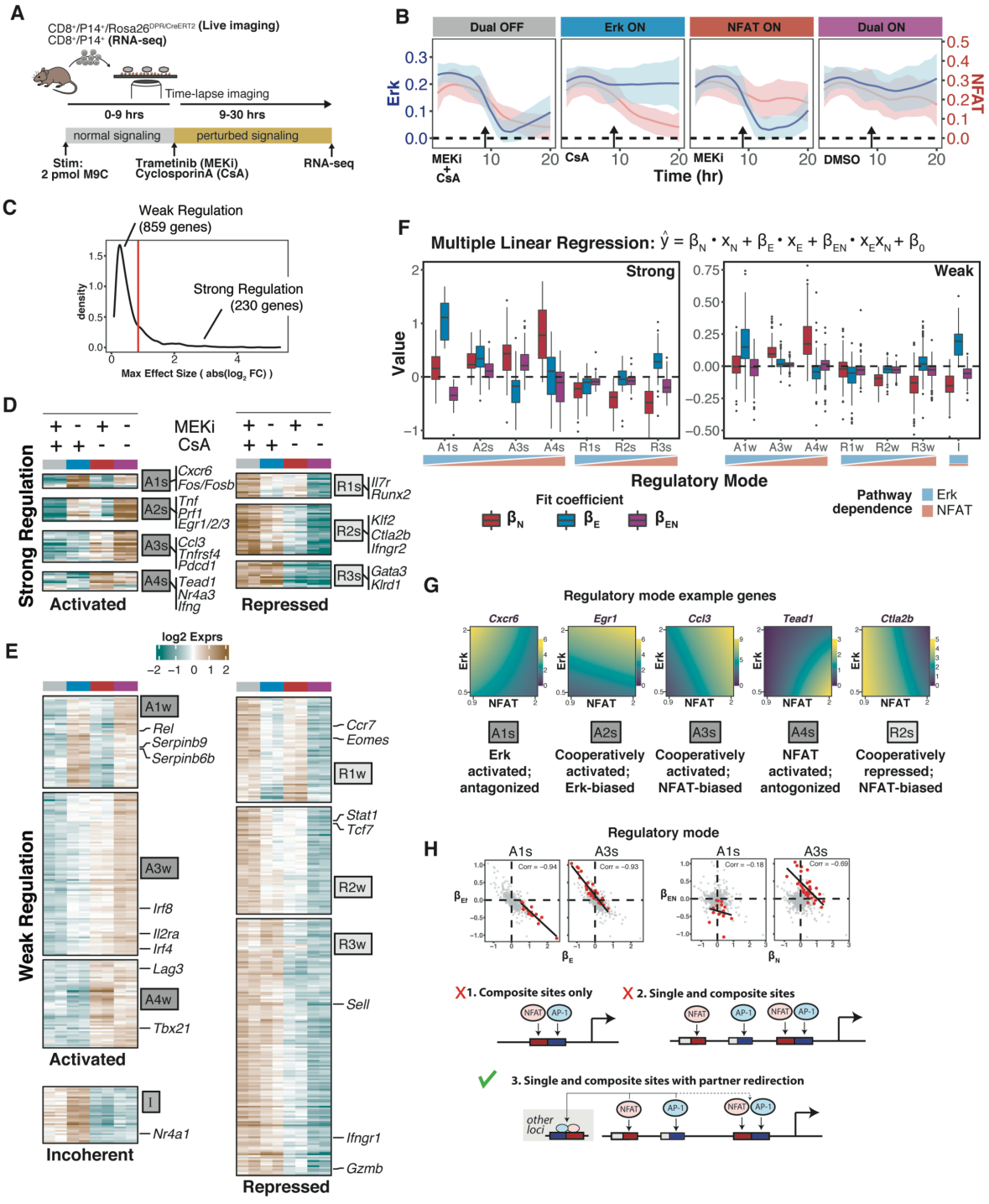
A
CD8+/P14+/Rosa26DPR/CreERT2 (Live imaging)
CD8+/P14+ (RNA-seq)
Time-lapse imaging
0-9 hrs
9-30 hrs
normal signaling
perturbed signaling
Stim:
2 pmol M9C
Trametinib (MEKi)
CyclosporinA (CsA)
RNA-seq
B
Dual OFF
Erk ON
NFAT ON
Dual ON
Erk
NFAT
MEKi + CsA
CsA
MEKi
DMSO
Time (hr)
C
Weak Regulation
(859 genes)
Strong Regulation
(230 genes)
density
Max Effect Size (abs(log2 FC))
D
MEKi
CsA
Strong Regulation
A1s
A2s
A3s
A4s
Cxcr6
Fos/Fosb
Tnf
Prf1
Egr1/2/3
Ccl3
Tnfrsf4
Pdcd1
Tead1
Nr4a3
Ifng
R1s
R2s
R3s
Il7r
Runx2
Klf2
Ctla2b
Ifngr2
Gata3
Klrd1
Activated
Repressed
E
log2 Exprs
Weak Regulation
A1w
Rel
Serpinb9
Serpinb6b
A3w
Irf8
Il2ra
Irf4
Lag3
A4w
Tbx21
Activated
I
Nr4a1
Incoherent
Ccr7
Eomes
R1w
Stat1
Tcf7
R2w
R3w
Sell
Ifngr1
Gzmb
Repressed
F
Multiple Linear Regression: ŷ = βN • xN + βE • xE + βEN • xExN + β0
Strong
Weak
Value
A1s
A2s
A3s
A4s
R1s
R2s
R3s
A1w
A3w
A4w
R1w
R2w
R3w
I
Regulatory Mode
Fit coefficient
βN
βE
βEN
Pathway dependence
Erk
NFAT
G
Regulatory mode example genes
Cxcr6
Egr1
Ccl3
Tead1
Ctla2b
Erk
NFAT
A1s
Erk activated; antagonized
A2s
Cooperatively activated; Erk-biased
A3s
Cooperatively activated; NFAT-biased
A4s
NFAT activated; antogonized
R2s
Cooperatively repressed; NFAT-biased
H
Regulatory mode
A1s
A3s
Corr = −0.94
Corr = −0.93
Corr = −0.18
Corr = −0.69
βEI
βE
βEN
βN
X 1. Composite sites only
X 2. Single and composite sites
3. Single and composite sites with partner redirection
NFAT
AP-1
other loci

Figure 3.1 Target Genes of Erk and NFAT Show Distinct Modes for Decoding Signaling Activity.

(A) Live imaging and bulk RNA sequencing were done on reporter, and non-reporter $CD8^+$ T cells, respectively following 30 hrs of stimulation with 2 pmol M9C and MEKi and/or CsA treatment after the first 9 hrs.
(B) Mean +/- SD from 110 (MEKi+CsA), 109 (CsA), 104 (MEKi), and 96 (DMSO) single cell Erk and NFAT activity traces in response to each perturbation.
(C) Bulk RNAseq was performed 30 hrs after initial stimulation. Differentially expressed genes were identified based on a q-value threshold of 0.001 and classified as being strongly or weakly regulated by NFAT and/or Erk relative to a maximum fold change from any treatment of 1.8.
(D-E) Heatmap representation of hierarchical clustering of genes strongly (D) and weakly (E) regulated by Erk and NFAT signaling. Classification of regulatory modes was determined by distinct patterns of expression change due to inhibitor treatments. Genes of interest are identified from each regulatory mode. "A" = Activated, "R" = Repressed, "I" = Incoherent, "s" = strong, "w" = weak.
(F) Boxplots of β coefficients from multiple linear regression models fit to each DEG and grouped by regulatory mode. β coefficients result from fitting each model to the normalized expression of each gene ($\hat{y} = y/\bar{y}$).
(G) Characterization of five regulatory modes. Example genes for each mode are shown with a model prediction of their expression with changing levels of Erk and NFAT signaling.
(H) Representative pairwise correlations between β_{EN} vs β_E and β_{EN} vs β_N for the A1s and A3s regulatory mode genes. All DEGs are shown in gray dots with genes of each regulatory mode shown in red. Linear regressions are shown in black. Pearson correlation coefficients are indicated. *trans*-TF partner redirection is required to reproduce the observed β coefficient correlations between single and combinatorial signaling sensitivities.

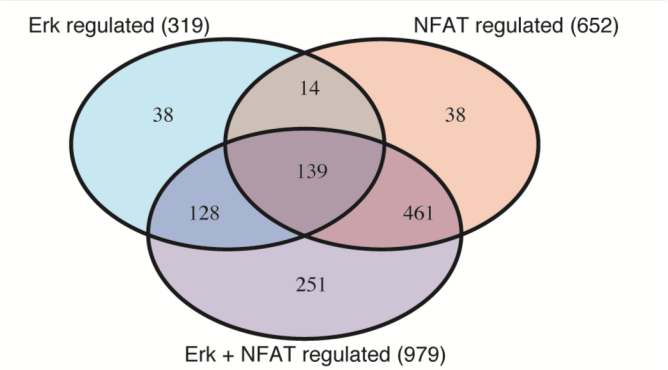

Figure 3.2 Erk and NFAT Target Genes.

Numbers of differentially expressed genes that are regulated by late NFAT, Erk, or combined signaling.

Analysis of strongly- and weakly-regulated genes using hierarchical clustering and linear regression (**Fig. 3.1D-F**) revealed a spectrum of regulatory modes by which distinct clusters of genes differentially integrate Erk and NFAT signaling inputs. Up-regulated genes could be either primarily activated by Erk (A1s, A1w, A2s, A2w) or by NFAT (A3s, A3w, A4s, A4w) (**Fig. 3.1D-E**), with these two subsets having highest sensitivity coefficients for Erk (β_E) and NFAT (β_N) in the linear models (**Fig. 3.1F**). Erk-biased genes include the AP-1 subunits (*Fos*, *Fosb*) and known target genes (*Egr1, Tnf*), as expected [1], whereas genes activated primarily by NFAT included key regulators of exhaustion and effector function (*Pdcd1*, *Lag3, Nr4a3, Ccl3, Ccl4, Ifng*), consistent with known roles of NFAT in driving these gene programs [2]. Interestingly, while Erk and NFAT work cooperatively in some modes (A2s, A3s, A3w) and show a positive sensitivity coefficient for combined Erk/NFAT signaling ($\beta_{EN} > 0$), they antagonize one another in other modes (A1s, A4s; $\beta_{EN} < 0$). Repressed target genes, which include canonical memory and self-renewal genes such as *Tcf7*, *Il7r*, and *Sell*, also showed a range of Erk and NFAT dependencies (R1s-R3s, R1w-R3w, I).

Intriguingly, across all these regulatory modes, we observed a marked negative correlation between the sensitivity to combined Erk/NFAT inputs (β_{EN}) and the sensitivities for individual inputs, most prominently for Erk (β_E) but also for NFAT (β_N) (**Fig. 3.1H and Fig 3.3**). This pervasive negative correlation suggests a global mechanism generating antagonism between single and combinatorial binding modes. In other systems [3,4], TFs can be redirected from one set of binding sites to another by a trans-acting binding partner. In T cells, AP-1 and NFAT could redirect each other's binding from sites where they bind with other partners to those where they bind together. To test whether such a mechanism could explain the inverse relationship between single and combined Erk/NFAT sensitivities, we analyzed a series of candidate mathematical models

describing different *cis*-regulatory mechanisms by which AP-1 and NFAT may regulate their target genes (**Appendix B, Section 1**). From modeling, we find that the observed range of sensitivities to single and combined inputs for different target genes (β_E, β_N vs. β_{EN}) cannot be readily explained by having composite AP-1:NFAT binding sites alone (**Model 1**), but most likely reflect binding of these factors at multiple singleton and composite sites, which could each vary in their transcriptional activity (**Model 2**). However, having multiple sites alone would give rise to uncorrelated single and combined input sensitivities if these sites act independently from each other to control transcriptional activity. In contrast, when AP-1 and NFAT can redirect each other away from single sites to composite sites through co-binding, negative relationships between the single (β_E, β_N), and combined (β_{EN}) input sensitivities then arise (**Fig. 3.1H, Model 3**), in agreement with experimental data. Importantly, because partner re-direction occurs in *trans*, affecting TF availability across all target genes, negative correlations arise across a range of *cis*-regulatory architectures with different input sensitivities. Indeed, negative correlations are pervasive across different regulatory architectures, consistent with the prediction of this model.

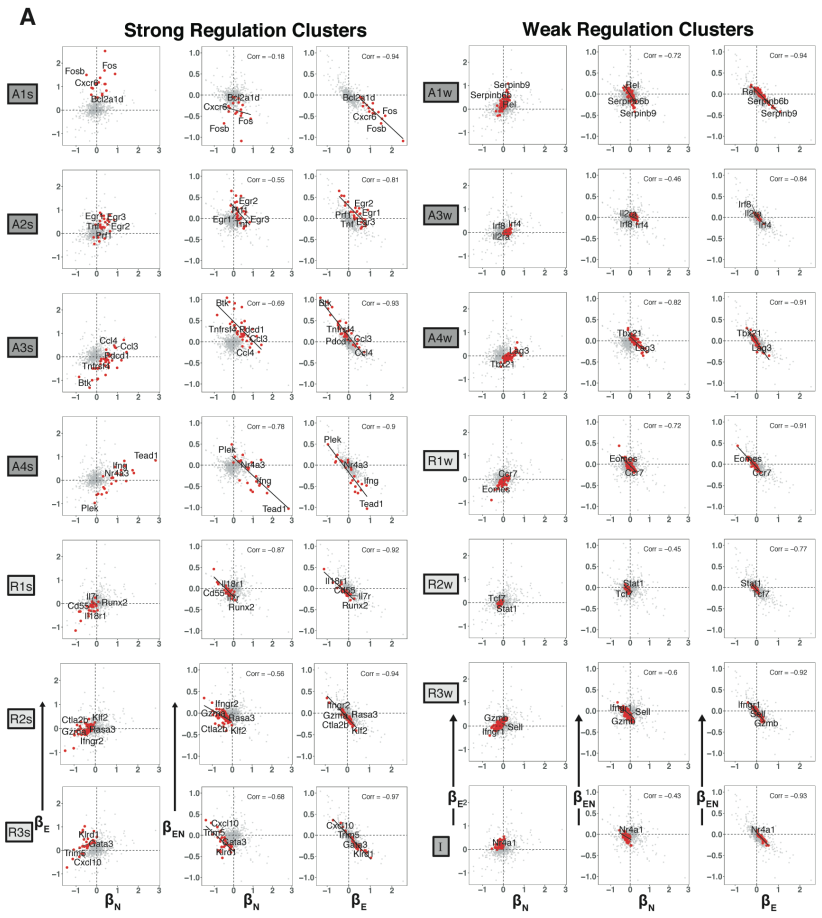

B

β_{EN} vs. β_N

Regulatory mode	β_{EN} vs. β_N Corr	$\beta_{EN} = m \cdot \beta_N + b_0$ m	Intercept
A1s	−0.18	−0.13	−0.34
A2s	−0.55	−0.53	0.28
A3s	−0.69	−0.46	0.48
A4s	−0.78	−0.42	0.17
R1s	−0.87	−0.46	−0.19
R2s	−0.56	−0.26	−0.20
R3s	−0.68	−0.42	−0.38
A1w	−0.72	−0.67	−0.02
A3w	−0.46	−0.19	0.03
A4w	−0.82	−0.44	0.10
R1w	−0.72	−0.47	−0.04
R2w	−0.45	−0.30	−0.06
R3w	−0.60	−0.35	−0.09
I	−0.43	−0.27	−0.11

β_{EN} vs. β_E

Regulatory mode	β_{EN} vs. β_E Corr	$\beta_{EN} = m \cdot \beta_E + b_0$ m	Intercept
A1s	−0.94	−0.48	0.17
A2s	−0.81	−0.52	0.29
A3s	−0.93	−0.65	0.13
A4s	−0.90	−0.68	−0.17
R1s	−0.92	−0.47	−0.15
R2s	−0.94	−0.55	−0.11
R3s	−0.97	−0.54	−0.01
A1w	−0.94	−0.49	0.07
A3w	−0.84	−0.50	0.02
A4w	−0.91	−0.73	−0.03
R1w	−0.91	−0.55	−0.07
R2w	−0.77	−0.53	−0.05
R3w	−0.92	−0.63	−0.02
I	−0.93	−0.53	0.03

Figure 3.3 Correlations Between β Coefficients by Regulatory Mode.

(A) Pairwise correlations between β coefficients for each regulatory mode is plotted separately as scatter plots with genes comprising each regulatory mode shown in red (all other DEGs shown in gray). Linear regressions and Pearson correlation coefficients are shown for β_{EN} vs. β_N and β_E. **(B)** Table listing Pearson correlation coefficients and linear regression coefficients for β_{EN} vs. β_N and β_E for all regulatory modes identified from the bulk RNA seq hierarchical clustering analysis.

3.2 pMHC-Specific Transcriptional Regulation by Erk and NFAT

pMHC inputs of different affinity and dose may give rise to distinct gene programs, and do so as a result of decoding of pMHC-dependent Erk and NFAT signaling. To test this hypothesis, we performed single-cell RNA-sequencing (scRNA-seq) on $CD8^+$ T cells cultured with the pMHC conditions we used in our imaging experiments (**Fig. 2.3**) using a standard 10X Genomics platform. We obtained 11,412 cells from six conditions, including the five pMHC conditions, as well as a non-stimulated (rest) control. We performed UMAP dimensionality reduction, subsetting on the 1,089 Erk and NFAT target genes identified from bulk RNA-seq (**Fig. 3.1**), then clustered the cells on this 2D projection using Leiden community detection [5,6] (**Fig. 3.4A**). Cells activated with pMHCs of varying affinity and dose were localized to different regions of the UMAP and had distinct proportions within each cluster, suggesting the presence of pMHC-specific gene programs (**Fig. 3.4B and Fig. 3.5**). All stimulated cells showed a genomic state distinct from resting cells (Clusters 2-8 vs. 1), reflecting the large-scale changes accompanying activation. Amongst activated cells, those exposed to high affinity pMHC (M9C) acquired an effector-like state (Clusters 5-8), with up-regulation of canonical effector genes (*Irf4*, *Il2ra*) and down-regulation of genes associated with memory and lymph node homing (*Tcf7, Sell, Klf2*) (**Fig 3.4C and Fig. 3.5**). Cells exposed to higher doses of this pMHC increased expression of T cell homing chemokines (*Ccl3, Ccl4*); they also expressed higher levels of inhibitory receptors (*Pdcd1*, *Lag3*), suggesting a more rapid progression towards a state of exhaustion (Clusters 7-8). In contrast, cells exposed to low affinity pMHC (L6F) showed less effector differentiation and greater retention of memory programming (Clusters 2-4). Strikingly, these cells enhanced expression of other inhibitory receptors (*Ctla4, Cd47*) as well as *Il2rb* (CD122), a marker of suppressive CD8 T cells [7,8]. These distinct inhibitory receptor expression profiles suggest a need for multiple suppressive

programs depending on the stimulatory regime, and point to a low dose, high affinity pMHC regime for maintaining optimal effector function.

Having identified global differences in the transcriptional states of T cells stimulated with different pMHC inputs, we asked whether these differences arose from the decoding of long-term Erk and NFAT signaling, thus enabling cells to perceive differences in pMHC inputs. To do so, we sought to identify groups of closely co-expressed genes in single cells, as they are likely regulated by the same upstream TFs [6,9]. We used a regression model to compute pairwise gene-gene expression correlations, followed by hierarchical clustering on the regression coefficients to identify groups of co-expressed genes (**Fig. 3.4D**), which we term gene modules. We found eight gene modules that were either activated or repressed by pMHC stimulation (M1-M6 vs M7-M8) and which varied in both the direction and magnitude of regulation in response to different inputs. Notably, activated modules could be up- or down-regulated with increasing pMHC affinity (M1-4 vs M5-6), or further up-regulated at greater pMHC dose (M4).

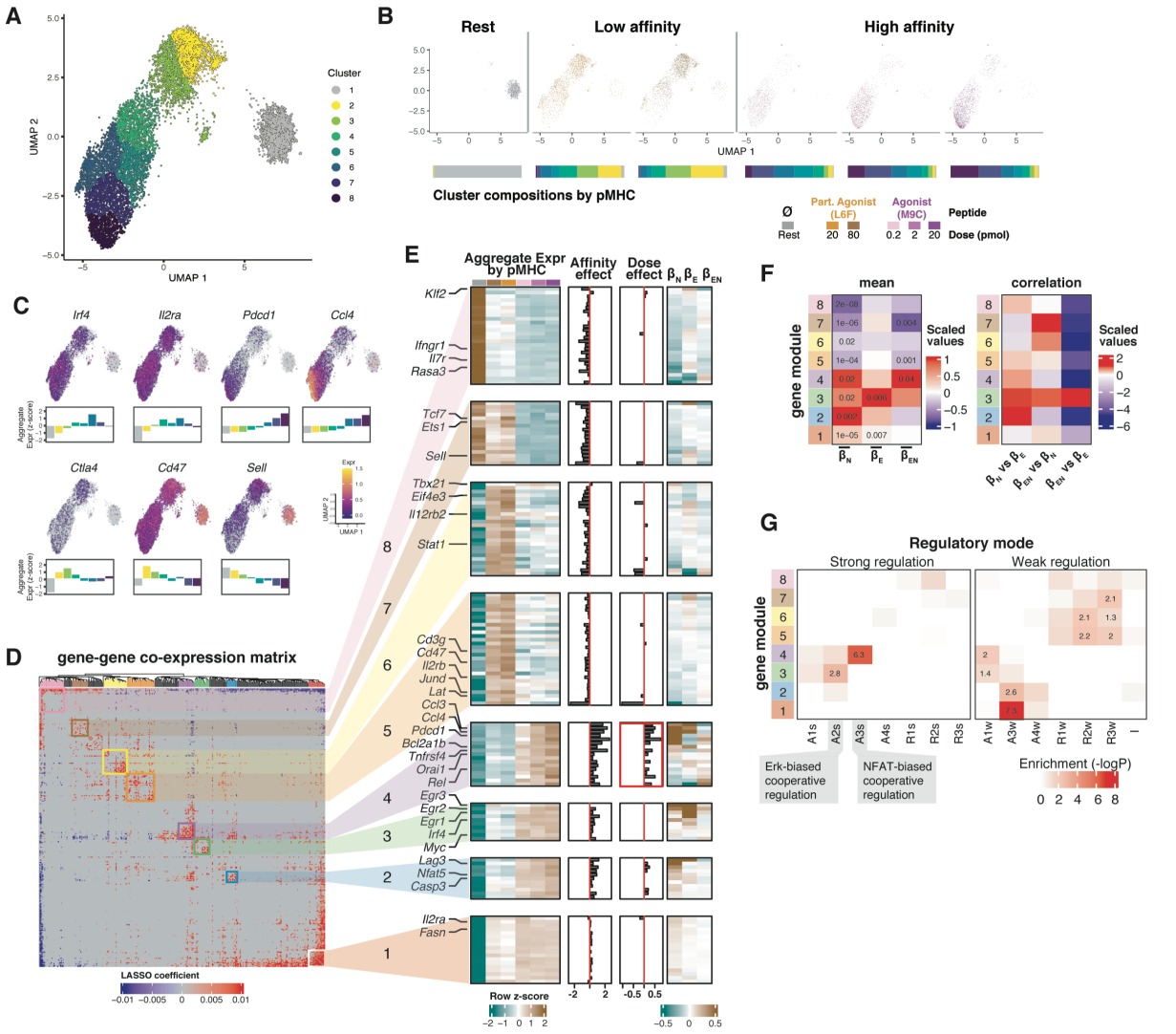

Figure 3.4 pMHCs of Varying Affinity and Dose Elicit Distinct T cell Functional Programs via Decoding of Erk and NFAT Signaling.

(A) UMAP dimensionality reduction of the 1,089 Erk and NFAT target genes identified in Fig. 4C-E from scRNAseq data of CD8⁺ T cells stimulated for 30 hrs with five different pMHC conditions. Cells were clustered using Leiden community detection [5] via Monocle3 [10].
(B) UMAP split by pMHC input. The proportion of cells from each pMHC condition belonging to each cluster in (A) are shown below each UMAP.
(C) Expression of select genes of interest overlaid on UMAP, and their scaled (z-score) aggregate expression by UMAP cluster shown as bar plots.
(D) Hierarchical clustering of a single cell gene-gene co-expression matrix of 309 genes that have at least one non-zero β coefficient from a LASSO regression model against all other genes used in the UMAP analysis. The matrix is colored by the regression β coefficients for each pair of genes (pairs of identical genes down the diagonal are colored as zero). Each value estimates

the magnitude and direction of co-expression between two genes in a single cell. Eight co-expression clusters are identified as gene modules.
(E) From left to right: Scaled aggregate expression by pMHC condition for each gene of the eight gene modules. Normalized effect of pMHC affinity and dose on gene expression determined by differential expression tests in Monocle3. β_N, β_E, and β_{EN} values from Fig. 4F for each gene of the gene modules.
(F) Summary statistics for β coefficients by gene module. t-test p-values are indicated for mean β coefficients significantly different from zero.
(G) Enrichment of regulatory modes identified in Fig 4 within each gene module, with p-values determined by Fisher's exact test.

To test the role of long-term Erk and NFAT signaling dynamics in generating these pMHC-dependent gene expression patterns, we analyzed the single and combinatorial Erk and NFAT dependencies (β_E, β_N, β_{EN}) of genes in each module obtained by signaling perturbation measurements (**Fig. 3.4E, right; Fig. 3.4F and Fig. 3.5**), as well as their enrichment in different Erk/NFAT regulatory modes (**Fig. 3.1F-G and Fig 3.4G**). We found that modules up-regulated with pMHC affinity (M1-M4) showed positive dependencies on Erk/NFAT regulation, whereas those down-regulated with affinity (M5-M8) showed negative dependencies (**Fig. 3.4E-F**). These results are consistent with pMHC affinity-dependent differences arising due to stronger Erk and NFAT signaling (**Fig. 2.5E**). As increasing pMHC dose further increases NFAT but not Erk signaling (**Fig. 2.5**), we predict that modules with strong pMHC dose-dependencies also show greater reliance on NFAT signaling compared to Erk signaling. Indeed, module M4, which showed the greatest pMHC dose sensitivity (**Fig. 3.5**), also showed strong sensitivity to NFAT and the greatest sensitivity to combinatorial NFAT/Erk activity compared with Erk activity ($\beta_N > \beta_E$; $\beta_{EN} > \beta_E$; $\beta_N > 0$; $\beta_{EN} > 0$) (**Fig. 3.4F**). Furthermore, this module was enriched for genes exhibiting an NFAT-biased mode for cooperative regulation (**mode "A3s", Fig. 3.4G**), thus identifying composite NFAT:AP-1 regulation as a regulatory mode for sensing pMHC dose. Similar NFAT-dominant regulation was also observed for the moderately dose-dependent module M2 ($\beta_N > \beta_E$; $\beta_N > 0$), though, interestingly, this module showed considerably weaker sensitivity to combined Erk/NFAT regulation (β_{EN}). In contrast, module M3, which was strongly up-regulated with increasing affinity but showed no dose-dependency, showed the greatest sensitivity to Erk signaling (β_E), and was also enriched for genes exhibiting an Erk-biased cooperative mode of regulation (mode "A2s"). This finding aligns with the pMHC affinity dependence and dose independence of this module, given that late Erk activity is the largest signaling difference between

high and low affinity pMHC (**Fig. 2.3 and Fig. 2.5**). Additionally, some modules showed weaker sensitivities to Erk and/or NFAT signaling, yet they showed distinctive dependencies on pMHC inputs (M1, M5, M8), suggesting the presence of additional *trans*- factors responsible for decoding pMHC inputs. Taken together, these results indicate that pMHC affinity- and dose-specific T cell states arise, at least in part, from decoding of long-term signaling dynamics by Erk and NFAT target genes.

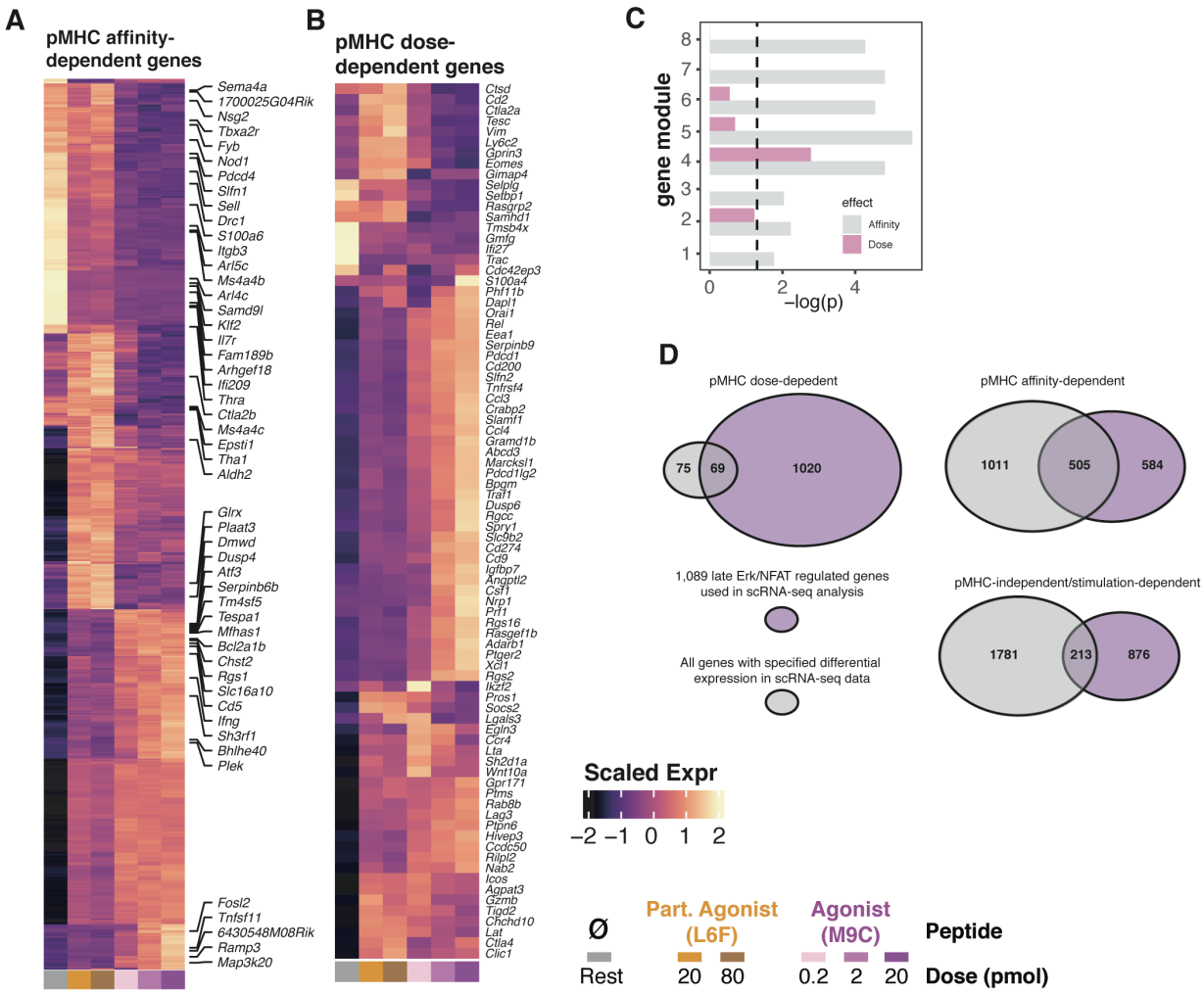

Figure 3.5 pMHC-dependent Gene Programs.

(A) Heatmap of 591 pMHC affinity-dependent Erk and NFAT target genes identified from DEG tests using Monocle3. Expression of each gene is aggregated by pMHC condition, and scaled as a z-score by row (color legend is shared with B). The top 50 DEGs based on effect size are annotated.
(B) Heatmap of 82 pMHC dose-dependent Erk and NFAT target genes identified from DEG tests using Monocle3. Expression of each gene is aggregated by pMHC condition, and scaled as a z-score by row.
(C) Wilcoxon signed rank tests comparing the affinity and dose dependencies of each gene module in Fig. 3.4D-E. All modules show affinity-dependence based on a p-value threshold of 0.05 (dashed line), while only cluster 4 is dose-dependent.
(D) Venn diagrams visualizing the overlap of Erk and NFAT target genes (1,089 DEGs identified from bulk RNA-seq) vs all genes identified in the scRNA-seq dataset as being pMHC affinity or dose dependent, or pMHC independent.

3.3 *CIS*-REGULATORY MECHANISMS TO DECODE ERK AND NFAT SIGNALING

To gain insights into the mechanisms integrating Erk and NFAT signaling inputs to generate pMHC-specific expression patterns, we analyzed mathematical models of candidate *cis*-regulatory mechanisms for selected target genes, to account for experimentally measured Erk and NFAT signaling responses and gene expression patterns. This approach utilizes quantitative measurements of both processes to identify and constrain candidate models of *cis*-regulatory element function, allowing us to determine whether the modeled mechanisms can explain experimental observations, and to determine the plausible parameter regimes under which these mechanisms operate.

We investigated two well-studied T cell activation genes, *Pdcd1* (encoding PD-1) and *Il2ra* (encoding CD25). These genes were chosen for their distinct pMHC affinity and dose dependencies, as well as their inclusion in distinct modules (M4 for *Pdcd1*, M1 for *Il2ra,*), allowing us to explore a range of *cis*-regulatory mechanisms for decoding signaling dynamics (**Fig 3.6A**). We used flow cytometry to measure PD-1 and CD25 levels in T cells activated by M9C and L6F at different doses, as above (**Fig 3.6C, D and Fig. 3.7**). We also perturbed cells with Erk and NFAT inhibitors after 9 hours of stimulation ("Late"). However, because some *cis*-regulatory elements can control activation timing without affecting maintenance of gene expression [4,11–13], as observed for *Il2ra* [11], we also perturbed signaling at the onset of stimulation ("Early"), as Erk and NFAT may play distinct roles in controlling activation versus maintenance of gene expression. Based on these measurements, we developed and fit these data to dynamical models that describe the *cis*-regulatory control of these two genes (**Appendix A**).

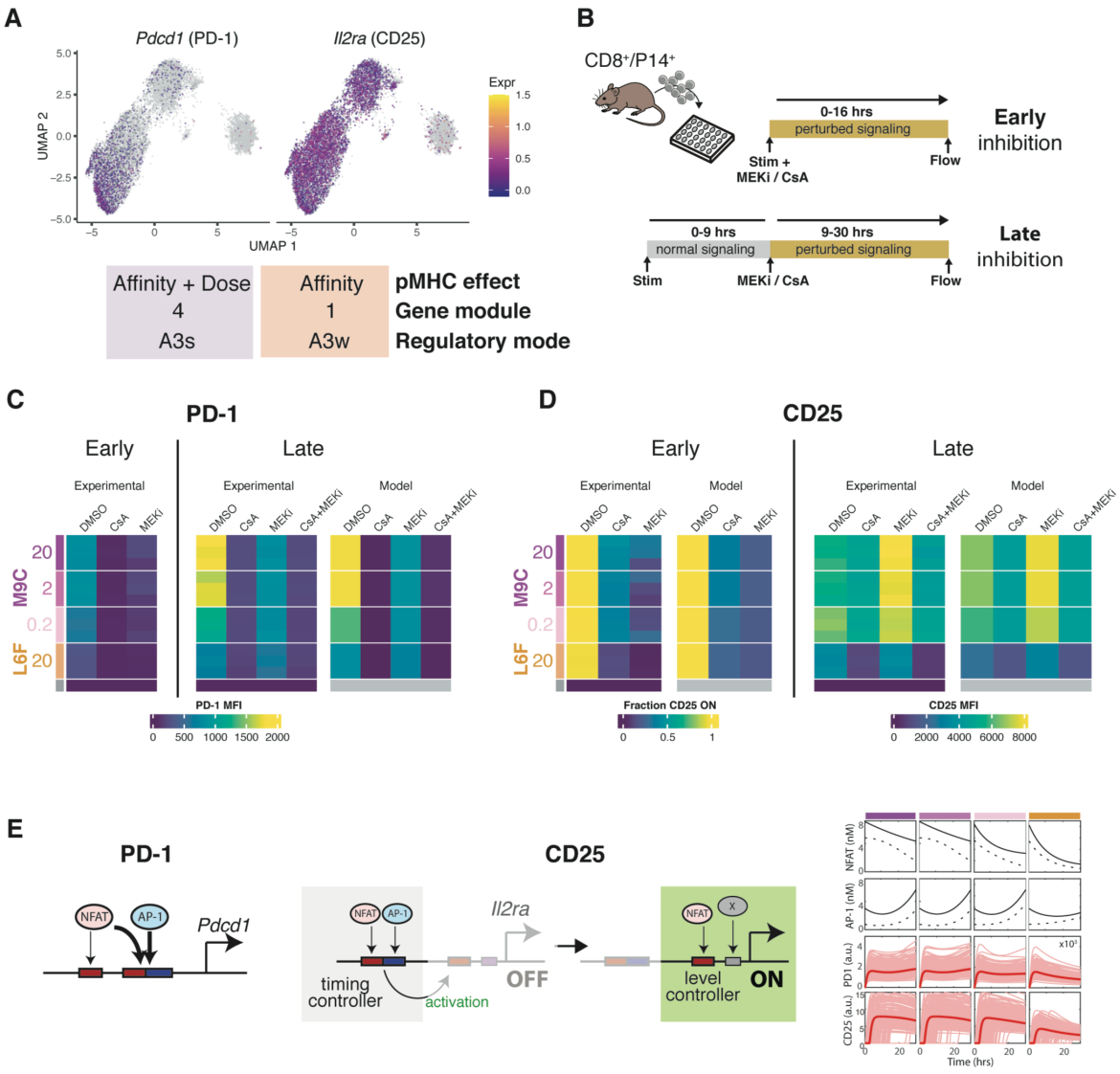

Figure 3.6 Temporal and Combinatorial *cis*-regulatory Mechanisms Work Together to Decode Erk and NFAT Signaling.

(A) scRNA-seq UMAPs overlaid with *Pdcd1* and *Il2ra* expression. *Pdcd1* represents a pMHC affinity- and dose-dependent gene, and belonging to gene module 4 and regulatory mode A3s. *Il2ra* represents a pMHC affinity-dependent gene, and belonging to gene module 1 and regulatory mode A3w.
(B) Non-reporter CD8⁺ T cells were stimulated with various pMHC conditions, treated with MEKi and/or CsA immediately (early) or 9 hrs (late) after stimulation, then assayed for PD-1 and CD25 expression after 16 (early) or 30 (late) hrs.
(C-D) Expression of PD-1 and CD25 in T cells following stimulation with different pMHC inputs and treated with different signaling inhibitors at early and late timepoints. Experimental results are compared with our model predictions.

(E) Proposed NFAT and AP-1 *cis*-regulatory mechanisms controlling PD-1 (*Pdcd1*) and CD25 (*Il2ra*) expression. Mathematical simulations for each pMHC input are shown for each gene, depicting the levels of active NFAT and AP-1 transcription factors, and the resulting expression of PD-1 and CD25.

This analysis revealed an array of regulatory mechanisms that collaborate in *cis*- and *trans*- to enable input-specific expression of these two genes downstream of Erk and NFAT signaling. PD-1 expression is predicted to depend on the concerted action of two elements, both of which are required for the observed dose, affinity and inhibitor dependencies in its expression: (1) an element that binds NFAT without AP-1, and (2) a composite NFAT:AP-1 binding site that acts independently (**Fig 3.6E**). This predicted bipartite architecture contrasts with an alternative where partnerless NFAT may play a dominant role in *Pdcd1* regulation [2], and highlights how target genes may utilize multiple elements that bind TFs in different combinations to construct input-specific responses. CD25 expression is also predicted to require two separate elements, but that have distinct regulatory functions: (1) a timing element consisting of an NFAT:AP-1 composite binding site, and (2) an element controlling expression levels that receives input from NFAT and an undetermined factor X (**Fig 3.6E**). As the timing element is required for initiation but not maintenance of expression, this system enables hysteresis in its regulation, allowing target genes to activate in response to prior signaling exposure. Interestingly, after activation, CD25 expression is regulated not only by a third, unidentified factor, but also by NFAT whose effects are revealed only upon attenuation of Erk signaling and presumably occur by NFAT redirection by AP-1 at other gene loci (**Fig 3.6D and Fig. 3.7B**). These results highlight how *trans*- mechanisms for TF partner redirection could generate additional dependencies for decoding combinatorial signaling states generated by diverse signaling inputs.

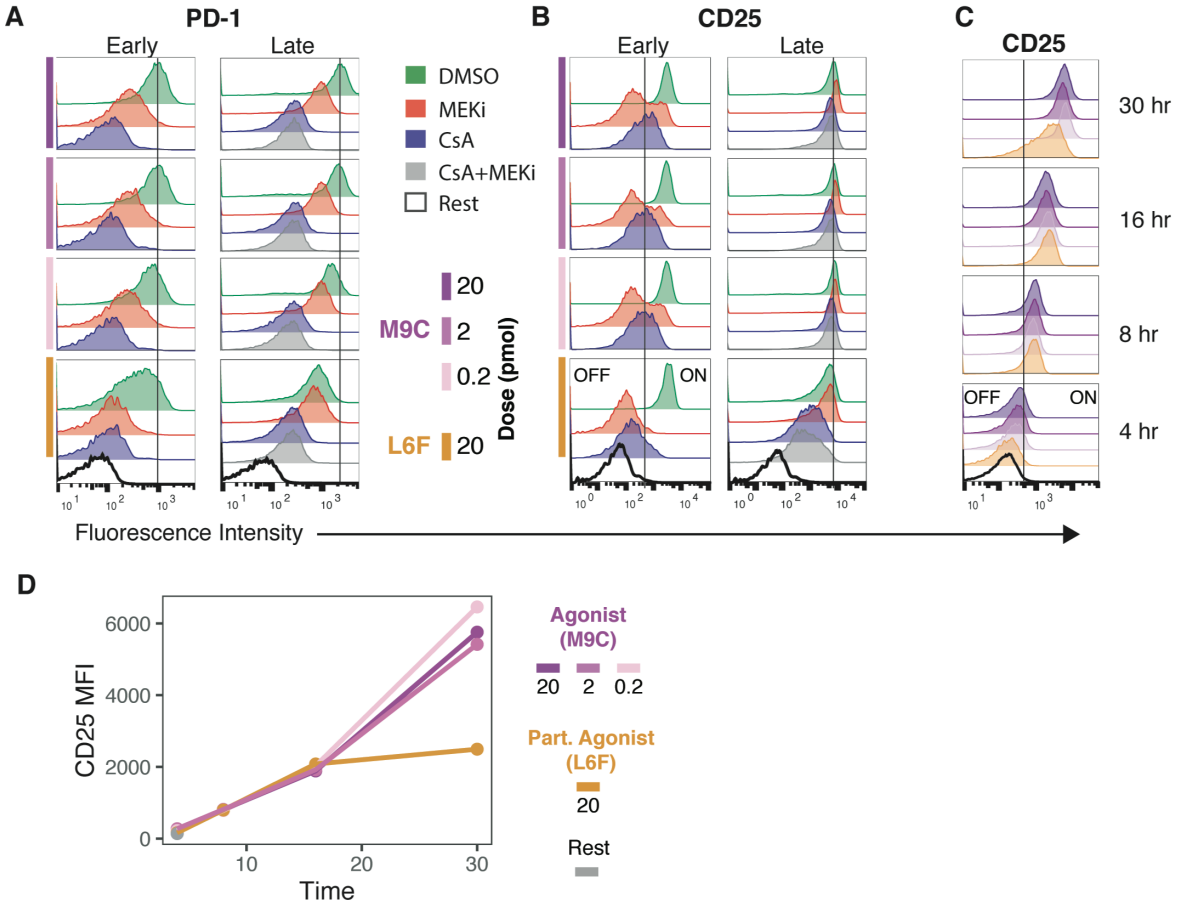

Figure 3.7 Regulation of PD-1 and CD25 by Erk and NFAT Signaling.

(A-B) Flow cytometry plots of PD-1 and CD25 expression in response to different pMHC inputs, and treated with MEKi and CsA at early or late timepoints. See Fig 6B for experimental design. pMHC condition is indicated with the colored bars on the left. Black lines are drawn for reference, with the line for early CD25 response demarcating CD25 ON vs OFF cells.
(C) Time course of CD25 expression in response to different pMHC inputs. Histograms are colored by pMHC condition. Black line shows CD25 ON vs OFF gate from B ("Early").
(D) MFI of CD25 expression over time from the data in (C).

3.4 METHODS

Bulk RNA sequencing

Cells were stimulated as described in Section 2.5, with six 96-wells used per condition to obtain sufficient cell numbers for total RNA yield. Every condition was coated identically, using 2 pmol M9C pMHC. After 9 hours of incubation, cells were treated with either 1 uM MEK inhibitor (Trametinib, Selleckchem Cat. no. S2673), 1 uM Cyclosporin A (Selleckchem Cat. no. 52286), 1 uM of both, or DMSO, yielding a 0.1% final DMSO concentration in all conditions. The cells were cultured for an additional 21 hours (30 hr total stimulation) before harvesting their RNA. To harvest total RNA, 450k total cells per condition were transferred to a pre-chilled 1.5 ml Eppendorf tube and centrifuged for 5 min at 300g and 4°C. Cells were washed 1x in ice-cold PBS. The PBS was removed and the cells were resuspended in 350 ul Trizol (Invitrogen Cat # 15596018) and vortexed for 30 sec to lyse the cells. The samples were then flash-frozen in liquid nitrogen and stored at -80°C for 12 days. RNA was isolated with the RNeasy Micro kit (Qiagen Cat # 74004) starting from step 2 of the manufacturer's protocol. Paired-end library preparation and transcriptome sequencing was conducted by Novogene Co., LTD (Sacramento, CA, USA).

Single-cell RNA sequencing

Cells were stimulated or rested, as described in Section 2.5 for 30 hrs and resuspended in Fc blocking solution (2.4G2 supernatant made in-house) and incubated with one of the six hashtag (HTO) antibodies (1 ug HTO per sample) for 30 min at 4°C. Cells were then washed 2x with FACS buffer. Propidium iodide (Alfa Aesar, Cat # J66584) was spiked into each tube of cells at 1:1,000 and sorted on a BD Aria III for live cells into a single tube, collecting 22,000 total cells (4k from each pMHC condition + 2k rested cells). Single cell library preparation was done with

the 10x Genomics platform, loading all 22k cells into a single lane [14], and following the manufacturer's recommended protocol (CG000205, Rev D, Single Cell 3' v3.1 with feature barcoding, 10x Genomics). Libraries were diluted to 2nM using Agilent Tapestation D1000 HS and loaded onto two NextSeq 2000 P2 100-cycle kits using the following conditions: read 1: 28 cycles; index 1: 8 cycles; read 2: 92 cycles. Data was converted to fastq using bcl2fastq. Cellranger (version 6.0.1, 10x Genomics) was used for transcriptome- and HTO-level UMI and cell demultiplexing, and for aligning the transcriptome to the GRCm38/mm10 reference genome. 1,252 doublets were removed based on HTO antibody counts, and cells with > 7.5% mitochondrial reads were removed. Next, only the DEGs from the bulkRNA-seq analysis (i.e NFAT and Erk regulated genes) expressed in at least 100 cells were included. The resulting scRNA-seq cell dataset contained 1,089 genes and 11,956 cells, with a median UMI (unique molecular identifier)/cell count of 5,972.

Flow cytometry

For extracellular staining following stimulation, cells were resuspended in 50 ul Fc blocking solution for 15 min at 4°C. 50 ul of antibody in Fc blocking solution was added and incubated for 20 min at 4°C. The amount of antibody used per sample was as follows: 1 ul BV605 anti-human CD69; 1 ul BV605 anti-mouse CD69; 1 ul APC anti-mouse CD69; 0.5 ul APC anti-mouse CD25; 1 ul e450 anti-mouse CD279 (PD-1). Cells were washed 1x and analyzed on an Attune Nxt cytometer (Thermo Fisher Scientific). For ppErk staining, cells were fixed in 2% formaldehyde (Fisher Scientific Cat # 50-980-487) in PBS for 20 min at RT. Cells were washed 1x and stored at 4°C until all time points were harvested, then permeabilized with ice-cold 90% MeOH at 4°C overnight. Next, cells were washed 1x, blocked for 15 min at 4°C with Fc blocking

solution. 0.1 ul anti-mouse ppErk1/2 antibody was added per sample in 50 ul Fc blocking solution, the cells were mixed by pipetting up and down 30x, and then incubated for 30 min at RT. The cells were washed 2x and re-suspended in 100 ul FACS buffer containing 0.1 ul Alexa Fluor Plus 555 Goat anti-mouse IgG per sample, and incubated for 20 min at RT in the dark. The cells were then washed 2x and analyzed. For NFAT1 staining, cells were fixed and permeabilized *in situ* using BD Cytofix/Cytoperm kit (BD, Cat # 554714) according to the manufacturer's protocol with some modifications. Following stimulation, half the media was carefully removed so as to not disturb the cells, and replaced with cytofix buffer and incubated for 5 min at RT. This process was repeated 2 more times with a final incubation time of 20 min at 4°C. Cells were gently washed 2x, the plate parfilmed, and stored at 4°C until all time points have been fixed. Cells were then washed 2x with 1x perm/wash buffer, and incubated for 10 min at RT after the second wash. Cells were washed 1x, stained with anti-mouse NFAT1 antibody at 1:200 in 50 ul FACS buffer and incubated for 1 hr at RT in the dark, washed 1x, stained with 0.1 ul Alexa Fluor Plus 488 Goat anti-rabbit IgG per sample in 100 ul FACS buffer and incubated for 1 hr at RT in the dark, and washed 1x. Cells were resuspended in 125 ul of a 1:1,000 dilution of DRAQ5 (Thermo Fisher Scientific, Cat # 62251) in FACS buffer and imaged using spinning disk confocal microscopy with a laser diode illuminator (AF488 - 470 Ex, 510/50 Em; DRAQ5 - 640 Ex, 700/75 Em) (89North) on the Leica DMi8 using for live imaging. Unless specified otherwise, all wash steps used FACS buffer and centrifugation at 300g for 5 min.

Computational analysis of RNA sequencing data

Bulk RNA-seq DEG analysis

Raw FASTQ files from paired-end transcriptome sequencing were aligned to the GRCm38/mm10 reference genome using Kallisto (v0.46.1) [15]. Transcripts were associated with gene names with *biomaRt* using the "mmusculus_gene_ensembl" dataset. Further analysis was performed with the *sleuth* package (v 0.30.0) [16], after first filtering out transcripts with < 5 counts (*sleuth* default). Differential expression analysis was performed following the Pachter lab walkthrough (https://pachterlab.github.io/sleuth_walkthroughs/boj/analysis.html), setting the "MEKi+CsA" treatment as the control condition for differential expression testing, as this condition represented the case where both pathways are inactive at late timepoints. We fit a "full" (multiple conditions) and "reduced" (intercept only) model, then computed the likelihood ratio test between these two models to determine genes regulated by late Erk and/or NFAT activity, as determined by expression changes with single inhibitor treatment or DMSO. From this test, we classified DEGs based on a q-value threshold of 0.001. Finally, to enable comparison with scRNAseq, we took the intersection of this DEG list (1,241 genes) and the list of expressed genes from the scRNA-seq dataset after quality control filtering, yielding 1,089 DEGs used in our analyses. To determine genes that are regulated by Erk, NFAT, or both pathways, we performed Wald tests in *sleuth* on each β coefficient from the "full" model (MEKi, CsA, DMSO). Genes with a q-value below 0.001 for any of the tests were classified as being regulated by the respective pathway(s).

Multiple linear regression models

We used multiple linear regression modeling (**Fig. 3.8**) to estimate the effect of late signaling activity on each DEG's expression level:

$$\hat{y}_{gene} = \beta_N \cdot x_N + \beta_E \cdot x_E + \beta_{EN} \cdot x_E x_N + \beta_o$$

$\hat{y}_{gene}$ is the $\log_2$ expression of a gene for a given treatment condition, measured by bulk RNA-seq, normalized by the mean expression of that gene across all treatment conditions.

x_N , x_E are the integrated activities of the NFAT and Erk pathways upon inhibitor treatment from 7-16 hours, measured by live imaging.

For two replicates of RNA-seq expression measurements (4 conditions x 2 replicates = 8 total data points for fitting), we fit a linear model to each of the 1,089 DEGs using the *lm* function within the *stats* package (v 4.1.2) in R with the following formula: $y \sim x_E * x_N$

List of regression parameters for all genes can be found in Appendix B.

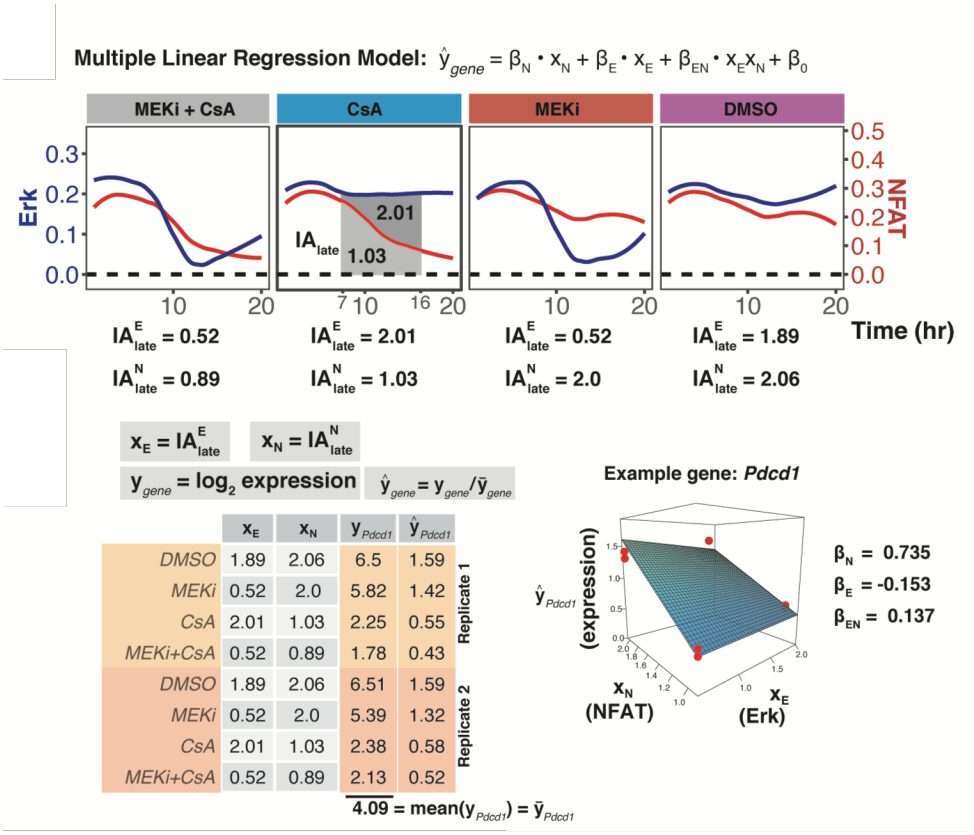

	x_E	x_N	y_{Pdcd1}	$\hat{y}_{Pdcd1}$	
DMSO	1.89	2.06	6.5	1.59	Replicate 1
MEKi	0.52	2.0	5.82	1.42	Replicate 1
CsA	2.01	1.03	2.25	0.55	Replicate 1
MEKi+CsA	0.52	0.89	1.78	0.43	Replicate 1
DMSO	1.89	2.06	6.51	1.59	Replicate 2
MEKi	0.52	2.0	5.39	1.32	Replicate 2
CsA	2.01	1.03	2.38	0.58	Replicate 2
MEKi+CsA	0.52	0.89	2.13	0.52	Replicate 2

Figure 3.8 Multiple Linear Regression Modeling.

Overview of the method for the multiple linear regression models presented in Fig 4F. The integrated activity from 7-16 hrs was calculated from the mean traces of Erk and NFAT activity from cells treated with DMSO, MEKi, CsA, or MEKi+CsA. These values served as predictor variables for modeling the expression of each gene under the same inhibitor conditions, which was determined by bulk RNA seq. Calculation of β coefficients for *Pdcd1* is shown as an example.

scRNA-seq UMAP clustering

Quality control, pre-processing, dimensionality reduction, and UMAP visualization was done with the *Monocle3* [10]package (v 1.2.9) in R following the Trapnell Lab walkthrough (https://cole-trapnell-lab.github.io/monocle3/docs/clustering/), with minor modifications. Following QC (details above), the cell dataset was reduced to 100 dimensions and visualized on a UMAP 2D projection. Cells were partitioned into 8 clusters using the *cluster_cells* function. These 8 clusters contained 95% of the cells, with additional outlier clusters containing the remaining 5% (544 cells) which were removed from the cell dataset for further analyses. To identify pMHC affinity- and dose-dependent genes, we followed the Trapnell Lab walkthrough (https://cole-trapnell-lab.github.io/monocle3/docs/differential/). To identify affinity-dependent DEGs, we subsetted our cell dataset on only cells from 2 or 20 pmol M9C, or L6F stimulation, thereby comparing affinity effects at saturating doses. We used the *fit_models* function and identified DEGs using a 0.05 q-value cutoff. We did the same to identify dose-dependent DEGs, but this time subsetted our cell dataset on only cells from M9C stimulation, thereby comparing dose effects of uniform affinity pMHC. To identify stimulation-dependent, but pMHC-independent genes, we fitted models comparing all stimulation conditions to the rest condition, and identified those genes that were stimulation-dependent, but not affinity or dose dependent. We performed these DEG tests on two cell data sets: (1) the 1,089 Erk and NFAT regulated genes identified from bulk RNA-seq, and (2) all genes identified by scRNA-seq that were expressed in at least 100 cells (**Fig 3.5**).

Single cell gene-gene co-expression analysis

We reasoned that genes co-expressed in single cells would be subject to the same regulatory mechanisms. To test this, we performed LASSO (least absolute shrinkage and selection operator)

regression using the *glmnet* package (v 4.1-4) [17] in R following a previously developed analysis method [6] with some modifications. First, genes expressed in fewer than 5% of the 11,412 cells in our cell dataset were excluded, leaving 810 genes. We scaled the expression of each gene as a z-score and ran the regression analysis for every pairwise set of genes. We used the pairwise regression coefficients, which estimate the correlation between two genes, to populate a gene-by-gene correlation matrix. For each pair of genes, two coefficients are generated (A ~ B and B ~ A), so we averaged the two to create a symmetrical matrix. We removed genes with no correlation to any other gene by excluding rows with a zero sum (a gene with no correlation to another gene yields a coefficient of zero), leaving 309 genes whose expression was correlated with at least one other gene. The resulting matrix was clustered using the "spearman" distance metric and the "average" hierarchical clustering method. Clusters of co-expressed genes were defined from this dendrogram by manually traversing the tree and setting cutoff heights that generated reasonable cluster boundaries based on regions of uniformly high correlation along the diagonal.

Mathematical modeling

Ordinary differential equations simulations of gene regulation models for *Pdcd1* and *Il2ra* were performed using MATLAB. Parameter values for these models were determined by the fitting gene expression values obtained by modeling to experimental measurements of mean fluorescence intensities (***Pdcd1* MFI, *Il2ra* late, Fig. 3.6C, D**) or gene activation percentages (***Il2ra* early, Fig 3.6D**). The sum-squared error of this fit was then minimized using the Nelder-Mead simplex method. In these models, cell-to-cell variability in gene expression was modeled using a cell-extrinsic distribution, via log-normally distributed differences in maximal

transcriptional activity. In our model, activation times for *Il2ra* were exponentially distributed. For simulations, these random activation times were determined through random number generation, followed by the distribution of likelihoods. More details, including equations used, can be found in Appendix C.

3.5 REFERENCES

1. Monje, P., Hernández-Losa, J., Lyons, R. J., Castellone, M. D. & Gutkind, J. S. Regulation of the Transcriptional Activity of c-Fos by ERK: A NOVEL ROLE FOR THE PROLYL ISOMERASE PIN1*. *J. Biol. Chem.* **280**, 35081–35084 (2005).
2. Martinez, G. J. *et al.* The Transcription Factor NFAT Promotes Exhaustion of Activated CD8 + T Cells. *Immunity* **42**, 265–278 (2015).
3. Luna-Zurita, L. *et al.* Complex Interdependence Regulates Heterotypic Transcription Factor Distribution and Coordinates Cardiogenesis. *Cell* **164**, 999–1014 (2016).
4. Chu, J. M., Pease, N. A. & Kueh, H. Y. In search of lost time: Enhancers as modulators of timing in lymphocyte development and differentiation. *Immunol. Rev.* **300**, 134–151 (2021).
5. Levine, J. H. *et al.* Data-Driven Phenotypic Dissection of AML Reveals Progenitor-like Cells that Correlate with Prognosis. *Cell* **162**, 184–197 (2015).
6. Cao, J., Zhou, W., Steemers, F., Trapnell, C. & Shendure, J. Sci-fate characterizes the dynamics of gene expression in single cells. *Nat. Biotechnol.* **38**, 980–988 (2020).
7. Konya, C., Goronzy, J. J. & Weyand, C. M. Treating autoimmune disease by targeting CD8(+) T suppressor cells. *Expert Opin. Biol. Ther.* **9**, 951–965 (2009).
8. Liu, J., Chen, D., Nie, G. D. & Dai, Z. CD8(+)CD122(+) T-Cells: A Newly Emerging Regulator with Central Memory Cell Phenotypes. *Front. Immunol.* **6**, 494 (2015).
9. Aibar, S. *et al.* SCENIC: single-cell regulatory network inference and clustering. *Nat. Methods* **14**, 1083–1086 (2017).
10. Trapnell, C. *et al.* The dynamics and regulators of cell fate decisions are revealed by pseudotemporal ordering of single cells. *Nat. Biotechnol.* **32**, 381–386 (2014).

11. Simeonov, D. R. *et al.* Discovery of stimulation-responsive immune enhancers with CRISPR activation. *Nature* **549**, 111–115 (2017).
12. Pease, N. A. *et al.* Tunable, division-independent control of gene activation timing by a polycomb switch. *Cell Rep.* **34**, 108888 (2021).
13. Ng, K. K. *et al.* A stochastic epigenetic switch controls the dynamics of T-cell lineage commitment. *eLife* **7**, e37851 (2018).
14. Stoeckius, M. *et al.* Cell Hashing with barcoded antibodies enables multiplexing and doublet detection for single cell genomics. *Genome Biol.* **19**, 224 (2018).
15. Bray, N. L., Pimentel, H., Melsted, P. & Pachter, L. Near-optimal probabilistic RNA-seq quantification. *Nat. Biotechnol.* **34**, 525–527 (2016).
16. Pimentel, H., Bray, N. L., Puente, S., Melsted, P. & Pachter, L. Differential analysis of RNA-seq incorporating quantification uncertainty. *Nat. Methods* **14**, 687–690 (2017).
17. Friedman, J. H., Hastie, T. & Tibshirani, R. Regularization Paths for Generalized Linear Models via Coordinate Descent. *J. Stat. Softw.* **33**, 1–22 (2010).

Chapter 4. Conclusions and Future Directions

4.1 Discussion

We developed an *in vitro* platform to continuously measure the dynamic Erk and NFAT signaling responses in individual T cells as they respond to varying pMHC inputs. We used this platform to show that T cells independently encode pMHC affinity and dose information using the long-term (9+ hrs) dynamics of these two pathways, with Erk and NFAT dynamics encoding affinity and dose information respectively. Through perturbation experiments, we identified target genes of Erk and NFAT signaling and further defined regulatory modes by which these genes decode Erk and NFAT dynamics. Lastly, using scRNA-seq, we identified gene programs that vary with pMHC affinity and dose, and show how their pMHC-dependent expression arises from decoding of Erk and NFAT dynamics at the *cis*-regulatory level. Analysis of these gene programs reveals a previously unappreciated role for long-timescale signaling dynamics in encoding T cell antigen information, and highlights how multiple signaling pathways that emanate from the T cell receptor can work together to encode distinct features of signaling inputs.

Our findings indicate that T cells initially activate uniformly, and elaborate pMHC-specific signaling and gene regulatory responses only after prolonged contact with various pMHC inputs. This shared molecular program for early activation, also observed in other studies [1–3], may enable T cells to prepare for a potential response before fully determining the nature of the threat. Such early response initiation may allow for rapid responses if a threat is indeed present, which may be critical as T cells reach the point of first cell division only ~30 hrs after pMHC encounter [4]. The lag in pMHC dose and affinity-dependent responses may be due to time-delayed negative feedback on signaling resulting in reduced sensitivity to pMHC inputs, such that only high affinity pMHC

can overcome this feedback. Indeed, T cell signaling is subject to multiple layers of negative feedback [5–8]. Some of these negative feedback loops, particularly those involving transcription of checkpoint inhibitory molecules [9,10], may act on extended time-scales similar to those we observed. Alternatively, the pMHC-specific response lag may reflect a need for T cells to integrate pMHC information over extended durations for accurate input discrimination [11–13]. In this picture, late divergent Erk and NFAT signaling levels would result from prior pMHC exposure along with immediate signaling inputs, potentially through cytokine feedback loops that could provide additional inputs into these pathways [12,14].

The multiple mechanisms by which gene regulatory elements can decode pMHC-dependent Erk and NFAT signals enables T cells to elaborate distinct functional programs in response to different pMHC inputs. Our transcriptomic studies of Erk and NFAT regulation, together with further in-depth analysis of *cis*-regulatory systems of specific genes (*Pdcd1* and *Il2ra*), indicate that target genes can be controlled through multiple *cis*-regulatory elements where Erk and NFAT can either act in combination, or singly; each of which may have different transcriptional outputs. Furthermore, Erk and NFAT can be readily redirected on a global level by the abundance of their partners, also observed in other contexts [5,15], and may enable a shift if the usage of these *cis*-regulatory elements depending on the cell's signaling state. Finally, Erk and NFAT signaling activity can modulate gene activation timing but not maintenance of expression, possibly through enhancer elements that control chromatin states [6,16,17], a finding that provides a mechanism by which cells can temporally-integrate cumulative Erk and NFAT signaling dynamics to generate stable pMHC-dependent changes in gene programming [18].

An ability to independently perceive pMHC affinity and dose may be critical for allowing T cells to selectively counter pathogens while suppressing responses to self that could lead to autoimmunity. While T cells with high affinity for self-pMHCs are eliminated during negative selection, those retained in the periphery can have affinities for self-pMHC that are very close to the sharp threshold for negative selection [7,19,20]. Though these T cells with lower-affinity TCRs are able to fully activate upon antigen encounter [2,3], they are far less efficient in mediating autoimmune destruction of healthy tissues compared to those with high-affinity TCRs [8], but may rely on a suppressive program, nonetheless, to prevent spurious effector responses. Our transcriptomic profiling showed that T cells activated by low-affinity pMHCs maintain a distinct functional program with attenuated effector programming (*Irf4* and others) and up-regulation of the immune checkpoint and suppressor function genes (i.e. *Ctla4*, *Cd47*, *Il2rb*). In contrast, T cells activated by high doses of high affinity pMHCs did not activate these suppressive genes, but instead upregulated distinct immune checkpoint genes (e.g. *Pdcd1*, *Lag3*), possibly reflecting a distinct inhibitory program for dampening hyperactive cytotoxic activities during severe pathology. Future studies should investigate these pMHC-dependent regulatory and functional states, particularly in contexts where T cell antigen recognition can result in initiation of autoimmune pathologies.

4.2 Future Directions

Not only does the work presented here extend our understanding of biological phenomena within several fields of study, including Immunology, Systems Biology, and Cell Biology, but it poses new important questions and provides guiding insight into testable hypotheses to address them. We suggest two possible models by which the TCR signaling network could generate the pMHC-specific long term Erk and NFAT dynamics we observed. First, an adaptation model whereby negative feedback following initial signaling filters out subsequent weak signals, and second, a temporal integration model whereby cumulative TCR and non-TCR inputs (i.e. cytokines) over extended timescales produces divergent late signaling activity. In our study, we kept the signaling inputs (pMHC) constant over the duration of our observation period. To test these two potential models, we would instead vary the pMHC input dynamics, as well as measure the effects of potential soluble inputs differentially secreted by the different pMHC inputs. T cells communicate with other immune cells to coordinate efficient responses, and much of this communication is achieved through soluble factors, such as cytokines. It would be interesting to investigate how known intercellular communication signals, such as IL-2, regulate Erk and NFAT signaling over the day- and week-long timescales of the various stages of the adaptive immune response. It would also be relevant to measure the dynamic response of the NF-kB pathway to variable pMHC inputs, which regulates many immune response genes and has been shown previously to activate in a pMHC-dependent manner in T cells [21].

Next, we suspect that the Erk and NFAT signaling responses elicited in tumor-specific T cells contribute to an impaired ability to eliminate tumors. We know that many factors within suppressive tumor environments contribute to failed tumor clearance, but understanding how

these signals are informing T cell states, whether through Erk and NFAT signaling or other signaling pathways will enable improvements in engineered T cell therapies. Indeed, targeting NFAT signaling is gaining interest for cancer therapeutics [22]. In this light, we identified a set of genes responsible for suppressing T cell function that are responsive to high levels of late NFAT signaling (i.e. *Pdcd1, Lag3*). Could signaling through these inhibitory receptors feed into the Erk and NFAT pathways to guide T cell fates? In the context of autoimmunity, are elevated levels of Erk and NFAT signaling in response to self-antigens causing autoimmune pathologies? Understanding the molecular mechanisms that lead T cells to initiate effector responses to low affinity self-antigens would provide tangible targets for developing therapies against autoimmune diseases.

Finally, our work sheds light on how cells interpret extracellular information to make decisions. The TCR and its downstream signaling network represent one of the most exquisite detection systems found in nature, and we have taken standard approaches for studying signal encoding and applied it to this highly complex signaling and regulatory system. Our work adds to the many signal encoding studies done before us and contributes to a framework for studying signal encoding and cellular decision making in other contexts. Advances in synthetic biology and protein engineering is rapidly expanding the toolbox of genetically encoded reporters, much like the ones we used here, as well as signal recorders [23,24] and designed signaling modulators [25–27]. It will be exciting to see these tools used to investigate a broader range of biological signal processing networks and how they can be leveraged to engineer therapeutic cells.

4.3 REFERENCES

1. Rosette, C. *et al.* The Impact of Duration versus Extent of TCR Occupancy on T Cell Activation: A Revision of the Kinetic Proofreading Model. 12 (2001).
2. Richard, A. C. *et al.* T cell cytolytic capacity is independent of initial stimulation strength. *Nat. Immunol.* **19**, 849–858 (2018).
3. Ma, C. Y., Marioni, J. C., Griffiths, G. M. & Richard, A. C. Stimulation strength controls the rate of initiation but not the molecular organisation of TCR-induced signalling. *eLife* **9**, e53948 (2020).
4. Marchingo, J. M. *et al.* T cell signaling. Antigen affinity, costimulation, and cytokine inputs sum linearly to amplify T cell expansion. *Science* **346**, 1123–1127 (2014).
5. Luna-Zurita, L. *et al.* Complex Interdependence Regulates Heterotypic Transcription Factor Distribution and Coordinates Cardiogenesis. *Cell* **164**, 999–1014 (2016).
6. Sen, S., Cheng, Z., Sheu, K. M., Chen, Y. H. & Hoffmann, A. Gene Regulatory Strategies that Decode the Duration of NFκB Dynamics Contribute to LPS- versus TNF-Specific Gene Expression. *Cell Syst.* S240547121930465X (2020) doi:10.1016/j.cels.2019.12.004.
7. Naeher, D. *et al.* A constant affinity threshold for T cell tolerance. *J. Exp. Med.* **204**, 2553–2559 (2007).
8. Koehli, S., Naeher, D., Galati-Fournier, V., Zehn, D. & Palmer, E. Optimal T-cell receptor affinity for inducing autoimmunity. *Proc. Natl. Acad. Sci.* **111**, 17248–17253 (2014).
9. Elliot, T. A. E. *et al.* Antigen and checkpoint receptor engagement recalibrates T cell receptor signal strength. *Immunity* **54**, 2481-2496.e6 (2021).
10. Greenwald, R. J., Freeman, G. J. & Sharpe, A. H. The B7 Family Revisited. *Annu. Rev. Immunol.* **23**, 515–548 (2005).

11. Harris, M. J., Fuyal, M. & James, J. R. Quantifying persistence in the T-cell signaling network using an optically controllable antigen receptor. *Mol. Syst. Biol.* **17**, e10091 (2021).
12. Tkach, K. E. *et al.* T cells translate individual, quantal activation into collective, analog cytokine responses via time-integrated feedbacks. *eLife* **2014**, 1–30 (2014).
13. Au-Yeung, B. B. *et al.* Quantitative and temporal requirements revealed for Zap70 catalytic activity during T cell development. *Nat. Immunol.* **15**, 687–694 (2014).
14. Achar, S. R. *et al.* Universal antigen encoding of T cell activation from high-dimensional cytokine dynamics. *Science* **376**, 880–884 (2022).
15. Hosokawa, H. *et al.* Transcription Factor PU.1 Represses and Activates Gene Expression in Early T Cells by Redirecting Partner Transcription Factor Binding. *Immunity* **48**, 1119-1134.e7 (2018).
16. Chu, J. M., Pease, N. A. & Kueh, H. Y. In search of lost time: Enhancers as modulators of timing in lymphocyte development and differentiation. *Immunol. Rev.* **300**, 134–151 (2021).
17. Simeonov, D. R. *et al.* Discovery of stimulation-responsive immune enhancers with CRISPR activation. *Nature* **549**, 111–115 (2017).
18. Pease, N. A. *et al.* Tunable, division-independent control of gene activation timing by a polycomb switch. *Cell Rep.* **34**, 108888 (2021).
19. Alam, S. M. *et al. T-cell-receptor affinity and thymocyte positive selection*. vol. 381 (1996).
20. Daniels, M. A. *et al.* Thymic selection threshold defined by compartmentalization of Ras/MAPK signalling. *Nature* **444**, 724–729 (2006).
21. Gallagher, M. P. *et al.* Hierarchy of signaling thresholds downstream of the T cell receptor and the Tec kinase ITK. *Proc. Natl. Acad. Sci.* **118**, e2025825118 (2021).

22. Flores, C., Fouquet, G., Moura, I. C., Maciel, T. T. & Hermine, O. Lessons to Learn From Low-Dose Cyclosporin-A: A New Approach for Unexpected Clinical Applications. *Front. Immunol.* **10**, (2019).
23. Kempton, H. R., Love, K. S., Guo, L. Y. & Qi, L. S. Scalable biological signal recording in mammalian cells using Cas12a base editors. *Nat. Chem. Biol.* **18**, 742–750 (2022).
24. Sheth, R. U. & Wang, H. H. DNA-based memory devices for recording cellular events. *Nat. Rev. Genet.* **19**, 718–732 (2018).
25. Roybal, K. T. *et al.* Engineering T Cells with Customized Therapeutic Response Programs Using Synthetic Notch Receptors. *Cell* **167**, 419-432.e16 (2016).
26. Roybal, K. T. *et al.* Precision Tumor Recognition by T Cells with Combinatorial Antigen-Sensing Circuits. *Cell* **164**, 770–779 (2016).
27. Ede, C., Chen, X., Lin, M. Y. & Chen, Y. Y. Quantitative Analyses of Core Promoters Enable Precise Engineering of Regulated Gene Expression in Mammalian Cells. *ACS Synth. Biol.* **5**, 395–404 (2016).

Appendix A – Representative Time-Lapse Imaging

Representative time-lapse movies (only the first frame is shown here) of individual well positions corresponding to each of the five pMHC conditions assayed in this study. Shown to the right of the movies for each condition is the mean +/- 99% confidence interval Erk and NFAT signaling responses for all cells analyzed from the specific well position shown in the movie. Nuclear and cytoplasmic segmentations are shown in dashed and solid lines, respectively. Scale bar = 5 um.

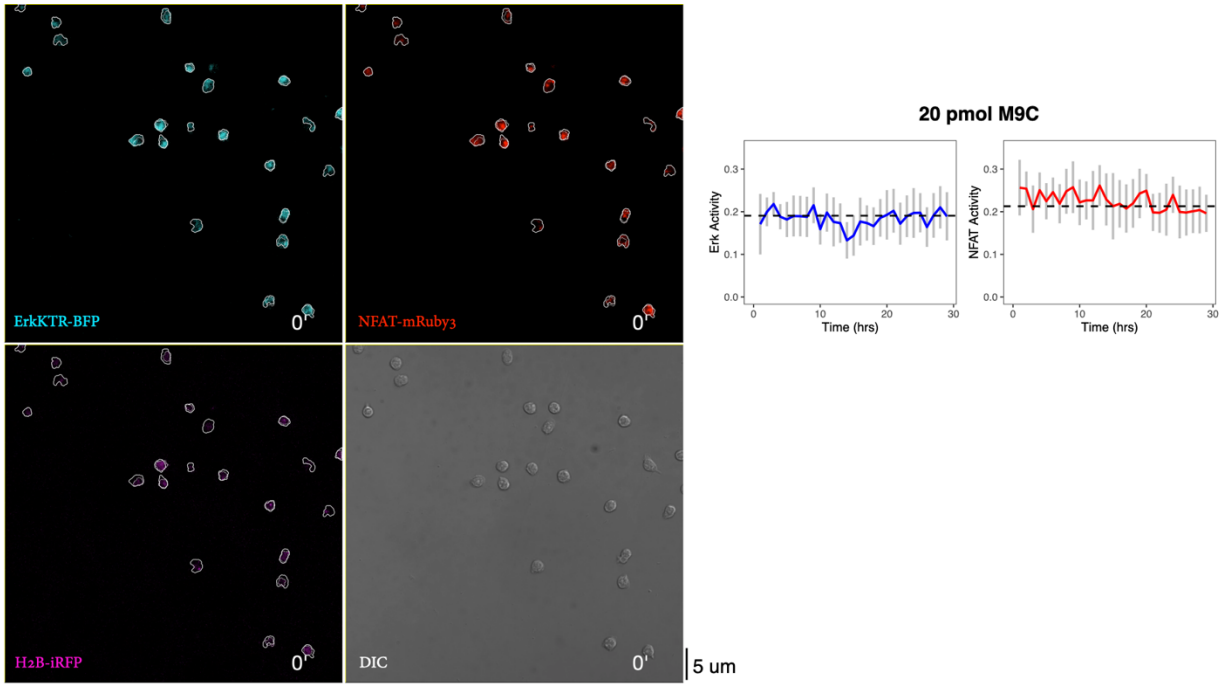

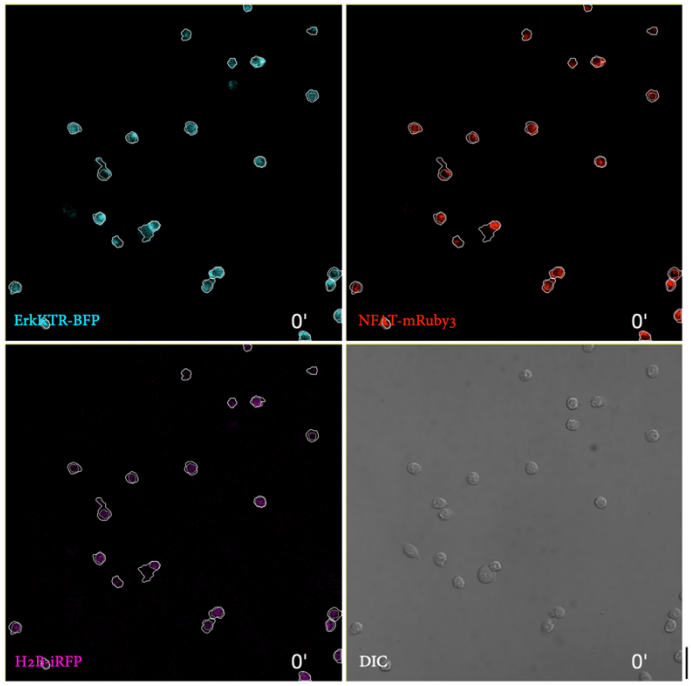
ErkKTR-BFP
0'
NFAT-mRuby3
0'
H2B-iRFP
0'
DIC
0'
5 um

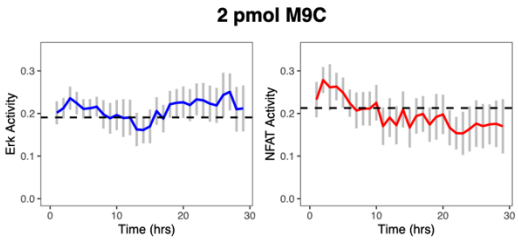
2 pmol M9C
Erk Activity
NFAT Activity
Time (hrs)
Time (hrs)

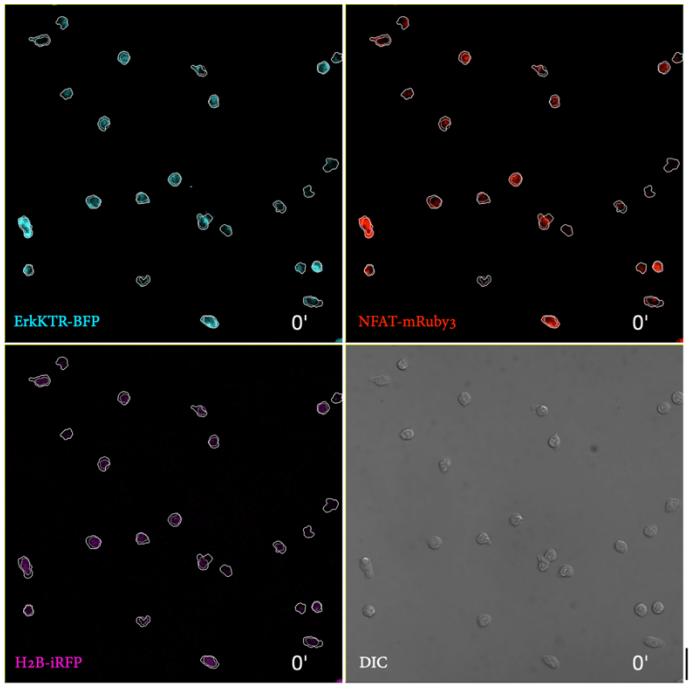
ErkKTR-BFP
0'
NFAT-mRuby3
0'
H2B-iRFP
0'
DIC
0'
5 um

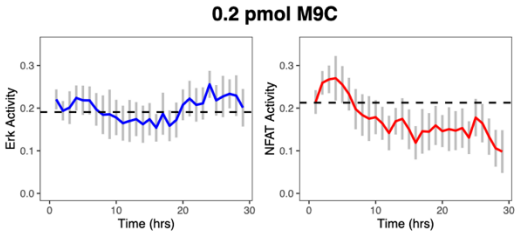
0.2 pmol M9C
Erk Activity
NFAT Activity
Time (hrs)
Time (hrs)

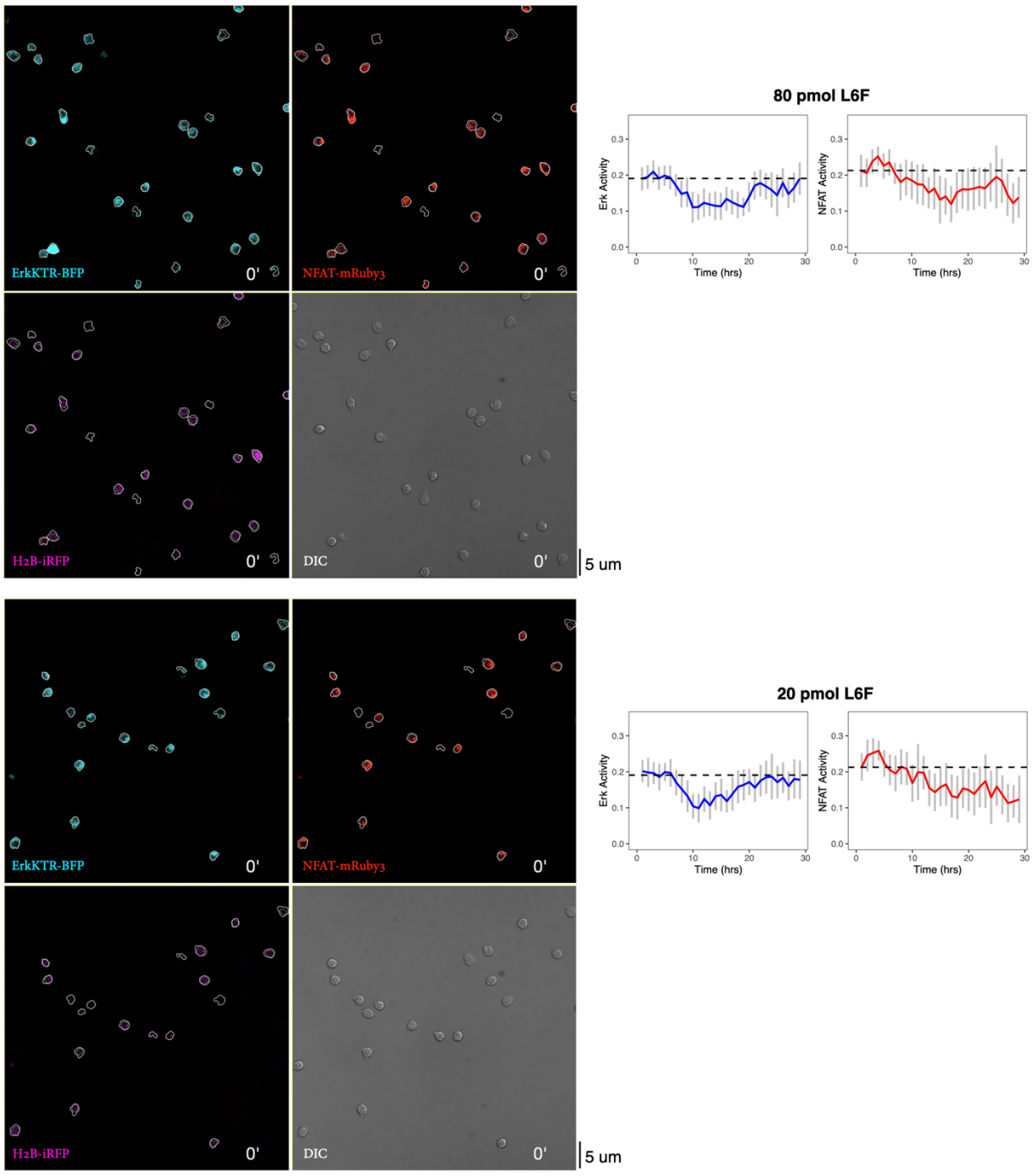
ErkKTR-BFP
0'
NFAT-mRuby3
0'
H2B-iRFP
0'
DIC
0'
5 um
80 pmol L6F
Erk Activity
NFAT Activity
Time (hrs)
20 pmol L6F

Appendix B – Linear Models

Multiple linear regression parameters for each of the 1,089 Erk and NFAT regulated genes. Provided are the 8 fitted, normalized $\log_2$ expression counts from two replicates of the four treatment conditions for each gene (DMSO, DMSO1, etc.), the β coefficients (Erk (E), NFAT (N), ErkNFAT (EN)) along with their p values and standard errors, the model intercept (B0), R^2, and residual standard error (RSE) values. The column "reg-mode" indicates the regulatory mode each gene was classified as based on its pattern of expression from inhibitor treatments.

Gene	Erk(E)	NFAT(N)	ErkNFAT(EN)	B0	R2	RSE	pval(E)	se(E)	pval(N)	se(N)	pval(EN)	se(EN)	DMSO	MEKi	CsA	MEKi+CsA	DMSO1	MEKi1	CsA1	MEKi+CsA1	reg_mode
Noc3l	0.030	0.075	0.009	0.835	0.925	0.017	0.292	0.025	0.026	0.022	0.597	0.016	1.080	1.009	0.990	0.921	1.080	1.009	0.990	0.921	A3w
Pdlim1	0.010	-0.090	-0.014	1.150	0.957	0.013	0.641	0.019	0.006	0.017	0.311	0.012	0.927	0.959	1.047	1.067	0.927	0.959	1.047	1.067	R3w
Arhgap19	-0.045	-0.102	-0.036	1.276	0.919	0.034	0.407	0.049	0.077	0.043	0.310	0.031	0.840	1.010	1.006	1.144	0.840	1.010	1.006	1.144	R2w
Rrp12	-0.007	0.066	0.028	0.859	0.899	0.021	0.827	0.030	0.071	0.027	0.229	0.020	1.088	1.016	0.969	0.927	1.088	1.016	0.969	0.927	A3w
Sfxn3	0.016	-0.198	-0.095	1.452	0.937	0.053	0.841	0.077	0.044	0.068	0.128	0.050	0.708	0.966	1.087	1.239	0.708	0.966	1.087	1.239	R3w
Pprc1	0.066	0.114	-0.021	0.788	0.951	0.013	0.027	0.019	0.003	0.017	0.162	0.012	1.064	1.028	0.993	0.915	1.064	1.028	0.993	0.915	A3w
Nolc1	0.013	0.071	0.008	0.864	0.897	0.017	0.622	0.024	0.029	0.021	0.652	0.016	1.063	1.021	0.978	0.938	1.063	1.021	0.978	0.938	A3w
Trim8	-0.072	0.108	0.048	0.838	0.980	0.014	0.023	0.020	0.004	0.018	0.020	0.013	1.111	1.066	0.904	0.919	1.111	1.066	0.904	0.919	A4w
Pdcd11	0.008	0.076	0.011	0.857	0.967	0.010	0.620	0.015	0.004	0.013	0.320	0.009	1.069	1.024	0.972	0.934	1.069	1.024	0.972	0.934	A3w
Add3	-0.005	-0.129	-0.041	1.274	0.945	0.027	0.914	0.040	0.022	0.035	0.189	0.026	0.843	0.971	1.049	1.137	0.843	0.971	1.049	1.137	R3w
Dusp5	0.168	-0.176	-0.041	1.131	0.987	0.017	0.002	0.025	0.001	0.022	0.061	0.016	0.928	0.824	1.204	1.043	0.928	0.824	1.204	1.043	I
Pdcd4	-0.144	-0.172	0.030	1.379	0.913	0.034	0.044	0.050	0.017	0.044	0.405	0.032	0.870	0.991	0.975	1.164	0.870	0.991	0.975	1.164	R2w
Ablim1	0.000	-0.066	-0.044	1.180	0.855	0.035	0.998	0.050	0.213	0.045	0.246	0.032	0.875	1.003	1.022	1.101	0.875	1.003	1.022	1.101	R2w
Plp2	0.026	-0.035	-0.032	1.081	0.846	0.020	0.417	0.028	0.235	0.025	0.152	0.018	0.932	0.990	1.030	1.048	0.932	0.990	1.030	1.048	R3w
Ddx3x	0.012	0.064	-0.002	0.894	0.945	0.009	0.383	0.013	0.005	0.011	0.797	0.008	1.039	1.025	0.979	0.956	1.039	1.025	0.979	0.956	A3w
Nkrf	-0.002	0.078	0.034	0.822	0.941	0.020	0.954	0.029	0.038	0.025	0.138	0.019	1.112	1.013	0.969	0.907	1.112	1.013	0.969	0.907	A3w
Sh2d1a	-0.298	0.319	0.087	0.729	0.980	0.039	0.006	0.057	0.003	0.050	0.076	0.037	1.161	1.304	0.637	0.899	1.161	1.304	0.637	0.899	A4
Sash3	-0.055	-0.108	0.011	1.209	0.969	0.011	0.028	0.016	0.002	0.015	0.352	0.011	0.926	0.975	1.010	1.089	0.926	0.975	1.010	1.089	R3w
Phf6	-0.007	0.118	0.016	0.803	0.984	0.010	0.669	0.015	0.001	0.013	0.166	0.009	1.094	1.051	0.943	0.912	1.094	1.051	0.943	0.912	A3w
Rtl8b	-0.049	-0.164	-0.026	1.355	0.878	0.048	0.517	0.070	0.057	0.062	0.591	0.045	0.823	0.974	1.033	1.170	0.823	0.974	1.033	1.170	R2w
Cd99l2	-0.136	-0.188	-0.044	1.531	0.967	0.039	0.073	0.056	0.020	0.050	0.290	0.036	0.717	1.038	0.974	1.271	0.717	1.038	0.974	1.271	R1w
Abcd1	-0.079	-0.182	-0.048	1.459	0.913	0.055	0.378	0.080	0.063	0.071	0.407	0.052	0.750	1.004	1.014	1.232	0.750	1.004	1.014	1.232	R2w
Flna	0.014	-0.078	-0.048	1.189	0.914	0.028	0.744	0.040	0.094	0.036	0.138	0.026	0.868	0.990	1.038	1.104	0.868	0.990	1.038	1.104	R3w
Gab3	-0.080	-0.462	-0.102	1.979	0.963	0.075	0.503	0.109	0.009	0.096	0.218	0.070	0.482	0.907	1.135	1.476	0.482	0.907	1.135	1.476	R2
Foxo4	0.243	0.062	-0.176	0.935	0.956	0.024	0.002	0.034	0.112	0.030	0.001	0.022	0.838	1.002	1.125	1.035	0.838	1.002	1.125	1.035	R3w
Btk	-1.312	-0.346	1.043	1.194	0.954	0.149	0.004	0.216	0.146	0.192	0.002	0.140	2.055	0.905	0.354	0.686	2.055	0.905	0.354	0.686	A3
Armcx2	0.399	-0.035	-0.168	0.872	0.971	0.032	0.001	0.047	0.453	0.042	0.005	0.030	0.902	0.835	1.292	0.971	0.902	0.835	1.292	0.971	I
Tsc22d3	0.096	-0.284	-0.165	1.613	0.913	0.093	0.515	0.135	0.076	0.120	0.131	0.087	0.570	0.923	1.175	1.332	0.570	0.923	1.175	1.332	R2
Kdm5c	0.014	0.032	0.015	0.907	0.969	0.007	0.244	0.010	0.025	0.009	0.094	0.007	1.057	0.994	0.999	0.950	1.057	0.994	0.999	0.950	A3w
Ctps2	-0.007	-0.113	-0.020	1.216	0.851	0.034	0.889	0.050	0.062	0.044	0.566	0.032	0.891	0.964	1.043	1.101	0.891	0.964	1.043	1.101	R3w
Gpm6b	-0.464	0.568	0.343	0.085	0.954	0.125	0.062	0.181	0.024	0.161	0.043	0.117	1.708	1.338	0.443	0.511	1.708	1.338	0.443	0.511	A3
Tmsb4x	0.053	-0.070	-0.018	1.073	0.910	0.017	0.102	0.025	0.034	0.022	0.318	0.016	0.958	0.942	1.070	1.030	0.958	0.942	1.070	1.030	I
Hccs	0.011	0.087	0.013	0.833	0.892	0.022	0.751	0.031	0.035	0.028	0.569	0.020	1.081	1.026	0.970	0.922	1.081	1.026	0.970	0.922	A3w

Gene	Erk(E)	NFAT(N)	ErkNFAT(EN)	B0	R2	RSE	pval(E)	se(E)	pval(N)	se(N)	pval(EN)	se(EN)	DMSO	MEKi	CsA	MEKi+CsA	DMSO1	MEKi1	CsA1	MEKi+CsA1	reg_mode
Tram1	0.036	-0.013	-0.047	1.062	0.865	0.019	0.264	0.028	0.624	0.025	0.061	0.018	0.922	1.006	1.025	1.047	0.922	1.006	1.025	1.047	R3w
Imp4	0.009	0.082	0.007	0.855	0.909	0.017	0.727	0.024	0.019	0.022	0.698	0.016	1.065	1.030	0.970	0.936	1.065	1.030	0.970	0.936	A3w
Neurl3	0.172	-0.431	-0.114	1.644	0.975	0.052	0.085	0.076	0.003	0.067	0.079	0.049	0.640	0.753	1.312	1.295	0.640	0.753	1.312	1.295	R3
Mitd1	-0.081	-0.174	0.030	1.305	0.938	0.022	0.064	0.032	0.004	0.028	0.222	0.021	0.909	0.945	1.025	1.121	0.909	0.945	1.025	1.121	R2w
Il18r1	-0.301	-0.294	-0.002	1.816	0.947	0.069	0.040	0.100	0.030	0.089	0.971	0.065	0.634	1.068	0.905	1.394	0.634	1.068	0.905	1.394	R1
Fhl2	0.128	0.473	-0.155	0.423	0.984	0.024	0.022	0.035	0.000	0.031	0.002	0.023	1.037	1.276	0.846	0.841	1.037	1.276	0.846	0.841	A4w
Slc39a10	0.063	0.205	0.021	0.577	0.987	0.017	0.068	0.025	0.001	0.022	0.261	0.016	1.199	1.042	0.957	0.803	1.199	1.042	0.957	0.803	A3w
Stat1	-0.038	-0.057	-0.013	1.156	0.892	0.021	0.276	0.030	0.100	0.027	0.550	0.020	0.918	1.009	0.995	1.079	0.918	1.009	0.995	1.079	R2w
Inpp1	0.102	-0.067	-0.091	1.144	0.924	0.031	0.087	0.045	0.171	0.040	0.035	0.029	0.845	0.968	1.092	1.095	0.845	0.968	1.092	1.095	R3w
Stk17b	0.020	-0.073	-0.026	1.133	0.939	0.016	0.425	0.023	0.023	0.020	0.152	0.015	0.919	0.970	1.045	1.066	0.919	0.970	1.045	1.066	R3w
Nop58	0.011	0.041	0.006	0.914	0.902	0.010	0.487	0.015	0.036	0.013	0.581	0.010	1.042	1.008	0.991	0.959	1.042	1.008	0.991	0.959	A3w
Abi2	0.089	0.069	0.063	0.671	0.939	0.041	0.210	0.060	0.267	0.053	0.181	0.039	1.223	0.919	1.049	0.808	1.223	0.919	1.049	0.808	A1w
Cd28	0.144	-0.001	-0.063	0.941	0.943	0.015	0.003	0.022	0.945	0.020	0.012	0.014	0.967	0.948	1.100	0.986	0.967	0.948	1.100	0.986	I
Ctla4	0.068	0.098	-0.115	0.984	0.878	0.034	0.237	0.049	0.085	0.043	0.021	0.032	0.867	1.097	0.983	1.054	0.867	1.097	0.983	1.054	R1w
Icos	0.044	0.123	0.007	0.750	0.866	0.033	0.411	0.048	0.045	0.043	0.843	0.031	1.111	1.026	0.978	0.886	1.111	1.026	0.978	0.886	A3w
Klf7	0.222	0.106	-0.253	1.037	0.857	0.075	0.109	0.108	0.330	0.096	0.022	0.070	0.695	1.103	1.072	1.130	0.695	1.103	1.072	1.130	R3w
Ikzf2	-0.330	-0.097	-0.035	1.618	0.949	0.070	0.032	0.102	0.342	0.090	0.623	0.066	0.660	1.215	0.783	1.341	0.660	1.215	0.783	1.341	R1
Ctdsp1	0.009	0.012	-0.045	1.054	0.900	0.017	0.734	0.025	0.607	0.022	0.050	0.016	0.922	1.037	0.992	1.049	0.922	1.037	0.992	1.049	R1w
Wnt10a	-0.129	0.411	0.452	-0.296	0.957	0.149	0.583	0.216	0.098	0.192	0.032	0.139	2.058	0.929	0.797	0.216	2.058	0.929	0.797	0.216	A3
Agfg1	-0.030	0.012	0.039	0.947	0.871	0.016	0.259	0.023	0.603	0.021	0.058	0.015	1.066	0.995	0.979	0.960	1.066	0.995	0.979	0.960	A4w
Sp140	-0.047	-0.184	0.020	1.297	0.953	0.021	0.190	0.030	0.002	0.027	0.373	0.020	0.905	0.925	1.053	1.117	0.905	0.925	1.053	1.117	R3w
Sp100	-0.001	-0.099	-0.047	1.237	0.963	0.021	0.973	0.030	0.021	0.027	0.073	0.019	0.849	0.989	1.036	1.126	0.849	0.989	1.036	1.126	R3w
Gpr55	-0.002	-0.676	-0.113	2.224	0.969	0.088	0.986	0.127	0.004	0.113	0.238	0.082	0.390	0.752	1.292	1.565	0.390	0.752	1.292	1.565	R2
Arl4c	-0.016	-0.336	-0.111	1.728	0.990	0.030	0.740	0.044	0.001	0.039	0.017	0.028	0.578	0.931	1.124	1.367	0.578	0.931	1.124	1.367	R2
Pdcd1	-0.153	0.735	0.137	-0.164	0.991	0.049	0.098	0.071	0.000	0.063	0.041	0.046	1.589	1.369	0.565	0.477	1.589	1.369	0.565	0.477	A3
St8sia4	0.298	0.174	-0.256	0.848	0.913	0.042	0.008	0.061	0.033	0.054	0.003	0.040	0.776	1.085	1.098	1.040	0.776	1.085	1.098	1.040	R3w
Ppip5k2	-0.025	0.155	0.032	0.740	0.998	0.006	0.033	0.008	0.000	0.007	0.003	0.005	1.136	1.070	0.914	0.880	1.136	1.070	0.914	0.880	A3w
Steap3	-0.403	-0.652	0.203	2.094	0.895	0.089	0.036	0.129	0.005	0.115	0.072	0.084	0.781	0.790	1.034	1.394	0.781	0.790	1.034	1.394	R3w
Cd55	-0.069	-0.279	-0.098	1.686	0.915	0.086	0.607	0.124	0.065	0.111	0.288	0.080	0.600	0.989	1.058	1.354	0.600	0.989	1.058	1.354	R1
Ikbke	-0.098	-0.174	0.026	1.333	0.825	0.042	0.185	0.062	0.033	0.055	0.542	0.040	0.891	0.960	1.011	1.138	0.891	0.960	1.011	1.138	R3w
Pik3c2b	-0.087	0.216	0.248	0.324	0.981	0.053	0.316	0.076	0.034	0.068	0.007	0.049	1.564	0.968	0.880	0.587	1.564	0.968	0.880	0.587	A3
Lax1	-0.030	-0.169	0.027	1.239	0.901	0.026	0.467	0.037	0.007	0.033	0.324	0.024	0.940	0.913	1.061	1.085	0.940	0.913	1.061	1.085	R3w
Btg2	0.078	-0.245	-0.044	1.352	0.986	0.020	0.057	0.030	0.001	0.026	0.082	0.019	0.825	0.856	1.167	1.153	0.825	0.856	1.167	1.153	R3w
Ptpn7	0.020	-0.025	0.024	0.968	0.877	0.016	0.429	0.023	0.286	0.020	0.179	0.015	1.047	0.954	1.032	0.968	1.047	0.954	1.032	0.968	A1w
Csrp1	-0.048	-0.052	-0.010	1.157	0.987	0.007	0.010	0.010	0.005	0.009	0.192	0.007	0.918	1.017	0.985	1.080	0.918	1.017	0.985	1.080	R1w
Kif21b	0.093	-0.115	-0.121	1.283	0.968	0.031	0.104	0.045	0.044	0.040	0.013	0.029	0.751	0.975	1.102	1.172	0.751	0.975	1.102	1.172	R3w
Dennd1b	0.047	-0.153	-0.031	1.229	0.864	0.042	0.482	0.061	0.048	0.054	0.471	0.040	0.882	0.914	1.102	1.102	0.882	0.914	1.102	1.102	R3w
Rgs2	1.110	0.379	-0.345	-0.294	0.967	0.089	0.001	0.130	0.030	0.115	0.015	0.084	1.240	0.682	1.613	0.465	1.240	0.682	1.613	0.465	A1
Rgs1	0.781	0.627	-0.180	-0.567	0.962	0.093	0.004	0.135	0.006	0.120	0.108	0.087	1.498	0.908	1.275	0.320	1.498	0.908	1.275	0.320	A2
1700025G04Rik	-0.049	-0.211	-0.168	1.689	0.982	0.045	0.494	0.066	0.023	0.058	0.017	0.042	0.510	1.067	1.027	1.396	0.510	1.067	1.027	1.396	R1
Rgs16	0.021	0.598	0.273	-0.428	0.941	0.157	0.930	0.228	0.042	0.202	0.137	0.147	1.900	1.063	0.790	0.246	1.900	1.063	0.790	0.246	A3
Rnasel	-0.164	-0.230	0.000	1.546	0.851	0.075	0.205	0.108	0.075	0.096	0.997	0.070	0.764	1.000	0.981	1.254	0.764	1.000	0.981	1.254	R2w
Stx6	0.049	0.099	0.014	0.765	0.916	0.026	0.258	0.037	0.040	0.033	0.602	0.024	1.115	1.004	0.994	0.886	1.115	1.004	0.994	0.886	A3w
Rabgap1l	-0.060	0.138	-0.003	0.874	0.903	0.029	0.224	0.042	0.020	0.037	0.906	0.027	1.032	1.115	0.889	0.964	1.032	1.115	0.889	0.964	A4w
Eef1aknmt	-0.038	0.123	0.047	0.775	0.889	0.037	0.518	0.054	0.061	0.048	0.248	0.035	1.139	1.051	0.922	0.888	1.139	1.051	0.922	0.888	A3w
Sell	0.134	-0.086	-0.114	1.176	0.996	0.009	0.001	0.013	0.002	0.012	0.000	0.009	0.808	0.955	1.121	1.116	0.808	0.955	1.121	1.116	R3w
Selp	0.656	-0.265	-0.263	1.077	0.992	0.035	0.000	0.051	0.004	0.045	0.001	0.033	0.747	0.613	1.580	1.060	0.747	0.613	1.580	1.060	A1
Xcl1	-0.243	0.585	0.300	-0.132	0.920	0.167	0.371	0.242	0.053	0.215	0.127	0.156	1.774	1.224	0.597	0.404	1.774	1.224	0.597	0.404	A3
Rcsd1	0.052	-0.164	-0.084	1.337	0.971	0.029	0.275	0.041	0.011	0.037	0.035	0.027	0.773	0.948	1.101	1.178	0.773	0.948	1.101	1.178	R3w
Pogk	-0.141	0.203	0.003	0.865	0.979	0.022	0.012	0.033	0.002	0.029	0.877	0.021	1.029	1.201	0.797	0.974	1.029	1.201	0.797	0.974	A4w
Uap1	0.173	-0.020	-0.061	0.929	0.958	0.018	0.003	0.026	0.434	0.023	0.021	0.017	0.979	0.916	1.131	0.974	0.979	0.916	1.131	0.974	A1w
Atf6	0.325	-0.089	-0.081	0.883	0.936	0.049	0.010	0.070	0.229	0.063	0.148	0.046	0.998	0.789	1.277	0.936	0.998	0.789	1.277	0.936	A1w
Cd48	0.007	-0.093	-0.011	1.151	0.972	0.010	0.645	0.015	0.002	0.013	0.314	0.010	0.930	0.957	1.047	1.066	0.930	0.957	1.047	1.066	R2w
Slamf1	-0.495	-0.182	0.425	1.092	0.952	0.061	0.005	0.088	0.080	0.078	0.002	0.057	1.432	0.912	0.787	0.869	1.432	0.912	0.787	0.869	A3
Pea15a	0.153	-0.140	-0.049	1.112	0.982	0.018	0.004	0.025	0.003	0.023	0.042	0.016	0.923	0.860	1.174	1.043	0.923	0.860	1.174	1.043	I
Ifi206	0.741	-0.785	-0.360	1.928	0.984	0.093	0.005	0.135	0.003	0.120	0.014	0.087	0.317	0.367	1.870	1.446	0.317	0.367	1.870	1.446	R3
Ifi214	0.867	-0.673	-0.402	1.683	0.988	0.077	0.001	0.112	0.002	0.099	0.005	0.072	0.377	0.369	1.907	1.348	0.377	0.369	1.907	1.348	R3
Ifi209	0.492	-0.428	-0.236	1.472	0.969	0.076	0.011	0.111	0.012	0.098	0.030	0.072	0.604	0.625	1.534	1.237	0.604	0.625	1.534	1.237	R3
Mnda1	-0.038	-0.267	-0.020	1.484	0.888	0.061	0.690	0.089	0.028	0.079	0.740	0.057	0.784	0.909	1.092	1.216	0.784	0.909	1.092	1.216	R3w
Ifi203	0.049	-0.139	-0.078	1.292	0.913	0.044	0.489	0.064	0.072	0.057	0.135	0.042	0.797	0.958	1.088	1.157	0.797	0.958	1.088	1.157	R3w
Adss	-0.024	0.130	-0.001	0.835	0.969	0.014	0.294	0.020	0.002	0.018	0.970	0.013	1.057	1.084	0.920	0.939	1.057	1.084	0.920	0.939	A4w
Itpkb	0.005	0.026	-0.068	1.082	0.890	0.029	0.913	0.042	0.527	0.037	0.065	0.027	0.880	1.066	0.978	1.076	0.880	1.066	0.978	1.076	R1w
Ephx1	-0.468	0.106	0.316	0.832	0.928	0.083	0.018	0.120	0.379	0.107	0.015	0.078	1.391	1.129	0.651	0.829	1.391	1.129	0.651	0.829	A3
Lbr	-0.006	-0.065	-0.007	1.117	0.927	0.012	0.767	0.018	0.014	0.016	0.596	0.011	0.946	0.976	1.025	1.052	0.946	0.976	1.025	1.052	R3w
Capn2	0.222	-0.060	-0.176	1.144	0.936	0.044	0.026	0.064	0.352	0.057	0.013	0.041	0.756	0.956	1.165	1.124	0.756	0.956	1.165	1.124	R3w
Dusp10	-0.061	-0.293	0.016	1.484	0.963	0.031	0.250	0.046	0.002	0.040	0.613	0.029	0.828	0.882	1.093	1.197	0.828	0.882	1.093	1.197	R3w

Gene	Erk(E)	NFAT(N)	ErkNFAT(EN)	B0	R2	RSE	pval(E)	se(E)	pval(N)	se(N)	pval(EN)	se(EN)	DMSO	MEKi	CsA	MEKi+CsA	DMSO1	MEKi1	CsA1	MEKi+CsA1	reg_mode
Smyd2	-0.001	0.094	0.011	0.842	0.881	0.022	0.970	0.032	0.031	0.029	0.635	0.021	1.073	1.040	0.957	0.930	1.073	1.040	0.957	0.930	A3w
Atf3	0.532	0.041	-0.057	0.387	0.892	0.117	0.035	0.169	0.798	0.150	0.632	0.109	1.256	0.687	1.381	0.676	1.256	0.687	1.381	0.676	A1
Lpgat1	0.121	0.227	-0.042	0.589	0.966	0.021	0.018	0.031	0.001	0.028	0.105	0.020	1.122	1.063	0.979	0.836	1.122	1.063	0.979	0.836	A3w
Traf3ip3	0.001	-0.104	-0.029	1.208	0.936	0.022	0.978	0.032	0.022	0.029	0.243	0.021	0.884	0.970	1.044	1.102	0.884	0.970	1.044	1.102	R2w
Fam107b	-0.041	-0.086	0.011	1.158	0.841	0.020	0.225	0.028	0.027	0.025	0.573	0.018	0.948	0.976	1.011	1.065	0.948	0.976	1.011	1.065	R3w
Gata3	0.173	-0.689	-0.145	2.086	0.966	0.092	0.266	0.134	0.004	0.119	0.168	0.087	0.433	0.646	1.428	1.493	0.433	0.646	1.428	1.493	R3
Itih5	0.566	0.884	-0.590	0.079	0.905	0.108	0.022	0.157	0.003	0.139	0.004	0.101	0.675	1.529	0.906	0.890	0.675	1.529	0.906	0.890	A4
Il2ra	0.050	0.140	-0.019	0.764	0.927	0.020	0.149	0.028	0.005	0.025	0.351	0.018	1.073	1.051	0.969	0.907	1.073	1.051	0.969	0.907	A3w
Vim	0.191	-0.032	-0.138	1.070	0.949	0.029	0.010	0.042	0.433	0.037	0.007	0.027	0.828	0.960	1.136	1.076	0.828	0.960	1.136	1.076	R3w
Arl5b	0.119	0.070	0.011	0.727	0.938	0.029	0.049	0.042	0.136	0.038	0.703	0.027	1.140	0.941	1.061	0.858	1.140	0.941	1.061	0.858	A1w
Commd3	0.013	-0.036	-0.042	1.115	0.987	0.007	0.279	0.011	0.020	0.010	0.004	0.007	0.904	1.007	1.019	1.071	0.904	1.007	1.019	1.071	R3w
Med22	0.023	0.076	0.010	0.839	0.978	0.009	0.154	0.013	0.003	0.012	0.286	0.008	1.078	1.014	0.984	0.924	1.078	1.014	0.984	0.924	A3w
Mrps2	0.007	0.097	-0.001	0.849	0.920	0.016	0.762	0.023	0.009	0.020	0.932	0.015	1.056	1.045	0.960	0.939	1.056	1.045	0.960	0.939	A4w
Lrrc8a	-0.043	-0.283	0.007	1.462	0.874	0.059	0.645	0.086	0.021	0.076	0.900	0.055	0.828	0.881	1.101	1.190	0.828	0.881	1.101	1.190	R3w
Ier5l	1.181	0.095	-0.439	0.216	0.968	0.091	0.001	0.132	0.463	0.117	0.007	0.085	0.939	0.564	1.782	0.715	0.939	0.564	1.782	0.715	A1
Fnbp1	0.026	-0.110	0.040	1.057	0.853	0.030	0.578	0.043	0.045	0.038	0.222	0.028	1.036	0.893	1.080	0.991	1.036	0.893	1.080	0.991	A1w
Ncs1	0.254	0.370	0.015	0.104	0.943	0.076	0.083	0.111	0.020	0.098	0.841	0.071	1.404	0.994	1.026	0.576	1.404	0.994	1.026	0.576	A2
Ass1	-0.089	0.125	0.003	0.917	0.941	0.024	0.062	0.034	0.015	0.031	0.899	0.022	1.019	1.124	0.873	0.984	1.019	1.124	0.873	0.984	A4w
Fam78a	-0.047	-0.197	-0.023	1.396	0.949	0.033	0.384	0.048	0.010	0.043	0.495	0.031	0.812	0.953	1.051	1.184	0.812	0.953	1.051	1.184	R3w
Fam102a	0.004	-0.312	-0.010	1.480	0.972	0.031	0.940	0.045	0.001	0.040	0.750	0.029	0.807	0.847	1.147	1.198	0.807	0.847	1.147	1.198	R3w
St6galnac4	-0.040	0.058	0.041	0.885	0.938	0.017	0.176	0.024	0.054	0.022	0.057	0.016	1.090	1.024	0.950	0.936	1.090	1.024	0.950	0.936	A3w
Sh2d3c	-0.034	-0.274	0.009	1.435	0.907	0.048	0.654	0.070	0.011	0.062	0.856	0.045	0.842	0.878	1.104	1.176	0.842	0.878	1.104	1.176	R3w
Stxbp1	0.151	-0.172	-0.073	1.207	0.877	0.056	0.135	0.081	0.075	0.072	0.233	0.052	0.854	0.865	1.183	1.098	0.854	0.865	1.183	1.098	R3w
Angptl2	-0.955	0.024	0.784	0.683	0.860	0.254	0.060	0.368	0.944	0.327	0.030	0.238	1.973	1.051	0.405	0.571	1.973	1.051	0.405	0.571	A3
Traf1	0.189	-0.110	-0.064	1.050	0.985	0.016	0.001	0.023	0.006	0.021	0.013	0.015	0.932	0.862	1.185	1.021	0.932	0.862	1.185	1.021	I
Dab2ip	0.411	0.871	0.057	-0.915	0.899	0.220	0.267	0.319	0.037	0.283	0.795	0.206	1.872	1.101	0.921	0.106	1.872	1.101	0.921	0.106	A3
Strbp	-0.096	0.079	0.054	0.898	0.972	0.014	0.010	0.021	0.013	0.019	0.016	0.014	1.092	1.064	0.900	0.945	1.092	1.064	0.900	0.945	A4w
Arhgap15	0.009	-0.083	-0.028	1.166	0.911	0.022	0.797	0.032	0.044	0.029	0.253	0.021	0.903	0.974	1.040	1.083	0.903	0.974	1.040	1.083	R2w
Rbm43	-0.072	-0.209	0.018	1.367	0.916	0.034	0.220	0.049	0.009	0.044	0.604	0.032	0.872	0.931	1.046	1.151	0.872	0.931	1.046	1.151	R3w
Gpd2	0.568	0.520	-0.238	-0.036	0.968	0.044	0.001	0.064	0.001	0.057	0.004	0.041	1.182	1.053	1.149	0.616	1.182	1.053	1.149	0.616	A2
Cytip	0.127	-0.085	-0.116	1.185	0.997	0.008	0.000	0.011	0.001	0.010	0.000	0.007	0.801	0.962	1.115	1.122	0.801	0.962	1.115	1.122	R3w
Dapl1	0.067	-0.102	-0.049	1.161	0.932	0.025	0.138	0.036	0.034	0.032	0.104	0.023	0.888	0.941	1.090	1.082	0.888	0.941	1.090	1.082	R3w
Rbms1	0.034	-0.158	-0.040	1.268	0.899	0.040	0.581	0.057	0.036	0.051	0.341	0.037	0.853	0.928	1.093	1.126	0.853	0.928	1.093	1.126	R3w
Dpp4	-0.094	-0.127	-0.032	1.364	0.910	0.045	0.221	0.065	0.094	0.058	0.495	0.042	0.804	1.029	0.980	1.187	0.804	1.029	0.980	1.187	R1w
Galnt3	0.205	-0.359	-0.046	1.369	0.989	0.027	0.006	0.039	0.001	0.035	0.143	0.025	0.839	0.709	1.318	1.134	0.839	0.709	1.318	1.134	I
Stk39	-0.075	0.205	-0.016	0.816	0.908	0.040	0.265	0.058	0.016	0.051	0.686	0.037	1.034	1.171	0.843	0.953	1.034	1.171	0.843	0.953	A4w
Itga6	0.112	0.287	-0.153	0.717	0.888	0.041	0.133	0.060	0.006	0.053	0.017	0.039	0.926	1.191	0.922	0.961	0.926	1.191	0.922	0.961	R1w
Map3k20	1.087	0.230	-0.418	0.093	0.977	0.064	0.000	0.093	0.050	0.083	0.002	0.060	0.995	0.683	1.650	0.672	0.995	0.683	1.650	0.672	A1w
Ccdc141	0.014	0.851	-0.268	0.209	0.949	0.098	0.925	0.141	0.002	0.126	0.043	0.091	0.947	1.642	0.559	0.852	0.947	1.642	0.559	0.852	A4w
Itga4	-0.028	-0.054	-0.158	1.409	0.945	0.061	0.765	0.088	0.525	0.078	0.050	0.057	0.633	1.122	0.972	1.272	0.633	1.122	0.972	1.272	R1
Slc43a1	-0.884	-0.571	0.436	2.133	0.890	0.090	0.002	0.130	0.008	0.116	0.007	0.084	0.983	0.984	0.670	1.363	0.983	0.984	0.670	1.363	R1w
Rapsn	1.540	0.879	-0.561	-1.171	0.946	0.146	0.002	0.211	0.009	0.187	0.015	0.136	1.366	0.805	1.669	0.160	1.366	0.805	1.669	0.160	A1
Madd	-0.025	-0.134	0.004	1.222	0.871	0.028	0.579	0.041	0.021	0.036	0.875	0.026	0.918	0.946	1.044	1.092	0.918	0.946	1.044	1.092	R3w
Hsd17b12	0.162	0.030	-0.029	0.808	0.922	0.026	0.013	0.038	0.425	0.034	0.312	0.025	1.065	0.923	1.105	0.907	1.065	0.923	1.105	0.907	A1w
Prr5l	0.394	-0.299	-0.408	1.721	0.973	0.084	0.032	0.122	0.051	0.109	0.007	0.079	0.265	0.902	1.364	1.468	0.265	0.902	1.364	1.468	R2
Cd44	0.299	0.081	-0.148	0.785	0.945	0.024	0.001	0.035	0.059	0.031	0.003	0.023	0.942	0.949	1.164	0.945	0.942	0.949	1.164	0.945	R3w
Nat10	-0.013	0.065	0.026	0.870	0.965	0.011	0.472	0.016	0.011	0.015	0.067	0.011	1.081	1.020	0.965	0.933	1.081	1.020	0.965	0.933	A3w
Qser1	0.339	0.597	-0.295	0.239	0.935	0.051	0.010	0.074	0.001	0.066	0.004	0.048	0.961	1.303	0.924	0.812	0.961	1.303	0.924	0.812	A4w
Prrg4	0.546	0.027	-0.263	0.776	0.962	0.045	0.001	0.065	0.660	0.057	0.003	0.042	0.840	0.840	1.357	0.963	0.840	0.840	1.357	0.963	I
Rcn1	-0.065	-0.031	-0.031	1.184	0.966	0.018	0.064	0.026	0.243	0.023	0.138	0.017	0.878	1.056	0.958	1.108	0.878	1.056	0.958	1.108	R1w
Spred1	0.625	0.354	-0.008	-0.286	0.946	0.122	0.024	0.176	0.087	0.157	0.947	0.114	1.590	0.739	1.316	0.355	1.590	0.739	1.316	0.355	A2
Fam98b	-0.004	0.095	-0.003	0.868	0.924	0.015	0.856	0.022	0.008	0.019	0.862	0.014	1.045	1.053	0.952	0.950	1.045	1.053	0.952	0.950	A4w
Knstrn	-0.033	-0.084	0.003	1.162	0.970	0.009	0.065	0.013	0.002	0.012	0.741	0.009	0.937	0.978	1.014	1.070	0.937	0.978	1.014	1.070	R3w
Nusap1	-0.088	-0.150	0.015	1.304	0.938	0.024	0.063	0.034	0.008	0.030	0.540	0.022	0.889	0.974	1.005	1.131	0.889	0.974	1.005	1.131	R3w
AA467197	-1.146	-1.022	0.461	3.084	0.977	0.077	0.001	0.111	0.001	0.099	0.003	0.072	0.609	0.922	0.684	1.785	0.609	0.922	0.684	1.785	R1
Slc30a4	-0.070	0.046	-0.062	1.133	0.884	0.045	0.340	0.065	0.469	0.057	0.210	0.042	0.855	1.124	0.912	1.109	0.855	1.124	0.912	1.109	R1w
Sppl2a	-0.069	-0.215	0.047	1.318	0.997	0.005	0.001	0.007	0.000	0.006	0.001	0.005	0.930	0.901	1.057	1.112	0.930	0.901	1.057	1.112	R3w
Dusp2	0.239	0.015	-0.044	0.764	0.928	0.037	0.011	0.054	0.771	0.048	0.277	0.035	1.076	0.873	1.169	0.882	1.076	0.873	1.169	0.882	A1w
Bcl2l11	0.083	-0.096	-0.107	1.239	0.909	0.045	0.278	0.066	0.178	0.059	0.066	0.043	0.785	0.980	1.088	1.147	0.785	0.980	1.088	1.147	R3w
Polr1b	0.030	0.128	0.003	0.766	0.934	0.021	0.378	0.031	0.009	0.027	0.895	0.020	1.097	1.041	0.964	0.898	1.097	1.041	0.964	0.898	A3w
Cdc25b	0.020	-0.115	-0.052	1.245	0.928	0.031	0.682	0.045	0.046	0.040	0.147	0.029	0.843	0.971	1.059	1.128	0.843	0.971	1.059	1.128	R3w
Rassf2	0.039	-0.121	-0.046	1.218	0.918	0.031	0.429	0.045	0.038	0.040	0.188	0.029	0.865	0.948	1.078	1.109	0.865	0.948	1.078	1.109	R3w
Gpcpd1	0.033	0.202	-0.114	0.869	0.870	0.043	0.626	0.063	0.023	0.056	0.049	0.041	0.905	1.172	0.909	1.014	0.905	1.172	0.909	1.014	R1w
Kif16b	0.067	0.248	-0.041	0.624	0.925	0.032	0.228	0.047	0.004	0.042	0.245	0.030	1.099	1.112	0.927	0.861	1.099	1.112	0.927	0.861	A3w
Bcl2l1	0.000	0.073	0.040	0.815	0.882	0.031	0.995	0.044	0.135	0.039	0.232	0.029	1.122	1.004	0.974	0.900	1.122	1.004	0.974	0.900	A3w
Plagl2	-0.021	-0.003	0.061	0.918	0.995	0.005	0.039	0.007	0.634	0.006	0.000	0.005	1.107	0.964	0.997	0.932	1.107	0.964	0.997	0.932	A3w

Gene	Erk(E)	NFAT(N)	ErkNFAT(EN)	B0	R2	RSE	pval(E)	se(E)	pval(N)	se(N)	pval(EN)	se(EN)	DMSO	MEKi	CsA	MEKi+CsA	DMSO1	MEKi1	CsA1	MEKi+CsA1	reg_mode
Dnmt3b	-0.055	0.426	-0.034	0.495	0.970	0.041	0.405	0.059	0.001	0.053	0.424	0.038	1.135	1.283	0.751	0.831	1.135	1.283	0.751	0.831	A4w
Pxmp4	-0.040	-0.006	-0.087	1.221	0.935	0.039	0.512	0.056	0.905	0.050	0.074	0.036	0.795	1.097	0.955	1.153	0.795	1.097	0.955	1.153	R1w
Trpc4ap	-0.051	0.008	-0.016	1.081	0.954	0.012	0.048	0.018	0.636	0.016	0.241	0.012	0.939	1.054	0.953	1.054	0.939	1.054	0.953	1.054	R1w
Sla2	-0.115	-0.273	-0.054	1.652	0.946	0.059	0.250	0.086	0.023	0.076	0.382	0.056	0.662	0.989	1.028	1.322	0.662	0.989	1.028	1.322	R2
Samhd1	0.023	-0.033	-0.056	1.125	0.889	0.026	0.582	0.038	0.385	0.034	0.088	0.025	0.884	1.013	1.022	1.081	0.884	1.013	1.022	1.081	R2w
Top1	0.019	0.035	0.014	0.898	0.913	0.013	0.362	0.019	0.106	0.017	0.325	0.012	1.060	0.993	1.001	0.946	1.060	0.993	1.001	0.946	A3w
Serinc3	0.023	-0.052	-0.050	1.142	0.983	0.010	0.196	0.015	0.017	0.013	0.006	0.009	0.885	0.999	1.032	1.084	0.885	0.999	1.032	1.084	R3w
Slc35c2	0.103	0.146	-0.035	0.719	0.967	0.014	0.007	0.020	0.001	0.018	0.055	0.013	1.079	1.029	1.005	0.887	1.079	1.029	1.005	0.887	A3w
Prex1	-0.133	-0.237	-0.012	1.539	0.946	0.044	0.106	0.064	0.014	0.057	0.794	0.041	0.757	0.984	1.006	1.252	0.757	0.984	1.006	1.252	R2w
Ptpn1	-0.051	0.102	0.015	0.883	0.915	0.021	0.175	0.031	0.021	0.028	0.504	0.020	1.054	1.076	0.915	0.954	1.054	1.076	0.915	0.954	A4w
Rbm38	0.108	0.032	-0.042	0.897	0.972	0.007	0.000	0.010	0.021	0.009	0.003	0.006	1.004	0.974	1.060	0.963	1.004	0.974	1.060	0.963	A1w
Zbp1	0.026	0.041	-0.068	1.033	0.958	0.014	0.268	0.020	0.082	0.018	0.006	0.013	0.903	1.058	0.987	1.052	0.903	1.058	0.987	1.052	R1w
Npepl1	0.022	0.106	-0.006	0.826	0.889	0.020	0.492	0.029	0.015	0.026	0.765	0.019	1.061	1.043	0.966	0.929	1.061	1.043	0.966	0.929	A3w
Slco4a1	0.307	-0.008	-0.041	0.710	0.964	0.037	0.004	0.053	0.870	0.047	0.297	0.034	1.113	0.810	1.233	0.844	1.113	0.810	1.233	0.844	A1w
Helz2	0.089	-0.081	-0.062	1.125	0.832	0.039	0.194	0.057	0.188	0.051	0.171	0.037	0.889	0.946	1.095	1.071	0.889	0.946	1.095	1.071	R3w
Fgf2	-0.932	0.055	0.913	0.369	0.851	0.330	0.123	0.477	0.903	0.424	0.042	0.309	2.264	0.944	0.434	0.358	2.264	0.944	0.434	0.358	A3
Spry1	-0.095	0.438	0.179	0.130	0.994	0.032	0.108	0.046	0.000	0.041	0.004	0.030	1.544	1.143	0.757	0.556	1.544	1.143	0.757	0.556	A3
Ankrd50	-0.034	0.271	0.044	0.554	0.895	0.063	0.731	0.091	0.029	0.081	0.494	0.059	1.220	1.125	0.856	0.799	1.220	1.125	0.856	0.799	A4w
Hspa4l	-0.020	0.180	0.028	0.705	0.907	0.039	0.736	0.056	0.023	0.050	0.488	0.036	1.144	1.083	0.905	0.868	1.144	1.083	0.905	0.868	A3w
Larp1b	0.108	0.178	-0.028	0.653	0.873	0.037	0.114	0.054	0.020	0.048	0.459	0.035	1.113	1.037	0.994	0.856	1.113	1.037	0.994	0.856	A3w
Mgst2	-0.090	-0.143	-0.061	1.439	0.993	0.015	0.016	0.022	0.002	0.020	0.013	0.014	0.737	1.043	0.985	1.235	0.737	1.043	0.985	1.235	R1w
Foxo1	-0.024	-0.075	-0.052	1.240	0.907	0.036	0.661	0.052	0.177	0.046	0.196	0.034	0.837	1.022	1.006	1.135	0.837	1.022	1.006	1.135	R2w
Gpr171	0.083	-0.220	-0.018	1.259	0.983	0.019	0.038	0.027	0.001	0.024	0.360	0.018	0.894	0.844	1.164	1.098	0.894	0.844	1.164	1.098	I
P2ry1	0.330	0.162	-0.024	0.395	0.948	0.056	0.015	0.081	0.086	0.072	0.666	0.052	1.257	0.866	1.175	0.702	1.257	0.866	1.175	0.702	A1w
Ift80	-0.047	-0.057	-0.048	1.233	0.953	0.025	0.266	0.037	0.157	0.033	0.112	0.024	0.840	1.045	0.980	1.135	0.840	1.045	0.980	1.135	R1w
Ppid	0.012	0.049	0.011	0.892	0.851	0.017	0.656	0.025	0.089	0.022	0.535	0.016	1.057	1.007	0.988	0.947	1.057	1.007	0.988	0.947	A3w
Ctso	-0.044	-0.301	-0.070	1.633	0.890	0.086	0.743	0.125	0.054	0.111	0.437	0.081	0.662	0.936	1.093	1.308	0.662	0.936	1.093	1.308	R2
Gucy1a1	1.111	0.414	-0.431	-0.188	0.985	0.051	0.000	0.074	0.003	0.066	0.001	0.048	1.088	0.769	1.581	0.563	1.088	0.769	1.581	0.563	A1
Tmem131l	-0.213	0.052	0.115	0.972	0.989	0.013	0.000	0.018	0.034	0.016	0.001	0.012	1.122	1.084	0.834	0.960	1.122	1.084	0.834	0.960	A4w
Etv3	0.200	0.147	-0.045	0.617	0.952	0.027	0.007	0.039	0.013	0.034	0.146	0.025	1.122	0.968	1.077	0.832	1.122	0.968	1.077	0.832	A1w
Sh2d2a	-0.016	0.100	0.015	0.841	0.982	0.009	0.292	0.014	0.001	0.012	0.150	0.009	1.077	1.050	0.943	0.930	1.077	1.050	0.943	0.930	A3w
Crabp2	-0.214	0.379	0.532	-0.294	0.865	0.292	0.641	0.424	0.371	0.376	0.124	0.274	2.147	0.907	0.763	0.183	2.147	0.907	0.763	0.183	A2
Pmf1	-0.008	-0.018	-0.023	1.080	0.907	0.014	0.718	0.020	0.360	0.017	0.138	0.013	0.938	1.016	0.998	1.049	0.938	1.016	0.998	1.049	R1w
Sema4a	-0.156	-0.339	-0.044	1.781	0.940	0.071	0.204	0.103	0.021	0.092	0.547	0.067	0.619	0.976	1.029	1.375	0.619	0.976	1.029	1.375	R2
Lmna	1.024	-0.581	-0.535	1.601	0.986	0.089	0.001	0.128	0.007	0.114	0.003	0.083	0.262	0.412	1.959	1.367	0.262	0.412	1.959	1.367	R3
Ubqln4	0.094	0.117	-0.040	0.784	0.939	0.013	0.008	0.019	0.002	0.017	0.031	0.012	1.046	1.025	1.010	0.919	1.046	1.025	1.010	0.919	A3w
Sytl1	-0.022	-0.369	-0.016	1.609	0.942	0.056	0.799	0.081	0.007	0.072	0.769	0.052	0.745	0.842	1.153	1.260	0.745	0.842	1.153	1.260	R3w
Rusc1	0.081	0.159	-0.169	0.977	0.988	0.016	0.023	0.023	0.001	0.020	0.000	0.015	0.801	1.161	0.955	1.083	0.801	1.161	0.955	1.083	R1w
Fam189b	-0.049	-0.133	-0.064	1.379	0.988	0.018	0.135	0.026	0.005	0.023	0.020	0.017	0.764	1.020	1.012	1.204	0.764	1.020	1.012	1.204	R1w
S100a13	0.066	-0.035	-0.093	1.145	0.895	0.036	0.276	0.052	0.487	0.046	0.051	0.034	0.836	1.011	1.049	1.104	0.836	1.011	1.049	1.104	R3w
S100a4	0.214	-0.047	-0.206	1.189	0.889	0.069	0.097	0.099	0.622	0.088	0.033	0.064	0.699	0.992	1.147	1.162	0.699	0.992	1.147	1.162	R3w
S100a6	0.319	-0.094	-0.266	1.241	0.952	0.059	0.020	0.085	0.282	0.076	0.009	0.055	0.619	0.942	1.239	1.200	0.619	0.942	1.239	1.200	R3
S100a11	-0.022	-0.107	0.002	1.181	0.901	0.020	0.498	0.029	0.014	0.026	0.903	0.019	0.931	0.959	1.034	1.076	0.931	0.959	1.034	1.076	R3w
S100a10	0.073	-0.097	-0.049	1.146	0.960	0.018	0.052	0.027	0.015	0.024	0.048	0.017	0.895	0.938	1.093	1.074	0.895	0.938	1.093	1.074	R3w
Tdrkh	0.434	1.170	-0.386	-0.566	0.904	0.142	0.102	0.205	0.003	0.182	0.044	0.133	1.162	1.601	0.711	0.527	1.162	1.601	0.711	0.527	A4
Tnfaip8l2	0.088	-0.398	0.002	1.482	0.971	0.040	0.205	0.058	0.002	0.052	0.959	0.038	0.838	0.734	1.255	1.173	0.838	0.734	1.255	1.173	I
Ctss	0.032	-0.259	0.040	1.274	0.939	0.035	0.555	0.050	0.004	0.045	0.290	0.033	0.955	0.813	1.154	1.077	0.955	0.813	1.154	1.077	I
Sf3b4	-0.003	0.033	0.019	0.919	0.939	0.010	0.840	0.014	0.058	0.012	0.102	0.009	1.055	1.003	0.986	0.956	1.055	1.003	0.986	0.956	A3w
Txnip	-0.010	-0.199	-0.044	1.393	0.963	0.031	0.830	0.045	0.007	0.040	0.199	0.029	0.792	0.943	1.077	1.189	0.792	0.943	1.077	1.189	R3w
Polr3gl	0.020	-0.125	-0.056	1.268	0.971	0.021	0.552	0.031	0.010	0.028	0.048	0.020	0.829	0.968	1.063	1.140	0.829	0.968	1.063	1.140	R3w
Notch2	-0.154	0.181	0.044	0.839	0.867	0.056	0.132	0.082	0.067	0.073	0.456	0.053	1.089	1.167	0.804	0.940	1.089	1.167	0.804	0.940	A4w
Tent5c	-0.076	0.422	-0.025	0.509	0.995	0.016	0.033	0.024	0.000	0.021	0.178	0.015	1.137	1.289	0.738	0.835	1.137	1.289	0.738	0.835	A4w
Ptgfrn	0.308	0.140	-0.086	0.569	0.963	0.028	0.002	0.041	0.019	0.037	0.032	0.027	1.107	0.921	1.156	0.816	1.107	0.921	1.156	0.816	A1w
Cd2	0.037	-0.062	-0.051	1.141	0.921	0.023	0.327	0.033	0.103	0.029	0.076	0.021	0.887	0.984	1.047	1.081	0.887	0.984	1.047	1.081	R3w
Igsf3	0.094	0.713	-0.421	0.602	0.918	0.130	0.644	0.188	0.013	0.167	0.026	0.121	0.613	1.640	0.655	1.092	0.613	1.640	0.655	1.092	A4
Tspan2	0.037	0.273	-0.171	0.866	0.965	0.034	0.495	0.049	0.003	0.043	0.006	0.032	0.832	1.253	0.866	1.049	0.832	1.253	0.866	1.049	R1w
Tshb	0.427	1.722	-0.661	-0.869	0.970	0.124	0.076	0.180	0.000	0.160	0.005	0.116	0.911	2.112	0.392	0.584	0.911	2.112	0.392	0.584	A4
Sike1	-0.070	-0.207	0.014	1.370	0.948	0.027	0.147	0.039	0.004	0.035	0.603	0.025	0.867	0.933	1.046	1.154	0.867	0.933	1.046	1.154	R3w
Rsbn1	0.023	0.049	0.023	0.857	0.930	0.017	0.401	0.024	0.088	0.022	0.227	0.016	1.088	0.990	0.999	0.923	1.088	0.990	0.999	0.923	A3w
Magi3	0.341	-0.129	-0.113	0.983	0.954	0.044	0.006	0.064	0.085	0.057	0.052	0.041	0.922	0.784	1.302	0.993	0.922	0.784	1.302	0.993	I
Ppm1j	0.044	-0.077	-0.123	1.290	0.948	0.040	0.493	0.059	0.212	0.052	0.031	0.038	0.738	1.030	1.046	1.186	0.738	1.030	1.046	1.186	R2w
Mov10	-0.165	-0.331	-0.007	1.712	0.962	0.047	0.074	0.069	0.006	0.061	0.875	0.044	0.692	0.956	1.026	1.326	0.692	0.956	1.026	1.326	R2
Cd53	0.074	-0.170	0.035	1.099	0.946	0.028	0.144	0.041	0.009	0.036	0.253	0.026	1.023	0.832	1.144	1.001	1.023	0.832	1.144	1.001	A1w
Csf1	1.376	0.162	-0.404	-0.188	0.975	0.102	0.001	0.148	0.286	0.132	0.013	0.096	1.173	0.430	1.909	0.488	1.173	0.430	1.909	0.488	A1
Slc25a24	0.354	-0.145	-0.308	1.352	0.932	0.087	0.049	0.126	0.266	0.112	0.020	0.082	0.529	0.926	1.281	1.264	0.529	0.926	1.281	1.264	R3
Vav3	0.190	0.546	-0.162	0.252	0.991	0.021	0.003	0.030	0.000	0.027	0.001	0.020	1.103	1.274	0.859	0.764	1.103	1.274	0.859	0.764	A4w

Gene	Erk(E)	NFAT(N)	ErkNFAT(EN)	B0	R2	RSE	pval(E)	se(E)	pval(N)	se(N)	pval(EN)	se(EN)	DMSO	MEKi	CsA	MEKi+CsA	DMSO1	MEKi1	CsA1	MEKi+CsA1	reg_mode
S1pr1	0.227	-0.446	-0.317	1.977	0.976	0.082	0.127	0.118	0.013	0.105	0.014	0.076	0.258	0.872	1.322	1.548	0.258	0.872	1.322	1.548	R2
Cnn3	0.043	0.096	0.008	0.788	0.971	0.013	0.083	0.019	0.004	0.017	0.527	0.012	1.099	1.011	0.990	0.900	1.099	1.011	0.990	0.900	A3w
Abcd3	-0.071	0.156	0.061	0.743	0.985	0.017	0.041	0.024	0.002	0.021	0.017	0.016	1.163	1.080	0.884	0.873	1.163	1.080	0.884	0.873	A4w
Dnttip2	-0.017	0.046	0.028	0.901	0.949	0.012	0.357	0.017	0.037	0.015	0.060	0.011	1.071	1.013	0.971	0.946	1.071	1.013	0.971	0.946	A3w
Hadh	-0.054	0.045	-0.013	1.022	0.959	0.012	0.034	0.017	0.040	0.015	0.313	0.011	0.965	1.072	0.935	1.028	0.965	1.072	0.935	1.028	R1w
Slc9b2	-0.144	1.185	0.133	-0.840	0.995	0.055	0.144	0.079	0.000	0.071	0.061	0.051	1.839	1.595	0.359	0.207	1.839	1.595	0.359	0.207	A3
Ppp3ca	0.034	-0.253	-0.007	1.349	0.943	0.036	0.557	0.053	0.006	0.047	0.847	0.034	0.866	0.853	1.143	1.137	0.866	0.853	1.143	1.137	R3w
Metap1	0.003	0.088	0.028	0.812	0.883	0.028	0.936	0.041	0.070	0.036	0.353	0.026	1.107	1.020	0.967	0.906	1.107	1.020	0.967	0.906	A3w
Pdlim5	0.298	0.053	-0.127	0.790	0.896	0.038	0.005	0.054	0.338	0.048	0.023	0.035	0.968	0.918	1.181	0.934	0.968	0.918	1.181	0.934	A1w
Gbp5	-0.113	0.045	0.035	1.007	0.949	0.016	0.008	0.023	0.091	0.020	0.076	0.015	1.022	1.075	0.898	1.004	1.022	1.075	0.898	1.004	A4w
Gbp7	-0.052	-0.323	0.047	1.459	0.849	0.063	0.601	0.091	0.016	0.081	0.467	0.059	0.880	0.834	1.121	1.165	0.880	0.834	1.121	1.165	R3w
Gbp3	-0.143	-0.288	0.060	1.496	0.926	0.038	0.059	0.055	0.004	0.049	0.168	0.036	0.865	0.907	1.036	1.192	0.865	0.907	1.036	1.192	R3w
Syde2	0.036	0.563	-0.113	0.325	0.943	0.064	0.721	0.093	0.002	0.083	0.134	0.060	1.112	1.353	0.741	0.794	1.112	1.353	0.741	0.794	A4w
Mcoln2	0.022	0.291	-0.157	0.831	0.923	0.051	0.783	0.073	0.011	0.065	0.030	0.047	0.861	1.261	0.849	1.028	0.861	1.261	0.849	1.028	R1w
Zzz3	0.019	0.051	0.014	0.875	0.991	0.005	0.052	0.007	0.001	0.006	0.035	0.004	1.069	1.001	0.993	0.937	1.069	1.001	0.993	0.937	A3w
Acadm	0.202	-0.012	-0.082	0.922	0.955	0.020	0.002	0.029	0.669	0.026	0.012	0.019	0.959	0.917	1.145	0.978	0.959	0.917	1.145	0.978	I
Ankrd13c	0.019	-0.043	0.046	0.954	0.950	0.016	0.448	0.023	0.103	0.020	0.035	0.015	1.082	0.927	1.044	0.948	1.082	0.927	1.044	0.948	A1w
Wls	0.349	0.075	-0.246	0.916	0.908	0.050	0.008	0.072	0.304	0.064	0.006	0.046	0.773	0.991	1.186	1.050	0.773	0.991	1.186	1.050	R3w
Tox	-0.145	0.198	0.089	0.718	0.927	0.049	0.111	0.071	0.035	0.063	0.124	0.046	1.197	1.131	0.812	0.860	1.197	1.131	0.812	0.860	A4w
Chd7	0.141	-0.056	-0.038	0.980	0.948	0.020	0.008	0.029	0.098	0.026	0.113	0.019	0.984	0.902	1.128	0.986	0.984	0.902	1.128	0.986	A1w
Trp53inp1	0.133	-0.158	-0.191	1.428	0.901	0.085	0.340	0.123	0.222	0.109	0.074	0.080	0.612	0.982	1.139	1.267	0.612	0.982	1.139	1.267	R2
Mmp16	0.060	-0.006	-0.084	1.090	0.957	0.018	0.080	0.026	0.814	0.023	0.007	0.017	0.868	1.023	1.033	1.077	0.868	1.023	1.033	1.077	R2w
Cpne3	0.032	-0.024	-0.070	1.126	0.929	0.024	0.407	0.034	0.479	0.031	0.035	0.022	0.867	1.022	1.022	1.089	0.867	1.022	1.022	1.089	R2w
Mdn1	0.067	0.093	-0.001	0.781	0.984	0.009	0.008	0.014	0.002	0.012	0.909	0.009	1.094	1.000	1.008	0.898	1.094	1.000	1.008	0.898	A3w
Ddx58	-0.034	-0.379	-0.050	1.702	0.879	0.097	0.823	0.140	0.038	0.125	0.608	0.091	0.663	0.873	1.142	1.322	0.663	0.873	1.142	1.322	R2
B4galt1	0.004	-0.151	-0.046	1.307	0.975	0.021	0.911	0.030	0.005	0.027	0.077	0.019	0.825	0.959	1.064	1.152	0.825	0.959	1.064	1.152	R3w
Nol6	-0.036	0.068	0.030	0.887	0.947	0.014	0.157	0.021	0.020	0.018	0.090	0.013	1.075	1.036	0.946	0.943	1.075	1.036	0.946	0.943	A4w
Dnajb5	0.460	0.128	-0.145	0.511	0.988	0.022	0.000	0.031	0.010	0.028	0.002	0.020	1.079	0.855	1.267	0.798	1.079	0.855	1.267	0.798	A1w
Sit1	0.179	-0.202	-0.228	1.505	0.928	0.086	0.223	0.124	0.141	0.110	0.047	0.080	0.544	0.957	1.188	1.311	0.544	0.957	1.188	1.311	R2
Glipr2	-0.046	-0.221	0.004	1.381	0.934	0.034	0.403	0.049	0.007	0.044	0.915	0.032	0.853	0.918	1.069	1.161	0.853	0.918	1.069	1.161	R2w
Trim14	0.026	0.009	-0.120	1.178	0.877	0.054	0.755	0.078	0.905	0.069	0.075	0.050	0.780	1.084	0.992	1.143	0.780	1.084	0.992	1.143	R1w
Galnt12	-0.032	0.054	-0.042	1.037	0.965	0.014	0.190	0.020	0.038	0.018	0.031	0.013	0.924	1.085	0.941	1.049	0.924	1.085	0.941	1.049	R1w
Nr4a3	0.116	0.752	-0.106	-0.071	0.973	0.060	0.250	0.087	0.001	0.077	0.132	0.056	1.285	1.385	0.717	0.613	1.285	1.385	0.717	0.613	A4
Slc44a1	-0.080	-0.203	0.031	1.345	0.833	0.044	0.271	0.063	0.022	0.056	0.488	0.041	0.896	0.929	1.039	1.136	0.896	0.929	1.039	1.136	R3w
Tmem38b	-0.496	-0.074	0.473	0.843	0.866	0.142	0.073	0.205	0.704	0.183	0.023	0.133	1.589	0.928	0.745	0.738	1.589	0.928	0.745	0.738	A3
Tmem245	0.009	0.105	0.045	0.748	0.787	0.054	0.912	0.079	0.207	0.070	0.430	0.051	1.155	1.010	0.967	0.868	1.155	1.010	0.967	0.868	A3w
Pakap	0.224	-0.424	-0.138	1.614	0.945	0.081	0.129	0.117	0.015	0.104	0.143	0.076	0.630	0.738	1.345	1.288	0.630	0.738	1.345	1.288	R3
D630039A03Rik	-0.598	0.239	0.091	1.213	0.939	0.101	0.015	0.146	0.140	0.130	0.392	0.095	0.927	1.474	0.444	1.155	0.927	1.474	0.444	1.155	A4
Hsdl2	-0.054	-0.008	-0.036	1.146	0.921	0.025	0.219	0.037	0.815	0.033	0.205	0.024	0.888	1.064	0.955	1.093	0.888	1.064	0.955	1.093	R1w
Bspry	0.832	0.463	-0.236	-0.279	0.949	0.093	0.003	0.134	0.018	0.119	0.053	0.087	1.326	0.834	1.380	0.460	1.326	0.834	1.380	0.460	A1
Akna	0.041	-0.132	-0.064	1.266	0.898	0.043	0.546	0.062	0.074	0.055	0.186	0.040	0.824	0.956	1.081	1.139	0.824	0.956	1.081	1.139	R3w
Ttc39b	0.090	-0.033	0.012	0.916	0.924	0.023	0.055	0.034	0.330	0.030	0.620	0.022	1.064	0.909	1.088	0.939	1.064	0.909	1.088	0.939	A1w
Jak1	-0.096	-0.163	0.048	1.273	0.850	0.027	0.073	0.040	0.010	0.035	0.136	0.026	0.942	0.947	1.011	1.099	0.942	0.947	1.011	1.099	R3w
Mier1	-0.026	-0.086	-0.008	1.177	0.886	0.022	0.458	0.032	0.040	0.029	0.705	0.021	0.918	0.982	1.018	1.082	0.918	0.982	1.018	1.082	R3w
Usp24	0.015	0.068	0.012	0.858	0.851	0.022	0.664	0.032	0.073	0.028	0.593	0.021	1.072	1.014	0.982	0.932	1.072	1.014	0.982	0.932	A3w
Ssbp3	0.021	-0.001	-0.071	1.109	0.827	0.038	0.725	0.055	0.983	0.049	0.115	0.036	0.869	1.043	1.002	1.085	0.869	1.043	1.002	1.085	R1w
Lrp8	0.324	0.348	-0.150	0.359	0.878	0.052	0.013	0.075	0.006	0.067	0.037	0.049	1.104	1.068	1.058	0.770	1.104	1.068	1.058	0.770	A3w
Osbpl9	0.049	-0.077	-0.033	1.115	0.843	0.028	0.295	0.041	0.100	0.036	0.279	0.026	0.923	0.953	1.067	1.057	0.923	0.953	1.067	1.057	R3w
Cdkn2c	-0.029	-0.103	-0.068	1.317	0.957	0.032	0.554	0.046	0.064	0.041	0.082	0.030	0.786	1.025	1.012	1.177	0.786	1.025	1.012	1.177	R2w
Spata6	0.158	-0.200	-0.129	1.345	0.873	0.078	0.237	0.113	0.118	0.101	0.153	0.073	0.730	0.892	1.190	1.188	0.730	0.892	1.190	1.188	R3w
Faah	-0.028	-0.126	-0.019	1.259	0.892	0.033	0.592	0.048	0.041	0.042	0.572	0.031	0.873	0.971	1.034	1.122	0.873	0.971	1.034	1.122	R3w
Plk3	0.257	0.174	0.039	0.350	0.937	0.071	0.066	0.102	0.128	0.091	0.588	0.066	1.344	0.872	1.125	0.659	1.344	0.872	1.125	0.659	A2
Hivep3	0.158	-0.117	0.104	0.786	0.873	0.089	0.287	0.129	0.363	0.114	0.278	0.083	1.248	0.741	1.198	0.813	1.248	0.741	1.198	0.813	A1w
Ctps	0.027	0.107	-0.001	0.810	0.921	0.018	0.376	0.027	0.011	0.024	0.941	0.017	1.075	1.036	0.970	0.919	1.075	1.036	0.970	0.919	A3w
Smap2	0.031	-0.144	-0.044	1.259	0.950	0.027	0.469	0.039	0.014	0.034	0.153	0.025	0.851	0.941	1.083	1.126	0.851	0.941	1.083	1.126	R3w
Ppt1	0.004	0.129	-0.010	0.821	0.978	0.010	0.818	0.015	0.001	0.013	0.356	0.010	1.055	1.071	0.940	0.934	1.055	1.071	0.940	0.934	A4w
Pabpc4	-0.002	0.070	0.018	0.864	0.942	0.014	0.933	0.020	0.017	0.018	0.244	0.013	1.074	1.022	0.969	0.934	1.074	1.022	0.969	0.934	A3w
Inpp5b	-0.058	0.092	0.035	0.869	0.902	0.025	0.187	0.037	0.047	0.032	0.209	0.024	1.085	1.059	0.919	0.937	1.085	1.059	0.919	0.937	A4w
Marcksl1	0.104	0.247	0.039	0.430	0.882	0.075	0.395	0.109	0.064	0.097	0.613	0.071	1.284	1.019	0.972	0.724	1.284	1.019	0.972	0.724	A3w
Lck	-0.072	-0.103	0.037	1.174	0.934	0.011	0.009	0.015	0.002	0.014	0.020	0.010	0.970	0.968	1.000	1.061	0.970	0.968	1.000	1.061	R3w
Sfn	-0.096	-0.302	0.057	1.463	0.969	0.025	0.055	0.036	0.001	0.032	0.069	0.023	0.883	0.869	1.079	1.170	0.883	0.869	1.079	1.170	R3w
Sh3bgrl3	-0.025	-0.042	-0.006	1.105	0.863	0.015	0.328	0.022	0.099	0.020	0.673	0.014	0.947	1.002	0.999	1.052	0.947	1.002	0.999	1.052	R2w
Rsrp1	0.008	-0.056	-0.013	1.098	0.887	0.015	0.728	0.021	0.041	0.019	0.409	0.014	0.948	0.976	1.030	1.046	0.948	0.976	1.030	1.046	R3w
E2f2	-0.028	-0.114	-0.053	1.305	0.904	0.043	0.669	0.062	0.108	0.055	0.253	0.040	0.810	1.007	1.021	1.163	0.810	1.007	1.021	1.163	R2w
Iffo2	0.551	0.020	-0.185	0.633	0.949	0.058	0.003	0.084	0.801	0.074	0.027	0.054	0.998	0.768	1.381	0.854	0.998	0.768	1.381	0.854	A1w
Thap3	-0.029	-0.087	-0.037	1.235	0.963	0.020	0.369	0.029	0.026	0.025	0.114	0.018	0.858	1.007	1.011	1.124	0.858	1.007	1.011	1.124	R2w

Gene	Erk(E)	NFAT(N)	ErkNFAT(EN)	B0	R2	RSE	pval(E)	se(E)	pval(N)	se(N)	pval(EN)	se(EN)	DMSO	MEKi	CsA	MEKi+CsA	DMSO1	MEKi1	CsA1	MEKi+CsA1	reg_mode
Gtf2ird1	0.053	-0.111	-0.051	1.196	0.883	0.036	0.372	0.053	0.077	0.047	0.207	0.034	0.869	0.948	1.083	1.100	0.869	0.948	1.083	1.100	R3w
Rasa4	0.575	0.002	-0.350	0.938	0.870	0.104	0.019	0.151	0.987	0.134	0.023	0.098	0.671	0.877	1.375	1.077	0.671	0.877	1.375	1.077	R3
Alkbh4	-0.013	-0.110	-0.019	1.215	0.945	0.020	0.670	0.029	0.013	0.026	0.372	0.019	0.892	0.969	1.038	1.101	0.892	0.969	1.038	1.101	R2w
Orai2	-0.033	-0.289	-0.001	1.474	0.859	0.066	0.748	0.096	0.028	0.086	0.989	0.062	0.814	0.878	1.110	1.198	0.814	0.878	1.110	1.198	R3w
Plod3	0.062	0.219	-0.018	0.628	0.862	0.046	0.402	0.067	0.021	0.059	0.705	0.043	1.129	1.081	0.942	0.848	1.129	1.081	0.942	0.848	A3w
Dnaaf5	-0.198	-0.252	0.083	1.467	0.933	0.030	0.010	0.043	0.003	0.039	0.041	0.028	0.897	0.945	0.981	1.176	0.897	0.945	0.981	1.176	R2w
Adap1	0.249	0.091	-0.266	1.053	0.938	0.051	0.028	0.074	0.238	0.065	0.005	0.048	0.676	1.087	1.097	1.140	0.676	1.087	1.097	1.140	R3w
Gpr146	0.092	-0.221	-0.140	1.477	0.974	0.041	0.192	0.059	0.013	0.052	0.021	0.038	0.653	0.938	1.147	1.262	0.653	0.938	1.147	1.262	R1
Chst12	-0.011	-0.094	-0.070	1.285	0.932	0.037	0.844	0.054	0.118	0.048	0.114	0.035	0.799	1.018	1.022	1.162	0.799	1.018	1.022	1.162	R2w
Lfng	-0.105	-0.152	0.000	1.357	0.965	0.023	0.034	0.033	0.007	0.029	0.994	0.021	0.846	0.998	0.990	1.166	0.846	0.998	0.990	1.166	R2w
Card11	0.067	-0.055	-0.087	1.162	0.879	0.039	0.305	0.057	0.341	0.051	0.076	0.037	0.837	0.996	1.060	1.107	0.837	0.996	1.060	1.107	R3w
Rnf216	0.112	0.336	-0.021	0.397	0.971	0.033	0.078	0.048	0.001	0.042	0.540	0.031	1.221	1.107	0.925	0.747	1.221	1.107	0.925	0.747	A3w
Samd9l	-0.240	-0.993	0.053	2.681	0.972	0.093	0.150	0.135	0.001	0.120	0.576	0.087	0.393	0.624	1.290	1.692	0.393	0.624	1.290	1.692	R2
Pon2	-0.033	-0.278	0.059	1.347	0.959	0.026	0.429	0.038	0.001	0.034	0.073	0.024	0.941	0.834	1.116	1.108	0.941	0.834	1.116	1.108	R3w
Mios	-0.061	0.072	0.046	0.882	0.944	0.018	0.081	0.026	0.036	0.023	0.052	0.017	1.094	1.042	0.928	0.936	1.094	1.042	0.928	0.936	A3w
Glcci1	-0.256	-0.224	0.044	1.568	0.953	0.040	0.011	0.058	0.012	0.051	0.301	0.037	0.797	1.034	0.915	1.255	0.797	1.034	0.915	1.255	R1w
Mdfic	-0.110	0.174	0.097	0.695	0.977	0.026	0.045	0.038	0.007	0.034	0.017	0.025	1.222	1.087	0.853	0.838	1.222	1.087	0.853	0.838	A4w
Fam3c	-0.019	0.155	-0.035	0.856	0.960	0.017	0.488	0.024	0.002	0.022	0.091	0.016	1.005	1.121	0.906	0.968	1.005	1.121	0.906	0.968	A4w
Ube2h	0.019	-0.142	-0.029	1.242	0.933	0.027	0.652	0.040	0.016	0.035	0.323	0.026	0.875	0.938	1.076	1.112	0.875	0.938	1.076	1.112	R3w
Akr1b10	-0.017	-0.068	-0.044	1.205	0.920	0.028	0.698	0.041	0.132	0.036	0.165	0.026	0.861	1.014	1.010	1.115	0.861	1.014	1.010	1.115	R2w
Bpgm	0.065	0.492	-0.141	0.447	0.978	0.033	0.245	0.048	0.000	0.042	0.010	0.031	1.034	1.320	0.791	0.855	1.034	1.320	0.791	0.855	A4w
Zc3hav1	0.013	-0.105	-0.017	1.173	0.916	0.022	0.705	0.031	0.020	0.028	0.452	0.020	0.915	0.951	1.056	1.078	0.915	0.951	1.056	1.078	R3w
Parp12	-0.059	-0.545	-0.076	2.029	0.952	0.088	0.668	0.127	0.008	0.113	0.405	0.082	0.502	0.828	1.195	1.475	0.502	0.828	1.195	1.475	R2
Kdm7a	0.223	-0.070	-0.118	1.049	0.972	0.023	0.002	0.033	0.075	0.029	0.005	0.021	0.868	0.902	1.182	1.048	0.868	0.902	1.182	1.048	R3w
Rab19	0.434	-0.186	-0.293	1.286	0.981	0.045	0.003	0.065	0.032	0.058	0.002	0.042	0.588	0.836	1.365	1.211	0.588	0.836	1.365	1.211	R3
Zyx	-0.061	-0.280	0.056	1.389	0.954	0.027	0.199	0.040	0.001	0.035	0.092	0.026	0.916	0.855	1.096	1.133	0.916	0.855	1.096	1.133	R3w
Ezh2	0.014	0.106	-0.028	0.876	0.939	0.012	0.470	0.017	0.002	0.015	0.068	0.011	1.013	1.067	0.955	0.965	1.013	1.067	0.955	0.965	A4w
Gimap8	-0.105	-0.210	0.061	1.329	0.951	0.019	0.018	0.027	0.001	0.024	0.026	0.018	0.937	0.919	1.029	1.115	0.937	0.919	1.029	1.115	R3w
Gimap4	-0.035	-0.159	0.018	1.248	0.948	0.018	0.264	0.027	0.003	0.024	0.367	0.017	0.924	0.930	1.051	1.096	0.924	0.930	1.051	1.096	R3w
Gimap6	-0.004	-0.133	0.021	1.166	0.922	0.019	0.877	0.027	0.005	0.024	0.299	0.017	0.964	0.919	1.063	1.054	0.964	0.919	1.063	1.054	R3w
Gimap7	0.057	-0.238	-0.036	1.351	0.962	0.032	0.285	0.046	0.004	0.041	0.300	0.030	0.832	0.868	1.149	1.152	0.832	0.868	1.149	1.152	R3w
Osbpl3	-0.218	-0.229	0.002	1.609	0.885	0.075	0.115	0.109	0.077	0.097	0.983	0.070	0.732	1.039	0.939	1.290	0.732	1.039	0.939	1.290	R2w
Jazf1	-0.992	-0.224	0.944	0.801	0.940	0.177	0.018	0.257	0.382	0.228	0.005	0.166	2.132	0.820	0.525	0.524	2.132	0.820	0.525	0.524	A3
Mturn	-0.728	-1.434	0.359	3.373	0.973	0.104	0.008	0.150	0.000	0.134	0.021	0.097	0.445	0.497	1.181	1.877	0.445	0.497	1.181	1.877	R3
Nod1	-0.288	-0.375	-0.080	2.064	0.902	0.135	0.215	0.195	0.097	0.174	0.560	0.126	0.440	1.082	0.937	1.541	0.440	1.082	0.937	1.541	R1
Herc6	-0.037	-0.354	-0.054	1.676	0.959	0.053	0.653	0.077	0.007	0.069	0.339	0.050	0.668	0.891	1.126	1.314	0.668	0.891	1.126	1.314	R2
Herc3	-0.002	-0.074	-0.059	1.223	0.918	0.033	0.971	0.047	0.154	0.042	0.124	0.031	0.838	1.013	1.021	1.128	0.838	1.013	1.021	1.128	R2w
Tigd2	-0.175	0.070	0.108	0.909	0.927	0.034	0.023	0.049	0.180	0.043	0.026	0.032	1.144	1.072	0.853	0.931	1.144	1.072	0.853	0.931	A4w
Gprin3	-0.579	0.067	0.202	1.241	0.970	0.050	0.001	0.073	0.361	0.065	0.013	0.047	1.066	1.283	0.560	1.091	1.066	1.283	0.560	1.091	A4
Tnip3	0.307	1.784	-0.507	-1.102	0.968	0.139	0.203	0.202	0.001	0.179	0.018	0.131	1.180	2.102	0.301	0.417	1.180	2.102	0.301	0.417	A4
Il12rb2	0.115	-0.002	-0.084	1.019	0.945	0.016	0.008	0.024	0.911	0.021	0.005	0.015	0.903	0.986	1.073	1.037	0.903	0.986	1.073	1.037	R3w
Eif2ak3	-0.131	-0.347	0.048	1.592	0.964	0.034	0.055	0.049	0.001	0.043	0.206	0.032	0.816	0.878	1.071	1.235	0.816	0.878	1.071	1.235	R3w
Cd8b1	-0.032	-0.074	-0.006	1.161	0.967	0.010	0.102	0.015	0.005	0.014	0.604	0.010	0.926	0.990	1.009	1.075	0.926	0.990	1.009	1.075	R2w
Polr1a	0.013	0.074	0.007	0.859	0.949	0.012	0.479	0.017	0.008	0.015	0.537	0.011	1.065	1.022	0.977	0.936	1.065	1.022	0.977	0.936	A3w
St3gal5	0.717	0.227	-0.320	0.370	0.928	0.067	0.002	0.097	0.057	0.086	0.007	0.063	0.950	0.865	1.385	0.799	0.950	0.865	1.385	0.799	A1w
Capg	0.201	-0.132	-0.043	1.028	0.968	0.027	0.006	0.039	0.019	0.034	0.161	0.025	0.971	0.825	1.209	0.996	0.971	0.825	1.209	0.996	I
Smyd5	0.041	0.144	0.020	0.697	0.982	0.015	0.140	0.022	0.002	0.020	0.228	0.014	1.148	1.027	0.968	0.856	1.148	1.027	0.968	0.856	A3w
Mxd1	0.057	-0.221	-0.134	1.508	0.951	0.056	0.519	0.081	0.038	0.072	0.064	0.053	0.644	0.957	1.121	1.278	0.644	0.957	1.121	1.278	R1
Arhgap25	0.089	-0.088	-0.115	1.236	0.920	0.044	0.233	0.064	0.193	0.057	0.049	0.041	0.776	0.986	1.088	1.150	0.776	0.986	1.088	1.150	R3w
Lrig1	-0.217	0.428	0.124	0.398	0.952	0.074	0.114	0.107	0.011	0.095	0.149	0.069	1.348	1.270	0.656	0.725	1.348	1.270	0.656	0.725	A3
Eif4e3	-0.170	-0.083	0.025	1.288	0.949	0.025	0.009	0.036	0.060	0.032	0.346	0.023	0.893	1.059	0.913	1.136	0.893	1.059	0.913	1.136	R1w
Bhlhe40	0.383	0.304	-0.176	0.400	0.883	0.048	0.005	0.069	0.008	0.061	0.017	0.045	1.066	1.025	1.119	0.790	1.066	1.025	1.119	0.790	A1w
Edem1	0.013	-0.042	-0.032	1.108	0.952	0.012	0.524	0.018	0.058	0.016	0.049	0.012	0.919	0.996	1.023	1.062	0.919	0.996	1.023	1.062	R3w
Raf1	-0.047	0.081	-0.032	0.997	0.965	0.014	0.087	0.021	0.012	0.018	0.072	0.013	0.950	1.101	0.920	1.030	0.950	1.101	0.920	1.030	R1w
Mbd4	-0.004	-0.050	-0.052	1.177	0.935	0.024	0.922	0.035	0.181	0.031	0.082	0.023	0.864	1.020	1.010	1.106	0.864	1.020	1.010	1.106	R1w
Il17ra	-0.052	-0.104	-0.008	1.235	0.892	0.028	0.277	0.041	0.046	0.036	0.766	0.027	0.891	0.991	1.007	1.111	0.891	0.991	1.007	1.111	R2w
Ptpn6	-0.017	0.073	0.011	0.891	0.991	0.005	0.061	0.007	0.000	0.006	0.063	0.004	1.052	1.040	0.955	0.953	1.052	1.040	0.955	0.953	A4w
Lag3	0.019	0.525	-0.041	0.268	0.988	0.030	0.686	0.043	0.000	0.038	0.216	0.028	1.225	1.286	0.760	0.728	1.225	1.286	0.760	0.728	A4w
Ptms	-0.012	0.140	-0.025	0.852	0.921	0.021	0.717	0.030	0.006	0.027	0.266	0.020	1.020	1.100	0.920	0.959	1.020	1.100	0.920	0.959	A4w
Cd27	-0.053	-0.056	0.003	1.142	0.882	0.017	0.102	0.025	0.066	0.022	0.860	0.016	0.941	1.007	0.986	1.066	0.941	1.007	0.986	1.066	R2w
Cd9	0.199	-0.025	-0.093	0.966	0.990	0.010	0.000	0.014	0.110	0.012	0.000	0.009	0.927	0.921	1.147	1.004	0.927	0.921	1.147	1.004	I
Ccnd2	-0.029	0.007	0.034	0.963	0.914	0.010	0.118	0.015	0.614	0.013	0.025	0.010	1.053	0.997	0.980	0.970	1.053	0.997	0.980	0.970	A4w
Cd69	0.087	-0.012	0.048	0.821	0.884	0.044	0.246	0.064	0.845	0.057	0.308	0.041	1.147	0.893	1.082	0.879	1.147	0.893	1.082	0.879	A1w
Klrd1	0.465	-0.618	-0.274	1.861	0.992	0.050	0.003	0.072	0.001	0.064	0.004	0.046	0.403	0.579	1.595	1.423	0.403	0.579	1.595	1.423	R3
Etv6	-0.088	-0.044	0.112	0.967	0.980	0.013	0.009	0.019	0.056	0.017	0.001	0.012	1.143	0.949	0.975	0.933	1.143	0.949	0.975	0.933	A1w
Dusp16	0.046	-0.074	0.148	0.779	0.965	0.041	0.482	0.060	0.234	0.053	0.019	0.039	1.286	0.808	1.100	0.806	1.286	0.808	1.100	0.806	A1w

Gene	Erk(E)	NFAT(N)	ErkNFAT(EN)	B0	R2	RSE	pval(E)	se(E)	pval(N)	se(N)	pval(EN)	se(EN)	DMSO	MEKi	CsA	MEKi+CsA	DMSO1	MEKi1	CsA1	MEKi+CsA1	reg_mode
Cdkn1b	-0.024	-0.236	-0.020	1.420	0.950	0.036	0.669	0.052	0.007	0.046	0.582	0.033	0.812	0.913	1.088	1.186	0.812	0.913	1.088	1.186	R3w
Arhgdib	-0.021	-0.068	0.009	1.110	0.892	0.011	0.270	0.017	0.010	0.015	0.430	0.011	0.967	0.973	1.017	1.043	0.967	0.973	1.017	1.043	R3w
Ldhb	-0.195	0.087	0.066	0.987	0.967	0.022	0.004	0.032	0.038	0.029	0.033	0.021	1.056	1.129	0.822	0.994	1.056	1.129	0.822	0.994	A4w
Cmas	0.088	-0.096	-0.038	1.105	0.977	0.013	0.010	0.019	0.005	0.017	0.037	0.012	0.928	0.920	1.105	1.048	0.928	0.920	1.105	1.048	I
St8sia1	0.071	-0.386	0.006	1.478	0.965	0.042	0.309	0.061	0.002	0.054	0.893	0.039	0.841	0.749	1.237	1.173	0.841	0.749	1.237	1.173	I
Kras	-0.048	0.087	0.017	0.897	0.921	0.018	0.147	0.027	0.021	0.024	0.374	0.017	1.052	1.064	0.926	0.958	1.052	1.064	0.926	0.958	A4w
Stk38l	0.142	0.543	-0.156	0.304	0.922	0.064	0.198	0.092	0.003	0.082	0.059	0.059	1.083	1.302	0.824	0.790	1.083	1.302	0.824	0.790	A4w
Resf1	0.106	-0.142	-0.044	1.163	0.966	0.022	0.028	0.031	0.007	0.028	0.098	0.020	0.901	0.888	1.140	1.071	0.901	0.888	1.140	1.071	I
Mboat7	0.024	0.019	0.058	0.834	0.985	0.012	0.246	0.018	0.291	0.016	0.008	0.012	1.143	0.945	1.021	0.891	1.143	0.945	1.021	0.891	A1w
Slc1a5	-0.032	0.031	0.044	0.910	0.871	0.021	0.363	0.031	0.319	0.028	0.093	0.020	1.086	1.002	0.969	0.942	1.086	1.002	0.969	0.942	A3w
Ppp5c	0.057	0.071	-0.008	0.839	0.890	0.017	0.084	0.025	0.033	0.022	0.631	0.016	1.060	1.002	1.009	0.928	1.060	1.002	1.009	0.928	A3w
Dmwd	0.388	0.518	0.171	-0.571	0.968	0.117	0.085	0.170	0.027	0.151	0.195	0.110	1.888	0.844	1.092	0.176	1.888	0.844	1.092	0.176	A2
Fosb	1.499	-0.497	-0.671	1.142	0.940	0.216	0.009	0.313	0.149	0.278	0.030	0.203	0.344	0.227	2.260	1.169	0.344	0.227	2.260	1.169	A1
Cd3eap	0.071	0.181	-0.023	0.684	0.887	0.033	0.213	0.048	0.013	0.042	0.504	0.031	1.102	1.060	0.965	0.873	1.102	1.060	0.965	0.873	A3w
Bcam	-0.033	1.416	0.125	-1.307	0.918	0.267	0.936	0.387	0.015	0.344	0.643	0.250	2.025	1.639	0.335	0.000	2.025	1.639	0.335	0.000	A4
Bcl3	-0.134	-0.181	-0.020	1.472	0.958	0.036	0.064	0.053	0.018	0.047	0.594	0.034	0.772	1.020	0.978	1.231	0.772	1.020	0.978	1.231	R1w
Pvr	0.544	0.270	-0.206	0.308	0.936	0.053	0.002	0.077	0.017	0.068	0.014	0.050	1.091	0.917	1.253	0.739	1.091	0.917	1.253	0.739	A1w
Kcnn4	-0.036	-0.053	-0.008	1.138	0.930	0.014	0.147	0.020	0.043	0.018	0.597	0.013	0.932	1.006	0.995	1.068	0.932	1.006	0.995	1.068	R2w
Plaur	-0.056	-0.281	-0.132	1.735	0.985	0.040	0.394	0.059	0.006	0.052	0.025	0.038	0.539	1.007	1.062	1.393	0.539	1.007	1.062	1.393	R1
Tgfb1	0.074	0.005	-0.001	0.903	0.990	0.006	0.001	0.008	0.553	0.007	0.887	0.005	1.050	0.950	1.055	0.945	1.050	0.950	1.055	0.945	A1w
Sertad3	0.110	-0.265	-0.121	1.485	0.907	0.077	0.382	0.112	0.057	0.100	0.170	0.073	0.679	0.887	1.185	1.249	0.679	0.887	1.185	1.249	R2
Zfp36	0.152	-0.070	-0.060	1.028	0.905	0.030	0.026	0.044	0.148	0.039	0.103	0.028	0.939	0.905	1.138	1.017	0.939	0.905	1.138	1.017	I
Gmfg	0.066	-0.154	-0.047	1.236	0.957	0.025	0.149	0.037	0.009	0.033	0.118	0.024	0.861	0.914	1.114	1.111	0.861	0.914	1.114	1.111	R3w
Fbxo17	-0.190	0.399	0.041	0.560	0.937	0.069	0.133	0.101	0.011	0.089	0.560	0.065	1.184	1.304	0.674	0.837	1.184	1.304	0.674	0.837	A4w
Gramd1a	0.050	-0.131	-0.007	1.147	0.961	0.017	0.111	0.024	0.004	0.022	0.692	0.016	0.945	0.904	1.098	1.053	0.945	0.904	1.098	1.053	I
Nkg7	-0.306	-0.068	0.115	1.265	0.982	0.016	0.000	0.024	0.032	0.021	0.002	0.015	0.994	1.090	0.818	1.098	0.994	1.090	0.818	1.098	R1w
Vrk3	-0.009	-0.096	-0.077	1.297	0.935	0.038	0.881	0.055	0.123	0.049	0.098	0.036	0.785	1.021	1.023	1.171	0.785	1.021	1.023	1.171	R2w
Emp3	0.073	-0.127	-0.086	1.260	0.979	0.021	0.073	0.030	0.009	0.027	0.012	0.020	0.803	0.954	1.099	1.144	0.803	0.954	1.099	1.144	R2w
Spty2d1	0.168	-0.084	-0.045	1.002	0.921	0.032	0.022	0.046	0.109	0.041	0.205	0.030	0.972	0.874	1.160	0.994	0.972	0.874	1.160	0.994	I
Fam169b	-0.089	-0.088	-0.028	1.294	0.942	0.031	0.114	0.044	0.087	0.039	0.382	0.029	0.836	1.042	0.967	1.155	0.836	1.042	0.967	1.155	R1w
Mctp2	0.161	-0.246	-0.144	1.437	0.932	0.066	0.170	0.096	0.045	0.085	0.081	0.062	0.677	0.879	1.211	1.234	0.677	0.879	1.211	1.234	R2
Slco3a1	0.141	-0.147	-0.092	1.216	0.997	0.008	0.000	0.012	0.000	0.011	0.000	0.008	0.825	0.899	1.160	1.115	0.825	0.899	1.160	1.115	R3w
Kif7	0.153	0.386	-0.078	0.379	0.820	0.079	0.250	0.114	0.019	0.101	0.348	0.074	1.159	1.151	0.922	0.768	1.159	1.151	0.922	0.768	A3w
Tm6sf1	0.238	0.030	-0.190	1.017	0.880	0.050	0.031	0.073	0.669	0.065	0.016	0.047	0.788	1.002	1.132	1.079	0.788	1.002	1.132	1.079	R3w
Il16	0.000	-0.094	-0.032	1.200	0.899	0.028	0.998	0.041	0.061	0.036	0.290	0.027	0.882	0.979	1.037	1.101	0.882	0.979	1.037	1.101	R2w
Sytl2	0.776	-0.682	-0.360	1.732	0.965	0.126	0.013	0.183	0.014	0.163	0.038	0.118	0.397	0.395	1.849	1.360	0.397	0.395	1.849	1.360	R3
Neu3	0.038	-0.176	-0.025	1.264	0.922	0.034	0.486	0.049	0.016	0.044	0.472	0.032	0.875	0.904	1.107	1.114	0.875	0.904	1.107	1.114	R3w
Pde2a	-0.128	-0.896	0.009	2.482	0.929	0.141	0.564	0.205	0.008	0.182	0.951	0.132	0.431	0.630	1.322	1.617	0.431	0.630	1.322	1.617	R2
Trim34a	0.157	-0.304	-0.118	1.479	0.991	0.025	0.011	0.036	0.001	0.032	0.007	0.023	0.695	0.830	1.241	1.234	0.695	0.830	1.241	1.234	R3w
Trim5	0.111	-0.822	-0.050	2.185	0.950	0.114	0.540	0.165	0.005	0.147	0.665	0.107	0.510	0.545	1.461	1.484	0.510	0.545	1.461	1.484	R3
Trim12a	0.039	-0.371	0.007	1.493	0.990	0.022	0.278	0.031	0.000	0.028	0.736	0.020	0.832	0.778	1.206	1.185	0.832	0.778	1.206	1.185	R3w
Trim12c	0.084	-0.134	-0.072	1.229	0.882	0.046	0.279	0.067	0.088	0.060	0.173	0.043	0.835	0.931	1.113	1.120	0.835	0.931	1.113	1.120	R3w
Trim30d	0.098	-0.226	-0.111	1.423	0.895	0.072	0.405	0.105	0.072	0.093	0.178	0.068	0.713	0.907	1.160	1.220	0.713	0.907	1.160	1.220	R3w
Gvin1	0.021	-0.122	-0.014	1.184	0.892	0.027	0.630	0.039	0.025	0.035	0.608	0.025	0.916	0.935	1.070	1.078	0.916	0.935	1.070	1.078	R3w
Tmem9b	0.037	-0.037	-0.044	1.092	0.986	0.007	0.022	0.010	0.015	0.009	0.003	0.007	0.915	0.991	1.037	1.057	0.915	0.991	1.037	1.057	R3w
Dennd5a	0.215	-0.256	-0.020	1.155	0.978	0.031	0.009	0.046	0.003	0.040	0.530	0.029	0.955	0.733	1.282	1.029	0.955	0.733	1.282	1.029	I
Swap70	0.280	0.639	-0.277	0.214	0.950	0.051	0.020	0.075	0.001	0.066	0.005	0.048	0.984	1.351	0.862	0.803	0.984	1.351	0.862	0.803	A4w
Tead1	0.846	2.829	-1.030	-2.355	0.971	0.190	0.037	0.276	0.000	0.245	0.004	0.178	1.063	2.677	0.124	0.136	1.063	2.677	0.124	0.136	A4
Rras2	-0.081	0.027	-0.027	1.108	0.973	0.015	0.022	0.022	0.234	0.020	0.135	0.014	0.909	1.093	0.920	1.078	0.909	1.093	0.920	1.078	R1w
Pde3b	0.027	-0.246	-0.011	1.355	0.958	0.031	0.581	0.045	0.003	0.040	0.729	0.029	0.858	0.865	1.134	1.144	0.858	0.865	1.134	1.144	R3w
Arl6ip1	0.069	0.007	-0.060	1.015	0.987	0.005	0.001	0.008	0.338	0.007	0.000	0.005	0.928	1.004	1.038	1.030	0.928	1.004	1.038	1.030	R3w
Dcun1d3	0.441	-0.158	-0.171	1.008	0.954	0.056	0.005	0.081	0.093	0.072	0.031	0.052	0.855	0.745	1.381	1.019	0.855	0.745	1.381	1.019	I
Il21r	-0.367	-0.235	0.166	1.495	0.953	0.026	0.001	0.038	0.002	0.034	0.003	0.025	0.964	1.006	0.860	1.170	0.964	1.006	0.860	1.170	R1w
Lat	-0.068	-0.133	0.049	1.192	0.938	0.012	0.017	0.018	0.001	0.016	0.012	0.011	0.980	0.941	1.019	1.060	0.980	0.941	1.019	1.060	R3w
Coro1a	0.003	-0.038	-0.013	1.078	0.886	0.012	0.890	0.017	0.072	0.015	0.295	0.011	0.953	0.990	1.017	1.039	0.953	0.990	1.017	1.039	R2w
Ypel3	-0.231	-0.476	0.044	1.915	0.921	0.081	0.119	0.117	0.010	0.104	0.590	0.075	0.671	0.888	1.053	1.389	0.671	0.888	1.053	1.389	R2
AI467606	0.034	-0.130	-0.046	1.240	0.966	0.021	0.329	0.030	0.008	0.027	0.076	0.020	0.855	0.948	1.078	1.119	0.855	0.948	1.078	1.119	R3w
Itga1	0.002	-0.116	0.061	1.057	0.875	0.028	0.964	0.041	0.033	0.036	0.082	0.026	1.059	0.889	1.068	0.983	1.059	0.889	1.068	0.983	A1w
Tacc2	0.274	0.298	-0.018	0.251	0.953	0.055	0.027	0.080	0.014	0.071	0.740	0.052	1.309	0.970	1.069	0.652	1.309	0.970	1.069	0.652	A2
Irf7	-0.053	-0.810	-0.071	2.407	0.899	0.174	0.845	0.252	0.022	0.224	0.685	0.163	0.368	0.685	1.325	1.622	0.368	0.685	1.325	1.622	R2
Ctsd	-0.098	-0.100	0.026	1.223	0.982	0.009	0.001	0.013	0.001	0.011	0.032	0.008	0.932	0.998	0.976	1.094	0.932	0.998	0.976	1.094	R1w
Lsp1	0.066	-0.085	-0.074	1.183	0.957	0.023	0.117	0.033	0.046	0.030	0.026	0.022	0.846	0.971	1.076	1.107	0.846	0.971	1.076	1.107	R3w
Tspan32	0.260	0.166	-0.191	0.787	0.768	0.044	0.016	0.064	0.044	0.057	0.010	0.042	0.877	1.055	1.086	0.982	0.877	1.055	1.086	0.982	R3w
Tnfrsf26	0.259	-0.337	-0.195	1.548	0.952	0.075	0.075	0.109	0.025	0.096	0.050	0.070	0.586	0.804	1.320	1.290	0.586	0.804	1.320	1.290	R3
Tnfrsf23	0.815	-0.138	-0.407	0.957	0.921	0.121	0.010	0.176	0.425	0.156	0.023	0.114	0.634	0.681	1.615	1.070	0.634	0.681	1.615	1.070	R3
Osbpl5	0.156	-0.092	-0.204	1.324	0.847	0.097	0.329	0.141	0.501	0.125	0.089	0.091	0.639	1.009	1.124	1.228	0.639	1.009	1.124	1.228	R2

Gene	Erk(E)	NFAT(N)	ErkNFAT(EN)	B0	R2	RSE	pval(E)	se(E)	pval(N)	se(N)	pval(EN)	se(EN)	DMSO	MEKi	CsA	MEKi+CsA	DMSO1	MEKi1	CsA1	MEKi+CsA1	reg_mode
Nol9	0.001	0.078	0.021	0.843	0.948	0.015	0.977	0.022	0.016	0.020	0.213	0.014	1.087	1.022	0.968	0.923	1.087	1.022	0.968	0.923	A3w
Kcnab2	-0.030	-0.019	-0.016	1.096	0.942	0.012	0.152	0.017	0.281	0.015	0.211	0.011	0.937	1.026	0.982	1.056	0.937	1.026	0.982	1.056	R1w
Atad3a	0.030	0.111	-0.010	0.816	0.879	0.021	0.391	0.031	0.015	0.027	0.652	0.020	1.062	1.043	0.969	0.926	1.062	1.043	0.969	0.926	A3w
Tnfrsf4	-0.169	0.199	0.180	0.577	0.941	0.064	0.143	0.093	0.073	0.082	0.040	0.060	1.364	1.074	0.812	0.750	1.364	1.074	0.812	0.750	A3
Abcb1a	0.248	-0.377	-0.197	1.624	0.919	0.105	0.180	0.153	0.050	0.136	0.116	0.099	0.552	0.794	1.329	1.325	0.552	0.794	1.329	1.325	R3
Rsbn1l	0.064	-0.019	-0.091	1.118	0.873	0.036	0.292	0.053	0.712	0.047	0.056	0.034	0.848	1.020	1.040	1.092	0.848	1.020	1.040	1.092	R2w
Gsap	0.347	0.183	-0.259	0.781	0.807	0.060	0.016	0.087	0.077	0.077	0.010	0.056	0.806	1.058	1.131	1.005	0.806	1.058	1.131	1.005	R3w
Napepld	-0.095	-0.027	-0.168	1.469	0.925	0.084	0.482	0.122	0.817	0.109	0.101	0.079	0.585	1.192	0.906	1.317	0.585	1.192	0.906	1.317	R1
Drc1	-0.283	0.036	-0.074	1.433	0.984	0.038	0.007	0.056	0.511	0.050	0.110	0.036	0.687	1.281	0.750	1.282	0.687	1.281	0.750	1.282	R1
Cad	0.027	0.102	0.003	0.809	0.972	0.011	0.175	0.016	0.002	0.014	0.810	0.011	1.080	1.031	0.973	0.916	1.080	1.031	0.973	0.916	A3w
Nrbp1	0.066	-0.064	-0.050	1.108	0.969	0.013	0.027	0.019	0.020	0.017	0.016	0.012	0.906	0.962	1.071	1.062	0.906	0.962	1.071	1.062	R3w
Fosl2	0.115	0.113	0.075	0.549	0.910	0.066	0.295	0.095	0.251	0.085	0.288	0.062	1.290	0.913	1.051	0.746	1.290	0.913	1.051	0.746	A1w
Mxd4	-0.340	-0.851	0.149	2.413	0.873	0.151	0.194	0.218	0.012	0.194	0.349	0.141	0.602	0.689	1.165	1.544	0.602	0.689	1.165	1.544	R1
Sh3bp2	0.037	-0.040	0.045	0.929	0.853	0.033	0.473	0.047	0.398	0.042	0.214	0.030	1.093	0.916	1.056	0.935	1.093	0.916	1.056	0.935	A1w
Add1	0.012	-0.054	-0.028	1.118	0.819	0.025	0.761	0.037	0.175	0.033	0.302	0.024	0.921	0.987	1.029	1.063	0.921	0.987	1.029	1.063	R3w
Jakmip1	-0.093	-0.278	-0.016	1.560	0.959	0.040	0.184	0.058	0.006	0.051	0.691	0.037	0.751	0.939	1.055	1.255	0.751	0.939	1.055	1.255	R3w
Lap3	0.026	0.120	-0.010	0.808	0.865	0.024	0.505	0.035	0.018	0.031	0.679	0.023	1.064	1.051	0.962	0.924	1.064	1.051	0.962	0.924	A3w
Rbpj	0.261	0.122	-0.081	0.645	0.964	0.022	0.001	0.033	0.013	0.029	0.018	0.021	1.076	0.941	1.129	0.853	1.076	0.941	1.129	0.853	A1w
Tlr1	-0.062	-0.354	-0.020	1.642	0.967	0.042	0.369	0.061	0.003	0.054	0.645	0.040	0.721	0.881	1.114	1.284	0.721	0.881	1.114	1.284	R3w
Tmem156	0.220	-0.044	-0.093	0.967	0.921	0.033	0.010	0.047	0.354	0.042	0.038	0.031	0.931	0.897	1.172	1.000	0.931	0.897	1.172	1.000	I
Ugdh	-0.077	0.180	0.029	0.773	0.951	0.028	0.132	0.041	0.008	0.036	0.335	0.026	1.109	1.122	0.862	0.907	1.109	1.122	0.862	0.907	A4w
Rhoh	-0.092	-0.152	0.018	1.307	0.994	0.007	0.001	0.010	0.000	0.009	0.049	0.007	0.891	0.974	1.004	1.131	0.891	0.974	1.004	1.131	R2w
Txk	0.093	-0.277	-0.104	1.492	0.989	0.025	0.060	0.036	0.001	0.032	0.011	0.023	0.696	0.879	1.181	1.245	0.696	0.879	1.181	1.245	R3w
Tec	-0.262	-0.453	0.074	1.863	0.908	0.077	0.079	0.112	0.010	0.099	0.366	0.072	0.723	0.897	1.024	1.355	0.723	0.897	1.024	1.355	R2
Srd5a3	-0.034	-0.100	-0.031	1.249	0.902	0.033	0.514	0.047	0.077	0.042	0.368	0.031	0.859	0.999	1.014	1.127	0.859	0.999	1.014	1.127	R2w
Igfbp7	0.726	1.300	-0.242	-1.388	0.973	0.109	0.010	0.159	0.001	0.141	0.077	0.102	1.715	1.340	0.904	0.042	1.715	1.340	0.904	0.042	A3
Stap1	0.263	-0.182	-0.072	1.083	0.935	0.050	0.022	0.073	0.047	0.065	0.197	0.047	0.923	0.779	1.274	1.024	0.923	0.779	1.274	1.024	I
Dck	-0.057	-0.040	-0.008	1.146	0.931	0.016	0.073	0.024	0.129	0.021	0.634	0.015	0.924	1.027	0.973	1.076	0.924	1.027	0.973	1.076	R1w
Sdad1	-0.030	0.049	0.046	0.878	0.968	0.012	0.174	0.018	0.038	0.016	0.017	0.012	1.100	1.008	0.963	0.928	1.100	1.008	0.963	0.928	A3w
Cxcl10	-0.141	-0.720	0.078	2.105	0.916	0.108	0.419	0.157	0.007	0.139	0.484	0.101	0.661	0.672	1.244	1.424	0.661	0.672	1.244	1.424	R3
Scarb2	-0.053	-0.139	-0.012	1.296	0.980	0.015	0.072	0.022	0.002	0.019	0.442	0.014	0.863	0.977	1.022	1.138	0.863	0.977	1.022	1.138	R3w
Ccng2	-0.060	-0.365	-0.009	1.636	0.873	0.083	0.643	0.121	0.027	0.107	0.913	0.078	0.738	0.866	1.122	1.274	0.738	0.866	1.122	1.274	R3w
Rasgef1b	-0.030	0.163	0.394	0.059	0.969	0.104	0.854	0.150	0.289	0.134	0.015	0.097	1.867	0.780	0.979	0.374	1.867	0.780	0.979	0.374	A2
Ptpn13	0.926	-0.195	-0.309	0.724	0.931	0.132	0.008	0.191	0.315	0.170	0.067	0.124	0.870	0.493	1.747	0.890	0.870	0.493	1.747	0.890	A1
Hsd17b11	-0.118	-0.240	0.038	1.434	0.925	0.035	0.081	0.051	0.006	0.045	0.313	0.033	0.865	0.931	1.029	1.175	0.865	0.931	1.029	1.175	R3w
Gbp8	-0.034	-0.148	-0.095	1.438	0.949	0.047	0.649	0.068	0.072	0.061	0.098	0.044	0.705	1.027	1.024	1.244	0.705	1.027	1.024	1.244	R1w
Gbp9	0.041	-0.155	-0.058	1.289	0.878	0.049	0.593	0.071	0.071	0.063	0.274	0.046	0.823	0.940	1.093	1.145	0.823	0.940	1.093	1.145	R3w
Gbp4	0.049	-0.035	-0.053	1.092	0.981	0.009	0.021	0.013	0.039	0.012	0.003	0.009	0.905	0.991	1.044	1.061	0.905	0.991	1.044	1.061	R2w
Gbp6	0.045	-0.014	-0.083	1.120	0.963	0.018	0.168	0.027	0.579	0.024	0.009	0.017	0.855	1.029	1.025	1.092	0.855	1.029	1.025	1.092	R2w
Lrrc8d	0.004	-0.212	0.008	1.298	0.921	0.034	0.935	0.049	0.008	0.043	0.818	0.032	0.899	0.883	1.104	1.114	0.899	0.883	1.104	1.114	R3w
Gfi1	-0.293	0.058	0.168	0.962	0.927	0.045	0.011	0.066	0.381	0.059	0.017	0.043	1.181	1.100	0.780	0.939	1.181	1.100	0.780	0.939	A4w
Evi5	0.607	1.356	-0.447	-0.945	0.967	0.093	0.011	0.135	0.000	0.120	0.007	0.087	1.256	1.621	0.746	0.377	1.256	1.621	0.746	0.377	A4
Mtf2	0.021	0.038	0.013	0.894	0.894	0.015	0.392	0.021	0.116	0.019	0.408	0.014	1.061	0.994	1.001	0.945	1.061	0.994	1.001	0.945	A3w
Dr1	0.026	0.130	-0.026	0.823	0.932	0.016	0.321	0.023	0.003	0.020	0.145	0.015	1.037	1.070	0.953	0.940	1.037	1.070	0.953	0.940	A4w
Tpst2	0.016	-0.106	-0.037	1.209	0.992	0.008	0.256	0.012	0.001	0.011	0.008	0.008	0.875	0.966	1.055	1.104	0.875	0.966	1.055	1.104	R3w
Selplg	-0.045	-0.109	-0.009	1.236	0.970	0.015	0.102	0.021	0.005	0.019	0.539	0.014	0.891	0.985	1.014	1.110	0.891	0.985	1.014	1.110	R3w
Ung	0.003	0.080	0.006	0.865	0.946	0.012	0.865	0.018	0.007	0.016	0.613	0.011	1.059	1.033	0.966	0.941	1.059	1.033	0.966	0.941	A3w
Unc119b	0.113	-0.035	-0.067	1.037	0.975	0.011	0.002	0.017	0.078	0.015	0.003	0.011	0.919	0.957	1.090	1.034	0.919	0.957	1.090	1.034	R3w
Pxn	0.056	-0.070	-0.040	1.111	0.870	0.026	0.215	0.038	0.105	0.034	0.173	0.024	0.915	0.958	1.068	1.059	0.915	0.958	1.068	1.059	R3w
Tesc	-0.445	-0.413	0.160	1.870	0.957	0.047	0.003	0.068	0.002	0.060	0.022	0.044	0.800	0.978	0.881	1.342	0.800	0.978	0.881	1.342	R1w
Rbm19	-0.042	0.040	0.071	0.858	0.974	0.015	0.129	0.022	0.105	0.019	0.007	0.014	1.139	0.992	0.963	0.906	1.139	0.992	0.963	0.906	A3w
Oas3	0.180	-0.483	-0.104	1.693	0.988	0.039	0.033	0.057	0.001	0.050	0.046	0.037	0.636	0.712	1.345	1.307	0.636	0.712	1.345	1.307	R3
Ptpn11	-0.004	0.111	0.007	0.826	0.957	0.014	0.863	0.021	0.004	0.019	0.654	0.014	1.073	1.054	0.946	0.927	1.073	1.054	0.946	0.927	A4w
Trafd1	-0.020	-0.230	0.013	1.344	0.903	0.039	0.744	0.057	0.011	0.051	0.748	0.037	0.884	0.887	1.095	1.134	0.884	0.887	1.095	1.134	R3w
Naa25	0.050	0.089	-0.003	0.811	0.971	0.011	0.031	0.015	0.003	0.014	0.779	0.010	1.077	1.012	0.997	0.915	1.077	1.012	0.997	0.915	A3w
Aldh2	-0.089	-0.086	-0.032	1.299	0.934	0.034	0.142	0.049	0.118	0.043	0.364	0.032	0.828	1.047	0.965	1.160	0.828	1.047	0.965	1.160	R1w
Hvcn1	-0.230	-0.199	0.067	1.457	0.966	0.024	0.003	0.035	0.003	0.031	0.040	0.022	0.873	1.009	0.928	1.190	0.873	1.009	0.928	1.190	R1w
Atp2a2	0.044	0.044	0.000	0.880	0.975	0.007	0.011	0.010	0.008	0.009	0.952	0.006	1.054	0.990	1.014	0.942	1.054	0.990	1.014	0.942	A1w
Orai1	0.019	0.070	0.024	0.827	0.959	0.015	0.424	0.022	0.022	0.019	0.157	0.014	1.100	1.002	0.987	0.911	1.100	1.002	0.987	0.911	A3w
Rhof	0.158	-0.129	-0.089	1.165	0.967	0.026	0.013	0.037	0.017	0.033	0.021	0.024	0.850	0.895	1.165	1.090	0.850	0.895	1.165	1.090	R3w
Hip1r	0.030	-0.197	-0.083	1.411	0.979	0.028	0.494	0.040	0.005	0.035	0.033	0.026	0.742	0.947	1.099	1.212	0.742	0.947	1.099	1.212	R3w
Vps37b	0.027	-0.464	-0.018	1.694	0.997	0.014	0.270	0.021	0.000	0.019	0.256	0.014	0.721	0.760	1.235	1.285	0.721	0.760	1.235	1.285	R3w
Abcb9	-0.271	-0.839	0.197	2.223	0.942	0.087	0.099	0.126	0.002	0.112	0.074	0.082	0.749	0.606	1.223	1.422	0.749	0.606	1.223	1.422	R3
Pitpnm2	-0.006	0.169	-0.013	0.780	0.926	0.025	0.877	0.036	0.006	0.032	0.595	0.023	1.064	1.101	0.914	0.922	1.064	1.101	0.914	0.922	A4w
Rilpl2	-0.017	0.236	0.015	0.641	0.863	0.056	0.842	0.081	0.031	0.072	0.787	0.053	1.152	1.120	0.879	0.850	1.152	1.120	0.879	0.850	A3w
Ncf1	-0.001	-0.015	-0.136	1.276	0.984	0.025	0.973	0.036	0.664	0.032	0.004	0.023	0.717	1.105	0.979	1.199	0.717	1.105	0.979	1.199	R1w

Gene	Erk(E)	NFAT(N)	ErkNFAT(EN)	B0	R2	RSE	pval(E)	se(E)	pval(N)	se(N)	pval(EN)	se(EN)	DMSO	MEKi	CsA	MEKi+CsA	DMSO1	MEKi1	CsA1	MEKi+CsA1	reg_mode
Crtam	-0.163	-0.151	0.307	0.856	0.838	0.119	0.398	0.172	0.379	0.153	0.051	0.111	1.428	0.787	1.006	0.779	1.428	0.787	1.006	0.779	A2
Thy1	-0.027	0.010	-0.027	1.070	0.909	0.017	0.324	0.024	0.674	0.022	0.160	0.016	0.933	1.047	0.969	1.051	0.933	1.047	0.969	1.051	R1w
Cd3g	-0.022	-0.071	0.005	1.123	0.846	0.016	0.408	0.023	0.027	0.021	0.746	0.015	0.957	0.975	1.018	1.051	0.957	0.975	1.018	1.051	R3w
Mpzl2	-0.032	0.928	0.066	-0.470	0.938	0.148	0.888	0.214	0.008	0.190	0.660	0.138	1.633	1.440	0.553	0.374	1.633	1.440	0.553	0.374	A4
Il10ra	-0.051	0.081	-0.111	1.148	0.973	0.028	0.283	0.041	0.090	0.036	0.014	0.027	0.789	1.169	0.901	1.142	0.789	1.169	0.901	1.142	R1w
Pts	-0.019	-0.060	-0.028	1.166	0.968	0.013	0.380	0.019	0.023	0.017	0.082	0.012	0.897	1.006	1.008	1.089	0.897	1.006	1.008	1.089	R2w
Pstpip1	-0.006	-0.083	-0.011	1.152	0.964	0.011	0.741	0.016	0.005	0.015	0.340	0.011	0.927	0.971	1.032	1.070	0.927	0.971	1.032	1.070	R3w
Peak1	0.221	0.075	-0.078	0.761	0.928	0.024	0.003	0.035	0.071	0.031	0.025	0.022	1.028	0.945	1.120	0.907	1.028	0.945	1.120	0.907	A1w
Ptpn9	0.334	0.211	-0.109	0.476	0.943	0.036	0.003	0.053	0.011	0.047	0.033	0.034	1.116	0.958	1.138	0.789	1.116	0.958	1.138	0.789	A1w
Neil1	0.065	-0.061	-0.108	1.211	0.970	0.024	0.135	0.035	0.120	0.031	0.009	0.022	0.791	1.012	1.057	1.140	0.791	1.012	1.057	1.140	R3w
Sema7a	-0.067	0.305	0.065	0.506	0.920	0.065	0.514	0.093	0.021	0.083	0.344	0.060	1.258	1.149	0.818	0.774	1.258	1.149	0.818	0.774	A3w
Nptn	-0.008	-0.126	0.019	1.163	0.944	0.015	0.722	0.021	0.003	0.019	0.247	0.014	0.962	0.927	1.056	1.055	0.962	0.927	1.056	1.055	R3w
Smad3	0.135	-0.241	-0.145	1.463	0.950	0.057	0.179	0.083	0.031	0.074	0.055	0.054	0.661	0.900	1.189	1.250	0.661	0.900	1.189	1.250	R2
Dennd4a	-0.091	-0.118	0.010	1.270	0.913	0.026	0.075	0.038	0.025	0.034	0.713	0.025	0.894	0.997	0.987	1.122	0.894	0.997	0.987	1.122	R2w
Rab8b	-0.040	0.199	-0.002	0.757	0.944	0.028	0.380	0.041	0.005	0.036	0.938	0.026	1.081	1.131	0.876	0.912	1.081	1.131	0.876	0.912	A4w
Anxa2	0.262	-0.157	-0.194	1.272	0.988	0.026	0.002	0.038	0.010	0.034	0.001	0.025	0.691	0.893	1.238	1.178	0.691	0.893	1.238	1.178	R3w
Ccnb2	-0.076	-0.094	0.011	1.213	0.947	0.016	0.028	0.023	0.009	0.020	0.491	0.015	0.920	0.998	0.988	1.095	0.920	0.998	0.988	1.095	R2w
Adam10	-0.063	0.052	0.028	0.948	0.966	0.010	0.011	0.014	0.014	0.013	0.036	0.009	1.045	1.048	0.933	0.974	1.045	1.048	0.933	0.974	A4w
Fam214a	-0.256	-0.504	0.077	1.927	0.919	0.078	0.086	0.113	0.007	0.100	0.353	0.073	0.704	0.865	1.053	1.378	0.704	0.865	1.053	1.378	R2
Mapk6	0.070	0.121	-0.032	0.792	0.887	0.019	0.061	0.027	0.007	0.024	0.142	0.017	1.049	1.038	0.991	0.922	1.049	1.038	0.991	0.922	A3w
Cgas	0.089	-0.119	-0.063	1.186	0.944	0.028	0.089	0.040	0.028	0.036	0.071	0.026	0.864	0.927	1.113	1.096	0.864	0.927	1.113	1.096	R3w
Tmem30a	0.035	-0.085	-0.009	1.101	0.960	0.012	0.107	0.017	0.005	0.015	0.446	0.011	0.956	0.939	1.065	1.039	0.956	0.939	1.065	1.039	I
Hmgn3	0.189	0.628	-0.173	0.150	0.943	0.062	0.103	0.090	0.001	0.080	0.041	0.058	1.127	1.326	0.818	0.730	1.127	1.326	0.818	0.730	A4w
Bcl2a1d	0.688	0.261	-0.174	0.085	0.881	0.122	0.018	0.177	0.173	0.157	0.202	0.114	1.244	0.783	1.376	0.597	1.244	0.783	1.376	0.597	A1
Bcl2a1b	0.375	0.166	0.005	0.280	0.931	0.084	0.036	0.121	0.198	0.108	0.954	0.078	1.347	0.812	1.213	0.627	1.347	0.812	1.213	0.627	A2
Tbc1d2b	-0.140	0.035	-0.005	1.130	0.936	0.029	0.030	0.043	0.401	0.038	0.855	0.028	0.918	1.123	0.874	1.086	0.918	1.123	0.874	1.086	R1w
Plscr1	0.138	0.259	-0.049	0.535	0.844	0.054	0.151	0.078	0.020	0.069	0.383	0.050	1.136	1.073	0.976	0.815	1.136	1.073	0.976	0.815	A3w
Dipk2a	-0.091	0.044	-0.002	1.051	0.950	0.017	0.020	0.025	0.115	0.022	0.913	0.016	0.961	1.089	0.908	1.041	0.961	1.089	0.908	1.041	R1w
Chst2	0.001	-0.003	0.111	0.795	0.916	0.046	0.985	0.067	0.968	0.059	0.061	0.043	1.224	0.906	1.024	0.846	1.224	0.906	1.024	0.846	A1w
Rasa2	0.190	-0.017	-0.028	0.844	0.926	0.032	0.015	0.047	0.700	0.042	0.402	0.030	1.057	0.879	1.149	0.915	1.057	0.879	1.149	0.915	A1w
Hyal2	-0.036	0.178	0.079	0.632	0.859	0.067	0.728	0.098	0.110	0.087	0.279	0.063	1.235	1.051	0.904	0.809	1.235	1.051	0.904	0.809	A3w
Uba7	0.093	-0.088	-0.145	1.287	0.944	0.045	0.230	0.065	0.205	0.058	0.026	0.042	0.718	1.009	1.084	1.189	0.718	1.009	1.084	1.189	R2w
Bsn	-0.620	-0.009	0.065	1.657	0.950	0.092	0.009	0.133	0.942	0.118	0.488	0.086	0.723	1.385	0.537	1.355	0.723	1.385	0.537	1.355	A4
Shisa5	0.059	-0.035	-0.024	1.025	0.917	0.012	0.029	0.018	0.089	0.016	0.099	0.011	0.970	0.960	1.057	1.013	0.970	0.960	1.057	1.013	I
Ccr4	-0.496	0.048	0.389	0.815	0.929	0.092	0.021	0.133	0.704	0.119	0.011	0.086	1.489	1.059	0.671	0.781	1.489	1.059	0.671	0.781	A3
Tgfbr2	-0.013	-0.277	-0.026	1.479	0.952	0.041	0.833	0.059	0.006	0.052	0.527	0.038	0.783	0.891	1.114	1.212	0.783	0.891	1.114	1.212	R3w
Eomes	-0.202	-0.114	0.017	1.386	0.957	0.031	0.011	0.045	0.046	0.040	0.579	0.029	0.840	1.072	0.901	1.187	0.840	1.072	0.901	1.187	R1w
Acaa1a	-0.054	-0.003	-0.022	1.112	0.894	0.023	0.182	0.034	0.925	0.030	0.369	0.022	0.919	1.055	0.955	1.071	0.919	1.055	0.955	1.071	R1w
Cxcr6	0.952	-0.252	-0.390	0.928	0.945	0.124	0.006	0.179	0.188	0.159	0.028	0.116	0.692	0.512	1.777	1.018	0.692	0.512	1.777	1.018	A1
Akap12	0.292	0.984	-0.632	0.345	0.862	0.214	0.400	0.311	0.023	0.276	0.035	0.201	0.469	1.810	0.640	1.082	0.469	1.810	0.640	1.082	A4
Ulbp1	0.423	-0.170	-0.193	1.091	0.931	0.070	0.014	0.101	0.131	0.090	0.042	0.065	0.791	0.769	1.369	1.070	0.791	0.769	1.369	1.070	I
Zc3h12d	-0.001	0.298	0.014	0.530	0.975	0.029	0.975	0.042	0.001	0.037	0.636	0.027	1.195	1.141	0.862	0.803	1.195	1.141	0.862	0.803	A3w
Phactr2	-0.161	0.070	0.378	0.390	0.903	0.146	0.490	0.212	0.728	0.188	0.051	0.137	1.697	0.840	0.918	0.546	1.697	0.840	0.918	0.546	A2
Heca	0.016	-0.240	-0.002	1.341	0.970	0.024	0.663	0.035	0.002	0.031	0.945	0.023	0.873	0.868	1.125	1.135	0.873	0.868	1.125	1.135	R3w
Ifngr1	-0.014	-0.233	-0.038	1.437	0.978	0.026	0.722	0.037	0.002	0.033	0.188	0.024	0.783	0.923	1.091	1.203	0.783	0.923	1.091	1.203	R3w
Myb	-0.207	-0.024	0.018	1.256	0.946	0.032	0.012	0.047	0.603	0.042	0.577	0.030	0.889	1.121	0.855	1.135	0.889	1.121	0.855	1.135	R1w
Themis	-0.082	-0.034	-0.058	1.259	0.845	0.059	0.394	0.086	0.676	0.076	0.356	0.055	0.811	1.089	0.941	1.159	0.811	1.089	0.941	1.159	R1w
Ncoa7	0.200	-0.157	-0.080	1.137	0.950	0.036	0.019	0.052	0.028	0.047	0.077	0.034	0.881	0.843	1.213	1.064	0.881	0.843	1.213	1.064	I
Tspyl4	0.026	-0.143	-0.152	1.463	0.860	0.097	0.861	0.141	0.319	0.125	0.171	0.091	0.631	1.034	1.057	1.278	0.631	1.034	1.057	1.278	R1
Slc16a10	0.367	-0.139	-0.067	0.880	0.989	0.025	0.001	0.036	0.013	0.032	0.046	0.024	1.026	0.722	1.336	0.916	1.026	0.722	1.336	0.916	A1w
Cdk19	-0.047	-0.207	-0.056	1.473	0.930	0.052	0.562	0.075	0.035	0.066	0.308	0.048	0.739	0.975	1.049	1.236	0.739	0.975	1.049	1.236	R3w
Sesn1	0.128	-0.171	-0.083	1.253	0.977	0.024	0.022	0.035	0.005	0.031	0.021	0.023	0.820	0.890	1.163	1.128	0.820	0.890	1.163	1.128	R3w
Bend3	0.056	0.232	0.020	0.546	0.988	0.018	0.093	0.026	0.001	0.023	0.288	0.017	1.208	1.061	0.939	0.792	1.208	1.061	0.939	0.792	A3w
Cd24a	0.179	0.198	-0.198	0.852	0.859	0.046	0.056	0.067	0.029	0.060	0.010	0.043	0.828	1.136	1.006	1.030	0.828	1.136	1.006	1.030	R1w
Crybg1	0.254	-0.081	-0.242	1.259	0.993	0.020	0.001	0.029	0.035	0.026	0.000	0.019	0.631	0.976	1.187	1.206	0.631	0.976	1.187	1.206	R1
Man1a	0.199	0.050	-0.104	0.873	0.958	0.014	0.001	0.021	0.055	0.018	0.002	0.013	0.949	0.968	1.110	0.973	0.949	0.968	1.110	0.973	R3w
Mcu	0.103	0.251	-0.045	0.581	0.974	0.019	0.021	0.028	0.001	0.025	0.067	0.018	1.117	1.091	0.953	0.839	1.117	1.091	0.953	0.839	A3w
Psap	-0.057	-0.070	0.002	1.171	0.883	0.020	0.125	0.029	0.055	0.026	0.903	0.019	0.928	1.003	0.989	1.079	0.928	1.003	0.989	1.079	R2w
Prf1	0.212	0.231	0.154	0.107	0.948	0.097	0.207	0.141	0.139	0.125	0.167	0.091	1.578	0.839	1.087	0.497	1.578	0.839	1.087	0.497	A2
Ddx21	0.012	0.050	0.013	0.886	0.915	0.014	0.565	0.020	0.045	0.018	0.378	0.013	1.062	1.006	0.988	0.943	1.062	1.006	0.988	0.943	A3w
Egr2	0.483	0.405	0.241	-0.649	0.931	0.206	0.181	0.299	0.202	0.266	0.281	0.193	2.027	0.662	1.232	0.079	2.027	0.662	1.232	0.079	A2
Adora2a	0.231	-0.046	-0.159	1.078	0.971	0.025	0.003	0.037	0.232	0.033	0.003	0.024	0.805	0.942	1.169	1.084	0.805	0.942	1.169	1.084	R3w
Chchd10	-0.049	-0.016	-0.029	1.138	0.891	0.026	0.272	0.038	0.668	0.034	0.301	0.025	0.900	1.051	0.964	1.085	0.900	1.051	0.964	1.085	R1w
Slc19a1	0.027	0.089	0.035	0.767	0.899	0.033	0.592	0.047	0.100	0.042	0.312	0.031	1.139	0.997	0.986	0.878	1.139	0.997	0.986	0.878	A3w
Pofut2	0.262	0.082	-0.074	0.692	0.969	0.022	0.001	0.031	0.041	0.028	0.021	0.020	1.067	0.916	1.149	0.868	1.067	0.916	1.149	0.868	A1w
Adarb1	-0.335	0.121	0.540	0.228	0.946	0.143	0.182	0.207	0.547	0.184	0.016	0.134	1.938	0.857	0.791	0.414	1.938	0.857	0.791	0.414	A2

Gene	Erk(E)	NFAT(N)	ErkNFAT(EN)	B0	R2	RSE	pval(E)	se(E)	pval(N)	se(N)	pval(EN)	se(EN)	DMSO	MEKi	CsA	MEKi+CsA	DMSO1	MEKi1	CsA1	MEKi+CsA1	reg_mode
Arhgef18	-0.014	-0.150	-0.124	1.472	0.948	0.055	0.865	0.079	0.100	0.070	0.073	0.051	0.657	1.036	1.035	1.272	0.657	1.036	1.035	1.272	R2
Irs2	0.370	-0.258	-0.128	1.167	0.927	0.075	0.027	0.109	0.056	0.097	0.144	0.070	0.839	0.710	1.382	1.070	0.839	0.710	1.382	1.070	I
Rasa3	0.096	-0.396	-0.080	1.624	0.973	0.048	0.238	0.069	0.003	0.061	0.145	0.045	0.677	0.797	1.244	1.282	0.677	0.797	1.244	1.282	R2
Champ1	0.010	0.093	0.029	0.794	0.980	0.012	0.600	0.018	0.004	0.016	0.066	0.012	1.117	1.016	0.970	0.897	1.117	1.016	0.970	0.897	A3w
Slc25a15	-0.117	0.245	0.036	0.712	0.946	0.040	0.114	0.058	0.009	0.052	0.389	0.038	1.134	1.178	0.802	0.886	1.134	1.178	0.802	0.886	A4w
Plekha2	0.025	-0.107	-0.056	1.233	0.941	0.028	0.564	0.040	0.040	0.036	0.097	0.026	0.843	0.974	1.058	1.124	0.843	0.974	1.058	1.124	R3w
Nsd3	-0.049	-0.096	0.005	1.194	0.942	0.015	0.090	0.022	0.008	0.019	0.727	0.014	0.925	0.982	1.009	1.085	0.925	0.982	1.009	1.085	R3w
Saraf	-0.088	-0.131	0.072	1.171	0.968	0.007	0.001	0.011	0.000	0.010	0.001	0.007	1.014	0.937	1.008	1.041	1.014	0.937	1.008	1.041	A1w
Dusp4	1.117	-0.026	-0.193	0.020	0.932	0.174	0.011	0.252	0.913	0.224	0.300	0.163	1.323	0.347	1.838	0.492	1.323	0.347	1.838	0.492	A1
Mfhas1	0.029	0.074	0.020	0.818	0.889	0.025	0.472	0.036	0.085	0.032	0.447	0.023	1.100	1.000	0.992	0.908	1.100	1.000	0.992	0.908	A3w
Casp3	0.104	0.176	-0.058	0.716	0.904	0.022	0.030	0.032	0.003	0.028	0.048	0.020	1.051	1.062	0.987	0.901	1.051	1.062	0.987	0.901	A3w
Dctd	-0.015	0.179	0.031	0.694	0.864	0.049	0.844	0.071	0.047	0.063	0.536	0.046	1.153	1.076	0.911	0.860	1.153	1.076	0.911	0.860	A3w
Sh3rf1	-0.083	0.341	0.120	0.369	0.950	0.066	0.436	0.096	0.016	0.085	0.125	0.062	1.380	1.134	0.800	0.687	1.380	1.134	0.800	0.687	A3
Tma16	0.037	0.145	0.017	0.706	0.939	0.027	0.399	0.039	0.014	0.035	0.536	0.025	1.140	1.033	0.964	0.863	1.140	1.033	0.964	0.863	A3w
Slc25a42	-0.140	0.217	0.095	0.671	0.946	0.045	0.101	0.066	0.021	0.059	0.088	0.043	1.223	1.132	0.809	0.836	1.223	1.132	0.809	0.836	A4w
Isyna1	-0.002	0.086	0.006	0.863	0.938	0.014	0.935	0.020	0.008	0.018	0.653	0.013	1.059	1.040	0.960	0.941	1.059	1.040	0.960	0.941	A3w
Jund	-0.035	-0.134	0.026	1.196	0.964	0.012	0.107	0.017	0.001	0.015	0.075	0.011	0.954	0.935	1.041	1.069	0.954	0.935	1.041	1.069	R3w
Il12rb1	0.157	0.064	-0.036	0.776	0.920	0.024	0.011	0.035	0.105	0.031	0.188	0.022	1.067	0.950	1.084	0.900	1.067	0.950	1.084	0.900	A1w
Ano8	0.083	-0.140	-0.081	1.258	0.863	0.055	0.355	0.080	0.118	0.071	0.190	0.052	0.812	0.936	1.114	1.138	0.812	0.936	1.114	1.138	R3w
Tpm4	0.116	0.001	-0.054	0.955	0.943	0.012	0.003	0.018	0.950	0.016	0.009	0.011	0.968	0.961	1.079	0.991	0.968	0.961	1.079	0.991	I
Klf2	0.250	-0.019	-0.284	1.247	0.985	0.033	0.006	0.048	0.687	0.043	0.001	0.031	0.580	1.045	1.146	1.229	0.580	1.045	1.146	1.229	R2
Zfp827	-0.313	0.177	0.196	0.756	0.989	0.027	0.001	0.038	0.007	0.034	0.001	0.025	1.291	1.153	0.714	0.843	1.291	1.153	0.714	0.843	A3
Abce1	0.014	0.054	0.003	0.896	0.946	0.009	0.330	0.013	0.008	0.011	0.723	0.008	1.046	1.015	0.986	0.953	1.046	1.015	0.986	0.953	A3w
Adgre5	-0.152	-0.114	0.031	1.301	0.914	0.029	0.021	0.042	0.036	0.037	0.309	0.027	0.899	1.025	0.942	1.133	0.899	1.025	0.942	1.133	R1w
Podnl1	-0.367	-1.157	0.293	2.636	0.951	0.107	0.078	0.156	0.001	0.138	0.043	0.101	0.703	0.435	1.316	1.547	0.703	0.435	1.316	1.547	R3
Zswim4	0.157	-0.033	0.075	0.715	0.886	0.073	0.213	0.106	0.746	0.094	0.333	0.069	1.236	0.809	1.152	0.803	1.236	0.809	1.152	0.803	A1w
Nfix	-0.180	0.222	0.130	0.648	0.863	0.086	0.220	0.124	0.114	0.110	0.180	0.080	1.270	1.135	0.782	0.813	1.270	1.135	0.782	0.813	A4w
Tnpo2	0.053	0.092	-0.011	0.818	0.971	0.009	0.017	0.014	0.002	0.012	0.266	0.009	1.063	1.018	0.996	0.923	1.063	1.018	0.996	0.923	A3w
N4bp1	0.076	0.038	-0.111	1.056	0.917	0.029	0.139	0.042	0.364	0.037	0.014	0.027	0.847	1.056	1.019	1.078	0.847	1.056	1.019	1.078	R1w
Heatr3	0.009	0.089	0.001	0.855	0.884	0.018	0.764	0.027	0.020	0.024	0.966	0.017	1.057	1.038	0.965	0.940	1.057	1.038	0.965	0.940	A3w
Snx20	0.004	-0.185	0.005	1.263	0.931	0.028	0.929	0.040	0.006	0.035	0.856	0.026	0.909	0.899	1.091	1.101	0.909	0.899	1.091	1.101	R3w
Cyld	-0.008	-0.108	-0.007	1.185	0.902	0.022	0.810	0.032	0.019	0.029	0.756	0.021	0.920	0.957	1.043	1.080	0.920	0.957	1.043	1.080	R3w
Rbl2	-0.016	-0.104	-0.078	1.320	0.902	0.050	0.836	0.073	0.185	0.065	0.172	0.047	0.774	1.023	1.021	1.183	0.774	1.023	1.021	1.183	R2w
Rrad	0.408	-0.131	-0.227	1.115	0.929	0.068	0.015	0.099	0.209	0.088	0.024	0.064	0.735	0.828	1.332	1.105	0.735	0.828	1.332	1.105	R3
Ranbp10	-0.062	-0.163	0.010	1.302	0.874	0.035	0.290	0.051	0.023	0.045	0.769	0.033	0.889	0.953	1.031	1.128	0.889	0.953	1.031	1.128	R3w
Psmb10	-0.014	-0.067	-0.044	1.199	0.900	0.031	0.766	0.044	0.162	0.039	0.203	0.029	0.865	1.012	1.012	1.111	0.865	1.012	1.012	1.111	R2w
Sntb2	-0.080	-0.372	-0.002	1.659	0.947	0.053	0.358	0.077	0.006	0.068	0.964	0.050	0.734	0.870	1.112	1.283	0.734	0.870	1.112	1.283	R3w
Nfat5	0.086	0.154	0.024	0.619	0.929	0.039	0.205	0.057	0.037	0.050	0.543	0.037	1.191	0.997	0.999	0.813	1.191	0.997	0.999	0.813	A3w
Zfp821	0.370	0.174	-0.052	0.379	0.954	0.052	0.008	0.075	0.059	0.066	0.345	0.048	1.235	0.866	1.195	0.705	1.235	0.866	1.195	0.705	A1w
Mlkl	0.218	-0.325	-0.067	1.342	0.914	0.074	0.113	0.108	0.027	0.096	0.389	0.070	0.824	0.734	1.308	1.134	0.824	0.734	1.308	1.134	I
Atmin	-0.048	0.070	0.064	0.834	0.948	0.022	0.213	0.032	0.071	0.029	0.036	0.021	1.138	1.017	0.943	0.902	1.138	1.017	0.943	0.902	A3w
6430548M08Rik	0.094	0.639	0.156	-0.362	0.885	0.192	0.753	0.277	0.060	0.247	0.432	0.179	1.735	1.129	0.804	0.332	1.735	1.129	0.804	0.332	A2
Gse1	-0.095	-0.166	-0.029	1.420	0.897	0.053	0.282	0.076	0.070	0.068	0.588	0.049	0.786	1.007	0.999	1.208	0.786	1.007	0.999	1.208	R2w
Irf8	0.078	0.145	-0.032	0.747	0.933	0.018	0.040	0.026	0.003	0.023	0.129	0.017	1.068	1.044	0.986	0.902	1.068	1.044	0.986	0.902	A3w
Rnf166	-0.121	-0.156	0.035	1.317	0.894	0.029	0.047	0.043	0.015	0.038	0.276	0.028	0.904	0.979	0.986	1.131	0.904	0.979	0.986	1.131	R2w
Cbfa2t3	-0.736	-0.773	0.141	2.801	0.911	0.168	0.039	0.243	0.023	0.216	0.421	0.157	0.370	1.019	0.821	1.790	0.370	1.019	0.821	1.790	R1
Urb2	-0.003	0.128	0.016	0.782	0.977	0.013	0.899	0.019	0.002	0.017	0.262	0.012	1.103	1.053	0.941	0.903	1.103	1.053	0.941	0.903	A3w
Tarbp1	-0.006	0.174	0.023	0.704	0.961	0.024	0.872	0.034	0.005	0.031	0.353	0.022	1.141	1.073	0.919	0.867	1.141	1.073	0.919	0.867	A3w
Nrp1	-0.359	0.373	0.111	0.679	0.894	0.108	0.084	0.157	0.056	0.140	0.335	0.102	1.200	1.354	0.570	0.876	1.200	1.354	0.570	0.876	A4
Itgb1	-0.027	0.063	0.023	0.897	0.966	0.010	0.127	0.014	0.008	0.013	0.067	0.009	1.063	1.032	0.954	0.950	1.063	1.032	0.954	0.950	A3w
Ccdc82	0.020	-0.049	-0.051	1.145	0.788	0.039	0.748	0.057	0.382	0.050	0.236	0.037	0.882	1.003	1.028	1.087	0.882	1.003	1.028	1.087	R2w
Sesn3	0.195	-0.054	-0.138	1.097	0.933	0.036	0.021	0.053	0.313	0.047	0.015	0.034	0.818	0.947	1.149	1.086	0.818	0.947	1.149	1.086	R3w
Izumo1r	-0.770	0.424	0.822	-0.213	0.976	0.146	0.022	0.211	0.087	0.187	0.004	0.136	2.394	1.089	0.369	0.148	2.394	1.089	0.369	0.148	A3
Panx1	-0.091	-0.166	0.038	1.290	0.906	0.024	0.061	0.036	0.006	0.032	0.175	0.023	0.923	0.950	1.014	1.112	0.923	0.950	1.014	1.112	R3w
Zfp426	-0.255	-0.170	0.213	1.172	0.954	0.023	0.002	0.034	0.005	0.030	0.001	0.022	1.168	0.920	0.925	0.986	1.168	0.920	0.925	0.986	A1w
Ilf3	0.017	0.055	0.003	0.891	0.980	0.005	0.097	0.008	0.001	0.007	0.534	0.005	1.049	1.013	0.988	0.950	1.049	1.013	0.988	0.950	A3w
AB124611	-0.007	-0.166	-0.090	1.423	0.994	0.015	0.780	0.022	0.001	0.020	0.003	0.014	0.722	0.994	1.055	1.229	0.722	0.994	1.055	1.229	R2w
Carm1	0.026	0.113	-0.001	0.801	0.981	0.009	0.132	0.014	0.001	0.012	0.912	0.009	1.078	1.040	0.967	0.915	1.078	1.040	0.967	0.915	A3w
Acp5	-0.414	-0.275	0.171	1.603	0.881	0.054	0.006	0.078	0.017	0.070	0.028	0.051	0.921	1.016	0.842	1.220	0.921	1.016	0.842	1.220	R1w
Bbs9	-0.124	-0.415	0.086	1.612	0.956	0.039	0.092	0.056	0.001	0.050	0.077	0.036	0.860	0.808	1.115	1.217	0.860	0.808	1.115	1.217	R3w
Dpy19l1	-0.012	-0.076	-0.011	1.150	0.929	0.015	0.607	0.022	0.018	0.020	0.483	0.014	0.927	0.979	1.024	1.070	0.927	0.979	1.024	1.070	R3w
St14	-0.280	-0.117	0.259	1.037	0.916	0.051	0.019	0.073	0.148	0.065	0.005	0.047	1.275	0.928	0.890	0.908	1.275	0.928	0.890	0.908	A4w
Fli1	-0.005	-0.078	-0.030	1.179	0.928	0.021	0.875	0.031	0.047	0.027	0.201	0.020	0.892	0.989	1.026	1.092	0.892	0.989	1.026	1.092	R2w
Ets1	-0.042	-0.044	-0.035	1.184	0.858	0.035	0.453	0.051	0.383	0.045	0.346	0.033	0.877	1.037	0.981	1.105	0.877	1.037	0.981	1.105	R1w
Vwa5a	-0.069	-0.020	-0.135	1.367	0.976	0.037	0.263	0.053	0.699	0.047	0.017	0.034	0.671	1.151	0.929	1.250	0.671	1.151	0.929	1.250	R1
Gramd1b	0.063	-0.078	0.051	0.945	0.900	0.035	0.275	0.050	0.154	0.045	0.194	0.032	1.099	0.873	1.096	0.932	1.099	0.873	1.096	0.932	A1w

Gene	Erk(E)	NFAT(N)	ErkNFAT(EN)	B0	R2	RSE	pval(E)	se(E)	pval(N)	se(N)	pval(EN)	se(EN)	DMSO	MEKi	CsA	MEKi+CsA	DMSO1	MEKi1	CsA1	MEKi+CsA1	reg_mode
Pwp2	0.008	0.117	0.015	0.787	0.870	0.031	0.863	0.045	0.042	0.040	0.627	0.029	1.102	1.041	0.954	0.903	1.102	1.041	0.954	0.903	A3w
Agpat3	-0.070	0.057	0.033	0.940	0.970	0.010	0.009	0.015	0.013	0.013	0.026	0.010	1.053	1.052	0.926	0.969	1.053	1.052	0.926	0.969	A4w
Wdr18	0.070	0.113	-0.026	0.794	0.911	0.017	0.046	0.024	0.007	0.022	0.179	0.016	1.057	1.028	0.996	0.919	1.057	1.028	0.996	0.919	A3w
Abca7	0.065	-0.176	-0.062	1.298	0.932	0.039	0.313	0.057	0.025	0.050	0.164	0.037	0.818	0.915	1.121	1.146	0.818	0.915	1.121	1.146	R3w
Arhgap45	0.045	-0.152	-0.045	1.254	0.930	0.033	0.391	0.047	0.022	0.042	0.217	0.031	0.854	0.927	1.097	1.121	0.854	0.927	1.097	1.121	R3w
Cbarp	0.511	0.222	-0.215	0.438	0.982	0.023	0.000	0.034	0.002	0.030	0.001	0.022	1.024	0.923	1.249	0.803	1.024	0.923	1.249	0.803	A1w
Midn	0.220	0.061	-0.074	0.775	0.902	0.029	0.007	0.043	0.183	0.038	0.055	0.028	1.028	0.935	1.127	0.910	1.028	0.935	1.127	0.910	A1w
Thop1	-0.003	0.113	0.018	0.802	0.860	0.031	0.944	0.045	0.048	0.040	0.576	0.029	1.097	1.045	0.948	0.910	1.097	1.045	0.948	0.910	A3w
Tbxa2r	-0.093	-0.310	-0.047	1.667	0.987	0.028	0.084	0.041	0.001	0.036	0.149	0.026	0.670	0.948	1.064	1.318	0.670	0.948	1.064	1.318	R2
Nfic	-0.009	0.061	-0.117	1.138	0.977	0.023	0.800	0.034	0.111	0.030	0.006	0.022	0.792	1.134	0.941	1.133	0.792	1.134	0.941	1.133	R1w
S1pr4	0.064	-0.205	-0.077	1.370	0.993	0.015	0.041	0.022	0.000	0.019	0.005	0.014	0.772	0.913	1.131	1.184	0.772	0.913	1.131	1.184	R3w
Gna15	0.188	-0.669	-0.093	1.942	0.985	0.056	0.082	0.081	0.001	0.072	0.150	0.053	0.558	0.603	1.440	1.398	0.558	0.603	1.440	1.398	R3
Tle5	-0.016	0.008	-0.035	1.072	0.959	0.012	0.403	0.017	0.613	0.015	0.033	0.011	0.924	1.044	0.977	1.055	0.924	1.044	0.977	1.055	R1w
1500009L16Rik	-0.150	-0.593	0.013	2.047	0.941	0.086	0.296	0.125	0.006	0.111	0.877	0.081	0.596	0.796	1.164	1.444	0.596	0.796	1.164	1.444	R2
Tcp11l2	-0.152	-0.662	0.106	1.979	0.860	0.121	0.435	0.176	0.013	0.156	0.401	0.113	0.744	0.685	1.214	1.357	0.744	0.685	1.214	1.357	R3
Utp20	0.062	0.118	-0.007	0.761	0.912	0.023	0.137	0.033	0.016	0.030	0.751	0.021	1.092	1.022	0.991	0.896	1.092	1.022	0.991	0.896	A3w
Apaf1	0.042	-0.126	-0.045	1.220	0.884	0.037	0.481	0.054	0.059	0.048	0.272	0.035	0.866	0.942	1.083	1.108	0.866	0.942	1.083	1.108	R3w
Elk3	0.230	-0.133	-0.059	1.024	0.879	0.057	0.049	0.083	0.145	0.073	0.330	0.053	0.956	0.817	1.229	0.998	0.956	0.817	1.229	0.998	A1w
Plxnc1	0.003	0.368	0.013	0.421	0.954	0.048	0.967	0.070	0.004	0.062	0.780	0.045	1.236	1.173	0.833	0.758	1.236	1.173	0.833	0.758	A3w
Cradd	-0.241	0.017	0.011	1.251	0.913	0.052	0.033	0.075	0.813	0.067	0.827	0.049	0.875	1.172	0.808	1.145	0.875	1.172	0.808	1.145	R1w
Socs2	-0.436	0.131	0.124	1.111	0.977	0.038	0.001	0.056	0.057	0.050	0.026	0.036	1.039	1.277	0.626	1.058	1.039	1.277	0.626	1.058	R1w
Eea1	-0.056	0.356	0.044	0.454	0.987	0.027	0.223	0.039	0.001	0.035	0.153	0.025	1.253	1.185	0.798	0.764	1.253	1.185	0.798	0.764	A4w
Btg1	-0.047	-0.076	0.069	1.044	0.921	0.014	0.081	0.020	0.014	0.018	0.006	0.013	1.065	0.939	1.013	0.983	1.065	0.939	1.013	0.983	A1w
Dusp6	0.755	0.223	-0.023	-0.224	0.892	0.192	0.053	0.279	0.418	0.247	0.905	0.180	1.571	0.592	1.475	0.362	1.571	0.592	1.475	0.362	A2
Phlda1	0.574	0.100	-0.251	0.608	0.949	0.050	0.001	0.072	0.192	0.064	0.006	0.047	0.924	0.847	1.348	0.882	0.924	0.847	1.348	0.882	A1w
Glipr1	0.206	-0.371	-0.072	1.434	0.938	0.069	0.108	0.100	0.014	0.089	0.327	0.065	0.781	0.723	1.319	1.177	0.781	0.723	1.319	1.177	I
Rap1b	0.065	-0.023	-0.034	1.017	0.924	0.011	0.016	0.016	0.190	0.015	0.033	0.011	0.961	0.970	1.054	1.015	0.961	0.970	1.054	1.015	I
Ifng	0.824	1.326	-0.482	-1.100	0.973	0.081	0.002	0.117	0.000	0.104	0.003	0.076	1.309	1.480	0.920	0.291	1.309	1.480	0.920	0.291	A4
Ppm1h	-0.176	-0.025	-0.001	1.257	0.933	0.036	0.028	0.053	0.615	0.047	0.974	0.034	0.869	1.114	0.876	1.142	0.869	1.114	0.876	1.142	R1w
Mettl1	0.074	0.152	-0.022	0.722	0.878	0.029	0.155	0.042	0.016	0.038	0.473	0.027	1.090	1.042	0.982	0.886	1.090	1.042	0.982	0.886	A3w
Nab2	0.274	0.153	-0.059	0.542	0.974	0.026	0.002	0.037	0.010	0.033	0.070	0.024	1.146	0.929	1.129	0.795	1.146	0.929	1.129	0.795	A1w
Nemp1	-0.014	0.028	0.076	0.833	0.981	0.015	0.549	0.022	0.215	0.019	0.005	0.014	1.161	0.961	0.991	0.887	1.161	0.961	0.991	0.887	A3w
Stat2	0.101	-0.017	-0.133	1.149	0.980	0.020	0.023	0.028	0.534	0.025	0.002	0.018	0.788	1.029	1.060	1.124	0.788	1.029	1.060	1.124	R2w
Tespa1	0.245	0.211	0.069	0.254	0.938	0.081	0.105	0.117	0.113	0.104	0.413	0.076	1.417	0.875	1.104	0.603	1.417	0.875	1.104	0.603	A2
Sfi1	-0.156	0.223	0.078	0.713	0.941	0.046	0.078	0.066	0.019	0.059	0.142	0.043	1.181	1.160	0.791	0.868	1.181	1.160	0.791	0.868	A4w
Eif4enif1	-0.022	0.144	0.011	0.791	1.000	0.001	0.000	0.002	0.000	0.002	0.001	0.001	1.089	1.080	0.917	0.914	1.089	1.080	0.917	0.914	A3w
Pik3ip1	-0.130	-0.430	-0.011	1.824	0.869	0.106	0.446	0.154	0.035	0.137	0.915	0.100	0.651	0.884	1.099	1.366	0.651	0.884	1.099	1.366	R2
Osm	-0.052	0.030	-0.099	1.203	0.884	0.058	0.567	0.084	0.706	0.075	0.143	0.054	0.784	1.134	0.926	1.156	0.784	1.134	0.926	1.156	R1w
Lif	0.585	0.833	-0.089	-0.800	0.940	0.138	0.043	0.200	0.009	0.178	0.527	0.129	1.668	1.077	1.045	0.209	1.668	1.077	1.045	0.209	A2
Nefh	-0.067	0.107	0.039	0.850	0.924	0.025	0.139	0.036	0.030	0.032	0.169	0.024	1.096	1.070	0.906	0.929	1.096	1.070	0.906	0.929	A4w
Myo1g	0.076	-0.023	-0.086	1.101	0.962	0.018	0.041	0.026	0.362	0.023	0.007	0.017	0.863	1.004	1.053	1.079	0.863	1.004	1.053	1.079	R3w
Ccm2	0.025	-0.098	-0.023	1.158	0.865	0.028	0.568	0.040	0.052	0.036	0.435	0.026	0.916	0.951	1.061	1.072	0.916	0.951	1.061	1.072	R3w
Ramp3	2.517	0.397	-1.087	-0.676	0.968	0.174	0.001	0.252	0.151	0.224	0.003	0.163	0.670	0.295	2.546	0.489	0.670	0.295	2.546	0.489	A1
Plek	-0.963	-0.099	0.492	1.421	0.947	0.090	0.002	0.131	0.443	0.116	0.004	0.084	1.309	1.234	0.399	1.058	1.309	1.234	0.399	1.058	A4
Spred2	0.614	0.535	-0.200	-0.184	0.972	0.053	0.001	0.077	0.001	0.069	0.016	0.050	1.296	0.997	1.185	0.522	1.296	0.997	1.185	0.522	A2
Rel	0.028	-0.123	0.099	0.965	0.913	0.041	0.665	0.060	0.083	0.053	0.063	0.039	1.149	0.836	1.099	0.916	1.149	0.836	1.099	0.916	A1w
Nsg2	-0.098	-0.301	-0.079	1.718	0.974	0.047	0.221	0.067	0.007	0.060	0.144	0.044	0.608	0.982	1.050	1.360	0.608	0.982	1.050	1.360	R2
Ubtd2	-0.014	0.298	0.038	0.501	0.902	0.065	0.885	0.094	0.023	0.083	0.563	0.061	1.235	1.130	0.857	0.778	1.235	1.130	0.857	0.778	A4w
Lcp2	0.073	-0.004	0.019	0.881	0.938	0.020	0.064	0.029	0.869	0.026	0.364	0.019	1.083	0.930	1.062	0.925	1.083	0.930	1.062	0.925	A1w
Adam19	0.360	-0.499	-0.273	1.809	0.863	0.187	0.255	0.271	0.107	0.241	0.195	0.175	0.405	0.713	1.458	1.423	0.405	0.713	1.458	1.423	R3
Med7	0.194	0.054	-0.026	0.729	0.950	0.027	0.008	0.040	0.203	0.035	0.365	0.026	1.104	0.910	1.120	0.867	1.104	0.910	1.120	0.867	A1w
Irgm1	0.030	-0.037	-0.029	1.072	0.954	0.010	0.095	0.014	0.040	0.012	0.031	0.009	0.940	0.984	1.035	1.041	0.940	0.984	1.035	1.041	R3w
Tgtp1	0.043	-0.068	-0.037	1.117	0.906	0.021	0.227	0.030	0.064	0.027	0.134	0.020	0.916	0.965	1.058	1.061	0.916	0.965	1.058	1.061	R3w
9930111J21Rik2	0.152	-0.322	-0.183	1.634	0.968	0.060	0.156	0.087	0.014	0.078	0.031	0.056	0.549	0.879	1.232	1.340	0.549	0.879	1.232	1.340	R2
Jade2	-0.039	0.053	0.029	0.914	0.854	0.021	0.267	0.030	0.117	0.027	0.205	0.019	1.064	1.030	0.951	0.955	1.064	1.030	0.951	0.955	A4w
Ube2b	0.050	-0.052	-0.014	1.043	0.916	0.013	0.062	0.019	0.038	0.017	0.328	0.013	0.975	0.949	1.060	1.015	0.975	0.949	1.060	1.015	I
Tcf7	-0.020	-0.071	-0.029	1.184	0.846	0.032	0.690	0.047	0.165	0.042	0.397	0.030	0.890	1.002	1.012	1.097	0.890	1.002	1.012	1.097	R2w
Pdlim4	-0.924	-1.421	0.348	3.616	0.960	0.139	0.010	0.201	0.001	0.179	0.055	0.130	0.302	0.654	1.020	2.024	0.302	0.654	1.020	2.024	R2
Fnip1	-0.006	0.228	-0.020	0.705	0.978	0.018	0.828	0.026	0.001	0.023	0.289	0.017	1.083	1.137	0.885	0.896	1.083	1.137	0.885	0.896	A4w
Cdc42se2	0.014	-0.048	-0.027	1.104	0.928	0.014	0.516	0.020	0.057	0.018	0.110	0.013	0.928	0.988	1.028	1.056	0.928	0.988	1.028	1.056	R3w
Tnip1	-0.063	-0.179	0.061	1.232	0.960	0.014	0.034	0.020	0.001	0.018	0.009	0.013	0.981	0.904	1.047	1.068	0.981	0.904	1.047	1.068	R3w
Anxa6	-0.017	-0.061	-0.013	1.137	0.887	0.018	0.548	0.027	0.061	0.024	0.502	0.017	0.928	0.992	1.013	1.067	0.928	0.992	1.013	1.067	R2w
Galnt10	-0.011	-0.300	0.080	1.314	0.912	0.044	0.875	0.064	0.006	0.056	0.125	0.041	0.985	0.790	1.148	1.077	0.985	0.790	1.148	1.077	I
Gemin5	-0.006	0.092	0.015	0.841	0.968	0.012	0.757	0.017	0.004	0.015	0.239	0.011	1.078	1.038	0.956	0.928	1.078	1.038	0.956	0.928	A3w
Igtp	-0.008	-0.020	-0.030	1.096	0.981	0.007	0.514	0.011	0.109	0.010	0.012	0.007	0.922	1.021	0.997	1.060	0.922	1.021	0.997	1.060	R1w
Irgm2	-0.012	-0.057	-0.030	1.155	0.988	0.008	0.346	0.011	0.005	0.010	0.014	0.007	0.900	1.004	1.012	1.084	0.900	1.004	1.012	1.084	R2w

Gene	Erk(E)	NFAT(N)	ErkNFAT(EN)	B0	R2	RSE	pval(E)	se(E)	pval(N)	se(N)	pval(EN)	se(EN)	DMSO	MEKi	CsA	MEKi+CsA	DMSO1	MEKi1	CsA1	MEKi+CsA1	reg_mode
Trpv2	0.205	-0.133	-0.080	1.094	0.978	0.022	0.003	0.032	0.009	0.028	0.018	0.021	0.898	0.851	1.205	1.045	0.898	0.851	1.205	1.045	I
Hs3st3b1	0.103	-0.095	0.108	0.814	0.882	0.073	0.387	0.106	0.369	0.094	0.188	0.068	1.232	0.789	1.146	0.833	1.232	0.789	1.146	0.833	A1w
Elac2	-0.014	0.048	0.041	0.868	0.912	0.021	0.675	0.030	0.148	0.027	0.105	0.020	1.101	1.001	0.975	0.923	1.101	1.001	0.975	0.923	A3w
Pik3r5	0.011	-0.036	-0.115	1.254	0.990	0.016	0.650	0.024	0.156	0.021	0.002	0.015	0.756	1.068	1.003	1.173	0.756	1.068	1.003	1.173	R1w
Pfas	0.066	0.095	-0.018	0.809	0.915	0.016	0.047	0.024	0.010	0.021	0.311	0.015	1.061	1.015	1.003	0.920	1.061	1.015	1.003	0.920	A3w
Per1	0.059	0.041	0.023	0.823	0.911	0.025	0.183	0.037	0.276	0.033	0.389	0.024	1.108	0.960	1.031	0.902	1.108	0.960	1.031	0.902	A1w
Kdm6b	0.033	0.056	0.033	0.815	0.930	0.023	0.380	0.033	0.130	0.029	0.201	0.021	1.119	0.978	1.005	0.898	1.119	0.978	1.005	0.898	A3w
Nlgn2	0.193	0.341	-0.049	0.343	0.892	0.065	0.110	0.094	0.015	0.084	0.468	0.061	1.219	1.075	0.979	0.726	1.219	1.075	0.979	0.726	A3w
Tm4sf5	-0.465	0.980	0.302	-0.452	0.963	0.151	0.101	0.219	0.007	0.194	0.099	0.141	1.856	1.581	0.241	0.322	1.856	1.581	0.241	0.322	A3
Eno3	-0.065	0.228	-0.113	0.949	0.972	0.032	0.228	0.046	0.005	0.041	0.019	0.030	0.859	1.255	0.820	1.066	0.859	1.255	0.820	1.066	R1w
Rabep1	-0.049	0.011	0.059	0.934	0.984	0.008	0.012	0.011	0.310	0.010	0.001	0.007	1.093	0.992	0.969	0.946	1.093	0.992	0.969	0.946	A3w
Dhx33	0.078	0.126	-0.019	0.750	0.889	0.025	0.096	0.036	0.017	0.032	0.454	0.023	1.083	1.024	0.997	0.896	1.083	1.024	0.997	0.896	A3w
Pimreg	-0.081	-0.146	-0.040	1.392	0.912	0.048	0.308	0.069	0.078	0.062	0.421	0.045	0.784	1.017	0.998	1.201	0.784	1.017	0.998	1.201	R2w
Xaf1	0.225	-0.479	-0.226	1.858	0.969	0.079	0.123	0.115	0.009	0.102	0.039	0.074	0.423	0.782	1.354	1.442	0.423	0.782	1.354	1.442	R2
Mybbp1a	0.022	0.079	0.002	0.850	0.941	0.013	0.307	0.019	0.009	0.017	0.848	0.012	1.064	1.023	0.980	0.934	1.064	1.023	0.980	0.934	A3w
Cluh	0.021	0.154	-0.004	0.752	0.984	0.011	0.253	0.016	0.000	0.014	0.693	0.010	1.091	1.066	0.944	0.899	1.091	1.066	0.944	0.899	A3w
Tsr1	0.010	0.054	0.014	0.880	0.904	0.015	0.664	0.022	0.054	0.020	0.376	0.015	1.066	1.008	0.986	0.940	1.066	1.008	0.986	0.940	A3w
Slc43a2	-0.051	-0.135	-0.044	1.346	0.817	0.064	0.614	0.093	0.177	0.083	0.508	0.060	0.803	1.004	1.015	1.178	0.803	1.004	1.015	1.178	R2w
Inpp5k	-0.070	-0.126	-0.019	1.310	0.910	0.036	0.251	0.052	0.053	0.046	0.593	0.034	0.845	1.002	1.001	1.152	0.845	1.002	1.001	1.152	R2w
Abr	-0.043	-0.151	-0.054	1.379	0.890	0.054	0.618	0.079	0.097	0.070	0.348	0.051	0.779	0.998	1.027	1.196	0.779	0.998	1.027	1.196	R2w
Cpd	0.754	0.336	-0.111	-0.226	0.970	0.083	0.003	0.121	0.035	0.107	0.227	0.078	1.456	0.722	1.404	0.418	1.456	0.722	1.404	0.418	A2
Ankrd13b	-0.060	0.176	0.073	0.676	0.958	0.033	0.274	0.048	0.014	0.042	0.076	0.031	1.206	1.072	0.886	0.836	1.206	1.072	0.886	0.836	A3w
Git1	-0.013	0.065	0.014	0.894	0.962	0.009	0.392	0.013	0.006	0.012	0.193	0.009	1.055	1.031	0.962	0.951	1.055	1.031	0.962	0.951	A3w
Nf1	0.216	-0.005	0.029	0.687	0.870	0.075	0.116	0.108	0.960	0.096	0.703	0.070	1.196	0.819	1.176	0.810	1.196	0.819	1.176	0.810	A1w
Evi2a	0.101	-0.221	-0.053	1.305	0.960	0.033	0.106	0.048	0.007	0.043	0.163	0.031	0.834	0.860	1.171	1.135	0.834	0.860	1.171	1.135	R3w
Slfn8	0.409	-0.176	-0.190	1.111	0.946	0.061	0.010	0.088	0.087	0.078	0.029	0.057	0.785	0.774	1.362	1.079	0.785	0.774	1.362	1.079	I
Slfn2	-0.021	-0.071	0.064	1.013	0.865	0.023	0.563	0.034	0.076	0.030	0.042	0.022	1.075	0.927	1.029	0.969	1.075	0.927	1.029	0.969	A1w
Slfn1	0.417	-0.200	-0.333	1.405	0.996	0.024	0.000	0.035	0.003	0.031	0.000	0.022	0.487	0.874	1.351	1.288	0.487	0.874	1.351	1.288	R3
Ccl5	0.216	-0.290	-0.078	1.312	0.976	0.036	0.015	0.052	0.003	0.047	0.082	0.034	0.821	0.763	1.287	1.129	0.821	0.763	1.287	1.129	I
Ccl3	0.385	0.919	-0.045	-0.766	0.973	0.093	0.047	0.135	0.002	0.120	0.636	0.087	1.677	1.227	0.858	0.237	1.677	1.227	0.858	0.237	A3
Ccl4	0.482	0.841	-0.135	-0.600	0.983	0.061	0.005	0.088	0.000	0.078	0.076	0.057	1.513	1.194	0.952	0.342	1.513	1.194	0.952	0.342	A3
Tada2a	0.081	0.207	-0.023	0.634	0.932	0.029	0.130	0.043	0.005	0.038	0.446	0.028	1.122	1.066	0.961	0.851	1.122	1.066	0.961	0.851	A3w
Acaca	0.010	0.130	0.017	0.763	0.997	0.005	0.216	0.007	0.000	0.006	0.019	0.004	1.113	1.045	0.950	0.892	1.113	1.045	0.950	0.892	A3w
Ypel2	0.257	1.159	-0.263	-0.559	0.973	0.084	0.101	0.121	0.000	0.108	0.028	0.078	1.287	1.620	0.604	0.489	1.287	1.620	0.604	0.489	A4
Rad51c	0.017	-0.190	-0.089	1.428	0.901	0.063	0.860	0.092	0.080	0.082	0.209	0.059	0.726	0.964	1.085	1.225	0.726	0.964	1.085	1.225	R3w
Gm45716	0.148	-0.297	0.090	1.093	0.888	0.083	0.283	0.120	0.049	0.106	0.308	0.077	1.112	0.669	1.272	0.947	1.112	0.669	1.272	0.947	A1w
Mmd	0.112	-0.015	0.069	0.755	0.912	0.052	0.211	0.075	0.836	0.067	0.227	0.049	1.204	0.855	1.107	0.833	1.204	0.855	1.107	0.833	A1w
Tob1	0.094	-0.168	-0.026	1.183	0.986	0.014	0.011	0.021	0.001	0.019	0.123	0.014	0.914	0.869	1.146	1.070	0.914	0.869	1.146	1.070	I
Fam117a	0.004	-0.102	-0.060	1.259	0.931	0.033	0.936	0.047	0.072	0.042	0.123	0.031	0.825	0.994	1.039	1.142	0.825	0.994	1.039	1.142	R3w
Zfp652	-0.158	-0.128	0.016	1.356	0.807	0.057	0.129	0.083	0.157	0.074	0.778	0.053	0.858	1.035	0.941	1.166	0.858	1.035	0.941	1.166	R1w
Skap1	0.011	-0.115	-0.007	1.172	0.916	0.021	0.745	0.031	0.013	0.027	0.734	0.020	0.928	0.940	1.061	1.072	0.928	0.940	1.061	1.072	R3w
Tbx21	-0.133	0.210	0.066	0.728	0.898	0.056	0.173	0.080	0.042	0.072	0.273	0.052	1.164	1.148	0.812	0.877	1.164	1.148	0.812	0.877	A4w
Tbkbp1	-0.061	0.461	0.051	0.292	0.923	0.085	0.646	0.124	0.014	0.110	0.557	0.080	1.322	1.236	0.747	0.696	1.322	1.236	0.747	0.696	A3
Arl5c	-0.088	-0.344	-0.119	1.843	0.991	0.033	0.139	0.048	0.001	0.043	0.018	0.031	0.510	0.986	1.069	1.434	0.510	0.986	1.069	1.434	R2
Thra	0.244	0.028	-0.244	1.111	0.952	0.045	0.020	0.065	0.651	0.058	0.004	0.042	0.682	1.040	1.127	1.150	0.682	1.040	1.127	1.150	R3w
Rara	0.245	-0.196	-0.089	1.155	0.976	0.030	0.005	0.044	0.007	0.039	0.036	0.028	0.871	0.799	1.264	1.067	0.871	0.799	1.264	1.067	I
Ccr7	0.031	-0.016	-0.079	1.134	0.996	0.006	0.023	0.009	0.102	0.008	0.000	0.006	0.851	1.035	1.015	1.098	0.851	1.035	1.015	1.098	R1w
Cnp	-0.034	-0.110	-0.033	1.268	0.985	0.013	0.152	0.019	0.003	0.017	0.056	0.012	0.849	0.996	1.019	1.136	0.849	0.996	1.019	1.136	R3w
Psme3	-0.012	0.018	0.024	0.944	0.917	0.010	0.435	0.014	0.242	0.013	0.061	0.009	1.050	0.998	0.987	0.965	1.050	0.998	0.987	0.965	A3w
Etv4	0.882	0.162	0.199	-0.700	0.947	0.218	0.049	0.316	0.596	0.281	0.385	0.204	2.066	0.287	1.646	0.000	2.066	0.287	1.646	0.000	A2
Mpp2	0.027	-1.109	0.017	2.591	0.972	0.106	0.867	0.153	0.001	0.136	0.871	0.099	0.430	0.404	1.544	1.622	0.430	0.404	1.544	1.622	R3
Hdac5	0.078	-0.109	-0.058	1.176	0.963	0.020	0.058	0.030	0.014	0.026	0.038	0.019	0.872	0.937	1.100	1.091	0.872	0.937	1.100	1.091	R3w
Grn	0.041	0.030	-0.146	1.177	0.916	0.050	0.604	0.072	0.668	0.064	0.036	0.047	0.749	1.106	0.989	1.156	0.749	1.106	0.989	1.156	R1w
Fnnl1	0.047	-0.098	-0.034	1.152	0.940	0.020	0.180	0.029	0.019	0.026	0.142	0.019	0.907	0.945	1.076	1.073	0.907	0.945	1.076	1.073	R3w
Itgb3	0.162	-0.406	-0.252	1.874	0.982	0.061	0.142	0.089	0.007	0.079	0.012	0.058	0.370	0.885	1.266	1.479	0.370	0.885	1.266	1.479	R2
Tex2	-0.115	-0.045	0.001	1.208	0.906	0.029	0.051	0.042	0.294	0.037	0.977	0.027	0.901	1.059	0.932	1.108	0.901	1.059	0.932	1.108	R1w
Pecam1	-0.030	-0.102	-0.069	1.317	0.860	0.059	0.741	0.085	0.249	0.075	0.278	0.055	0.785	1.026	1.011	1.178	0.785	1.026	1.011	1.178	R2w
Nol11	-0.003	0.051	0.021	0.889	0.903	0.016	0.891	0.023	0.065	0.020	0.238	0.015	1.068	1.012	0.977	0.943	1.068	1.012	0.977	0.943	A3w
Prkca	-0.201	0.187	0.090	0.801	0.864	0.068	0.113	0.099	0.101	0.088	0.233	0.064	1.155	1.165	0.775	0.905	1.155	1.165	0.775	0.905	A4w
Rab37	-0.260	-0.649	0.085	2.132	0.927	0.093	0.127	0.135	0.006	0.120	0.385	0.087	0.638	0.787	1.120	1.456	0.638	0.787	1.120	1.456	R2
Slc9a3r1	0.000	-0.045	-0.021	1.106	0.942	0.012	0.998	0.017	0.039	0.015	0.132	0.011	0.933	0.994	1.017	1.056	0.933	0.994	1.017	1.056	R3w
Armc7	-0.272	-0.279	0.113	1.542	0.957	0.027	0.002	0.039	0.001	0.035	0.011	0.025	0.894	0.960	0.942	1.203	0.894	0.960	0.942	1.203	R1w
Trim65	-0.002	0.148	-0.115	0.994	0.973	0.023	0.963	0.033	0.007	0.029	0.006	0.021	0.851	1.170	0.907	1.072	0.851	1.170	0.907	1.072	R1w
Syngr2	0.001	0.042	0.020	0.898	0.878	0.017	0.965	0.024	0.122	0.021	0.266	0.016	1.065	1.004	0.985	0.946	1.065	1.004	0.985	0.946	A3w
Tha1	-0.039	-0.060	-0.175	1.464	0.977	0.044	0.568	0.064	0.349	0.057	0.013	0.041	0.588	1.142	0.963	1.307	0.588	1.142	0.963	1.307	R1
Cyth1	-0.039	-0.037	-0.029	1.156	0.889	0.026	0.363	0.038	0.336	0.034	0.307	0.024	0.896	1.033	0.982	1.089	0.896	1.033	0.982	1.089	R1w

Gene	Erk(E)	NFAT(N)	ErkNFAT(EN)	B0	R2	RSE	pval(E)	se(E)	pval(N)	se(N)	pval(EN)	se(EN)	DMSO	MEKi	CsA	MEKi+CsA	DMSO1	MEKi1	CsA1	MEKi+CsA1	reg_mode
Usp36	0.011	0.045	0.021	0.880	0.927	0.015	0.620	0.021	0.073	0.019	0.205	0.014	1.075	0.998	0.992	0.936	1.075	0.998	0.992	0.936	A3w
Lgals3bp	-0.023	-0.165	-0.029	1.330	0.980	0.018	0.437	0.026	0.002	0.023	0.160	0.017	0.833	0.956	1.054	1.156	0.833	0.956	1.054	1.156	R2w
Cbx4	0.011	0.075	-0.083	1.029	0.899	0.030	0.816	0.043	0.125	0.039	0.042	0.028	0.882	1.098	0.957	1.063	0.882	1.098	0.957	1.063	R1w
Mafg	0.121	0.168	-0.019	0.636	0.931	0.030	0.050	0.044	0.012	0.039	0.530	0.028	1.134	1.015	1.011	0.841	1.134	1.015	1.011	0.841	A3w
Fasn	0.043	0.073	-0.003	0.844	0.874	0.019	0.183	0.027	0.039	0.024	0.867	0.017	1.063	1.008	0.999	0.930	1.063	1.008	0.999	0.930	A3w
Cd7	-0.278	-0.981	-0.040	2.885	0.928	0.180	0.345	0.260	0.013	0.231	0.823	0.168	0.187	0.735	1.236	1.842	0.187	0.735	1.236	1.842	R2
Rab10	-0.044	0.092	0.002	0.913	0.961	0.012	0.069	0.018	0.004	0.016	0.851	0.012	1.027	1.076	0.924	0.973	1.027	1.076	0.924	0.973	A4w
Dnmt3a	0.014	0.052	0.030	0.850	0.810	0.032	0.775	0.046	0.276	0.041	0.374	0.030	1.098	0.992	0.993	0.918	1.098	0.992	0.993	0.918	A3w
Sdc1	0.086	0.681	0.022	-0.163	0.931	0.112	0.626	0.163	0.009	0.144	0.847	0.105	1.482	1.266	0.751	0.501	1.482	1.266	0.751	0.501	A3
Trib2	0.417	0.058	-0.163	0.702	0.968	0.031	0.001	0.044	0.213	0.039	0.005	0.029	0.975	0.865	1.263	0.896	0.975	0.865	1.263	0.896	A1w
Lpin1	0.122	-0.232	-0.092	1.367	0.901	0.065	0.263	0.093	0.049	0.083	0.204	0.060	0.764	0.871	1.185	1.180	0.764	0.871	1.185	1.180	R3w
Nol10	0.015	0.070	0.022	0.837	0.966	0.012	0.455	0.018	0.012	0.016	0.136	0.012	1.092	1.007	0.983	0.917	1.092	1.007	0.983	0.917	A3w
Odc1	0.043	0.080	-0.011	0.847	0.866	0.017	0.157	0.025	0.022	0.022	0.531	0.016	1.051	1.019	0.993	0.936	1.051	1.019	0.993	0.936	A3w
Id2	0.204	-0.249	-0.065	1.241	0.988	0.022	0.003	0.033	0.001	0.029	0.037	0.021	0.863	0.781	1.262	1.095	0.863	0.781	1.262	1.095	I
Rnf144a	-0.139	-0.166	-0.065	1.540	0.862	0.090	0.347	0.130	0.225	0.116	0.481	0.084	0.685	1.069	0.957	1.289	0.685	1.069	0.957	1.289	R1
Pik3cg	0.332	-0.182	-0.157	1.155	0.911	0.071	0.031	0.102	0.115	0.091	0.076	0.066	0.797	0.799	1.311	1.092	0.797	0.799	1.311	1.092	I
Sypl	0.625	0.258	-0.078	-0.012	0.956	0.087	0.008	0.126	0.082	0.112	0.391	0.081	1.395	0.748	1.347	0.510	1.395	0.748	1.347	0.510	A1
Tspan13	-0.090	-0.158	0.014	1.322	0.972	0.017	0.020	0.024	0.002	0.021	0.424	0.016	0.880	0.973	1.007	1.140	0.880	0.973	1.007	1.140	R3w
Dnajb9	0.014	-0.314	0.011	1.432	0.942	0.042	0.834	0.061	0.004	0.055	0.793	0.040	0.855	0.822	1.160	1.163	0.855	0.822	1.160	1.163	R3w
Egln3	-0.181	0.173	0.223	0.549	0.991	0.028	0.012	0.041	0.009	0.037	0.001	0.027	1.429	1.034	0.823	0.714	1.429	1.034	0.823	0.714	A3
Fam177a	0.011	0.005	-0.049	1.069	0.909	0.018	0.692	0.027	0.849	0.024	0.047	0.017	0.912	1.034	0.997	1.057	0.912	1.034	0.997	1.057	R1w
Frmd6	0.168	0.349	-0.060	0.384	0.941	0.043	0.054	0.062	0.003	0.055	0.209	0.040	1.184	1.106	0.955	0.755	1.184	1.106	0.955	0.755	A3w
Dhrs7	-0.111	-0.164	0.001	1.381	0.980	0.018	0.013	0.026	0.002	0.023	0.961	0.017	0.837	0.995	0.991	1.176	0.837	0.995	0.991	1.176	R2w
Slc38a6	0.084	-0.053	-0.014	1.002	0.931	0.017	0.025	0.024	0.068	0.021	0.408	0.016	0.996	0.925	1.087	0.992	0.996	0.925	1.087	0.992	A1w
Prkch	-0.217	-0.003	0.058	1.163	0.949	0.025	0.004	0.036	0.928	0.032	0.066	0.023	0.975	1.105	0.845	1.074	0.975	1.105	0.845	1.074	R1w
Zfp36l1	0.033	-0.051	0.034	0.972	0.932	0.017	0.259	0.025	0.084	0.022	0.101	0.016	1.062	0.923	1.056	0.960	1.062	0.923	1.056	0.960	A1w
Entpd5	-0.065	-0.050	-0.028	1.206	0.879	0.034	0.265	0.050	0.324	0.044	0.438	0.032	0.874	1.044	0.968	1.115	0.874	1.044	0.968	1.115	R1w
Npc2	-0.025	-0.098	-0.008	1.193	0.960	0.014	0.284	0.020	0.006	0.018	0.572	0.013	0.912	0.975	1.025	1.088	0.912	0.975	1.025	1.088	R2w
Fos	1.688	0.374	-0.490	-0.732	0.978	0.116	0.001	0.168	0.066	0.149	0.011	0.108	1.322	0.385	2.034	0.259	1.322	0.385	2.034	0.259	A1
Jdp2	-0.535	-0.395	0.013	2.228	0.900	0.149	0.068	0.216	0.108	0.192	0.930	0.140	0.455	1.172	0.774	1.599	0.455	1.172	0.774	1.599	R1
Irf2bpl	0.144	-0.006	-0.079	0.979	0.906	0.021	0.010	0.031	0.826	0.028	0.017	0.020	0.931	0.959	1.099	1.011	0.931	0.959	1.099	1.011	R3w
Gpr65	0.117	-0.100	-0.100	1.193	0.981	0.019	0.013	0.027	0.014	0.024	0.005	0.018	0.818	0.948	1.117	1.117	0.818	0.948	1.117	1.117	R3w
Ttc7b	-0.029	0.167	0.025	0.740	0.947	0.027	0.487	0.039	0.008	0.034	0.375	0.025	1.125	1.086	0.904	0.886	1.125	1.086	0.904	0.886	A4w
Gpr68	-0.852	-0.852	0.635	2.143	0.896	0.089	0.003	0.129	0.002	0.115	0.002	0.083	1.246	0.655	0.866	1.232	1.246	0.655	0.866	1.232	A3
Ifi27	0.141	-0.141	-0.134	1.286	0.820	0.083	0.308	0.121	0.258	0.107	0.162	0.078	0.743	0.937	1.149	1.171	0.743	0.937	1.149	1.171	R3w
Evl	0.068	-0.034	-0.034	1.030	0.852	0.019	0.064	0.027	0.233	0.024	0.120	0.017	0.957	0.962	1.062	1.019	0.957	0.962	1.062	1.019	R3w
Wars	-0.044	-0.037	-0.002	1.113	0.941	0.011	0.045	0.015	0.056	0.014	0.865	0.010	0.947	1.015	0.983	1.056	0.947	1.015	0.983	1.056	R1w
Ckb	0.423	0.230	-0.129	0.374	0.968	0.035	0.001	0.051	0.007	0.045	0.017	0.033	1.145	0.920	1.194	0.741	1.145	0.920	1.194	0.741	A1w
Gpr132	0.041	-0.054	-0.050	1.122	0.932	0.019	0.221	0.028	0.097	0.025	0.052	0.018	0.896	0.984	1.047	1.072	0.896	0.984	1.047	1.072	R3w
Crip1	-0.016	-0.057	-0.055	1.208	0.912	0.032	0.744	0.047	0.240	0.042	0.144	0.030	0.847	1.028	1.003	1.122	0.847	1.028	1.003	1.122	R1w
Ighm	-0.013	-0.058	-0.017	1.133	0.982	0.007	0.278	0.011	0.003	0.009	0.070	0.007	0.925	0.994	1.014	1.067	0.925	0.994	1.014	1.067	R3w
Zfp386	0.029	-0.238	-0.091	1.490	0.990	0.022	0.422	0.032	0.001	0.029	0.012	0.021	0.702	0.933	1.116	1.249	0.702	0.933	1.116	1.249	R3w
Sp4	-0.201	-0.176	0.064	1.392	0.880	0.038	0.022	0.055	0.023	0.049	0.149	0.036	0.899	1.002	0.939	1.159	0.899	1.002	0.939	1.159	R1w
Pitrm1	-0.028	0.094	0.021	0.855	0.985	0.009	0.083	0.012	0.001	0.011	0.057	0.008	1.077	1.051	0.938	0.934	1.077	1.051	0.938	0.934	A4w
Gtpbp4	0.027	0.085	0.004	0.833	0.925	0.016	0.323	0.024	0.016	0.021	0.788	0.015	1.074	1.020	0.982	0.924	1.074	1.020	0.982	0.924	A3w
Dip2c	0.107	0.779	-0.060	-0.184	0.945	0.097	0.491	0.141	0.003	0.125	0.546	0.091	1.386	1.368	0.705	0.540	1.386	1.368	0.705	0.540	A4
Trgv2	-0.322	-0.156	-0.062	1.746	0.924	0.098	0.085	0.141	0.281	0.126	0.534	0.091	0.578	1.202	0.812	1.409	0.578	1.202	0.812	1.409	R1
Cmah	-0.008	-0.167	-0.073	1.394	0.900	0.057	0.927	0.082	0.085	0.073	0.243	0.053	0.755	0.981	1.057	1.207	0.755	0.981	1.057	1.207	R2w
Ripor2	0.042	-0.184	-0.062	1.338	0.911	0.048	0.571	0.069	0.040	0.061	0.237	0.045	0.799	0.927	1.107	1.167	0.799	0.927	1.107	1.167	R3w
Dusp22	0.001	0.221	-0.071	0.802	0.899	0.037	0.989	0.053	0.010	0.047	0.107	0.034	0.980	1.170	0.883	0.966	0.980	1.170	0.883	0.966	A4w
Irf4	0.167	0.306	-0.057	0.442	0.986	0.018	0.003	0.027	0.000	0.024	0.030	0.017	1.167	1.082	0.975	0.776	1.167	1.082	0.975	0.776	A3w
Serpinb6b	0.743	0.154	-0.282	0.378	0.940	0.073	0.002	0.106	0.179	0.094	0.015	0.069	1.002	0.778	1.447	0.773	1.002	0.778	1.447	0.773	A1w
Serpinb9	0.825	0.175	-0.333	0.341	0.990	0.032	0.000	0.046	0.013	0.041	0.000	0.030	0.964	0.773	1.490	0.773	0.964	0.773	1.490	0.773	A1w
Nqo2	0.279	-0.105	-0.210	1.203	0.870	0.083	0.081	0.120	0.381	0.107	0.054	0.078	0.700	0.919	1.224	1.157	0.700	0.919	1.224	1.157	I
Tubb2a	0.035	-0.026	-0.086	1.156	0.939	0.027	0.420	0.039	0.502	0.035	0.027	0.026	0.834	1.033	1.022	1.111	0.834	1.033	1.022	1.111	R2w
Tubb2b	0.042	-0.200	-0.123	1.476	0.870	0.087	0.758	0.127	0.150	0.113	0.207	0.082	0.667	0.970	1.102	1.262	0.667	0.970	1.102	1.262	R2
Smim13	0.054	0.145	0.035	0.652	0.904	0.044	0.440	0.063	0.062	0.056	0.440	0.041	1.187	1.006	0.981	0.826	1.187	1.006	0.981	0.826	A3w
Nol7	-0.084	-0.020	0.058	1.026	0.832	0.016	0.021	0.023	0.377	0.020	0.017	0.015	1.051	1.002	0.956	0.991	1.051	1.002	0.956	0.991	A4w
Card19	0.157	-0.171	-0.126	1.296	0.978	0.029	0.020	0.042	0.010	0.037	0.010	0.027	0.753	0.904	1.177	1.166	0.753	0.904	1.177	1.166	R3w
Nol8	-0.027	0.031	0.050	0.894	0.958	0.014	0.256	0.020	0.160	0.018	0.018	0.013	1.101	0.993	0.975	0.931	1.101	0.993	0.975	0.931	A3w
Sema4d	-0.120	-0.107	0.027	1.259	0.935	0.020	0.015	0.030	0.015	0.026	0.234	0.019	0.915	1.010	0.962	1.113	0.915	1.010	0.962	1.113	R1w
Gadd45g	-0.404	0.173	0.087	1.078	0.978	0.039	0.002	0.057	0.027	0.051	0.078	0.037	1.009	1.305	0.624	1.062	1.009	1.305	0.624	1.062	R1w
Sptlc1	0.156	-0.030	-0.023	0.894	0.946	0.023	0.010	0.034	0.374	0.030	0.356	0.022	1.039	0.892	1.130	0.939	1.039	0.892	1.130	0.939	A1w
Mxd3	-0.013	-0.172	-0.099	1.458	0.990	0.021	0.689	0.030	0.003	0.027	0.007	0.020	0.695	1.004	1.051	1.251	0.695	1.004	1.051	1.251	R1
Rgs14	0.046	-0.174	-0.064	1.323	0.984	0.019	0.173	0.028	0.002	0.025	0.023	0.018	0.803	0.931	1.104	1.161	0.803	0.931	1.104	1.161	R2w
B4galt7	0.026	-0.131	-0.034	1.227	0.928	0.028	0.558	0.040	0.022	0.036	0.264	0.026	0.875	0.943	1.074	1.107	0.875	0.943	1.074	1.107	R3w

Gene	Erk(E)	NFAT(N)	ErkNFAT(EN)	B0	R2	RSE	pval(E)	se(E)	pval(N)	se(N)	pval(EN)	se(EN)	DMSO	MEKi	CsA	MEKi+CsA	DMSO1	MEKi1	CsA1	MEKi+CsA1	reg_mode
Idnk	-0.030	-0.111	0.018	1.169	0.901	0.017	0.292	0.025	0.007	0.022	0.318	0.016	0.955	0.950	1.033	1.062	0.955	0.950	1.033	1.062	R3w
Ctla2b	0.146	-0.861	-0.245	2.562	0.909	0.214	0.663	0.311	0.035	0.276	0.290	0.201	0.118	0.660	1.468	1.754	0.118	0.660	1.468	1.754	R2
Ctla2a	-0.108	-0.579	-0.048	2.088	0.957	0.083	0.417	0.120	0.006	0.106	0.570	0.077	0.508	0.823	1.178	1.491	0.508	0.823	1.178	1.491	R2
Zfp729a	0.106	-0.046	-0.002	0.942	0.939	0.021	0.024	0.030	0.159	0.026	0.912	0.019	1.039	0.903	1.103	0.956	1.039	0.903	1.103	0.956	A1w
Nsun2	-0.009	0.062	0.016	0.889	0.946	0.011	0.612	0.017	0.013	0.015	0.220	0.011	1.060	1.025	0.967	0.947	1.060	1.025	0.967	0.947	A3w
Slc6a19	0.289	-0.677	-0.285	2.186	0.999	0.021	0.001	0.031	0.000	0.027	0.000	0.020	0.233	0.684	1.485	1.598	0.233	0.684	1.485	1.598	R2
Brd9	-0.082	-0.091	0.016	1.207	0.879	0.023	0.065	0.033	0.035	0.029	0.491	0.021	0.928	1.000	0.982	1.091	0.928	1.000	0.982	1.091	R1w
Cast	0.019	-0.039	-0.050	1.128	0.864	0.028	0.665	0.041	0.341	0.037	0.134	0.027	0.890	1.007	1.023	1.080	0.890	1.007	1.023	1.080	R2w
Glrx	0.179	-0.153	-0.126	1.242	0.932	0.048	0.062	0.070	0.068	0.062	0.049	0.045	0.777	0.898	1.185	1.140	0.777	0.898	1.185	1.140	R3w
Homer1	0.122	0.095	0.022	0.666	0.961	0.028	0.039	0.040	0.056	0.036	0.448	0.026	1.177	0.943	1.054	0.826	1.177	0.943	1.054	0.826	A1w
F2r	-0.279	-0.273	0.166	1.444	0.982	0.012	0.000	0.017	0.000	0.015	0.000	0.011	0.999	0.925	0.945	1.131	0.999	0.925	0.945	1.131	A1w
Iqgap2	-0.028	-0.273	0.002	1.438	0.920	0.045	0.695	0.066	0.010	0.059	0.967	0.043	0.833	0.880	1.107	1.181	0.833	0.880	1.107	1.181	R3w
Hmgcr	0.079	-0.026	-0.010	0.961	0.897	0.017	0.036	0.025	0.309	0.023	0.569	0.016	1.016	0.939	1.071	0.974	1.016	0.939	1.071	0.974	A1w
Hexb	-0.054	-0.160	-0.027	1.357	0.939	0.034	0.329	0.049	0.021	0.044	0.442	0.032	0.820	0.980	1.028	1.172	0.820	0.980	1.028	1.172	R3w
Enc1	0.463	0.154	-0.158	0.492	0.948	0.044	0.002	0.064	0.053	0.057	0.019	0.041	1.070	0.876	1.255	0.798	1.070	0.876	1.255	0.798	A1w
Utp15	-0.009	0.060	0.025	0.875	0.866	0.022	0.782	0.032	0.097	0.028	0.289	0.020	1.078	1.017	0.969	0.936	1.078	1.017	0.969	0.936	A3w
Pik3r1	0.094	-0.021	-0.141	1.179	0.871	0.057	0.317	0.082	0.784	0.073	0.056	0.053	0.764	1.038	1.055	1.143	0.764	1.038	1.055	1.143	R2w
Adamts6	-0.136	0.545	0.163	0.050	0.981	0.060	0.192	0.087	0.002	0.077	0.044	0.056	1.547	1.240	0.671	0.542	1.547	1.240	0.671	0.542	A3
Elovl7	-0.107	-0.478	-0.039	1.920	0.953	0.073	0.368	0.105	0.007	0.094	0.595	0.068	0.583	0.866	1.134	1.417	0.583	0.866	1.134	1.417	R1
Depdc1b	-0.086	-0.333	-0.045	1.687	0.957	0.054	0.330	0.078	0.008	0.069	0.422	0.050	0.667	0.930	1.081	1.323	0.667	0.930	1.081	1.323	R2
Pde4d	-0.040	-0.280	-0.005	1.477	0.953	0.037	0.498	0.054	0.004	0.048	0.896	0.035	0.807	0.891	1.099	1.203	0.807	0.891	1.099	1.203	R2w
Gzma	0.096	-0.722	-0.118	2.180	0.956	0.107	0.569	0.156	0.006	0.138	0.304	0.101	0.419	0.662	1.390	1.530	0.419	0.662	1.390	1.530	R2
Parp8	-0.086	-0.348	0.149	1.349	0.891	0.051	0.309	0.074	0.006	0.066	0.035	0.048	1.049	0.762	1.126	1.062	1.049	0.762	1.126	1.062	A1w
Emb	-0.033	-0.140	0.018	1.217	0.981	0.010	0.075	0.014	0.000	0.012	0.110	0.009	0.936	0.937	1.044	1.082	0.936	0.937	1.044	1.082	R3w
BC147527	0.010	-0.318	-0.159	1.759	0.805	0.163	0.969	0.236	0.204	0.210	0.356	0.152	0.508	0.962	1.125	1.405	0.508	0.962	1.125	1.405	R2
Slc4a7	0.059	0.058	0.054	0.741	0.944	0.031	0.260	0.045	0.225	0.040	0.139	0.029	1.179	0.943	1.030	0.848	1.179	0.943	1.030	0.848	A1w
Kcnk5	-0.161	0.249	0.013	0.803	0.945	0.044	0.064	0.063	0.011	0.056	0.774	0.041	1.060	1.231	0.761	0.947	1.060	1.231	0.761	0.947	A4w
Vcl	0.454	0.054	-0.265	0.851	0.977	0.029	0.000	0.041	0.216	0.037	0.001	0.027	0.793	0.920	1.274	1.014	0.793	0.920	1.274	1.014	I
Anxa11	-0.043	-0.004	-0.019	1.094	0.924	0.016	0.135	0.023	0.852	0.021	0.284	0.015	0.932	1.044	0.965	1.059	0.932	1.044	0.965	1.059	R1w
Pde12	-0.055	0.082	0.057	0.839	0.936	0.024	0.184	0.034	0.055	0.031	0.063	0.022	1.125	1.034	0.930	0.911	1.125	1.034	0.930	0.911	A3w
Sh3bp5	-0.060	-0.124	-0.049	1.350	0.968	0.027	0.202	0.039	0.023	0.035	0.126	0.025	0.793	1.020	1.002	1.185	0.793	1.020	1.002	1.185	R2w
Prxl2a	0.437	-0.035	-0.159	0.808	0.936	0.053	0.005	0.077	0.640	0.069	0.034	0.050	0.945	0.800	1.323	0.932	0.945	0.800	1.323	0.932	A1w
Ptger2	-0.444	-0.116	0.652	0.508	0.934	0.159	0.126	0.230	0.601	0.205	0.012	0.149	1.960	0.722	0.840	0.477	1.960	0.722	0.840	0.477	A2
Lgals3	-0.152	-0.397	-0.111	1.987	0.946	0.094	0.325	0.136	0.030	0.121	0.275	0.088	0.454	0.999	1.046	1.501	0.454	0.999	1.046	1.501	R1
Zfp219	0.074	0.210	-0.088	0.758	0.989	0.008	0.004	0.012	0.000	0.011	0.000	0.008	0.989	1.126	0.941	0.944	0.989	1.126	0.941	0.944	A4w
Trdc	-0.057	-0.152	-0.007	1.310	0.920	0.031	0.277	0.045	0.019	0.040	0.830	0.029	0.864	0.969	1.026	1.141	0.864	0.969	1.026	1.141	R3w
Trac	0.063	-0.023	0.008	0.941	0.933	0.015	0.046	0.022	0.312	0.020	0.594	0.014	1.045	0.937	1.061	0.957	1.045	0.937	1.061	0.957	A1w
Irf9	-0.024	-0.121	-0.012	1.232	0.915	0.025	0.544	0.037	0.021	0.033	0.650	0.024	0.893	0.966	1.036	1.106	0.893	0.966	1.036	1.106	R2w
Dhrs1	0.100	-0.028	-0.107	1.117	0.949	0.025	0.049	0.036	0.424	0.032	0.010	0.023	0.834	1.002	1.070	1.095	0.834	1.002	1.070	1.095	R3w
Gzmb	0.141	-0.106	-0.118	1.203	0.879	0.054	0.149	0.079	0.207	0.070	0.082	0.051	0.795	0.942	1.135	1.127	0.795	0.942	1.135	1.127	R3w
Phf11b	0.006	-0.070	-0.067	1.221	0.966	0.021	0.855	0.031	0.064	0.028	0.030	0.020	0.830	1.015	1.024	1.131	0.830	1.015	1.024	1.131	R2w
Spata13	-0.003	-0.145	0.005	1.211	0.923	0.023	0.924	0.033	0.008	0.029	0.816	0.021	0.927	0.924	1.066	1.082	0.927	0.924	1.066	1.082	R3w
Ctsb	-0.034	0.126	-0.007	0.867	0.971	0.013	0.142	0.018	0.002	0.016	0.584	0.012	1.034	1.094	0.914	0.958	1.034	1.094	0.914	0.958	A4w
Egr3	0.501	0.595	0.103	-0.699	0.889	0.227	0.202	0.329	0.111	0.292	0.653	0.212	1.868	0.859	1.129	0.144	1.868	0.859	1.129	0.144	A2
Pdlim2	-0.033	-0.047	-0.030	1.166	0.930	0.021	0.337	0.030	0.156	0.027	0.204	0.020	0.892	1.024	0.991	1.093	0.892	1.024	0.991	1.093	R1w
Ppp3cc	-0.006	-0.098	-0.017	1.186	0.920	0.021	0.851	0.031	0.023	0.027	0.430	0.020	0.906	0.969	1.038	1.087	0.906	0.969	1.038	1.087	R3w
Polr3d	0.074	0.095	0.005	0.757	0.859	0.034	0.208	0.049	0.097	0.044	0.878	0.032	1.112	0.991	1.014	0.883	1.112	0.991	1.014	0.883	A3w
Dok2	0.132	-0.180	-0.020	1.144	0.942	0.034	0.055	0.049	0.015	0.044	0.557	0.032	0.944	0.831	1.182	1.043	0.944	0.831	1.182	1.043	I
Rcbtb2	-0.133	-0.092	-0.034	1.366	0.953	0.036	0.062	0.052	0.116	0.046	0.368	0.034	0.793	1.077	0.933	1.198	0.793	1.077	0.933	1.198	R1w
Lpar6	-0.246	-0.411	0.036	1.850	0.898	0.087	0.122	0.126	0.021	0.112	0.680	0.081	0.682	0.938	1.009	1.371	0.682	0.938	1.009	1.371	R2
Itm2b	-0.045	-0.122	-0.001	1.239	0.947	0.019	0.177	0.027	0.007	0.024	0.951	0.018	0.900	0.971	1.022	1.106	0.900	0.971	1.022	1.106	R3w
Epsti1	0.197	-0.291	-0.089	1.358	0.997	0.012	0.000	0.017	0.000	0.015	0.001	0.011	0.785	0.785	1.271	1.159	0.785	0.785	1.271	1.159	R3w
Tnfsf11	0.308	0.168	0.251	-0.099	0.885	0.209	0.367	0.303	0.568	0.270	0.269	0.196	1.802	0.658	1.210	0.331	1.802	0.658	1.210	0.331	A2
Rgcc	-0.067	-0.176	0.125	1.112	0.859	0.040	0.311	0.058	0.027	0.051	0.029	0.037	1.110	0.856	1.055	0.979	1.110	0.856	1.055	0.979	A1w
Tbc1d4	-0.238	0.152	-0.058	1.174	0.963	0.049	0.028	0.071	0.072	0.063	0.275	0.046	0.814	1.295	0.733	1.158	0.814	1.295	0.733	1.158	R1w
Kctd12	0.272	-0.062	-0.175	1.083	0.906	0.054	0.025	0.078	0.418	0.069	0.025	0.050	0.789	0.918	1.205	1.088	0.789	0.918	1.205	1.088	R3w
Slain1	0.031	0.048	-0.069	1.019	0.981	0.009	0.067	0.013	0.013	0.011	0.001	0.008	0.908	1.059	0.988	1.045	0.908	1.059	0.988	1.045	R1w
Dzip1	-0.074	-0.567	0.070	1.808	0.849	0.113	0.677	0.164	0.018	0.146	0.547	0.106	0.774	0.708	1.223	1.295	0.774	0.708	1.223	1.295	R3w
Dnajc3	0.012	-0.130	0.001	1.178	0.889	0.026	0.762	0.037	0.017	0.033	0.971	0.024	0.937	0.925	1.070	1.068	0.937	0.925	1.070	1.068	R3w
Farp1	-0.399	0.567	0.491	-0.268	0.962	0.145	0.131	0.210	0.039	0.187	0.023	0.136	2.048	1.169	0.523	0.260	2.048	1.169	0.523	0.260	A3
Tmtc4	-0.116	0.336	0.034	0.577	0.985	0.027	0.043	0.040	0.001	0.035	0.256	0.026	1.182	1.225	0.760	0.833	1.182	1.225	0.760	0.833	A4w
Ptger4	-0.079	0.214	0.042	0.700	0.996	0.010	0.005	0.014	0.000	0.013	0.010	0.009	1.153	1.130	0.847	0.869	1.153	1.130	0.847	0.869	A4w
Fyb	0.002	0.000	-0.085	1.156	0.910	0.036	0.966	0.052	0.995	0.046	0.065	0.034	0.830	1.068	0.985	1.117	0.830	1.068	0.985	1.117	R1w
Il7r	-0.020	-0.170	-0.153	1.562	0.974	0.047	0.785	0.068	0.047	0.060	0.025	0.044	0.584	1.053	1.034	1.328	0.584	1.053	1.034	1.328	R1
Basp1	0.432	-0.146	-0.194	1.046	0.965	0.047	0.003	0.069	0.075	0.061	0.012	0.044	0.809	0.776	1.365	1.051	0.809	0.776	1.365	1.051	I
Ank	0.221	-0.091	-0.100	1.049	0.850	0.055	0.051	0.080	0.271	0.071	0.126	0.052	0.891	0.878	1.194	1.037	0.891	0.878	1.194	1.037	I

Gene	Erk(E)	NFAT(N)	ErkNFAT(EN)	B0	R2	RSE	pval(E)	se(E)	pval(N)	se(N)	pval(EN)	se(EN)	DMSO	MEKi	CsA	MEKi+CsA	DMSO1	MEKi1	CsA1	MEKi+CsA1	reg_mode
Ankrd46	-0.102	0.046	0.083	0.902	0.892	0.031	0.086	0.045	0.315	0.040	0.045	0.029	1.128	1.027	0.916	0.929	1.128	1.027	0.916	0.929	A4w
Slc25a32	-0.094	0.033	0.082	0.913	0.920	0.025	0.058	0.036	0.359	0.032	0.023	0.023	1.124	1.016	0.928	0.932	1.124	1.016	0.928	0.932	A4w
Sntb1	0.242	-0.117	-0.173	1.197	0.959	0.040	0.014	0.059	0.088	0.052	0.010	0.038	0.744	0.910	1.208	1.139	0.744	0.910	1.208	1.139	R3w
Tmem65	0.069	0.555	-0.152	0.369	0.959	0.051	0.398	0.073	0.001	0.065	0.033	0.048	1.050	1.357	0.764	0.830	1.050	1.357	0.764	0.830	A4w
Myc	-0.024	0.082	0.018	0.873	0.919	0.018	0.401	0.025	0.022	0.023	0.329	0.016	1.067	1.044	0.947	0.942	1.067	1.044	0.947	0.942	A3w
Tmem71	-0.022	-0.701	-0.053	2.174	0.946	0.106	0.893	0.153	0.007	0.136	0.618	0.099	0.484	0.704	1.301	1.511	0.484	0.704	1.301	1.511	R2
Tg	0.134	-0.096	-0.183	1.319	0.950	0.050	0.141	0.073	0.212	0.065	0.018	0.047	0.665	1.006	1.112	1.217	0.665	1.006	1.112	1.217	R2
Ndrg1	0.280	-0.159	-0.155	1.180	0.932	0.055	0.025	0.080	0.090	0.071	0.040	0.052	0.781	0.847	1.260	1.112	0.781	0.847	1.260	1.112	I
Them6	-0.065	-0.015	-0.001	1.104	0.940	0.013	0.026	0.019	0.432	0.017	0.930	0.012	0.947	1.040	0.956	1.056	0.947	1.040	0.956	1.056	R1w
Ly6e	0.034	-0.078	-0.043	1.156	0.976	0.012	0.136	0.018	0.008	0.016	0.021	0.012	0.891	0.972	1.054	1.083	0.891	0.972	1.054	1.083	R3w
Ly6a	0.079	-0.057	-0.069	1.115	0.909	0.027	0.110	0.039	0.172	0.034	0.051	0.025	0.881	0.971	1.074	1.074	0.881	0.971	1.074	1.074	R3w
Ly6c1	0.283	-0.347	-0.189	1.521	0.811	0.155	0.275	0.224	0.156	0.199	0.262	0.145	0.609	0.777	1.344	1.270	0.609	0.777	1.344	1.270	R3
Ly6c2	0.210	-0.273	-0.124	1.379	0.953	0.054	0.055	0.079	0.017	0.070	0.071	0.051	0.734	0.813	1.266	1.187	0.734	0.813	1.266	1.187	R3w
Top1mt	0.010	0.146	0.037	0.700	0.913	0.037	0.860	0.054	0.037	0.048	0.345	0.035	1.163	1.037	0.947	0.854	1.163	1.037	0.947	0.854	A3w
Plec	0.314	-0.042	-0.218	1.081	0.891	0.066	0.030	0.096	0.649	0.085	0.024	0.062	0.741	0.934	1.219	1.106	0.741	0.934	1.219	1.106	R3w
Parp10	0.025	-0.085	-0.060	1.208	0.977	0.016	0.343	0.024	0.015	0.021	0.017	0.015	0.848	0.988	1.047	1.117	0.848	0.988	1.047	1.117	R2w
Vps28	-0.045	-0.061	0.004	1.139	0.915	0.013	0.084	0.020	0.025	0.017	0.781	0.013	0.944	0.998	0.994	1.063	0.944	0.998	0.994	1.063	R2w
Apol7e	0.028	-0.550	0.097	1.608	0.901	0.090	0.842	0.131	0.009	0.116	0.317	0.085	0.904	0.621	1.299	1.176	0.904	0.621	1.299	1.176	I
Il2rb	-0.015	-0.111	-0.016	1.214	0.969	0.014	0.513	0.021	0.004	0.019	0.298	0.014	0.896	0.968	1.037	1.099	0.896	0.968	1.037	1.099	R3w
C1qtnf6	0.098	-0.465	-0.051	1.668	0.915	0.090	0.494	0.131	0.016	0.116	0.577	0.084	0.700	0.736	1.284	1.280	0.700	0.736	1.284	1.280	R3
Cyth4	-0.025	-0.249	0.000	1.403	0.984	0.018	0.406	0.027	0.000	0.024	0.989	0.017	0.844	0.892	1.098	1.167	0.844	0.892	1.098	1.167	R3w
Sh3bp1	0.017	-0.105	-0.019	1.171	0.804	0.035	0.749	0.051	0.079	0.045	0.590	0.033	0.914	0.950	1.059	1.077	0.914	0.950	1.059	1.077	R3w
Lgals1	0.091	-0.076	-0.094	1.177	0.912	0.037	0.161	0.053	0.182	0.047	0.052	0.034	0.827	0.974	1.088	1.112	0.827	0.974	1.088	1.112	R3w
Csnk1e	0.093	0.135	0.010	0.663	0.892	0.041	0.192	0.060	0.063	0.053	0.803	0.039	1.158	0.994	1.011	0.838	1.158	0.994	1.011	0.838	A3w
Sun2	-0.059	-0.167	0.026	1.274	0.949	0.019	0.096	0.027	0.002	0.024	0.215	0.018	0.920	0.936	1.038	1.106	0.920	0.936	1.038	1.106	R2w
Grap2	0.016	-0.070	-0.049	1.177	0.918	0.026	0.686	0.038	0.104	0.034	0.114	0.024	0.872	0.993	1.036	1.099	0.872	0.993	1.036	1.099	R3w
Mrtfa	-0.079	-0.157	-0.001	1.334	0.854	0.045	0.288	0.065	0.053	0.058	0.978	0.042	0.858	0.978	1.012	1.152	0.858	0.978	1.012	1.152	R2w
Prr5	-0.822	-1.018	0.240	3.090	0.954	0.125	0.010	0.181	0.003	0.161	0.109	0.117	0.376	0.875	0.888	1.861	0.376	0.875	0.888	1.861	R2
Cerk	-0.217	-0.358	0.113	1.593	0.915	0.043	0.026	0.063	0.003	0.056	0.050	0.040	0.885	0.881	1.022	1.212	0.885	0.881	1.022	1.212	R3w
Hdac10	0.176	0.009	-0.014	0.795	0.843	0.049	0.069	0.072	0.894	0.064	0.772	0.046	1.091	0.890	1.129	0.889	1.091	0.890	1.129	0.889	A1w
Mapk11	0.539	-0.048	-0.047	0.493	0.941	0.090	0.014	0.130	0.699	0.116	0.610	0.084	1.230	0.628	1.431	0.711	1.230	0.628	1.431	0.711	A1
Pphln1	0.037	0.049	0.016	0.850	0.952	0.014	0.135	0.020	0.051	0.018	0.284	0.013	1.084	0.985	1.009	0.922	1.084	0.985	1.009	0.922	A1w
Prickle1	-0.525	0.471	0.244	0.490	0.935	0.120	0.039	0.174	0.038	0.154	0.096	0.112	1.414	1.414	0.421	0.750	1.414	1.414	0.421	0.750	A4
Wnt10b	0.020	-0.348	0.039	1.423	0.964	0.035	0.705	0.050	0.001	0.045	0.299	0.032	0.896	0.777	1.187	1.141	0.896	0.777	1.187	1.141	R3w
Tuba1a	0.090	-0.049	-0.051	1.057	0.898	0.022	0.047	0.032	0.159	0.028	0.066	0.021	0.928	0.953	1.082	1.037	0.928	0.953	1.082	1.037	I
Tmbim6	0.002	-0.075	-0.009	1.128	0.990	0.005	0.843	0.007	0.000	0.007	0.118	0.005	0.940	0.968	1.035	1.057	0.940	0.968	1.035	1.057	R3w
Racgap1	-0.053	-0.067	0.008	1.151	0.885	0.016	0.091	0.024	0.035	0.021	0.645	0.015	0.944	0.998	0.992	1.067	0.944	0.998	0.992	1.067	R2w
Larp4	0.041	0.092	-0.003	0.818	0.917	0.017	0.179	0.025	0.014	0.022	0.845	0.016	1.071	1.020	0.988	0.921	1.071	1.020	0.988	0.921	A3w
Bin2	-0.035	-0.127	-0.003	1.239	0.923	0.023	0.361	0.034	0.013	0.030	0.884	0.022	0.899	0.963	1.032	1.106	0.899	0.963	1.032	1.106	R3w
Galnt6	-0.018	-0.162	0.005	1.255	0.994	0.007	0.157	0.011	0.000	0.009	0.493	0.007	0.908	0.927	1.063	1.103	0.908	0.927	1.063	1.103	R2w
Nr4a1	0.084	-0.180	-0.002	1.169	0.943	0.029	0.113	0.042	0.008	0.037	0.936	0.027	0.949	0.850	1.149	1.051	0.949	0.850	1.149	1.051	I
Itgb7	-0.014	-0.151	-0.069	1.371	0.941	0.041	0.823	0.059	0.046	0.053	0.144	0.038	0.767	0.991	1.046	1.197	0.767	0.991	1.046	1.197	R2w
Socs1	-0.088	-0.154	0.000	1.338	0.914	0.034	0.148	0.049	0.024	0.044	0.991	0.032	0.857	0.984	1.004	1.154	0.857	0.984	1.004	1.154	R2w
Rmi2	-0.078	-0.106	0.016	1.224	0.952	0.015	0.022	0.022	0.005	0.019	0.309	0.014	0.923	0.989	0.992	1.096	0.923	0.989	0.992	1.096	R2w
Litaf	0.004	0.214	0.037	0.607	0.945	0.037	0.944	0.054	0.011	0.048	0.351	0.035	1.197	1.075	0.910	0.818	1.197	1.075	0.910	0.818	A3w
Rrn3	0.028	0.068	0.007	0.851	0.912	0.016	0.308	0.024	0.031	0.021	0.673	0.015	1.070	1.009	0.991	0.930	1.070	1.009	0.991	0.930	A3w
B3gnt5	0.171	0.302	-0.360	1.007	0.970	0.056	0.102	0.081	0.014	0.072	0.002	0.052	0.555	1.327	0.919	1.198	0.555	1.327	0.919	1.198	A4
Eif4g1	0.016	0.058	0.000	0.893	0.975	0.006	0.129	0.008	0.001	0.008	0.992	0.005	1.043	1.018	0.985	0.953	1.043	1.018	0.985	0.953	A3w
Tmem41a	-0.039	0.132	0.029	0.797	0.950	0.022	0.288	0.032	0.009	0.028	0.231	0.021	1.107	1.071	0.914	0.908	1.107	1.071	0.914	0.908	A3w
Ccdc50	0.030	0.070	0.031	0.801	0.975	0.014	0.206	0.020	0.017	0.018	0.073	0.013	1.121	0.988	0.997	0.894	1.121	0.988	0.997	0.894	A3w
Nrros	0.122	-0.085	-0.055	1.079	0.919	0.027	0.036	0.040	0.072	0.035	0.096	0.026	0.920	0.915	1.123	1.041	0.920	0.915	1.123	1.041	R3w
Pcyt1a	-0.062	-0.252	0.031	1.397	0.948	0.029	0.216	0.042	0.003	0.038	0.324	0.027	0.880	0.891	1.076	1.153	0.880	0.891	1.076	1.153	R3w
Pdia5	-0.238	-0.791	0.094	2.301	0.988	0.044	0.020	0.064	0.000	0.057	0.084	0.041	0.590	0.692	1.205	1.513	0.590	0.692	1.205	1.513	R2
Slc49a4	-0.204	-0.371	0.035	1.741	0.906	0.071	0.120	0.104	0.016	0.092	0.625	0.067	0.730	0.928	1.024	1.318	0.730	0.928	1.024	1.318	R2
Parp14	0.024	-0.091	-0.048	1.196	0.958	0.020	0.443	0.028	0.023	0.025	0.059	0.018	0.868	0.976	1.052	1.104	0.868	0.976	1.052	1.104	R2w
Dtx3l	0.027	-0.032	-0.090	1.184	0.940	0.030	0.575	0.044	0.450	0.039	0.033	0.028	0.817	1.039	1.018	1.126	0.817	1.039	1.018	1.126	R1w
Parp9	0.000	-0.083	-0.055	1.226	0.859	0.043	0.999	0.062	0.204	0.055	0.242	0.040	0.843	1.003	1.028	1.126	0.843	1.003	1.028	1.126	R2w
Eaf2	0.574	0.670	-0.351	-0.056	0.888	0.073	0.006	0.106	0.002	0.094	0.007	0.068	1.042	1.218	1.060	0.680	1.042	1.218	1.060	0.680	A4w
Lrrc58	0.036	0.130	-0.013	0.784	0.976	0.011	0.076	0.015	0.001	0.014	0.257	0.010	1.071	1.051	0.964	0.914	1.071	1.051	0.964	0.914	A3w
Qtrt2	0.112	0.254	-0.075	0.623	0.988	0.011	0.002	0.016	0.000	0.014	0.002	0.010	1.064	1.111	0.953	0.873	1.064	1.111	0.953	0.873	A4w
Zdhhc23	-0.147	0.706	-0.060	0.238	0.970	0.070	0.221	0.101	0.001	0.090	0.411	0.065	1.180	1.512	0.544	0.764	1.180	1.512	0.544	0.764	A4
Sidt1	-0.118	-0.211	0.043	1.381	0.969	0.019	0.012	0.027	0.001	0.024	0.068	0.017	0.892	0.942	1.016	1.150	0.892	0.942	1.016	1.150	R2w
Nepro	0.019	0.096	0.035	0.767	0.892	0.033	0.709	0.048	0.088	0.043	0.324	0.031	1.138	1.006	0.977	0.879	1.138	1.006	0.977	0.879	A3w
Btla	-0.001	0.092	0.064	0.745	0.939	0.031	0.991	0.045	0.082	0.040	0.094	0.029	1.179	0.995	0.969	0.857	1.179	0.995	0.969	0.857	A3w
Cd200	-0.143	0.491	0.129	0.203	0.889	0.129	0.488	0.188	0.042	0.167	0.348	0.121	1.442	1.246	0.685	0.628	1.442	1.246	0.685	0.628	A3
Cd96	-0.197	-0.234	0.025	1.547	0.869	0.066	0.107	0.095	0.050	0.084	0.709	0.061	0.790	1.002	0.962	1.246	0.790	1.002	0.962	1.246	R2w

Gene	Erk(E)	NFAT(N)	ErkNFAT(EN)	B0	R2	RSE	pval(E)	se(E)	pval(N)	se(N)	pval(EN)	se(EN)	DMSO	MEKi	CsA	MEKi+CsA	DMSO1	MEKi1	CsA1	MEKi+CsA1	reg_mode
Trat1	-0.423	-0.402	0.068	1.995	0.960	0.064	0.010	0.092	0.008	0.082	0.315	0.060	0.637	1.042	0.875	1.446	0.637	1.042	0.875	1.446	R1
Cd47	-0.045	-0.038	-0.021	1.150	0.909	0.021	0.221	0.031	0.241	0.028	0.362	0.020	0.908	1.030	0.979	1.083	0.908	1.030	0.979	1.083	R1w
Alcam	0.037	0.095	0.090	0.644	0.901	0.059	0.684	0.085	0.276	0.075	0.175	0.055	1.260	0.947	1.002	0.791	1.260	0.947	1.002	0.791	A3w
Cep97	0.002	-0.205	-0.012	1.326	0.951	0.029	0.968	0.041	0.005	0.037	0.674	0.027	0.862	0.905	1.095	1.138	0.862	0.905	1.095	1.138	R3w
St3gal6	0.320	-0.163	-0.157	1.141	0.952	0.048	0.010	0.070	0.059	0.062	0.026	0.045	0.801	0.817	1.293	1.089	0.801	0.817	1.293	1.089	I
Pros1	-0.484	0.020	0.384	0.852	0.975	0.051	0.003	0.074	0.778	0.066	0.001	0.048	1.471	1.040	0.692	0.796	1.471	1.040	0.692	0.796	A3
Samsn1	0.075	0.364	-0.109	0.567	0.979	0.022	0.081	0.032	0.000	0.029	0.006	0.021	1.033	1.221	0.866	0.880	1.033	1.221	0.866	0.880	A4w
Ifnar2	-0.137	-0.142	0.021	1.343	0.968	0.020	0.008	0.028	0.005	0.025	0.314	0.018	0.873	1.009	0.965	1.154	0.873	1.009	0.965	1.154	R1w
Il10rb	-0.042	-0.157	-0.052	1.384	0.943	0.039	0.495	0.056	0.034	0.050	0.222	0.036	0.779	0.993	1.031	1.197	0.779	0.993	1.031	1.197	R2w
Ifnar1	0.012	-0.211	-0.036	1.367	0.981	0.021	0.700	0.030	0.001	0.027	0.141	0.019	0.818	0.913	1.102	1.168	0.818	0.913	1.102	1.168	R3w
Ifngr2	-0.189	-0.508	0.069	1.864	0.868	0.097	0.251	0.141	0.015	0.125	0.491	0.091	0.731	0.821	1.105	1.343	0.731	0.821	1.105	1.343	R2
Gart	-0.029	0.045	0.025	0.922	0.946	0.011	0.129	0.015	0.030	0.014	0.062	0.010	1.057	1.023	0.961	0.958	1.057	1.023	0.961	0.958	A3w
Slc5a3	0.130	0.259	-0.021	0.493	0.827	0.069	0.263	0.100	0.043	0.089	0.756	0.064	1.187	1.056	0.975	0.782	1.187	1.056	0.975	0.782	A3w
Hlcs	-0.460	-0.107	0.300	1.170	0.818	0.084	0.020	0.122	0.377	0.108	0.019	0.079	1.245	1.028	0.754	0.973	1.245	1.028	0.754	0.973	A4w
Snx9	0.176	-0.039	-0.001	0.843	0.961	0.027	0.011	0.039	0.318	0.034	0.975	0.025	1.091	0.855	1.154	0.900	1.091	0.855	1.154	0.900	A1w
Sytl3	-0.059	-0.220	0.012	1.379	0.886	0.043	0.399	0.062	0.017	0.056	0.781	0.040	0.862	0.921	1.060	1.157	0.862	0.921	1.060	1.157	R3w
Ezr	0.074	0.040	-0.066	0.972	0.862	0.015	0.027	0.022	0.109	0.019	0.009	0.014	0.937	1.022	1.026	1.016	0.937	1.022	1.026	1.016	R3w
Tagap	-0.080	-0.054	0.138	0.924	0.946	0.030	0.136	0.043	0.227	0.038	0.008	0.028	1.195	0.916	0.991	0.898	1.195	0.916	0.991	0.898	A1w
Rnaset2a	-0.047	-0.096	-0.006	1.211	0.892	0.025	0.269	0.036	0.041	0.032	0.815	0.023	0.904	0.990	1.008	1.099	0.904	0.990	1.008	1.099	R2w
Agpat4	0.299	0.051	-0.093	0.728	0.890	0.046	0.011	0.066	0.438	0.059	0.097	0.043	1.036	0.888	1.189	0.886	1.036	0.888	1.189	0.886	A1w
Chd1	0.065	0.075	-0.011	0.830	0.916	0.016	0.045	0.023	0.020	0.020	0.475	0.015	1.061	1.001	1.013	0.925	1.061	1.001	1.013	0.925	A3w
Vmn2r97	0.130	0.093	-0.029	0.755	0.926	0.021	0.014	0.031	0.028	0.028	0.221	0.020	1.078	0.978	1.051	0.892	1.078	0.978	1.051	0.892	A1w
Zfp945	-0.335	-0.792	0.105	2.403	0.914	0.126	0.139	0.182	0.008	0.162	0.423	0.117	0.548	0.752	1.133	1.568	0.548	0.752	1.133	1.568	R1
Paqr4	-0.134	-0.244	-0.045	1.614	0.923	0.067	0.238	0.097	0.047	0.086	0.509	0.062	0.685	1.009	1.002	1.304	0.685	1.009	1.002	1.304	R1
Itpr3	-0.150	-0.257	0.041	1.492	0.875	0.052	0.117	0.075	0.018	0.067	0.449	0.049	0.841	0.944	1.012	1.204	0.841	0.944	1.012	1.204	R3w
Def6	0.022	-0.097	-0.018	1.152	0.984	0.009	0.162	0.013	0.001	0.011	0.097	0.008	0.924	0.950	1.059	1.068	0.924	0.950	1.059	1.068	R3w
Fkbp5	-0.008	-0.108	-0.023	1.214	0.966	0.016	0.762	0.023	0.006	0.021	0.194	0.015	0.887	0.970	1.040	1.103	0.887	0.970	1.040	1.103	R3w
Stk38	-0.043	-0.089	-0.017	1.217	0.884	0.029	0.372	0.042	0.077	0.038	0.566	0.027	0.888	0.999	1.005	1.107	0.888	0.999	1.005	1.107	R2w
Mtch1	-0.051	-0.076	0.008	1.162	0.983	0.007	0.006	0.010	0.001	0.009	0.286	0.006	0.940	0.992	0.998	1.071	0.940	0.992	0.998	1.071	R2w
Tbc1d22b	-0.070	-0.132	0.014	1.258	0.867	0.030	0.176	0.043	0.025	0.038	0.634	0.028	0.909	0.971	1.010	1.110	0.909	0.971	1.010	1.110	R3w
Dnah8	-0.087	-0.178	-0.090	1.540	0.829	0.104	0.598	0.151	0.257	0.135	0.409	0.098	0.662	1.046	0.998	1.293	0.662	1.046	0.998	1.293	R2
Rrp1b	0.039	0.106	-0.007	0.806	0.955	0.013	0.112	0.019	0.003	0.017	0.598	0.012	1.071	1.032	0.979	0.918	1.071	1.032	0.979	0.918	A3w
Pglyrp2	0.158	-0.599	-0.050	1.793	0.901	0.124	0.427	0.179	0.020	0.159	0.688	0.116	0.666	0.624	1.393	1.317	0.666	0.624	1.393	1.317	R3
Myo1f	-0.057	-0.770	-0.050	2.313	0.936	0.126	0.772	0.183	0.009	0.163	0.694	0.118	0.430	0.691	1.307	1.572	0.430	0.691	1.307	1.572	R2
Tapbp	0.006	-0.047	-0.021	1.101	0.964	0.009	0.660	0.013	0.015	0.012	0.068	0.008	0.936	0.989	1.023	1.053	0.936	0.989	1.023	1.053	R3w
H2-Oa	-0.204	-0.379	0.008	1.803	0.925	0.073	0.128	0.106	0.016	0.095	0.913	0.069	0.670	0.947	1.022	1.361	0.670	0.947	1.022	1.361	R2
H2-DMa	0.011	-0.141	-0.082	1.350	0.957	0.035	0.846	0.051	0.035	0.045	0.066	0.033	0.762	0.988	1.058	1.191	0.762	0.988	1.058	1.191	R2w
Gpsm3	-0.029	-0.156	0.026	1.221	0.965	0.014	0.217	0.020	0.001	0.018	0.115	0.013	0.946	0.921	1.055	1.078	0.946	0.921	1.055	1.078	R3w
Ppt2	0.027	0.226	-0.019	0.664	0.881	0.042	0.678	0.061	0.014	0.054	0.654	0.039	1.106	1.111	0.911	0.871	1.106	1.111	0.911	0.871	A4w
Clic1	0.017	-0.049	-0.020	1.089	0.957	0.009	0.263	0.013	0.014	0.012	0.082	0.009	0.944	0.979	1.032	1.045	0.944	0.979	1.032	1.045	R2w
Tnf	0.263	0.205	-0.005	0.378	0.980	0.033	0.005	0.048	0.008	0.042	0.878	0.031	1.277	0.920	1.106	0.697	1.277	0.920	1.106	0.697	A2
Lta	-0.144	0.078	0.155	0.773	0.865	0.067	0.213	0.098	0.420	0.087	0.070	0.063	1.262	1.015	0.883	0.840	1.262	1.015	0.883	0.840	A4w
H2-D1	0.008	-0.041	-0.013	1.076	0.959	0.007	0.455	0.010	0.011	0.009	0.114	0.007	0.955	0.984	1.023	1.037	0.955	0.984	1.023	1.037	R2w
H2-Q6	0.001	-0.049	-0.046	1.158	0.987	0.009	0.956	0.014	0.015	0.012	0.006	0.009	0.880	1.012	1.015	1.093	0.880	1.012	1.015	1.093	R2w
H2-Q7	-0.031	-0.074	-0.010	1.169	0.926	0.017	0.284	0.025	0.029	0.022	0.554	0.016	0.917	0.993	1.009	1.081	0.917	0.993	1.009	1.081	R2w
H2-Q10	-0.012	-0.210	-0.027	1.379	0.922	0.042	0.847	0.060	0.017	0.054	0.532	0.039	0.820	0.924	1.084	1.172	0.820	0.924	1.084	1.172	R3w
Tcf19	-0.040	-0.086	-0.004	1.185	0.936	0.016	0.168	0.024	0.015	0.021	0.824	0.015	0.918	0.988	1.009	1.085	0.918	0.988	1.009	1.085	R2w
Ddr1	0.145	0.622	-0.154	0.180	0.965	0.050	0.117	0.073	0.001	0.065	0.030	0.047	1.132	1.339	0.790	0.739	1.132	1.339	0.790	0.739	A4w
Flot1	0.065	-0.016	-0.127	1.179	0.954	0.031	0.223	0.045	0.718	0.040	0.012	0.029	0.778	1.050	1.032	1.140	0.778	1.050	1.032	1.140	R2w
Ppp1r18	0.026	-0.074	-0.022	1.120	0.934	0.015	0.304	0.022	0.020	0.020	0.194	0.014	0.930	0.962	1.051	1.057	0.930	0.962	1.051	1.057	R3w
H2-T23	-0.005	-0.130	0.006	1.189	0.895	0.024	0.891	0.034	0.013	0.030	0.803	0.022	0.936	0.933	1.058	1.073	0.936	0.933	1.058	1.073	R3w
H2-T22	-0.008	-0.082	-0.011	1.152	0.967	0.011	0.649	0.016	0.004	0.014	0.336	0.010	0.927	0.973	1.030	1.070	0.927	0.973	1.030	1.070	R2w
Trim26	0.013	-0.159	0.010	1.203	0.881	0.031	0.788	0.045	0.016	0.040	0.743	0.029	0.940	0.902	1.086	1.072	0.940	0.902	1.086	1.072	R3w
H2-M3	0.081	-0.304	-0.006	1.366	0.925	0.052	0.340	0.075	0.010	0.067	0.900	0.049	0.869	0.793	1.204	1.134	0.869	0.793	1.204	1.134	I
Tnfrsf21	-0.122	0.217	0.109	0.624	0.893	0.070	0.292	0.101	0.073	0.090	0.169	0.065	1.262	1.108	0.825	0.805	1.262	1.108	0.825	0.805	A3w
Runx2	0.076	0.080	-0.276	1.300	0.969	0.056	0.397	0.081	0.327	0.072	0.006	0.052	0.538	1.213	0.967	1.282	0.538	1.213	0.967	1.282	R1
Slc29a1	-0.015	0.156	0.023	0.742	0.946	0.025	0.711	0.037	0.009	0.033	0.388	0.024	1.124	1.071	0.920	0.885	1.124	1.071	0.920	0.885	A3w
Gtpbp2	0.004	-0.084	-0.037	1.189	0.912	0.026	0.923	0.037	0.065	0.033	0.203	0.024	0.882	0.985	1.035	1.099	0.882	0.985	1.035	1.099	R3w
Xpo5	0.002	0.096	0.007	0.841	0.972	0.010	0.916	0.015	0.002	0.013	0.505	0.010	1.070	1.042	0.957	0.931	1.070	1.042	0.957	0.931	A3w
Zfp318	0.274	0.147	-0.071	0.575	0.956	0.030	0.003	0.043	0.018	0.038	0.062	0.028	1.117	0.937	1.129	0.817	1.117	0.937	1.129	0.817	A1w
Ptcl2	-0.080	-0.065	0.009	1.179	0.888	0.021	0.058	0.030	0.073	0.027	0.661	0.020	0.930	1.017	0.970	1.083	0.930	1.017	0.970	1.083	R1w
Satb1	0.141	-0.120	-0.087	1.168	0.986	0.016	0.004	0.023	0.004	0.020	0.004	0.015	0.849	0.910	1.148	1.093	0.849	0.910	1.148	1.093	R3w
Tnfaip8l1	-0.181	-0.432	0.061	1.755	0.947	0.052	0.075	0.076	0.003	0.067	0.279	0.049	0.763	0.860	1.075	1.302	0.763	0.860	1.075	1.302	R3w
Ptprs	0.044	0.177	0.012	0.658	0.966	0.023	0.248	0.033	0.004	0.029	0.601	0.021	1.153	1.048	0.954	0.845	1.153	1.048	0.954	0.845	A3w
Dennd1c	0.066	-0.233	-0.049	1.359	0.860	0.066	0.527	0.095	0.051	0.085	0.467	0.062	0.813	0.875	1.150	1.162	0.813	0.875	1.150	1.162	R3w
Tnfsf14	-0.368	0.398	0.187	0.512	0.994	0.029	0.001	0.043	0.000	0.038	0.002	0.027	1.360	1.311	0.566	0.762	1.360	1.311	0.566	0.762	A3

Gene	Erk(E)	NFAT(N)	ErkNFAT(EN)	B0	R2	RSE	pval(E)	se(E)	pval(N)	se(N)	pval(EN)	se(EN)	DMSO	MEKi	CsA	MEKi+CsA	DMSO1	MEKi1	CsA1	MEKi+CsA1	reg_mode
Pja2	0.221	0.069	-0.080	0.773	0.973	0.014	0.000	0.021	0.019	0.018	0.004	0.013	1.021	0.943	1.122	0.913	1.021	0.943	1.122	0.913	A1w
Twsg1	0.118	0.235	-0.051	0.597	0.963	0.021	0.018	0.031	0.001	0.027	0.064	0.020	1.107	1.076	0.971	0.846	1.107	1.076	0.971	0.846	A3w
Myl12b	-0.090	-0.066	0.013	1.186	0.852	0.025	0.069	0.037	0.111	0.033	0.608	0.024	0.930	1.020	0.964	1.086	0.930	1.020	0.964	1.086	R1w
Smchd1	0.021	-0.050	-0.028	1.101	0.944	0.012	0.304	0.018	0.035	0.016	0.074	0.012	0.929	0.982	1.034	1.054	0.929	0.982	1.034	1.054	R3w
Wdr43	0.019	0.056	0.001	0.890	0.900	0.012	0.333	0.018	0.023	0.016	0.923	0.011	1.047	1.014	0.989	0.951	1.047	1.014	0.989	0.951	A3w
Ehd3	-0.083	-0.315	0.005	1.564	0.888	0.066	0.431	0.095	0.020	0.084	0.939	0.061	0.779	0.895	1.084	1.241	0.779	0.895	1.084	1.241	R3w
Crim1	0.011	0.320	-0.051	0.603	0.908	0.049	0.882	0.071	0.007	0.063	0.323	0.046	1.084	1.197	0.848	0.871	1.084	1.197	0.848	0.871	A4w
Eif2ak2	0.141	-0.026	-0.118	1.084	0.842	0.046	0.099	0.066	0.678	0.059	0.051	0.043	0.840	0.982	1.098	1.079	0.840	0.982	1.098	1.079	R3w
Cdc42ep3	0.097	-0.232	-0.093	1.400	0.819	0.091	0.503	0.132	0.119	0.117	0.337	0.085	0.745	0.889	1.165	1.200	0.745	0.889	1.165	1.200	R3w
Hnrnpll	0.099	0.168	-0.028	0.680	0.983	0.012	0.005	0.017	0.000	0.015	0.066	0.011	1.102	1.038	0.992	0.868	1.102	1.038	0.992	0.868	A3w
Mta3	0.000	0.001	-0.037	1.067	0.910	0.016	0.984	0.023	0.961	0.020	0.064	0.015	0.926	1.031	0.992	1.051	0.926	1.031	0.992	1.051	R1w
Haao	0.024	-0.162	-0.131	1.456	0.897	0.077	0.838	0.112	0.177	0.099	0.143	0.072	0.660	1.008	1.069	1.263	0.660	1.008	1.069	1.263	R2
Zfp36l2	-0.020	-0.162	0.035	1.201	0.932	0.020	0.528	0.028	0.003	0.025	0.129	0.018	0.967	0.903	1.068	1.063	0.967	0.903	1.068	1.063	R3w
Npc1	-0.091	-0.129	-0.023	1.346	0.949	0.031	0.110	0.044	0.031	0.039	0.473	0.029	0.823	1.018	0.985	1.173	0.823	1.018	0.985	1.173	R2w
Rnf125	-0.070	-0.179	0.000	1.354	0.937	0.030	0.184	0.044	0.010	0.039	0.993	0.028	0.854	0.960	1.030	1.157	0.854	0.960	1.030	1.157	R3w
Bin1	-0.134	-0.356	0.097	1.517	0.956	0.031	0.039	0.044	0.001	0.039	0.028	0.029	0.908	0.835	1.083	1.174	0.908	0.835	1.083	1.174	R3w
Camk4	-0.032	-0.067	-0.019	1.174	0.934	0.018	0.290	0.026	0.047	0.024	0.337	0.017	0.904	1.005	1.003	1.089	0.904	1.005	1.003	1.089	R2w
Egr1	0.531	0.152	0.114	-0.094	0.876	0.207	0.151	0.299	0.599	0.266	0.587	0.193	1.661	0.603	1.362	0.373	1.661	0.603	1.362	0.373	A2
Zfp608	0.127	0.538	0.200	-0.334	0.983	0.075	0.307	0.108	0.005	0.096	0.046	0.070	1.789	1.017	0.886	0.308	1.789	1.017	0.886	0.308	A3
Gramd3	-0.115	-0.335	0.020	1.605	0.997	0.010	0.002	0.015	0.000	0.013	0.108	0.010	0.777	0.896	1.072	1.255	0.777	0.896	1.072	1.255	R3w
Slc12a2	0.057	0.134	0.010	0.710	0.962	0.020	0.121	0.029	0.007	0.026	0.629	0.019	1.133	1.019	0.983	0.865	1.133	1.019	0.983	0.865	A3w
Synpo	0.205	1.430	-0.073	-1.254	0.966	0.144	0.382	0.209	0.002	0.186	0.618	0.135	1.789	1.639	0.474	0.098	1.789	1.639	0.474	0.098	A3
Ndst1	-0.198	0.089	0.017	1.079	0.885	0.051	0.054	0.073	0.242	0.065	0.741	0.047	0.955	1.173	0.808	1.063	0.955	1.173	0.808	1.063	R1w
Tcof1	0.005	0.042	0.020	0.894	0.991	0.005	0.459	0.007	0.002	0.006	0.010	0.004	1.067	1.001	0.988	0.944	1.067	1.001	0.988	0.944	A3w
Mppe1	-0.038	-0.201	-0.002	1.351	0.956	0.026	0.372	0.037	0.004	0.033	0.943	0.024	0.859	0.926	1.065	1.150	0.859	0.926	1.065	1.150	R2w
Smad7	-0.030	-0.532	0.089	1.667	0.961	0.051	0.706	0.074	0.001	0.066	0.136	0.048	0.860	0.678	1.244	1.217	0.860	0.678	1.244	1.217	R3w
Setbp1	0.122	0.783	-0.180	0.014	0.941	0.086	0.379	0.124	0.002	0.110	0.088	0.080	1.156	1.458	0.692	0.694	1.156	1.458	0.692	0.694	A4w
Pard6g	-0.042	0.433	-0.107	0.605	0.911	0.071	0.699	0.102	0.009	0.091	0.180	0.066	0.999	1.338	0.743	0.920	0.999	1.338	0.743	0.920	A4w
Nfatc1	-0.081	0.095	0.070	0.827	0.870	0.041	0.239	0.059	0.142	0.052	0.137	0.038	1.143	1.048	0.907	0.902	1.143	1.048	0.907	0.902	A4w
Cndp2	-0.109	-0.025	-0.001	1.173	0.967	0.016	0.009	0.023	0.283	0.020	0.972	0.015	0.914	1.066	0.927	1.093	0.914	1.066	0.927	1.093	R1w
Cyb5a	-0.082	-0.052	0.000	1.179	0.967	0.013	0.012	0.019	0.034	0.017	0.997	0.012	0.918	1.032	0.961	1.089	0.918	1.032	0.961	1.089	R1w
Unc93b1	-0.098	-0.095	-0.024	1.306	0.940	0.031	0.098	0.045	0.079	0.040	0.461	0.029	0.835	1.042	0.964	1.159	0.835	1.042	0.964	1.159	R1w
Cdk2ap2	0.054	-0.079	-0.022	1.093	0.965	0.012	0.034	0.017	0.006	0.015	0.117	0.011	0.946	0.939	1.075	1.040	0.946	0.939	1.075	1.040	I
Tbc1d10c	-0.045	-0.115	0.000	1.226	0.990	0.008	0.016	0.011	0.000	0.010	0.972	0.007	0.907	0.974	1.019	1.100	0.907	0.974	1.019	1.100	R3w
Slc29a2	0.309	0.454	-0.108	0.141	0.865	0.088	0.071	0.127	0.016	0.113	0.257	0.082	1.239	1.098	1.005	0.658	1.239	1.098	1.005	0.658	A3
Capn1	-0.059	-0.036	-0.011	1.147	0.877	0.024	0.160	0.034	0.307	0.031	0.643	0.022	0.919	1.033	0.969	1.079	0.919	1.033	0.969	1.079	R1w
Map4k2	-0.059	-0.114	0.003	1.237	0.889	0.027	0.200	0.038	0.029	0.034	0.902	0.025	0.904	0.982	1.008	1.106	0.904	0.982	1.008	1.106	R3w
Rasgrp2	0.061	-0.203	-0.213	1.625	0.976	0.053	0.470	0.077	0.041	0.068	0.012	0.049	0.496	1.029	1.100	1.375	0.496	1.029	1.100	1.375	R2
Plaat3	-0.131	-0.086	-0.034	1.353	0.983	0.020	0.012	0.030	0.031	0.026	0.152	0.019	0.798	1.078	0.932	1.192	0.798	1.078	0.932	1.192	R1w
Stx5a	0.031	-0.129	-0.028	1.207	0.951	0.021	0.371	0.031	0.009	0.027	0.227	0.020	0.891	0.936	1.079	1.095	0.891	0.936	1.079	1.095	R3w
Tmem179b	-0.045	-0.126	0.018	1.209	0.955	0.013	0.083	0.020	0.002	0.017	0.218	0.013	0.937	0.953	1.028	1.082	0.937	0.953	1.028	1.082	R3w
Rom1	-0.095	-0.300	-0.039	1.637	0.944	0.056	0.308	0.082	0.014	0.073	0.504	0.053	0.692	0.948	1.059	1.301	0.692	0.948	1.059	1.301	R1
Ahnak	0.299	-0.270	-0.233	1.468	0.981	0.045	0.010	0.066	0.010	0.058	0.005	0.043	0.574	0.840	1.312	1.274	0.574	0.840	1.312	1.274	R3
Fth1	0.045	-0.044	-0.021	1.049	0.982	0.006	0.005	0.008	0.004	0.007	0.016	0.005	0.962	0.963	1.051	1.024	0.962	0.963	1.051	1.024	R3w
Cd5	0.141	-0.021	-0.003	0.863	0.918	0.031	0.034	0.045	0.626	0.040	0.914	0.029	1.074	0.891	1.119	0.917	1.074	0.891	1.119	0.917	A1w
Cd6	0.069	-0.106	0.024	1.029	0.925	0.025	0.130	0.037	0.031	0.032	0.372	0.024	1.033	0.877	1.108	0.981	1.033	0.877	1.108	0.981	A1w
Ccdc86	0.011	0.118	0.031	0.753	0.946	0.024	0.768	0.034	0.018	0.031	0.239	0.022	1.135	1.027	0.959	0.879	1.135	1.027	0.959	0.879	A3w
Ms4a4c	0.139	-0.378	-0.138	1.651	0.868	0.121	0.475	0.176	0.073	0.156	0.291	0.114	0.600	0.822	1.257	1.321	0.600	0.822	1.257	1.321	R2
Ms4a4b	0.039	-0.193	-0.060	1.351	0.964	0.030	0.422	0.044	0.008	0.039	0.103	0.028	0.797	0.923	1.109	1.171	0.797	0.923	1.109	1.171	R3w
Ms4a6c	0.016	-0.264	-0.061	1.489	0.877	0.074	0.892	0.108	0.051	0.096	0.433	0.070	0.740	0.904	1.124	1.232	0.740	0.904	1.124	1.232	R3w
Ms4a6b	0.003	-0.141	-0.024	1.252	0.948	0.024	0.930	0.034	0.010	0.030	0.342	0.022	0.875	0.946	1.064	1.116	0.875	0.946	1.064	1.116	R2w
Lpxn	0.114	-0.198	-0.033	1.217	0.972	0.024	0.031	0.035	0.003	0.031	0.214	0.022	0.896	0.846	1.174	1.084	0.896	0.846	1.174	1.084	I
Ostf1	0.023	-0.058	-0.049	1.151	0.932	0.021	0.503	0.031	0.103	0.028	0.069	0.020	0.883	0.995	1.035	1.087	0.883	0.995	1.035	1.087	R2w
Nmrk1	-0.043	-0.279	-0.061	1.585	0.950	0.052	0.598	0.076	0.014	0.068	0.281	0.049	0.691	0.940	1.085	1.284	0.691	0.940	1.085	1.284	R2
Ak3	-0.049	-0.034	-0.027	1.161	0.977	0.012	0.051	0.018	0.093	0.016	0.078	0.011	0.895	1.039	0.973	1.092	0.895	1.039	0.973	1.092	R1w
Jak2	-0.094	-0.180	0.143	1.119	0.904	0.033	0.123	0.048	0.013	0.043	0.010	0.031	1.126	0.858	1.040	0.976	1.126	0.858	1.040	0.976	A1w
Insl6	-0.045	-0.264	-0.067	1.574	0.864	0.088	0.744	0.128	0.081	0.114	0.464	0.083	0.688	0.953	1.076	1.283	0.688	0.953	1.076	1.283	R2
Cd274	0.258	-0.029	-0.057	0.832	0.956	0.031	0.004	0.045	0.502	0.040	0.117	0.029	1.036	0.848	1.202	0.914	1.036	0.848	1.202	0.914	A1w
Pdcd1lg2	0.370	-0.065	0.157	0.347	0.894	0.157	0.180	0.228	0.766	0.203	0.347	0.147	1.522	0.573	1.348	0.557	1.522	0.573	1.348	0.557	A2
Sgms1	0.346	-0.169	-0.237	1.267	0.966	0.051	0.009	0.074	0.062	0.066	0.008	0.048	0.652	0.861	1.300	1.186	0.652	0.861	1.300	1.186	R3
Pten	-0.006	-0.103	-0.018	1.195	0.899	0.025	0.887	0.036	0.033	0.032	0.485	0.024	0.902	0.966	1.041	1.091	0.902	0.966	1.041	1.091	R3w
Fas	-0.012	-0.254	-0.030	1.450	0.937	0.044	0.865	0.064	0.011	0.057	0.508	0.041	0.789	0.904	1.104	1.202	0.789	0.904	1.104	1.202	R2w
Lipa	0.096	-0.209	-0.042	1.273	0.869	0.057	0.307	0.082	0.046	0.073	0.471	0.053	0.860	0.860	1.164	1.116	0.860	0.860	1.164	1.116	R3w
Ifit2	-0.108	-0.446	0.025	1.752	0.987	0.028	0.057	0.041	0.000	0.036	0.389	0.026	0.731	0.830	1.131	1.309	0.731	0.830	1.131	1.309	R3w
Pcgf5	-0.008	0.176	-0.067	0.873	0.947	0.023	0.821	0.034	0.004	0.030	0.037	0.022	0.958	1.150	0.898	0.994	0.958	1.150	0.898	0.994	R1w
Exoc6	-0.092	0.106	0.034	0.893	0.981	0.012	0.007	0.018	0.003	0.016	0.042	0.012	1.067	1.092	0.886	0.955	1.067	1.092	0.886	0.955	A4w

Appendix C – Mathematical Modeling

1. Modeling gene regulation to understand the relationships between Erk/NFAT signaling coefficients

What is the basis for the strong observed negative correlation between the sensitivity coefficient for combined Erk and NFAT regulation (β_{EN}) and the sensitivity coefficients for the individual pathways alone (β_E and β_N)? Here, we examine the possibility that these correlations impose constraints on the *cis*-regulatory logic of target gene regulation by Erk or NFAT. To do so, we analyze a series of mathematical models of gene regulation, then derive from these models predicted relationships between these sensitivity terms, to determine whether these models can plausibly explain experimental data. First, recall that the linear model for fitting Erk and NFAT gene expression is given by:

$$y(x_N, x_E) = \beta_0 + \beta_E \cdot x_E + \beta_N \cdot x_N + \beta_{EN} \cdot x_E x_N \quad (1)$$

We will now construct a series of gene regulation functions for different models, incorporating different regulatory schemes for binding of NFAT or AP-1, which acts downstream of Erk activation. We will then use these gene regulation functions for different models to calculate predicted sensitivity coefficients. We will examine how sensitivity coefficients are constrained to vary with each other to see whether their modes of covariation are consistent with those observed experimentally (**Fig. 3.1H**). In these models, we make the assumption that TF binding is fast and reaches thermodynamic equilibrium [1,2], and that each binding configuration supports a distinct transcription rate.

1.1: Model I: Regulation by a single composite site for cooperative activation

NFAT and AP-1 are known to bind cooperatively to composite sites on *cis*-regulatory elements, a mode of regulation known to occur for many T cell activation genes, and is therefore thought to underlie the activation of many target genes of T cell signaling. In our first model, we consider whether this mode of regulation is sufficient to account for the observed dependencies of genes on NFAT and/or Erk signaling. In this model, a single composite NFAT and AP-1 binding can be occupied jointly by both NFAT and AP-1, or singly by one factor alone. Occupancy by both factors is required for activation, though occupancy with a single factor can result in partial activation. The probabilities of finding this composite element in different transcription factor occupancy states is given by:

$$\frac{dp_N}{dt} = \alpha_1 n \cdot p_0 - \beta_1 \cdot p_N - \alpha_4 a \cdot p_N + \beta_4 p_C \quad (2)$$

$$\frac{dp_A}{dt} = \alpha_2 a \cdot p_0 - \beta_2 \cdot p_A - \alpha_3 n \cdot p_A + \beta_3 p_C \quad (3)$$

$$\frac{dp_C}{dt} = \alpha_4 a \cdot p_N - \beta_4 \cdot p_C + \alpha_3 n \cdot p_A - \beta_3 p_C \quad (4)$$

where p_N , p_A and p_C are the probabilities of finding the element in the NFAT bound, AP-1 bound and doubly state, and a and n are the normalized levels of active AP-1 and NFAT transcription factors. Here, we will choose the normalization factor for these TFs such that the magnitude of these variables is unity when the corresponding factor is fully active, to enable comparison with Equation (1). Additionally, from conservation of probabilities:

$$p_0 + p_N + p_A + p_C = 1. \quad (5)$$

where p_0 is the probability of finding the element in an unbound state. Now, let the transcription rates of the gene locus in NFAT and AP-1 singly bound and doubly bound states be v_N , v_A and v_C. By solving equations (2)-(5), and by additionally assuming that the system is in thermodynamic equilibrium by invoking detailed balance of forward and reverse reaction rates for individual chemical binding and unbinding reactions, we get that the average rate of transcription from this gene locus as a function of NFAT and AP-1 activity levels is given by:

$$v(n,a) = \frac{v_A a/K_A + v_N n/K_N + v_C an/K_C}{1 + a/K_A + n/K_N + an/K_C}. \quad (6)$$

where $K_N = \beta_1/\alpha_1$, $K_A = \beta_2/\alpha_2$ and $K_C = \beta_2\beta_3/\alpha_2\alpha_3 = \beta_1\beta_4/\alpha_1\alpha_4$ are the dissociation constants for the TFs singly and in combination, in normalized units. We note that the expression for K_C implies that a relationship between the binding and unbinding rate constants that must be satisfied for the system to be at steady state. This condition corresponds to the requirement that the system is at thermodynamic equilibrium. Now, modeling the gene expression (y) using a synthesis and first-order degradation term:

$$\frac{dy}{dt} = v(n,a) - \delta y \quad (7)$$

and hence the steady state expression level of the gene will be:

$$y = v(n,a)/\delta \quad (8)$$

Now, we consider the regime where NFAT and AP-1 bind in a highly cooperative manner such that binding of one TF enhances affinity for binding of the second TF, such that $K_C \ll K_N$, and $K_C \ll K_A$. This biochemical regime is observed with the extensive contacts between the NFAT and AP-1 upon binding to DNA [3]. In this regime, by incorporating the expression for steady-state expression levels, we get:

$$y_N = v(1,0)/\delta = \frac{v_N/\delta}{1+K_N} \quad (9)$$

$$y_A = v(0,1)/\delta = \frac{v_A/\delta}{1+K_A} \quad (10)$$

$$y_C = v(1,1)/\delta = \frac{v_C/\delta}{1+K_C} \quad (11)$$

Finally, assuming that gene is not transcribed in the absence of AP-1 or NFAT activity, we set $y_0 = 0$. Here, we note that because NFAT and AP-1 bind cooperatively ($K_C \ll K_N$, and $K_C \ll K_A$), the transcription rate when only one TF is present (Eq. 9-10) will be much lower than that when both are present (Eq. 11), and thus $y_C \gg y_A$, and $y_C \gg y_N$.

We can now solve equation (1) to get their relationship between gene expression levels and the sensitivity coefficients obtained from analysis of RNA-seq data::

$$\beta_0 = y_0 (= 0) \quad (12)$$

$$\beta_N = y_N \quad (13)$$

$$\beta_E = y_A \quad (14)$$

$$\beta_C = y_C - y_A - y_N - y_0 \ (\sim y_C \gg y_A, y_N) \quad (15)$$

From these equations, we get that these requirements translate to the condition that the sensitivity coefficients $\beta_{EN} \gg \beta_N, \beta_{EN} \gg \beta_E$. This is inconsistent with observations that, for most target genes, the sensitivity coefficients for single regulation (β_N, β_A) are not negligible in magnitude compared to that for joint regulation (β_C). A greater range of single-input sensitivities can be observed when the requirements for NFAT and AP-1 cooperativity are relaxed, such that these factors bind independently to the same composite site; however, such a binding scheme would not be consistent with the known interaction and binding between these factors observed at a biochemical and structural level.

1.2: Model II: Regulation by multiple single and composite sites

Our analysis of a single NFAT/AP-1 composite binding site suggest that additional elements, where NFAT or AP-1 bind either singly or combination with other factors, may be required in order to explain the observed sensitivity coefficients for target genes, where the sensitivity coefficients for single NFAT or AP-1 regulation are comparable in magnitude to that for their joint regulation, (i.e. $\beta_N \sim \beta_C$ or $\beta_A \sim \beta_C$). We thus considered another *cis*-regulatory element that contains both a composite NFAT/AP-1 element, as well as two additional regulatory elements that contain binding sites for NFAT or AP-1 alone. These binding sites may either involve partnerless binding of these factors [4], or could involve binding of these factors with other partners not explicitly modeled. In any case, we can describe the binding of NFAT or AP-1 to those additional sites using additional probabilities, as follows:

$$\frac{dq_N}{dt} = \alpha_5 n \cdot q_0 - \beta_5 \cdot q_N \tag{16}$$

$$\frac{dr_A}{dt} = \alpha_6 a \cdot r_0 - \beta_6 \cdot r_A \quad (17)$$

where the conservation of probabilities dictates that:

$$q_0 + q_N = 1 \quad (18)$$

$$r_0 + r_A = 1 \quad (19)$$

Additionally, the binding of NFAT and AP-1 to the composite element is described by the same equation described above (2)-(4). Now, let us assume that each of these elements control transcription in an independent manner, such that the total average rate of transcription is given by the sum of the average transcription rates from each element [1]. In such a situation, the average transcription rate from the locus is given by:

$$v(n,a) = \frac{v_C an}{K_C + an} + \frac{v_A a}{K_A + a} + \frac{v_N n}{K_N + n} \quad (20)$$

Here, we take the maximal rates of the transcription of the NFAT and AP-1 only elements to be v_N and v_A, and the dissociation constants for these TFs from their respective elements to be $K_N = \beta_5/\alpha_5$ and $K_A = \beta_6/\alpha_6$. Furthermore, we have incorporated the assumption that NFAT and AP-1 binding to the composite is highly cooperative such that there is negligible fraction of the element that is singly bound. In this regime, the expression level of the gene is given by:

$$y_N = v(1,0)/\delta = \frac{v_N/\delta}{1+K_N} \quad (21)$$

$$y_A = v(0,1)/\delta = \frac{v_A/\delta}{1+K_A} \tag{22}$$

$$y_C = v(1,1)/\delta = \frac{v_N/\delta}{1+K_N} + \frac{v_A/\delta}{1+K_A} + \frac{v_C/\delta}{1+K_C}$$

Using equations (12)-(15), and assuming that there is no basal transcription, we then determine that the values for the sensitivity coefficients are given by:

$$\beta_0 = 0 \tag{23}$$

$$\beta_N = \frac{v_N/\delta}{1+K_N} \tag{24}$$

$$\beta_E = \frac{v_A/\delta}{1+K_A} \tag{25}$$

$$\beta_C = \frac{v_C/\delta}{1+K_C} \tag{26}$$

With this regulatory system, we note that the maximal transcription velocities and the dissociation constants for each of the binding elements can be tuned independently, thus allowing the measured sensitivity coefficients to vary freely from each other. Such a situation can account for the variation in sensitivity coefficients between different genes, as we observed (**Fig. 3.1**); however, such a situation would be hard to reconcile with experimental observations showing the strong negative correlation between the joint sensitivity coefficient β_C and the single NFAT or AP-1 sensitivity coefficients β_A, and β_N. The strength of this negative correlation and its pervasiveness across multiple gene clusters suggest the existence of additional regulatory mechanisms dictating TF occupancy and transcription rate that involve pervasive antagonism between these two transcription factors.

1.3: Model III: Regulation by multiple sites with partner competition

What is the basis for the observed negative correlations between the combined NFAT/AP-1 sensitivity coefficient β_C and the single sensitivity coefficients β_E, and β_N? In developmental systems, it has been observed that a transcription factor can globally redirect the binding of its partner away from other sites towards the composite sites binding both TFs [5,6]. With such a partner redirection, NFAT (or AP-1), when expressed in the cell, preferentially redirect AP-1 (or NFAT) towards composite NFAT and AP-1 elements for both TFs, at the expense of binding to elements containing only AP-1 (or NFAT) binding sites. Here, we consider a simple mathematical model for AP-1 and NFAT redirection, where these two TFs can form a heterodimer to bind the composite element:

$$\frac{d[AN]}{dt} = k_{ON}[A][N] - k_{OFF}[AN] \tag{27}$$

here, the conservation relationships for the two factors are:

$$[A] + [AN] = A_T \tag{28}$$

$$[N] + [AN] = N_T$$

where A_T and N_T are the total concentration of NFAT and AP-1 present when signaling is fully active. We take these quantities to be unity upon full signaling, and zero when the signaling pathway is inhibited. A full solution of (27) and (28) would involve solving a quadratic equation.

Here, to gain intuition into the behavior of the system, we consider the regime where NFAT and AP-1 bind tightly to each other, and where NFAT is in abundance relative to AP-1 ($N_T > A_T$). In this regime, when signaling is fully active:

$$[\mathrm{A}] = 0 \qquad a = 0 \tag{29}$$

$$[\mathrm{N}] = N_T - A_T \qquad n = 1 - (A_T/N_T) > 0 \tag{30}$$

$$[\mathrm{AN}] = A_T \qquad c = 1 \tag{31}$$

where $\rho = A_T/N_T$ is the ratio of total AP-1 to NFAT, and where we have defined c to be a variable describing the NFAT/AP-1 complex. Now, from (20), the rate of transcription is given by:

$$v(n,a) = \frac{v_C c}{K_C + c} + \frac{v_A a}{K_A + a} + \frac{v_N n}{K_N + n} \tag{32}$$

By inserting (29)-(31) into (32), we get that:

$$y_C = v(1,1)/\delta = \frac{v_N(1-\rho)/\delta}{(1-\rho)+K_N} + \frac{v_C/\delta}{1+K_C} \tag{33}$$

$$y_A = v(0,1)/\delta = \frac{v_A/\delta}{K_A+1} \tag{34}$$

$$y_N = v(1,0)/\delta = \frac{v_N/\delta}{K_N+1} \tag{35}$$

Using (12)-(15), and assuming negligible basal transcription, we now get that:

$$\beta_0 = 0 \tag{36}$$

$$\beta_N = \frac{v_N/\delta}{1+K_N} \tag{37}$$

$$\beta_E = \frac{v_A/\delta}{1+K_A} \tag{38}$$

$$\beta_C = \frac{v_C/\delta}{1+K_C} + \frac{v_N(1-\rho)/\delta}{(1-\rho)+K_N} - \frac{v_N/\delta}{K_N+1} - \frac{v_A/\delta}{K_A+1} \tag{39}$$

We now note that, unlike the sensitivity coefficients derived for the multiple sites model without any partner redirection (Model II), the sensitivity coefficients for single and joint NFAT and AP-1 effects are no longer independent; specifically, when there are variations in the maximal transcription rates and dissociation constants for the NFAT and AP-1 singly bound elements (v_N, v_A, K_N, K_A), β_C would now vary in the opposite direction from β_E and β_N. For instance, in this case, amid variations in the binding parameters for the AP-1 only binding site (v_A or K_A), we expect the following relationship:

$$\beta_C(v_A, K_A) = C - \beta_E(v_A, K_A) \tag{40}$$

where:

$$C = \frac{v_C/\delta}{1+K_C} + \frac{v_N(1-\rho)/\delta}{(1-\rho)+K_N} - \frac{v_N/\delta}{K_N+1}. \tag{41}$$

Thus, in this case, the joint sensitivity coefficient would decrease linearly with an increasing value for the AP-1 sensitivity coefficient, with an intercept given by the parameters for NFAT and composite site activity, as well as the ratios of NFAT and AP-1 levels. From these equations (36-39), we expect this inverse relationship to arise regardless of the relative strengths of the

NFAT or AP-1 only site, their transcriptional rates, and we also expect this inverse relationship when the composite site is absent, such that the interaction between NFAT and AP-1 is a *trans*-effect that results in redirection of these factors towards other gene loci. These different regimes are captured by the observed regulatory modes (**"A1-4" Fig. 3.1**). By the same argument, we also expect similar inverse relationships to arise from the redirection of binding partners from the repressive binding sites. Thus, from analysis of the mathematical model, we conclude that the *trans*- redirection of NFAT and/or AP-1 binding from *cis*-regulatory elements with different strengths can plausibly explain the negative correlation between the sensitivity coefficients that is broadly observed across many different regulatory modes and clusters.

2. Mathematical models of PD-1 and CD25 regulation

In this section, we build a model describing the regulation of PD-1 or CD25 at the *cis*-regulatory level. We will first approximate the experimentally observed signaling dynamics using a series of simple functions. We approximate the time-dependent activity of Erk and NFAT using the following time-dependent function:

$$y = b + (a - b)exp(-t/c) + d \cdot (t/t_{end})^e \quad (42)$$

This function consists of two parts: (1) an exponential decay from an initial value *a* to a final value *b,* occurring with time constant c; and (2) a rise in activity, from an initial value of zero to a value of *d* at the end time t_{end}, occurring with an exponent *e*. The function captures the initial decay in signaling from a maximum value that occurs straight after signaling onset, whereas the

second value captures the late rise in signaling activity that can occur with variable amplitude and sharpness. These two components of the function, together with chosen parameters, give rise to a time trace (**Fig. 3.6E**) that approximates the signaling activities observed by live cell measurements.

Parameter	Description	Value (signaling condition)
a	initial value	4 nM (AP-1) 9 nM (NFAT)
b	asymptotic value of initial decay	2 nM (AP-1) 1 nM (NFAT, L6C, 0.2 pmol M9C) 3 nM (NFAT, 2 and 20 pmol M9C)
c	timescale of drop off	8 hr (AP-1) 10 hr (NFAT, L6C, 0.2 pmol M9C) 50 hr (NFAT, 2 and 20 pmol M9C)
d	magnitude of late rise	1 nM (AP-1, L6F) 5 nM (AP-1, M9C) 0 nM (NFAT)
e	exponent of late rise	3 (AP-1) 3 (NFAT)

Table 1: Parameters used for Erk and NFAT signaling dynamics in mathematical models.

The Erk and NFAT signaling levels provide a readout of the total concentration of TF in the system. Due to combinatorial action of NFAT and AP-1 transcription factors through their co-binding to common regulatory elements, there is lower free concentration of these TFs in the nucleus. To model the sequestration of free NFAT and AP-1 by binding of these factors to other elements, we utilize a simplified version of the model, where AP-1 and NFAT exist in either unbound (A_0, N_0), singly-bound (A_1, N_1) or doubly bound (C) species on DNA. Binding and unbinding reactions occur rapidly and reach equilibrium, with affinity constants that describe the initial binding of AP-1 or NFAT to DNA (K_N, K_A), or the subsequent binding of each of these factors to form a dimeric complex on DNA (K_C):

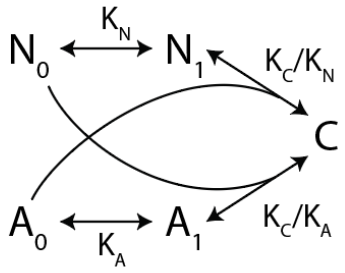

With this binding reaction scheme, it can be shown that the concentration of unbound NFAT or AP-1 that is free to act regulate the target genes is now given by to these two quadratic equations:

$$K_C(1+K_N)N_0^2 + [(1+K_N)(1+K_A) + K_C(A_T - N_T)]N_0 - (1+K_A)N_T = 0 \quad (43)$$

$$K_C(1+K_A)A_0^2 + [(1+K_N)(1+K_A) + K_C(N_T - A_T)]N_0 - (1+K_N)N_T = 0 \quad (44)$$

where N_T and A_T correspond to the total concentration of active NFAT and AP-1 factors in the nucleus as a result of signaling. For this model, we will use these equations to solve for the concentration of unbound AP-1 and NFAT given the total concentrations of these factors. These free TF concentrations along with the binding affinities of these TFs on relevant *cis*-regulatory elements at the gene locus, will then determine transcription rates for the two gene loci we consider below.

Parameter	Description	Value (units)
K_N	affinity constant for NFAT to unoccupied binding site	0.01 (1/nM)
K_A	affinity constant for AP-1 to unoccupied binding site	0.01 (1/nM)
K_C	affinity constant for composite NFAT and AP-1 binding site	0.5 ($1/nM^2$)

2.1: Pdcd1

From the scRNA-seq and flow cytometry data, we find that levels of *Pdcd1* transcripts, as well as PD-1 surface levels, increase in an NFAT dependent manner with both increasing affinity and

dose. This suggests that a model where NFAT may bind to the *Pdcd1* locus to drive its transcription. However, because PD1 levels also increase with increasing affinity, this suggests that NFAT may function cooperatively with AP-1 factors induced by the elevated Erk signaling under stronger pMHC affinity inputs. Here, to test this hypothesis, we built a *cis*-regulatory element model of *Pdcd1* regulation, to determine whether it can plausibly explain the pMHC-dependent regulation of this gene, as mediated by NFAT and Erk/AP-1 activation. This model consists of two *cis*-regulatory elements controlling *Pdcd1* transcription: (1) a partnerless NFAT binding site; and (2) a composite NFAT/AP-1 binding site, that would be engaged in a regime with high Erk signaling levels. These two binding sites regulate *Pdcd1* transcription in an additive and independent manner, and can do so with different rates of transcription. The equation describing this mode of PD1 regulation is given by the following:

$$\frac{dx}{dt} = \frac{v_1 N_0}{N_0 + K_1} + \frac{v_2 (N_0 A_0)}{(N_0 A_0) + K_2} - \delta_m x \tag{45}$$

$$\frac{dy}{dt} = \alpha_p x - \delta_p y \tag{46}$$

where x and y refer to the mRNA and protein levels for PD-1. For simulations, we modeled stochastic effects on transcription by treating the maximal transcription rates of both *cis*-regulatory elements (v_1, v_2) as a random variable that is log-normally distributed, corresponding to the stable cell-extrinsic heterogeneity in gene expression states.

We find that the *cis*-regulatory model we describe here captures the distinct dependencies of PD-1 expression on pMHC affinity, dose and addition of signaling inhibitors. Consistent with experimental data, PD-1 expression was higher at low doses of high-affinity pMHC M9C

compared to high doses of low-affinity of L6F, reflecting engagement of the NFAT:AP1 composite element due to stronger Erk signaling. PD-1 was then further up-regulated by increasing doses of M9C, reflecting increasing joint NFAT/AP-1 occupancy due to the accompanying increase in NFAT signaling. While inhibition of NFAT signaling with CsA, abolished PD-1 expression, MEKi inhibition dropped PD1 levels to those found upon stimulation with L6C, consistent with a scheme where an NFAT-only site sustains PD-1 expression in a regime where signaling activity is low. Taken together, these results are consistent with a model, where PD-1 is regulated by a bipartite non-coding element architecture, where NFAT acts singly on one site and in combination with AP-1 on the other to enable the pMHC dose and affinity specific expression of this gene.

Parameter	**Description**	**Value (Units)**
K_1	Concentration required for half-maximal binding of NFAT to its partnerless site	4 (nM)
v_1	Maximal transcription rate induced by partnerless NFAT binding site on *Pdcd1* locus	μ = 0.2 (1/hr; mean) $ln(v_N) = N(ln(\mu),0.2)$
K_2	Concentration required for half-maximal binding of the NFAT	1900 (nM^2)

	AP-1 complex to the *cis*-regulatory site	
v_2	Maximal transcription rate induced by NFAT / AP-1 composite site on *Pdcd1*	66.2 (1/hr; mean) $ln(v_N) = N(ln(\mu),0.2)$
δ_m	mRNA degradation rate	1 (1/hr)
α_p	protein synthesis rate per mRNA	2.2×10^4(a.u./hr)
δ_p	protein degradation rate	3 (1/hr)

Table 2: Parameters for the *Pdcd1* gene regulation model.

2.2: Il2ra

To describe the *Il2ra* (CD25) regulation, we utilize a standard ordinary differential equation framework for gene regulation, incorporating an additional random variable to describe temporal control in the opening of this gene locus. In this model, *Il2ra* is initially in a closed state, but then transitions into an open state that can then be accessed by transcription factors for expression regulation. Based on prior studies [7,8], we model this chromatin transition as a first-order stochastic process that occurs with a rate that is set by levels of AP-1 and NFAT transcription factors. Let P_1 be a binary random variable that is unity when the locus is open, and zero when closed. The probability:

$$Pr(P_1 = 1 | \, t > \tau) = 1 - e^{-kt} \quad (47)$$

where the first order transition rate:

$$k = \frac{v_{on}(N_0 A_0)}{(N_0 A_0)+K} \quad (48)$$

Parameter	Description	Value (Units)
K	Concentration product required for half-maximal enhancement of *Il2ra* locus opening rate	1.01 (nM^2)
v_{on}	Maximal first-order rate for *Il2ra* locus opening	0.31 (1/hr)
v_N	Maximal transcription rate induced by partnerless NFAT binding site on *Il2ra* locus	$\mu = 0.7$ (1/hr; mean) $ln(v_N) = N(ln(\mu),0.2)$
K_N	Concentration for half-maximal binding / transcription	2.7 (nM)
v_X	Transcription rate due to factor X	$\mu = 0.59$ (1/hr, mean, M9C) $\mu = 0.18$ (1/hr, mean, L6F)

		$ln(v_N) = N(ln(\mu),0.2)$
δ_m	mRNA degradation rate	1 (1/hr)
α_p	protein synthesis rate per mRNA	2.2×10^4(a.u./hr)
δ_p	protein degradation rate	3 (1/hr)

Table 3: Parameters for the *Il2ra* gene regulation model, incorporating regulation by NFAT and AP-1 (Erk dependent).

The ordinary differential equations describing *Il2ra* regulation are given by the following variables:

$$\frac{dx}{dt} = [\frac{v_N \cdot N_0}{N_0 + K_N} + v_X(t)] \cdot P_1 - \delta_m x \quad (49)$$

$$\frac{dy}{dt} = \alpha_p x - \delta_p y \quad (50)$$

Here, transcription of *Il2ra* is controlled by two elements, (1) a partnerless NFAT element, which dissociation constant K_N and maximum transcription rate v_N; and (2) a separate element controlled by an unidentified transcription factor *X*, that drives transcription at a rate v_X. We note that this element has greater activity with high affinity pMHC (M9C) compared to with low affinity pMHC stimulation (L6F). Transcription from *Il2ra* is only possible when its locus is open, and henceforth $P_1 = 1$. One expressed, mRNA transcripts are then degraded at rate δ_m;

they are also translated at a rate of α_p per mRNA copy, and translated proteins are then degraded at a rate δ_p. As locus opening occurs stochastically to the single-cell level, we ran multiple individual simulations of this model, each instance having a different time for locus opening dictated by the temporal probabilities, and also having varying maximal transcriptional rate by NFAT (v_N) and also the unidentified factor (v_X). These cell-to-cell variations, modeled using a log-normal distribution, provide an approximation of stable cell-to-cell heterogeneity in gene transcription due to extrinsic sources. We constrained the rate constants of the model using (1) the fractions of cells that have activated CD25 at 16 hrs (**Fig. 3.6D**), both after stimulation by the different pMHC inputs considered above and upon addition with MEKi or CsA at the onset of pMHC exposure; and (2) the mean CD25 fluorescence intensities at 30 hrs (**Fig. 3.6D**), in response to different pMHC inputs and upon inhibitor addition at 9 hrs.

This mathematical model captures both the effects of pMHC ligands, and in particular, the differential effects of signaling inhibitors on CD25 expression. In the model, early inhibition of Erk and NFAT substantially reduced the fraction of cells activating CD25, consistent with experimental observations, a consequence of disrupting NFAT or AP-1 binding at the *Il2ra* timing enhancer. In contrast, later inhibition of signaling inhibitors at 9 hrs, a time point where CD25 had already largely fully activated, resulted in much weaker effects on gene expression. NFAT inhibition moderately decreased CD25 levels, whereas MEK inhibition increased CD25 levels. These changes were explained in the model through a partnerless NFAT element whose occupancy decreased with CsA addition, but increased with MEKi addition due to redirection of NFAT away from AP-1/NFAT composite sites. We note that the reduced CD25 levels observed upon stimulation by lower-affinity L6F could not be recapitulated by the partnerless NFAT site

alone, as NFAT levels are also low when the higher-affinity M9C is present at low doses. In our model, these affinity-dependent changes in expression are instead accounted for by a separate regulatory element, controlled by a separate unidentified factor X, whose activity varies with pMHC affinity.

References

1. Bintu, L. *et al.* Transcriptional regulation by the numbers: models. *Curr. Opin. Genet. Dev.* **15**, 116–124 (2005).
2. Ackers, G. K., Johnson, A. D. & Shea, M. A. Quantitative model for gene regulation by lambda phage repressor. *Proc. Natl. Acad. Sci. U. S. A.* **79**, 1129–1133 (1982).
3. Chen, L., Glover, J. N., Hogan, P. G., Rao, A. & Harrison, S. C. Structure of the DNA-binding domains from NFAT, Fos and Jun bound specifically to DNA. *Nature* **392**, 42–48 (1998).
4. Martinez, G. J. *et al.* The Transcription Factor NFAT Promotes Exhaustion of Activated CD8 + T Cells. *Immunity* **42**, 265–278 (2015).
5. Luna-Zurita, L. *et al.* Complex Interdependence Regulates Heterotypic Transcription Factor Distribution and Coordinates Cardiogenesis. *Cell* **164**, 999–1014 (2016).
6. Hosokawa, H. *et al.* Transcription Factor PU.1 Represses and Activates Gene Expression in Early T Cells by Redirecting Partner Transcription Factor Binding. *Immunity* **48**, 1119-1134.e7 (2018).
7. Simeonov, D. R. *et al.* Discovery of stimulation-responsive immune enhancers with CRISPR activation. *Nature* **549**, 111–115 (2017).
8. Chu, J. M., Pease, N. A. & Kueh, H. Y. In search of lost time: Enhancers as modulators of timing in lymphocyte development and differentiation. *Immunol. Rev.* **300**, 134–151 (2021).

VITA

Matthew Wither was born in Cleveland, OH in 1989. He received his Bachelor of Science in Chemistry from Regis University in 2011 and a Bachelor of Science in Biology from Metropolitan State University of Denver in 2013. He worked as a Research Assistant from 2014-2016 at the University of Colorado Anschutz Medical Campus in the Proteomics and Metabolomics Mass Spectrometry Core Facility. He earned his Ph.D. in Bioengineering from the University of Washington in 2023.

FIELD OF STUDY

Signal transduction and gene regulation in T cells.

PUBLICATIONS

First-author publications:

Abadie K, Pease NA, **Wither MJ**, Kueh HY. Order by chance: origins and benefits of stochasticity in immune cell fate control. Curr Opin Syst Biol. **2019** Dec;18:95-103. doi: 10.1016/j.coisb.2019.10.013.

Wither MJ, Hansen KC, Reisz JA. Mass Spectrometry-Based Bottom-Up Proteomics: Sample Preparation, LC-MS/MS Analysis, and Database Query Strategies. Curr Protoc Protein Sci. **2016** Nov 1;86:16.4.1-16.4.20. doi: 10.1002/cpps.18.

Wither M, Dzieciatkowska M, Nemkov T, Strop P, D'Alessandro A, Hansen KC. Hemoglobin oxidation at functional amino acid residues during routine storage of red blood cells. Transfusion. **2016** Feb;56(2):421-6. doi: 10.1111/trf.13363.

Hill RC, **Wither MJ**, Nemkov T, Barrett A, D'Alessandro A, Dzieciatkowska M, Hansen KC. Preserved Proteins from Extinct Bison latifrons Identified by Tandem Mass Spectrometry; Hydroxylysine Glycosides are a Common Feature of Ancient Collagen. Mol Cell Proteomics. **2015** Jul;14(7):1946-58. doi: 10.1074/mcp.M114.047787.

Contributing-author publications:

D'Alessandro A, Howie HL, Hay AM, Dziewulska KH, Brown BC, **Wither MJ**, Karafin M, Stone EF, Spitalnik SL, Hod EA, Francis RO, Fu X, Thomas T, Zimring JC. Hematologic and systemic metabolic alterations due to Mediterranean class II G6PD deficiency in mice. JCI Insight. 2021 Jul 22;6(14):e147056. doi: 10.1172/jci.insight.147056.

Moore HB, D'Alessandro A, Moore EE, **Wither M**, Lawson PJ, Huebner BR, Hansen K, Choudhury R, Nydam TL. Increase in post-reperfusion sensitivity to tissue plasminogen activator-mediated fibrinolysis during liver transplantation is associated with abnormal metabolic changes and increased blood product utilisation. Blood Transfus. 2019 Jul;17(4):312-320. doi: 10.2450/2019.0205-18.

Clendenen N, Nunns GR, Moore EE, Gonzalez E, Chapman M, Reisz JA, Peltz E, Fragoso M, Nemkov T, **Wither MJ**, Sauaia A, Silliman CC, Hansen K, Banerjee A, D'Alessandro A, Moore HB. Selective organ ischaemia/reperfusion identifies liver as the key driver of the post-injury plasma metabolome derangements. Blood Transfus. 2019 Sep;17(5):347-356. doi: 10.2450/2018.0188-18.

Fox BM, Gil HW, Kirkbride-Romeo L, Bagchi RA, Wennersten SA, Haefner KR, Skrypnyk NI, Brown CN, Soranno DE, Gist KM, Griffin BR, Jovanovich A, Reisz JA, **Wither MJ**, D'Alessandro A, Edelstein CL, Clendenen N, McKinsey TA, Altmann C, Faubel S. Metabolomics assessment reveals oxidative stress and altered energy production in the heart after ischemic acute kidney injury in mice. Kidney Int. 2019 Mar;95(3):590-610. doi: 10.1016/j.kint.2018.10.020.

Reisz JA, **Wither MJ**, Moore EE, Slaughter AL, Moore HB, Ghasabyan A, Chandler J, Schaub LJ, Fragoso M, Nunns G, Silliman CC, Hansen KC, Banerjee A, Sheppard FR, D'Alessandro A. All animals are equal but some animals are more equal than others: Plasma lactate and succinate in hemorrhagic shock-A comparison in rodents, swine, nonhuman primates, and injured patients. J Trauma Acute Care Surg. 2018 Mar;84(3):537-541. doi: 10.1097/TA.0000000000001721.

Nemkov T, Sun K, Reisz JA, Song A, Yoshida T, Dunham A, **Wither MJ**, Francis RO, Roach RC, Dzieciatkowska M, Rogers SC, Doctor A, Kriebardis A, Antonelou M, Papassideri I, Young CT, Thomas TA, Hansen KC, Spitalnik SL, Xia Y, Zimring JC, Hod EA, D'Alessandro A. Hypoxia modulates the purine salvage pathway and decreases red blood cell and supernatant levels of hypoxanthine during refrigerated storage. Haematologica. 2018 Feb;103(2):361-372. doi: 10.3324/haematol.2017.178608.

Barrett AS, **Wither MJ**, Hill RC, Dzieciatkowska M, D'Alessandro A, Reisz JA, Hansen KC. Hydroxylamine Chemical Digestion for Insoluble Extracellular Matrix Characterization. J Proteome Res. 2017 Nov 3;16(11):4177-4184. doi: 10.1021/acs.jproteome.7b00527.

Liu H, Wang C, Lee S, Deng Y, **Wither M**, Oh S, Ning F, Dege C, Zhang Q, Liu X, Johnson AM, Zang J, Chen Z, Janknecht R, Hansen K, Marrack P, Li CY, Kappler JW, Hagman J, Zhang G. Clipping of arginine-methylated histone tails by JMJD5 and JMJD7. Proc Natl Acad Sci U S A. 2017 Sep 12;114(37):E7717-E7726. doi: 10.1073/pnas.1706831114.

D'Alessandro A, Moore HB, Moore EE, Reisz JA, **Wither MJ**, Ghasasbyan A, Chandler J, Silliman CC, Hansen KC, Banerjee A. Plasma succinate is a predictor of mortality in critically injured patients. J Trauma Acute Care Surg. 2017 Sep;83(3):491-495. doi: 10.1097/TA.0000000000001565.

Clendenen N, Nunns GR, Moore EE, Reisz JA, Gonzalez E, Peltz E, Silliman CC, Fragoso M, Nemkov T, **Wither MJ**, Hansen K, Banerjee A, Moore HB, D'Alessandro A. Hemorrhagic shock and tissue injury drive distinct plasma metabolome derangements in swine. J Trauma Acute Care Surg. 2017 Oct;83(4):635-642. doi: 10.1097/TA.0000000000001504.

D'alessandro A, Nemkov T, Reisz J, Dzieciatkowska M, **Wither MJ**, Hansen KC. Omics markers of the red cell storage lesion and metabolic linkage. Blood Transfus. 2017 Mar;15(2):137-144. doi: 10.2450/2017.0341-16.

Slaughter AL, D'Alessandro A, Moore EE, Banerjee A, Silliman CC, Hansen KC, Reisz JA, Fragoso M, **Wither MJ**, Bacon AW, Moore HB, Peltz ED. Glutamine metabolism drives succinate accumulation in plasma and the lung during hemorrhagic shock. J Trauma Acute Care Surg. 2016 Dec;81(6):1012-1019. doi: 10.1097/TA.0000000000001256.

Reisz JA, **Wither MJ**, Dzieciatkowska M, Nemkov T, Issaian A, Yoshida T, Dunham AJ, Hill RC, Hansen KC, D'Alessandro A. Oxidative modifications of glyceraldehyde 3-phosphate dehydrogenase regulate metabolic reprogramming of stored red blood cells. Blood. 2016 Sep 22;128(12):e32-42. doi: 10.1182/blood-2016-05-714816.

D'alessandro A, Nemkov T, Moore HB, Moore EE, **Wither M**, Nydam T, Slaughter A, Silliman CC, Banerjee A, Hansen KC. Metabolomics of trauma-associated death: shared and fluid-specific features of human plasma vs lymph. Blood Transfus. 2016 May;14(2):185-94. doi: 10.2450/2016.0208-15.

Tzounakas VL, Kriebardis AG, Georgatzakou HT, Foudoulaki-Paparizos LE, Dzieciatkowska M, **Wither MJ**, Nemkov T, Hansen KC, Papassideri IS, D'Alessandro A, Antonelou MH. Glucose 6-phosphate dehydrogenase deficient subjects may be better "storers" than donors of red blood cells. Free Radic Biol Med. 2016 Jul;96:152-65. doi: 10.1016/j.freeradbiomed.2016.04.005.

D'Alessandro A, Moore HB, Moore EE, **Wither MJ**, Nemkov T, Morton AP, Gonzalez E, Chapman MP, Fragoso M, Slaughter A, Sauaia A, Silliman CC, Hansen KC, Banerjee A. Plasma First Resuscitation Reduces Lactate Acidosis, Enhances Redox Homeostasis, Amino Acid and Purine Catabolism in a Rat Model of Profound Hemorrhagic Shock. Shock. 2016 Aug;46(2):173-82. doi: 10.1097/SHK.0000000000000588.

D'Alessandro A, Slaughter AL, Peltz ED, Moore EE, Silliman CC, **Wither M**, Nemkov T, Bacon AW, Fragoso M, Banerjee A, Hansen KC. Trauma/hemorrhagic shock instigates aberrant metabolic flux through glycolytic pathways, as revealed by preliminary (13)C-glucose labeling metabolomics. J Transl Med. 2015 Aug 5;13:253. doi: 10.1186/s12967-015-0612-z.

D'Alessandro A, Moore HB, Moore EE, **Wither M**, Nemkov T, Gonzalez E, Slaughter A, Fragoso M, Hansen KC, Silliman CC, Banerjee A. Early hemorrhage triggers metabolic responses that build up during prolonged shock. Am J Physiol Regul Integr Comp Physiol. 2015 Jun 15;308(12):R1034-44. doi: 10.1152/ajpregu.00030.2015.